(2)

LTR-91-GV-022

INFLATABLE TORUS SOLAR ARRAY TECHNOLOGY PROGRAM PHASE I

FINAL REPORT

Gordon Veal
Program Manager

L'Garde, Inc.

December 1991

DARPA
Defense Advanced Research
Projects Agency

LTR-91-GV-022

INFLATABLE TORUS SOLAR ARRAY TECHNOLOGY PROGRAM PHASE I

Prepared by

Billy Derbes
Koorosh Guidanean
Pat Malone
Art Palisoc
Gordon Veal
George Vendura

L'Garde, Inc.
15181 Woodlawn Avenue
Tustin, CA 92680

December 1991

FINAL REPORT
For Period 08 March 1990 - 8 October 1991

Contract F29601-90-C-006

Prepared for

DARPA
Defense Advanced Research
Projects Agency

Phillips Laboratory
Kirtland AFB, NM 87117-6008

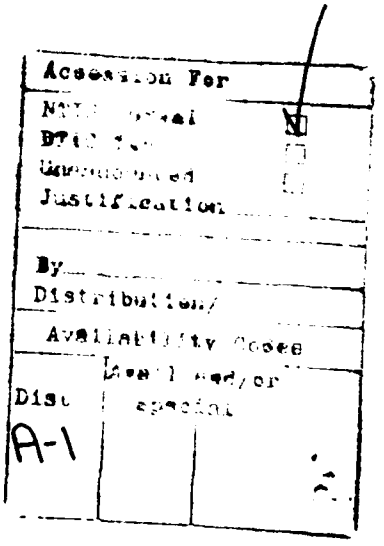

REPORT DOCUMENTATION PAGE	1. REPORT NO.	2.	3. Recipient's Accession No.

4. Title and Subtitle

INFLATABLE TORUS SOLAR ARRAY TECHNOLOGY PROGRAM
PHASE I

5. Report Date
October 15, 1991

6.

7. Author(s) Billy Derbis, Koorosh Guidanean, Pat Malone
Art Palisoc, Gordon Veal, George Vendura

8. Performing Organization Rept. No.
LTR-91-GV-022

9. Performing Organization Name and Address

L'Garde, Inc.
15181 Woodlawn Avenue
Tustin, CA 92680

10. Project/Task/Work Unit No.

11. Contract(C) or Grant(G) No.
(C) F29601-90-C-0006
(G)

12. Sponsoring Organization Name and Address

Defense Advanced Research Projects Agency (DARPA)
3701 North Fairfax Drive
Arlington, VA 22203-1714

13. Type of Report & Period Covered
Final Report
Mar 90 - Oct 91

14.

15. Supplementary Notes

16. Abstract (Limit: 200 words)

This Phase I of the Inflatable Torus Solar Array Technology (ITSAT) Program demonstrated the feasibility of an inflatably deployed solar array. During the program, several array conceptual designs for various orbits and power levels were prepared. A flexible amorphous silicon solar array was fabricated and mounted in a lightweight inflatably deployed rigidizable structure. This prototype unit was successfully packaged and deployed.

17. Document Analysis a. Descriptors

Inflatable Solar Array
Inflatable Structures
Rigidized Structures
Flexible Solar Arrays

b. Identifiers/Open-Ended Terms

c. COSATI Field/Group

18. Availability Statement	19. Security Class (This Report)	21. No. of Pages
Unlimited	Unclassified	147 + Appen.
	20. Security Class (This Page) Unclassified	22. Price

(See ANSI-Z39.18) See Instructions on Reverse OPTIONAL FORM 272 (4-77)

* GPO : 1993 0 - 301-526 (8393)

TABLE OF CONTENTS

TABLE OF CONTENTS
(Continued)

TABLE OF CONTENTS
(Continued)

LIST OF FIGURES

LIST OF FIGURES (Continued)

LIST OF FIGURES (Continued)

LIST OF FIGURES (Continued)

LIST OF TABLES

LIST OF TABLES (Continued)

ACRONYMS AND ABBREVIATIONS

AMO - Air Mass 0
AO - Atomic Oxygen
APSA - Advanced Photovoltaic Solar Array
AR - Anti Reflective
ASTM - American Society for Testing Materials
ASTP - Advanced Space Technology Program
BOL - Beginning of Life
BSF - Back Surface Field
BSR - Back Surface Reflector
CIS - Copper-Indium Diselenide
COTR - Contracting Officer's Technical Representative
DARPA - Defense Advanced Research Projects Agency
EOL - End of Life
FEM - Finite Element Method
GEO - Geosynchronous Equatorial Orbit
ITO - Indium Tin Oxide
ITSAT - Inflatable Torus Solar Array Technology
JPL - Jet Propulsion Laboratory
LEO - Low Earth Orbit
MOCVD - Metal Organic Chemical Vapor Deposition
NASA - National Aeronautics and Space Administration
PFRT - Preflight Readiness Test
PL - Phillips Laboratory
PV - Photovoltaic
PVF - Polyvinyl Fluoride
S/A - Solar Array
SBIR - Small Business Innovative Research
SERI - Solar Electric Research Institute
STEP - Space Technology Experiment Program
TCO - Transparent Conductive Oxide
TF - Temperature Degradation Factor
UV - Ultraviolet

ACRONYMS AND ABBREVIATIONS
(Continued)

aSi - Amorphous Silicon
cm - Centimeter
CO_2 - Carbon Dioxide
dia - Diameter
Fe - Iron
ft - Foot
g - 32ft/sec^2; gram
GaAs - Gallium Arsenide
GN_2 - Gaseous Nitrogen
Hz - Hertz
in - Inch
K - Solar Cell Temperature Coeff.
Kg - Kilogram
km - Kilometer
lb - Pound
lbf - Pound Force
M - Mass
Mev - Million Electron Volts
mil - .001 inch
oz - Ounce
P - Power
psi - Pounds per Square Inch
R - Gas Constant
ROM - Rough Order of Magnitude
sec - Second
Si - Silicon
SiO_2 - Silicon Dioxide

SUMMARY

The Defense Advanced Research Projects Agency (DARPA) Advanced Space Technology Program (ASTP) is defining, developing, and demonstrating high payoff technology applications to improve space system operational support to military commanders. ASTP will advance the state-of-the-art for more capable, smaller, and lower mass satellite systems, subsystems and components.

Under the ASTP effort, a number of small satellites are being designed. These satellites typically with a mass of a few hundred kilograms or less, have stowed volumes that are less than a cubic meter, and require electrical power levels ranging from a few watts up to a few kilowatts. Body mounted solar cells can meet some of the lower power requirements. For power levels above about 100 watts, deployed solar arrays are needed. Current solar array designs for more than 100 watts will exceed mass and volume restrictions both of which are critical.

In order to meet the solar array requirements of these smallsats, it was clear a new and unique approach was required - one that would involve a thin, flexible structure and thin flexible solar array. This type of system, if it could be developed, would be inherently low mass but equally (and probably more importantly), would require less volume and have the ability to be packaged in shapes that would provide the spacecraft designer the versatility needed to make smallsats feasible.

Towards this end, in February 1989 L'Garde proposed the development of an experiment to demonstrate the packaging and deployment in space of a flexible solar array mounted on an inflatable structure.

The program was broken into 3 phases, Phase 1 - proof of principle design, optional Phase 2 - preflight readiness test, and optional Phase 3 - space flight experiment operations. This final report describes the activities and results of Phase 1 only. It consisted of 6 tasks: Task 1 inflatable solar array concept definition; Task 2 prototype array design; Task 3 array fabrication; Task 4 testing for packaging, deployment, and functional characteristics; Task 5 analysis of test results and recommendations for optional work; and Task 6 project management and documentation.

L'Garde, from it's inception almost 20 years ago until the present, has been designing and developing inflatable structures for space applications. These structures range from short-lived decoys for re-entry vehicles to large aperture space based antennas and solar concentrators. In addition, L'Garde has studied both fully inflatable structures plus inflatably deployed and subsequently rigidized structures. L'Garde's expertise, therefore, is ideal for solving one half of the problem - development of a lightweight flexible structure.

Apogee Corporation had for some time been in the process of developing a lightweight flexible solar array of amorphous silicon which at the time was the leading candidate for a flexible solar array. While not as efficient as existing crystalline silicon arrays, the large difference in weight per unit area promised

an overall higher power to weight ratio. This then provided the potential solution for the second half of the problem - development of a lightweight flexible solar array.

The ITSAT team was Apogee Corporation providing the amorphous silicon array and L'Garde providing the flexible structure and integration. During Task I - Concept Definition a matrix of designs was developed to provide data on power to weight ratio, packaged volume, deployed dimensions and cost. The matrix consisted of sixteen basic concepts all employing an amorphous silicon array as the baseline that included:

a. Six orbits - LEO, GEO, Molniya, 3000 kilometer, 10,000 kilometer and a one way LEO/GEO transfer orbit.

b. Four power levels - 200 watts (3 year EOL), 1000 watts (1 year EOL), 2500 watts (1 year EOL) and 5000 watts (end of transfer orbit).

c. Three physical configurations - spherical (no pointing required), pillow (structure resembles an inflated mattress) and tubular (structure consisted of an inflated tubular framework surrounding the array).

d. Two types of structures - fully inflatable and inflatably deployed and rigidized.

e. Three satellite buses - STEP type, Techstars type and a generic type.

In developing the various point designs, launch loads, on-orbit loads, orbit environments, and thermal effects were all considered. The purpose of the concept study was three-fold - first to determine the concept to be carried forward, second to provide preliminary data to potential spacecraft designers, and third to provide data to the COTR to allow comparisons to be made between ITSAT technology and competitive technologies.

Evaluations of the various point designs provides the following:

a. Rigidizable systems are much better than fully inflated unless the life requirement is only a few days.

b. The tubular configuration is the best.

c. High wattage arrays provide higher power to weight ratios (overhead weights such as inflation tanks, pointing systems, support arms, etc. do not scale directly with wattage).

d. The inflatably deployed rigidized tubular configuration with a flexible array has the potential to meet the smallsat requirements (200 watt system in LEO/GEO achieved 39 watts/kg).

e. A radiation shield for the aSi array is not available and will require development.

Task 2 called for design and development of a prototype unit to be fabricated and tested to demonstrate the feasibility of packaging and deploying an inflatable system. The structure was the rigidized tubular configuration selected as a result of the concept definition studies.

This type of structure is fabricated from a laminate of plastic film - aluminum foil-plastic film which results in a structure thin and flexible enough to be folded and packaged. It is inflated under low pressure to deploy it (1-2 psi) and then rigidized by increasing the pressure to 13 psi. This pressure is sufficient to yield the aluminum to remove the packaging wrinkles and result in a smooth tubular structure. Once rigidized, the inflatant is vented leaving a strong lightweight structure.

Several materials were evaluated and a laminate of AN19 plastic film - 3 mil aluminum - AN19 plastic film was selected. The AN19 is a half mil polyvinyl fluoride reinforced with an open weave nylon fabric.

Off-the-shelf adhesives were selected for fabrication of the proof of principle prototype unit due to the very expensive nature of "space qualified" adhesives and the cost of an extensive adhesives survey. Materials will be selected for Phase II and III units that will meet the space environments and outgassing requirements.

The array used was an amorphous silicon array supplied by Apogee Corporation. This is the array that had been originally proposed by L'Garde and because of the long lead time was placed on order immediately after the start of the contract.

During the radiation studies of Task 1 and fabrication of the array, two major problems surfaced. The first is that no appropriate flexible radiation shield for the array exists, and second the method used for attachment of the bus bars is not acceptable for flight hardware. Although this type of array is potentially a good solution to the flexible array problem, it appears these problems will require more time and funding to resolve than is available for this program.

As a result of these concerns with amorphous silicon, several other array technologies were investigated - copper-indium diselenide, gallium arsenide, Cleft gallium arsenide and the advance photovoltaic solar array type blanket (APSA). Of these the APSA type appears most promising for the ITSAT program.

The APSA type is a very thin (2 mil) crystalline silicon cell mounted on two mil kapton sheet with a two to three mil cover glass. The cells are mounted on the kapton and electrically connected in such a manner as to allow the array to be accordion folded for packaging. This array system has been through space qualification tests and flown on the shuttle.

The packaging and testing of the rigidizable structure and amorphous silicon flexible array definitely established the feasibility of the basic concept. Factors of safety on the order of 8 on the design loads of .03 "g" were demonstrated after packaging and deployment. In addition, it was shown that the amorphous silicon array could be packaged and deployed with no damage to the

array. The two problems identified during the testing - excessive leakage at the torus corner joints and warpage of the torus have been resolved.

The final task was to develop a design of a Preflight Readiness Test unit using all information and data developed from Phase 1. The PFRT design employs an inflatably deployed rigidizable structure to support an APSA type array. L'Garde recommends carrying this configuration into Phases 2 and 3.

1.0 INTRODUCTION

Since almost the beginning of the Space Program, crystalline silicon solar cells have been the primary source of electrical power for spacecraft. The reasons are simple enough: The sun is, for all practical purposes, an inexhaustible source of energy and the photoelectric effect has been known for over one hundred years and well understood since about 1900. As importantly, photovoltaic technology has long reached a substantial level of maturity and solar cell arrays have donned almost all spacecraft flown to date, that had any significant power requirements.

Impressive as the progress and the contributions of the crystalline cell array technology may have been, it has had some serious disadvantages. We mention two significant ones: Crystalline solar cells are easily damaged under flexure; and they suffer considerable degradation when exposed to intense radiation fields, as for instance the ones that comprise the Van Allen belts. The first one has been countered by using rigid, therefore heavy substrates and/or intricate array folding schemes, which in turn require mechanically complex, thus heavy, volume intensive and, in a number of recorded cases, unreliable deployment mechanisms. Similarly, radiation degradation has been dealt with by utilizing glass: inexpensive, transparent but inflexible, a decent radiation shield but due to its relatively low density, finite thicknesses must be used, which further exacerbates the inflexibility problem, resulting in either complex and/or heavy deployment mechanisms as well.

About two decades ago amorphous silicon (aSi, or alpha-silicon) started being widely recognized as a promising photocell material by the photovoltaics community. Though it has a relatively low conversion efficiency compared to its crystalline counterpart (up to 7% reported in some cases, vs 13% for crystalline) it offers some significant advantages: it is much easier, thus much less expensive to manufacture, it is very flexible and it can use thin film substrates as backing material. In addition, due to its non-crystalline nature considerably smaller operational cell thicknesses are possible, since one doesn't have to worry about slicing a minimum thickness from a crystalline ingot. Thus, it is fair to expect that radiation damage should be smaller than in the crystalline cell case, where both the crystal lattice can suffer from charged particle bombardment and the larger thicknesses involved can absorb a much larger number of damage inducing particles.

Development of this material has been strong enough to bring about a fair number of terrestrial applications, where flexibility and survival in inclement environments are required. Sovonics, Inc. has been spearheading the aSi movement in the United States, with the corporate giants Sanyo and Canon following suit in Japan. Three years ago, Apogee Corporation, under the direction of Dr. Joseph Hanak had already started the effort towards the utilization of aSi in Space.

In parallel, a number of other photovoltaic technologies are being developed, both of the crystalline and flexible variety, such as gallium arsenide (GaAs) and copper-indium diselenide (or CIS), respectively. Both of these cell varieties claim higher efficiencies and better radiation resistance than their traditional silicon counterparts. In particular CIS has been the subject of

considerable R&D by International Solar Energy Technology and at least one large Aerospace firm in this country is seriously looking into CIS producibility on thin film substrates, strictly for use in space. It is worth noting that as of this writing CIS is considered to be even better than amorphous silicon in radiation resistance and it boasts roughly a 10% efficiency, twice better than that of amorphous silicon.

Recently, some advances have also been observed in the crystalline silicon array technology, namely, thinner cells have been possible to manufacture and adhere onto thin film substrates, such as a few thousandths of an inch of kapton. This results in lighter arrays and a larger variety of folding schemes. Still, the relative rigidity of the crystalline cells limits the latter, as well as the possible deployment mechanisms, and the form factor of the final package.

L'Garde, Inc. was formed twenty years ago by a few individuals who keenly recognized that much of this country's Space effort would be severely limited by the payload mass and volume constraints imposed upon the space transport vehicles. Based on some pioneering work that these engineers and scientists had done with inflatable space objects for the Department of Defense, they were among a handful of individuals in the western world to discover that amide and polyimide films offered significant structural strength under stress, excellent pressure containment and reasonable space environment survival characteristics. Early space flights in the Advanced Ballistic Missile program, which utilized objects designed, built, ground-tested and launch-supported by L'Garde, verified their initial intuition and analyses.

Today, with L'Garde building the world's first Large Aperture Inflatable Antenna for use in Space, it is easy to see how the flexible solar cell technology and L'Garde's space inflatables experience offer an unprecedented opportunity to combine the two technologies for the next quantum step in the development of Space PV Arrays: much lower cost, lower launch mass and volume, much better conformity to launch vehicle shape and higher operational reliability. For instance, assuming that the shape of the array to be flown is rectangular, a highly accurate inflatable rectangular torus can be constructed that can support the rectangular array "blanket"; i.e. the array is "framed" by the torus. The torus can be designed to meet all flight structural and dynamic loads, while it can be packaged along with the array in a very small volume. The form factor and launch volume of the package will depend mainly on the flexibility of the array.

This opportunity was also perceived by DARPA's Advanced Space Technology Program whose charter is to define, develop and demonstrate high payoff technology applications to improve space system operational support to military commanders. In this connection ASTP will advance the state-of-art for more capable, smaller and lower mass satellite systems, subsystems and components. Thus, the Inflatable Torus Solar Array Technology Demonstration Program was initiated in March of 1990 by DARPA to accomplish the following work:

1. Proof of Principle Design (Phase 1)
2. Pre-flight Readiness Test (Phase 2, Optional)
3. Space-flight Experiment Operations (Phase 3, Optional)

Phase 1 consists of the following distinct tasks:

- Inflatable Solar Array Concept Definition, including 16 point designs for a variety of Orbits and Power outputs, based on a design methodology that was developed specifically for this task.
- Prototype Array design based on the results of the first task.
- Prototype Array Fabrication
- Testing for packaging, deployment in Laboratory conditions, and functional characteristics.
- Analysis of test results and recommendations for optional work.
- Project Management and documentation.

All of the Phase 1 tasks have been successfully completed and much progress has been achieved. In addition, an amorphous silicon solar cell array has been built by Apogee Corporation and tested at L'Garde. Also, as a result of the first task, it was recognized that rigidization of the inflatable torus after inflation would be a very desirable characteristic to have. This was accomplished by increasing the scope of work in this first phase to design, fabricate and test a variety of aluminum foil/ film laminates that would meet the structural and dynamics requirements imposed by the array mass and the host spacecraft control system. Upon selection of the best material, a rectangular torus was fabricated and tested, then the aSi solar array was attached to it and the system was tested again successfully at ambient conditions.

In the following pages of this report, we present the results of these tasks in detail and we recommend proceeding with the program to make the Inflatable Solar Array a reality in Phases 2 and 3 of this high pay-off DARPA Program.

2.0 CONCEPT DEFINITION

In task one of the Statement of Work "Concept Definition", L'Garde was to develop 12 point designs for a completely self-contained ITSAT employing an amorphous silicon array for the following:

a. Nine designs which deliver 200 watts at the end of three years. These consist of a tubular torus configuration, a pillow configuration, and a spherical configuration; each in a polar Low Earth Orbit (LEO), a Geosynchronous Equatorial Orbit (GEO), and a six hour Molniya orbit.

b. Three contractor recommended configurations designed for a one year life. These consist of 1000 watt design in a 10,000 km, 60° orbit; a 2500 watt design in a 3000 km equatorial orbit; and a 5000 watt design in a LEO to GEO transfer mission.

The requirement was subsequently revised to add four additional point designs.

2.1 REQUIREMENTS

REQUIREMENT	VALUE	NOTE
Launch Vehicles:	Pegasus, Taurus, Delta II	The 200 watt designs were packaged into Pegasus, the larger designs into Delta-II. Delta-II launch loads are used for all designs.
Payload Diameter:	maximum launch vehicle payload envelope diameter	This eliminates the possibility of a sidemount array and the result is an aft-mount for all point designs. STEP and Techstars satellites were also examined.
Drive System:	single-axis with vehicle yawing continuously.	Contract mods to designs 4 and 7 are 2-axis aft-mount; (no yawing) 5 and 8 are 2-axis side-mount.
Vehicle Maneuvers:	1 ft/sec^2 max any direction.	This is the primary on-axis load.
Array Pull-Out:	1 lbf	
Voltage:	32 volt	
Outgassing	"avoid H_2O"; otherwise there is no specific direction.	UV-cured resin is used for the larger designs. Compatibility will be spacecraft specific.

2.2 LAUNCH VEHICLES AND PACKAGING

200 Watt Vehicles

Pegasus was used for these vehicles. The payload envelope is pictured in Figure 2.0-1. A generic 46 inch diameter satellite was used for the point designs. Since this is the full diameter of the payload bay, the array must be aft- mounted, with telescoping arms to extend the panels beyond the payload edge once on-orbit. The array resides in the interstage area, using up otherwise wasted space. Since it is desired to stack many vehicles in Pegasus, the relevant packaging parameter is solar array length penalty.

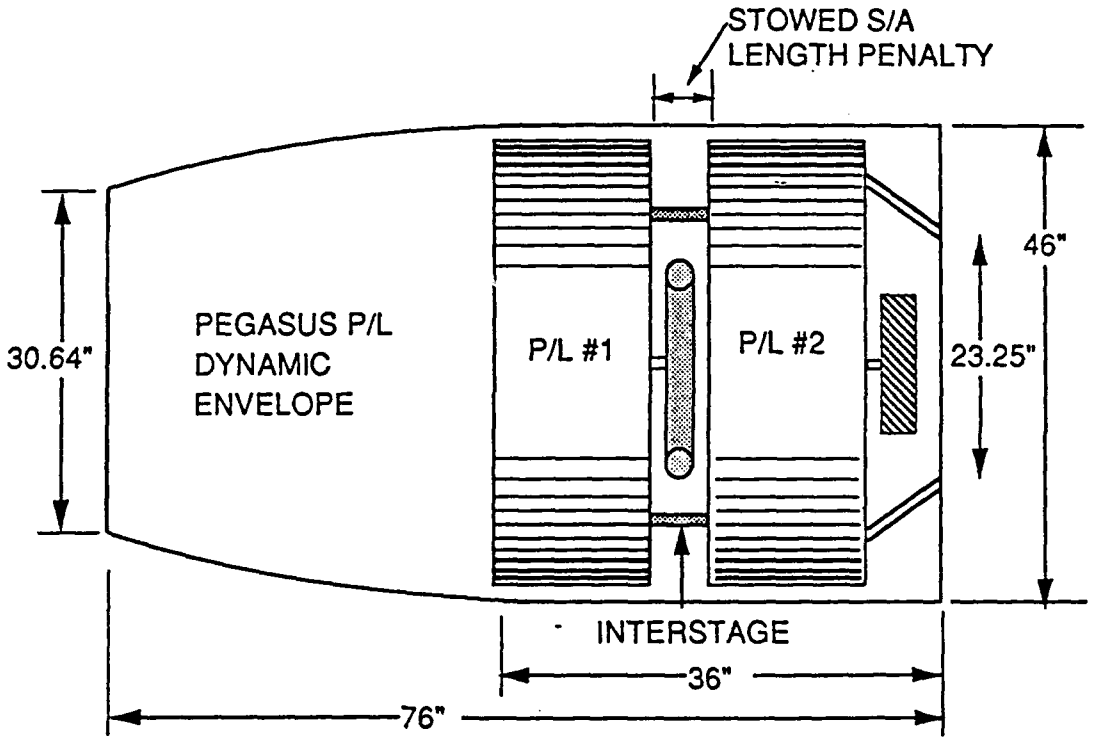

Figure 2.0-1. Pegasus Payload Envelope

1000, 2500, 5000 Watt Vehicles

Delta-II was used for these vehicles. The payload envelope is pictured in Figure 2.0-2. A generic 86 inch diameter satellite was used for the point designs.

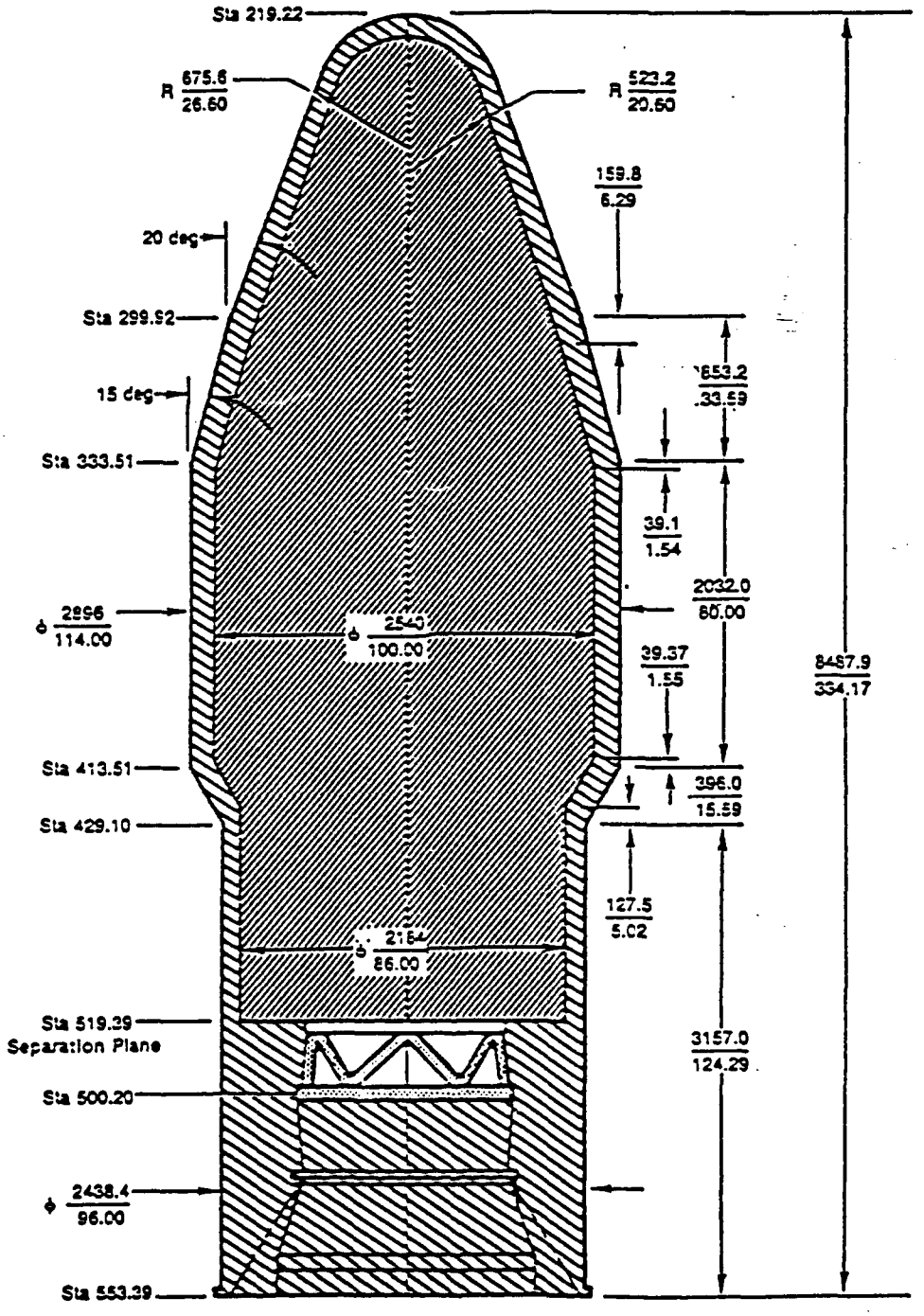

Figure 2.0-2. Delta-II Payload Envelope

2.3 POINTING

The use of a pointing system applies to planar arrays only. The spherical configuration does not need to be pointed.

The baseline aft-mount system achieves general sun pointing using a combination of single-axis drive and coordinated spacecraft yawing. This yawing may not be possible for surveillance or crosslinked satellites, in which case a dual-axis system, possibly side-mounted, must be used. Note, however, that side-mounts are not possible with satellites that occupy the full launch vehicle payload bay diameter.

For the equatorial orbits, it would be possible to simplify the planar systems even further by eliminating spacecraft yawing and upsizing the array for the earth tilt losses.

A solar array computer and motor controller are baselined, but the computer could be replaced by software in the spacecraft computers. Software calculates the sun position using navigation and attitude data, and orbit perturbations are handled using solar array current information to adjust pointing accuracy.

The 5000 watt LEO to GEO transfer concept is different from the others in that the vehicle 'z' axis is oriented along the velocity vector to accommodate constant ion engine thrusting, whereas the other concepts are earth pointed. The single-axis aft-mount system with continuous vehicle rolling will also work for this concept. Vehicle rolling would keep the solar array axis perpendicular to the sun vector, compensating for beta angle.

2-axis aft-mount and side-mount systems were also investigated, and are discussed in Sections 2.10.14 to 2.10.17.

Figures 2.0-3, -4 and -5 demonstrate the range of drive angles and vehicle yawing necessary to point in the Molniya orbit (single-axis aft mount system).

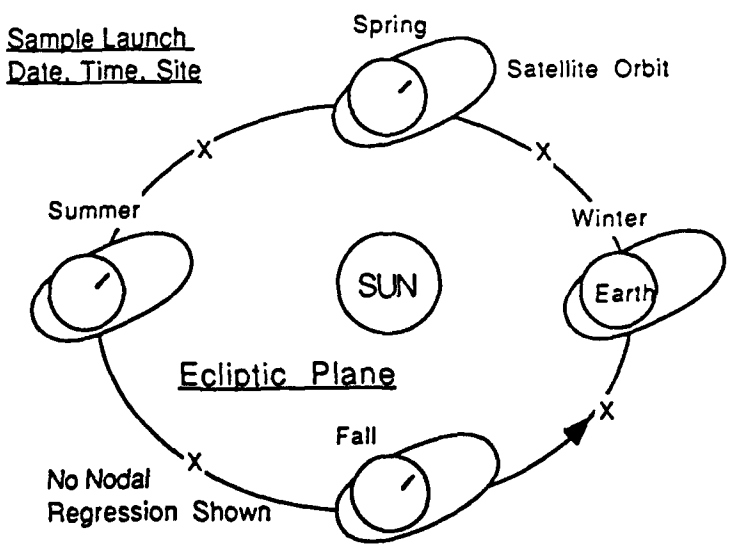

Molniya Orbit, Planar Arrays, Earth-Pointing Satellite, 3-Axis Stabilized

In this example, seasonal variations cause the sun's rays to face the satellite orbit in Winter and Summer; and to be edge-on to the orbit in Fall & Spring. Earth is tilted to Ecliptic 23.4349°

Figure 2.0-3. Sun-Orbit Geometry for Molniya Orbit

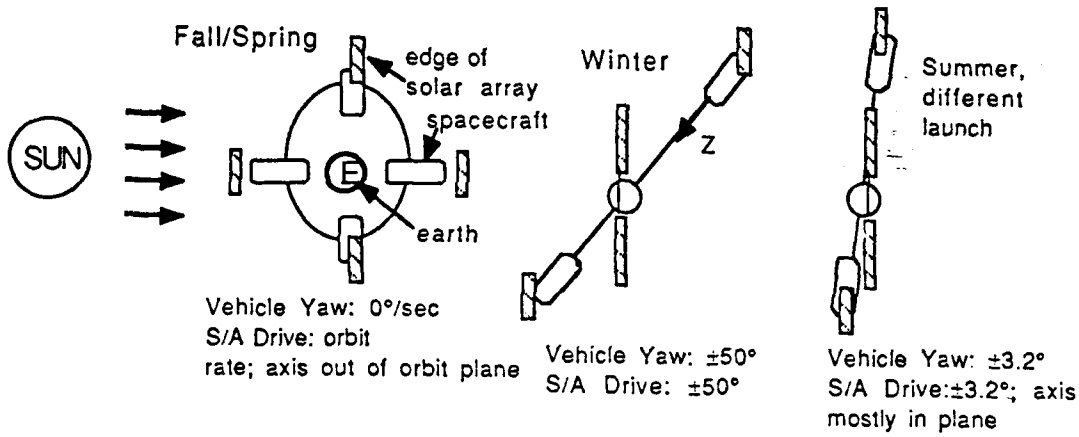

Figure 2.0-4. View Into Edge of Ecliptic Plane

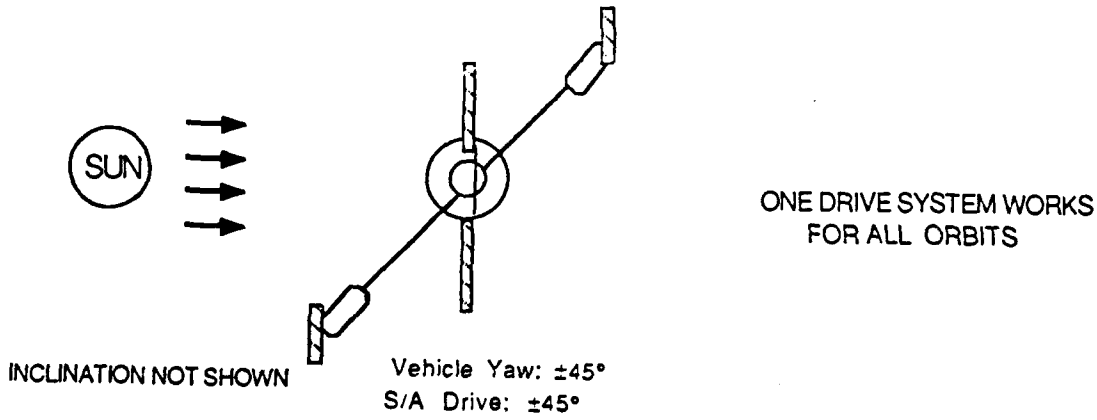

Figure 2.0-5. Plan View of Ecliptic Plane - Mid Season

2.4 GENERAL LOADS

2.4.1 Vehicle Stationkeeping

In order to maintain orbit parameters, the spacecraft must occasionally use thrusters, imparting a maximum acceleration of 1 ft/sec^2, any direction. This is the primary load. The most stressing geometry for the tubular configuration is shown in Figure 2.0-6. The result is a moment at the base. This puts the upper side of the tube in tension; the lower in compression, as shown in Figure 2.0-7. The lower side will buckle before the upper will fail in tension. For make-up gas systems, the compressive forces must be resisted by pressure. For rigidized systems, bending buckling failure data, presented in Appendix 1, must be used.

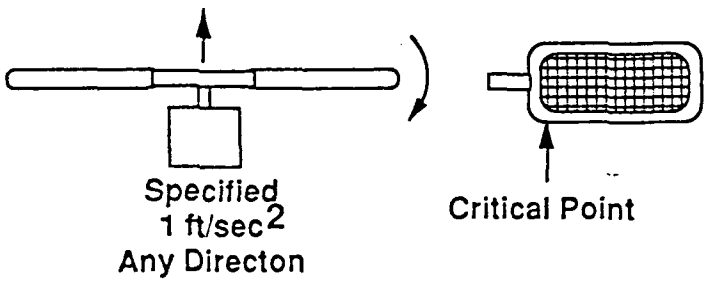

Figure 2.0-6. Critical On-Orbit Loading For Tubular Configuration

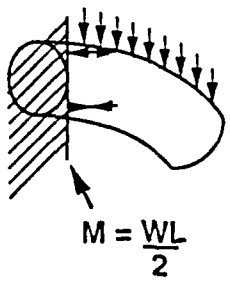

$\sigma_{\text{Critical Point}} = M/I\ y$

σ = stress
M = moment
L = length
W = mass X acceleration
I = moment of inertia
y = radius

Figure 2.0-7. Stresses Due to Bending

2.4.2 Array Pull-Out

In order for the array to become reasonably flat after deployment, and to stay flat, approximately one pound of force must be applied to its edges.

The planar arrays are tethered to the support structure from the array corners, so the 1 lbf requirement is achieved by resolving tie angles. For the spherical case, equivalent stress is used. (Figure 2.0-8)

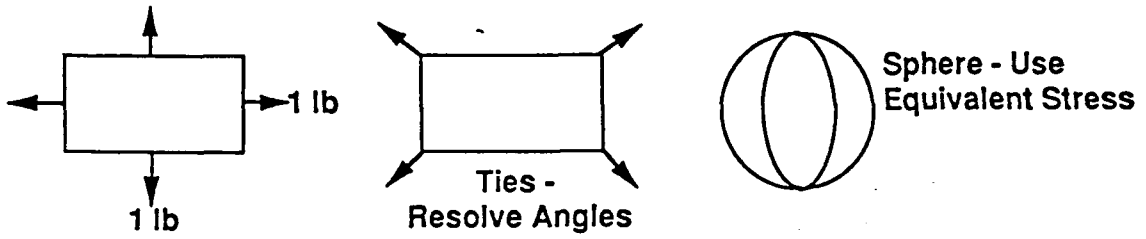

Figure 2.0-8. Array Pull-Out

The result is a minimum pressure requirement on the make-up gas structures (usually lower than the stationkeeping requirement). For the rigidized structures, the initial inflation pressure and tie/structure manufacturing details are affected.

2.4.3 Unwind

Because the power transfer cables have limited travel, it is necessary to unwind them once the drive is at +/-180°. The system is designed to reach end of travel while in eclipse, at which point the array is "quickly" unwound to be ready for sunrise. The minimum eclipse time is on the order of 28 minutes (worst case Molniya), so there is much time available to accelerate, unwind, and decelerate the array. Accelerating the array to the rotational speed subjects the drive arm to a torque, which the drive motor must supply (torque=[I_z]X[angular acceleration]+friction+cable moment).

The low acceleration rates necessary and the counterwinding for the cables result in extremely low torque required for the lightweight 200 watt arrays. Drive motors can be very small; a nominal size (~2 to 4 oz-in) was selected for the 200 watt conceptual designs. Actually, the stressing requirement on the drive motor for the detailed design will probably be maximum radial load during launch, as the arrays are cantilevered off the motor. The 200 watt array drive arms are 2.0 in. dia 1/32 in. thick which is sufficient to carry the torsional loads.

The larger arrays are much heavier due to radiation shielding and oversizing. This results in larger torques, but the motor and arm weights are still very small compared to overall array weight.

2.4.4 Dynamics

We assume the nature of the 1 ft/sec^2 translational maneuver to be a step input, as with a thruster. If we also assume the structure to have zero damping, the max dynamic stress will be twice the static stress. Therefore, a factor of 2 is used in all structural calculations. The assumption of zero damping builds a factor of safety into the designs, especially the pressurized versions, where damping is high.

2.4.5 Inflation

Inflation of a solar array can be made to proceed relatively slow. Solenoid valves are used in the inflation systems to reduce inflation speed and avoid high accelerations and stresses. Other provisions are also made, such as accordion-folding the rigidized aluminum tubes instead of rolling them in order to prevent localized pressure concentrations.

2.4.6 Launch

The worst structural condition for steady state acceleration is the resultant launch vehicle axial acceleration. This is due to the long moment arms involved and the fact that axial accelerations are much higher than transverse accelerations. The Delta II maximum axial acceleration of 12 g's is baselined for all designs.

The pyrotechnic shock environment is considered reasonable and will be investigated further in the Phase 2 detailed design phase. Natural frequencies will also be computed in the detailed design for consideration by the vehicle integrator.

2.4.7 Negligible Forces

The 200 watt LEO design was analyzed to determine the forces due to solar pressure, atmospheric drag, gravity gradient, and leaks. All were found to be less than 3×10^{-5} lbf, and so are considered negligible for all designs.

2.5 GENERAL ON-ORBIT ENVIRONMENT

There are many materials and techniques available to shield against atomic oxygen and radiation. The materials discussed below serve as a functional baseline for the conceptual study.

2.5.1 Atomic Oxygen

Atomic oxygen, prevalent at the lower altitudes, affects both the non-metallic structure and the array itself.

2.5.1.1 Kapton - The primary structural material for the make-up gas configuration is kapton. Material degradation and mass loss as a result of atomic oxygen (AO) attack are directly proportional to the reaction efficiency ($R\epsilon$) of a given material and AO total accumulated fluence (F_T). The equation used for surface erosion (ΔX) of a material in an AO environment is as follows:

$$\Delta x = F_T \; R\epsilon \qquad (1)$$

The F_T (AO fluence) is dependent on the attitude of a surface, solar activity and other factors. Studies by NASA [2-1] have shown that the atmosphere at altitudes about 200Km consists primarily of AO and that the relative AO concentration below 600Km decreases with altitude as plotted in Figure 2.0-9.

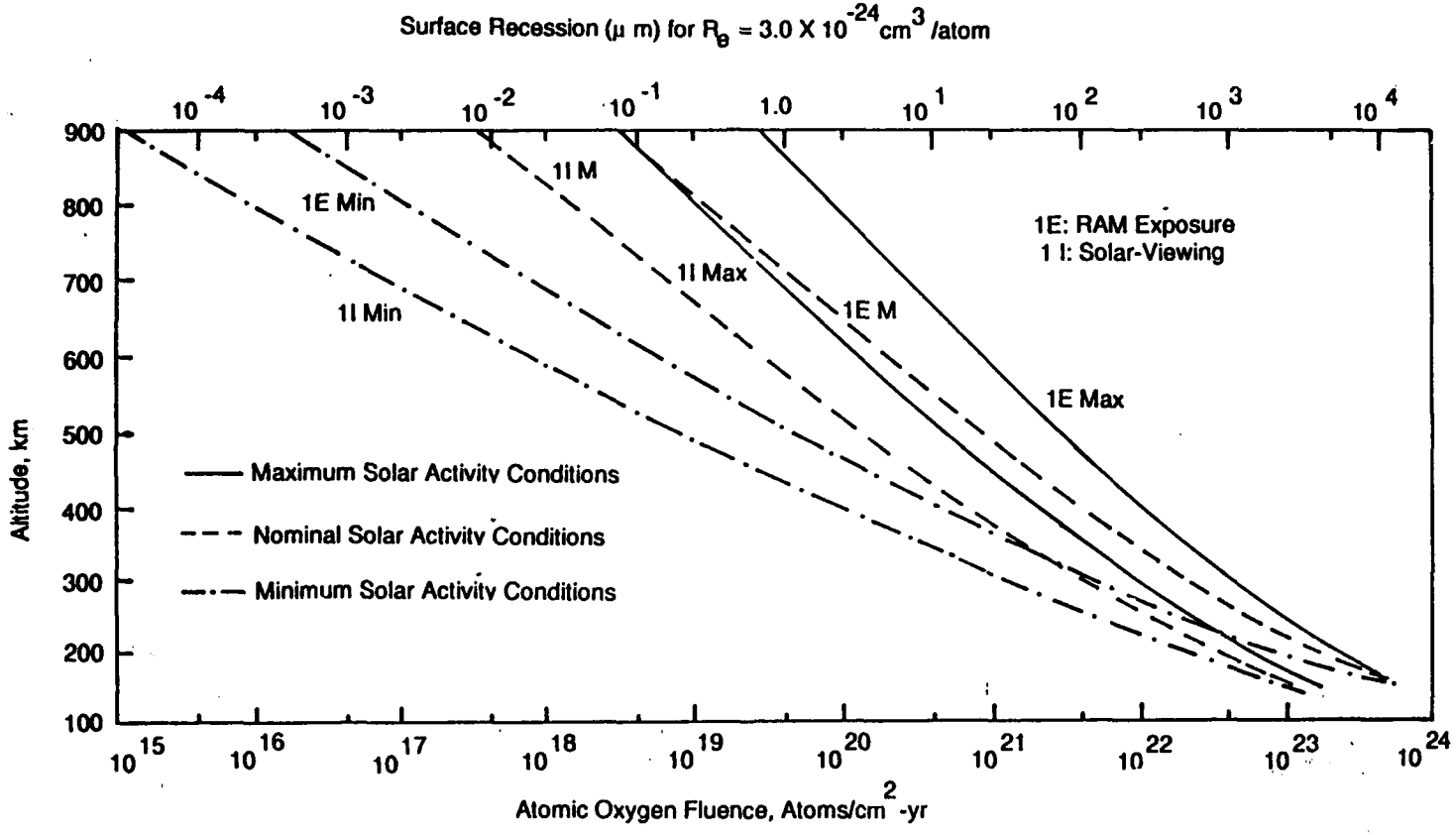

Figure 2.0-9. Atomic Oxygen Fluence, Atoms/cm^2-year

Figure 2.0-9 was used to obtain AO fluence in a 740 Km orbit. The reaction efficiency of kapton was obtained from these same NASA studies and assumed to be 3×10^{-24} CM^3/atom. An average value of ram and solar viewing for AO fluence was taken as the effective AO fluence for the particular solar activity.

Table 2.0-1 provides the AO fluence at different solar activity levels and surface erosion for regular kapton film (computed by equation 1).

TABLE 2.0-1. ATOMIC OXYGEN FLUENCE ATOM/YEAR CM^2 AND CORRESPONDING SURFACE EROSION FOR KAPTON FILM

	Solar Max	Nominal Solar Activity	Minimal Solar Activity
Ram	1.85×10^{20}	3.05×10^{19}	4.2×10^{17}
Solar Viewing	2.28×10^{19}	4.77×10^{18}	3.43×10^{16}
Average	1.039×10^{20}	$1,764 \times 10^{19}$	2.27×10^{17}
Surface Erosion Mils/year	0.13	0.0208	2.7×10^{-4}
Micron/year	(3.12)	(0.52)	(6.8×10^{-3})

Based on above analysis, the maximum surface recession of the kapton film (calculated for solar max condition at 740Km altitude is 0.13 mil/year. The resistance of kapton to AO, however, can further be enhanced by one or more of the following methods:

- Depositing SiO_2 and metals (Al, Au, Ni, etc.)
- Selection of Type F kapton (kapton film with a Teflon layer on one or both side.
- Dupont and Lockheed are currently developing AO-resistant kapton.

It is seen that because of the relative short duration (3 years) and low AO fluence, the damage to kapton film by AO is not significant in 740Km LEO.

2.5.1.2 Silicone-Based Polymers - Use of silicone-based polymers to protect the ITSAT arrays from AO and ionizing radiation is planned. Silicone-based polymers are known to resist atomic oxygen and are currently being utilized in a limited scale for the above purpose. Comparison of different commercially available silicones demonstrated that a silicone co-polymer Type CV1144 is superior to others in this respect. [2.0-2]

CV1144 is a flexible room temperature curing silicone and can be used for protecting space hardware from LEO environment and is available commercially (from Ghan Nusil).

CV1144 can be spray-applied for a fractional mil coating thickness or brushed on. It is non-corrosive and uses an oxime curing system that is not easily poisoned. It meets the NASA outgassing requirements as detailed in SP-R-0022 and ASTM E595 and provides an effective barrier against atomic oxygen.

The coating is currently being used to protect the Ku-Band reflector of the shuttle against LEO environment.

Recently, General Electric Aerospace has also developed a silicone based material for the same purpose. [2.0-3].

The amorphous silicon array front side coating has been baselined to be silicone rubber. The cell substrate will be stainless steel. These will be laminated to a sheet of kapton, which may then be coated with silicone rubber for radiation protection. Stainless steel is very resistant to atomic oxygen, and kapton was discussed above.

2.5.1.3 Rigidized Aluminum Structure - Aluminum is virtually unaffected by atomic oxygen.

2.5.1.4 Kevlar/UV-Cured Resin Structure - The Kevlar/Resin matrix will be encapsulated in an oxygen-resistant material such as kapton for stowage and initial inflation, which will also protect it throughout the mission.

2.5.2 Micrometeoroids & Debris

The debris and micrometeoroid environment affects all surfaces. The effect on the array is negligible, as total hole area expected in 3 years is very small, plus there is redundant power routing.

This environment is of primary concern to non-rigidized structural systems, which require make-up gas because of the leakage. Leakage is a function of pressure, time, and hole area, which is a function of material thickness and effective material area.

Tables 2.0-2 and 2.0-3 provide an estimate of meteoroid damage on kapton film in GEO and LEO environments. The numbers refer to hole area in CM^2/M^2.year. The values are calculated based on References [2.0-4] and [2.0-5].

L'Garde experience and test data have been used to estimate the second film damage (damage as it exits the inflatable structure). Assuming the second film damage is 50 times the particles projected area, the total hole area as a result of meteoroid attack for kapton film under GEO environment was calculated and is given in Table 2.0-4.

For thin films, the optimum material thickness, considering both first film and second film damage, is in the 1 to 2 mil range. We therefore baseline 2 mil kapton, which will erode to approximately 1.7 mil over the mission lifetime due to atomic oxygen.

TABLE 2.0-2. ESTIMATE FOR METEOROID DAMAGE IN KAPTON FILM AT GEO IN ONE YEAR

FILM THICKNESS	HOLE AREA 1ST FILM	PARTICLE PROJECTED AREA 2ND FILM
(mils)	(cm^2)	(cm^2)
0.250000	0.011283	0.001383
0.500000	0.016365	0.000837
0.750000	0.019447	0.000508
1.000000	0.021411	0.000313
1.250000	0.022776	0.000208
1.500000	0.023613	0.000151
1.750000	0.024208	0.000118
2.000000	0.024507	0.000100
2.250000	0.024786	0.000079
2.500000	0.024610	0.000067
2.750000	0.024760	0.000057
3.000000	0.024533	0.000048
3.250000	0.024192	0.000044
3.500000	0.024088	0.000038
3.750000	0.023597	0.000035
4.000000	0.023395	0.000030
4.250000	0.023158	0.000027
4.500000	0.022512	0.000025
4.750000	0.022211	0.000023
5.000000	0.021889	0.000021

TABLE 2.0-3. ESTIMATE FOR METEOROID DAMAGE IN KAPTON FILM AT LEO IN ONE YEAR

FILM THICKNESS	HOLE AREA 1ST FILM	PARTICLE PROJECTED AREA 2ND FILM
(mils)	(cm^2)	(cm^2)
0.000250	0.018749	0.003053
0.000500	0.026723	0.002187
0.000750	0.031519	0.001366
0.001000	0.034538	0.001330
0.001250	0.036602	0.001306
0.001500	0.037826	0.001290
0.001750	0.038659	0.001278
0.002000	0.029020	0.001271
0.002250	0.039343	0.001261
0.002500	0.038859	0.001254
0.002750	0.028503	0.001248
0.003000	0.037687	0.001242
0.003250	0.036801	0.001239
0.003500	0.036362	0.001233
0.003750	0.035372	0.001230
0.004000	0.034884	0.001224
0.004250	0.034380	0.001222
0.004500	0.033249	0.001219
0.004750	0.032683	0.001216
0.005000	0.032097	0.001214

TABLE 2.0-4. GEO TOTAL HOLE AREA

THICKNESS(mils)	HOLE AREA* 1ST FILM	PARTICLE PROJECTED AREA - 2ND FILM	TOTAL HOLE* AREA
1	0.021411	0.000313	0.03706
2	0.024507	0.000100	0.0295
5	0.021889	0.000021	0.021994

* CM^2/M^2.year

2.5.2.1 Free Molecular Flow Model For Gas Leakage - A simplified six-view projected area for the torus was calculated to be $1.8m^2$. An internal pressure of 0.1 psi was assumed at this stage.

The mass loss is computed by using the free molecular flow equation as follows:

$$\dot{m}/a = P/4\sqrt{\frac{8M}{\pi RT}} \quad \text{where}$$

$\dot{m}/a$ - mass loss rate per unit hole area per second
M - molecular weight of the inflating gas
P - pressure (0.1 psi)
R - universal gas constant
T - temperature of the gas (527° R)

The amount of gas lost as a function of life time, t (years), is calculated from:

$$m = \int (\text{hole area per year}).t.(\dot{m}/a)\, dt$$

Table 2.0-5 gives the amount of mass loss through the holes (given in Table 2.0-4 for GEO) as a function of torus skin thickness for kapton film using water as an inflatant.

TABLE 2.0-5. WATER MASS LOSS (FREE MOLECULAR)

LIFETIME PERIOD (year)	MASS LOSS (Water), POUNDS 1 MIL	2 MIL	5 MIL
1	172	137	106
2	686	548	426
3	1544	1232	954

2.5.2.2 Choked Flow Model For Gas Leakage - The assumed internal pressure of 0.1 psi is quite high and calculation of the mass loss by free molecular flow kinetic relation may not be applicable.

The mass loss through a hole is computed by using choked flow theory for the mass flux of perfect gases through a duct.

The mass flow rate through an orifice for perfect gases, assuming reversible adiabatic expansion through the orifice is:

$$\dot{W} = CA\,(P_A + \Delta P)\sqrt{\frac{gk}{RT}\left(\frac{2}{k+1}\right)^{\frac{k+1}{k-1}}}$$

where: $P_A / (P_A + \Delta P) < 0.53$

$\dot{W}$ = gas mass flow rate
C = orifice coefficient
A = Area of orifice
g = gravitational constant

K = gas specific heat ratio
R = gas constant
T = Temperature
$P_A + \Delta P$ = Internal pressure
P_A = Ambient (external) pressure

For the nitrogen gas, the above equation is reduced by using the following values for K, C, R, T and g:

K = 1.4 [2.0-6]
C = 0.65 [2.0-7]
R = 55.16 feet/°R
T = 530 R°
g = 32.17 ft/sec²

to the equation

$$\dot{W} = 0.0148\ AP$$

Where:

$\dot{W}$ = Mass loss flow rate, pounds/sec.
A = Total Hole area, IN^2 (= at)
$P = P_A + \Delta P$ Internal Pressure, PSI
a = hole area created in one year, IN^2
t = time years

The amount of nitrogen gas lost as a function of life time t is then given by:

$$m = 0.0148\ Pa \int t.dt = \frac{0.0148}{2}\ Pat^2$$

$$m = 7.4 \times 10^{-3} \times PAt^2 \quad \text{for Nitrogen Gas}$$

Similarly equations can be derived to provide the mass loss for other inflatants:

$m = 1.98 \times 10^{-3} \times Pat^2$ Hydrogen (K = 1.4) [2.0-6]

$m = 5.73 \times 10^{-3} \times Pat^2$ Water (K = 1.3) [2.0-6]

$m = 2.95 \times 10^{-3} \times Pat^2$ Helium (K = 1.67) [2.0-6]

Table 2.0-6 gives the amount of mass loss through the holes (given in Table 2.0-4 for GEO environment) as a function of torus skin thickness assuming use of regular kapton and water as an inflatant.

TABLE 2.06. WATER MASS LOSS (CHOKED FLOW)

LIFETIME PERIOD (year)	MASS LOSS (Water), POUNDS 1 MIL	2 MIL	5 MIL
1	187	149	111
2	748	596	444
3	1683	1341	999

Because of the relatively high pressure in the structure the amount of gas loss as a result of meteoroid damage will be substantial. If an inflatable system is used a large amount of make-up gas is needed to replenish the loss of inflatant.

It seems that even choosing hydrogen gas (the lightest inflatant, in spite of it being an unattractive choice, because of flammability, etc.) considerable make-up gas is still required to replenish the lost gas.

Table 2.07 gives the corresponding mass losses if hydrogen gas is used as an inflatant.

TABLE 2.07. HYDROGEN MASS LOSS (CHOKED FLOW)

LIFETIME PERIOD (year)	MASS LOSS (Hydrogen), POUNDS 1 MIL	2 MIL	5 MIL
1	65	52	38
2	260	206	153
3	585	464	342

Note that inflatant leakage in the LEO environment will be even worse because of:

- Higher meteoroid flux (hence, larger hole area)
- Gradual surface erosion of the skin (because of atomic oxygen attack).

Because of the above considerations it appears that a rigidized structure (plastic-aluminum-plastic laminate, gelatin/Kevlar fabric or un-cured polymers) are the system of choice for the torus system.

2.5.3 Radiation

The effect of radiation on the array itself is most pronounced at altitudes between LEO and GEO, such as the 200 watt Molniya orbit and the orbits of all the larger arrays. In evaluating the radiation effects on the array, the following assumptions were made:

- No solar flare protons are included.
- No atomic oxygen or micrometeoroid/debris effects are included (they are very small).
- Calculations are for a radiation shield of 2.5g/cm³ glass. To use 1g/cm³ silicone rubber, multiply thickness by ~2.5. This is conservative, as data for one type of silicone rubber indicates that a factor of 1.7 provides equivalence. At 1 MeV, Iron has a 50% higher range than SiO_2 for protons. Thus, the thickness of stainless steel (t_{fe}) required to substitute an equivalent thickness of silicone (t_{si}) is:

  $$t_{fe} = (\text{glass density/steel density})X1.5 = 0.48\ t_{si}$$

  Therefore, 2.4 mils of stainless steel provides a radiation shielding equivalent of 5 mils of glass.
- Shields must be provided for both sides of the array since radiation from both sides contributes to degradation.
- There is an additional efficiency loss due to the Staebler-Wronski effect. It is 11% relative for one year; 14.5% relative for three years (Dr. Hanak).
- The thermal degradation is included in these calculations. It is ~4% relative for the tubular configuration, ~ 9% relative for the pillow, and ~8% relative for the sphere (Figure 2.0-10). In general, however, a value of 5.5% relative is used to simplify the number of calculations.
- Data figures are as follows:

Figure 2.0-10	Normalized Pmax vs. temperature for amorphous silicone cells from Dr. Joe Hanak.
Figure 2.0-11	Phillips Laboratories fluence profiles as a function of shield thickness for crystalline silicon (using PL software). Data for amorphous silicon is unavailable, but it is thought to be more radiation resistant than crystalline silicon.
Figure 2.0-12	Maximum power degradation curve from Ref. 2.0-8, page 151.

- Pmax is power output at normal solar incidence (maximum); $Pmax_o$ is initial maximum power output.

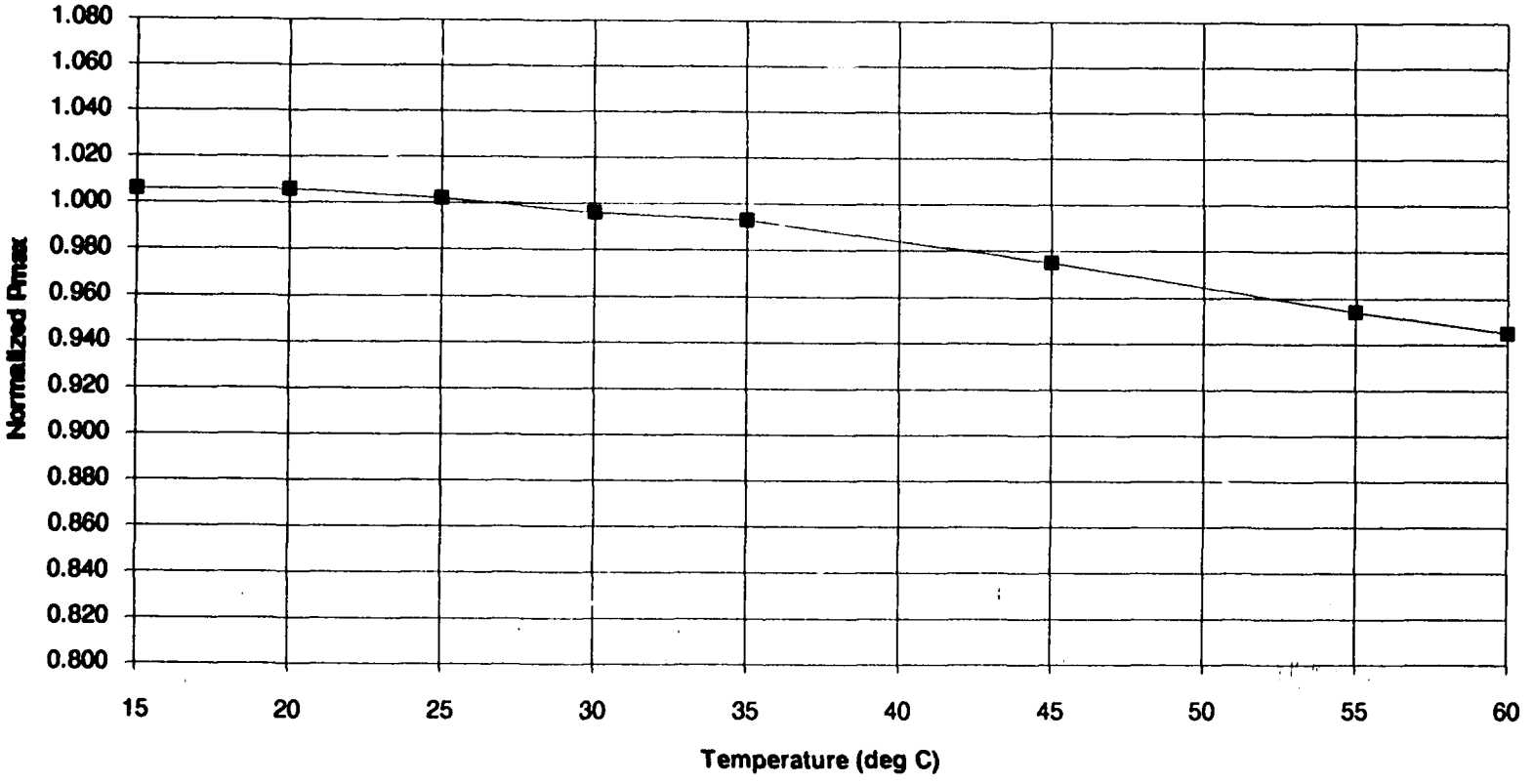

Figure 2.0-10. Pmax vs. Temperature

The calculation procedure is then:

1. Knowing orbit and life, get fluence vs. shield thickness from Figure 2.0-11.

2. Using this data, get $Pmax/Pmax_o$ vs. shield thickness from Figure 2.0-12.

   (NOTE: Radiation from both sides of the array contributes to degradation).

3. Subtract Staebler-Wronski and thermal degradation to get $(Pmax/Pmax_o)$ total.

4. Calculate total solar array area and weight and select a shield thickness that minimizes the total weight.

		shielding	0	25.4	76.4	152	305	509	764	1524
Low orbit	case 1,2,3									
altitude	inclination									
740	90									
combined electron/proton		fluence/yr	1.32E+15	7.46E+13	3.66E+13	2.24E+13	1.35E+13	9.34E+12	7.38E+12	5.30E+12
Mid orbit	case 11									
altitude	inclination									
3000	0									
combined electron/proton		fluence/yr	7.18E+16	5.88E+16	4.68E+16	3.76E+16	2.56E+16	1.46E+16	9.13E+15	3.85E+15
High orbit	case 10									
altitude	inclination									
10000	60									
combined electron/proton		fluence/yr	1.10E+19	6.64E+17	1.31E+17	2.90E+16	3.82E+15	9.13E+14	3.10E+14	5.83E+13
6hr Molniya	case 4,5,6									
altitude	inclination									
516/20287	63.4349									
combined electron/proton		fluence/yr	5.82E+18	1.58E+17	3.57E+16	1.15E+16	3.20E+15	1.13E+15	5.24E+14	1.52E+14
Orbit transfer	case 12									
from 300km 28	deg									
to 35794km 0	deg									
combined electron/proton		fluence/yr	8.10E+18	5.00E+17	1.40E+17	5.50E+16	1.80E+16	6.80E+15	3.20E+15	9.70E+14
Geo orbit	case 7,8,9									
altitude	inclination									
35794	0									
combined electron/proton		fluence/yr	5.30E+17	7.51E+13	6.19E+13	4.96E+13	3.44E+13	2.30E+13	1.47E+13	4.69E+12

Figure 2.0-11. Fluences vs. Orbit and Shield Thickness

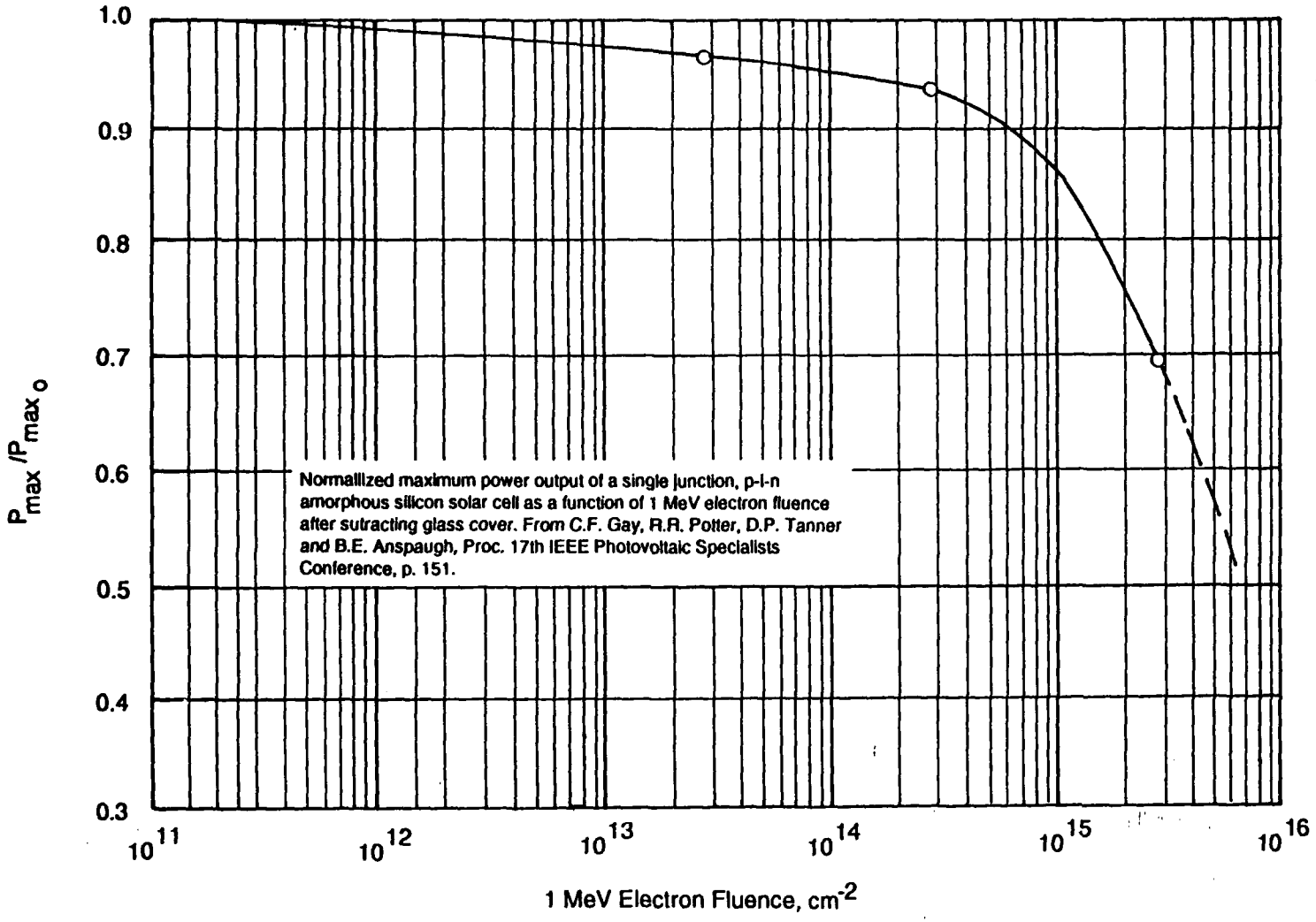

Figure 2.0-12. Power Degradation vs. Fluence

Array Backside - The baseline array is on a 1.0 mil stainless steel substrate, which provides an equivalent of 2 mils glass radiation protection. If additional shielding is needed, silicone rubber is added instead of stainless steel because it is a 1.5 times more effective shield on an equivalent glass/weight basis. Approximately 2.5 mils of silicone rubber is equivalent to one mil of glass, and it has a density of 1 gram/cm^3.

Array Front Side - The array is normally coated by 1.7 mils of transparent silicone rubber, which provides enough radiation protection for the LEO and GEO orbits. If additional protection is needed, extra thicknesses of silicone rubber are added.

LEO/GEO, 3 Year

With a 1 mil layer of SiO_2 (or 1.7 mils of silicone rubber equivalent), ($Pmax/Pmax_o$) total over three years life is 80%. No other shield thicknesses were considered because the shielding requirements are so small.

Molniya, 3 Year:

Shield Thickness (Glass, Mils)	1 MeV Equiv. Fluence (cm^{-2})	Pmax/Pmax0	(Pmax/Pmax0)total
60	$2.29X10^{14}$	.94	.775
30	$7.87X10^{14}$	.88	.715
20	$1.70X10^{15}$	.78	.615
12	$4.79X10^{15}$	.575	.410

10,000km Orbit, 1 year (1000 watt):

Shield Thickness (Glass, Mils)	1 MeV Equiv. Fluence (cm^{-2})	Pmax/Pmax0	(Pmax/Pmax0)total
60	$5.84X10^{13}$	.956	.791
30	$3.10X10^{14}$	.930	.765
20	$9.14X10^{14}$	.865	.700
12	$3.83X10^{15}$	.620	.455

3000km Orbit, 1 Year (2500 watt):

Shield Thickness (Glass, Mils)	1 MeV Equiv. Fluence (cm^{-2})	Pmax/Pmax0	(Pmax/Pmax0)total
60	$3.85X10^{15}$	.615	.450

LEO to GEO Transfer Mission, 1 Year (5000 watt):

Shield Thickness (Glass, Mils)	1 MeV Equiv. Fluence (cm^{-2})	Pmax/Pmax0	$(Pmax/Pmax_0)_{total}$
60	$9.70X10^{14}$	.950	.785
30	$3.20X10^{15}$	.660	.495
20	$6.80X10^{15}$	.505	.340

2.6 THERMAL EFFECTS

The array and structure experience temperature extremes and large variations in temperature as the spacecraft moves in and out of eclipse. The analysis is simplified somewhat by the fact that the array is always intentionally pointed at the sun.

2.6.1 Thermal Analysis

The models used in the thermal analysis of the three different ITSAT configurations are shown in Figure 2.0-13. The spherical array is modeled as a non-rotating thin-skinned balloon, the pillow configuration as a hollow rectangular parallelipiped, and the tubular configuration as a multilayer infinite slab. The thermal environment is assumed to be made up of the sun and earth only. The energy balance on an element is shown in Fig. 2.0-14.

2.6.1.1 Calculations Under Sun and Earth Shine - The thermal profile around the spherical balloon is calculated using a closed form solution and is shown in Figure 2.0-15 An absorptivity of $\alpha = 0.8$ is used with two different values of emissivities. The maximum temperature is at about 350 K (76 C).

A discrete radial energy balance is used for the pillow-type ITSAT. A computer program PILLO was written to do the analysis. This code was modified to investigate the case where the solar array is modeled as a cover slip that "floats" over the pillow. Figure 2.0-16 and 2.0-17 show the temperature profile over the pillow for the case where the solar array is an integral part of the pillow making up that side of the pillow facing the sun. When the array forms a "floating" cover slip over the top of the pillow, the temperature increases. The temperature increases as the array comes closer and closer to the pillow. This is shown pictorially in Figure 2.0-18 for a 1 x 2m solar array "floating" on top of a pillow of the same area and 1/2 meter thick. As the distance between the array and the pillow increases, the average temperature over the array approaches that of the tubular-type. It must be noted, too, that when the array shades only part of the pillow, that portion of the pillow that is shaded can get extremely cold relative to the sun-exposed portions.

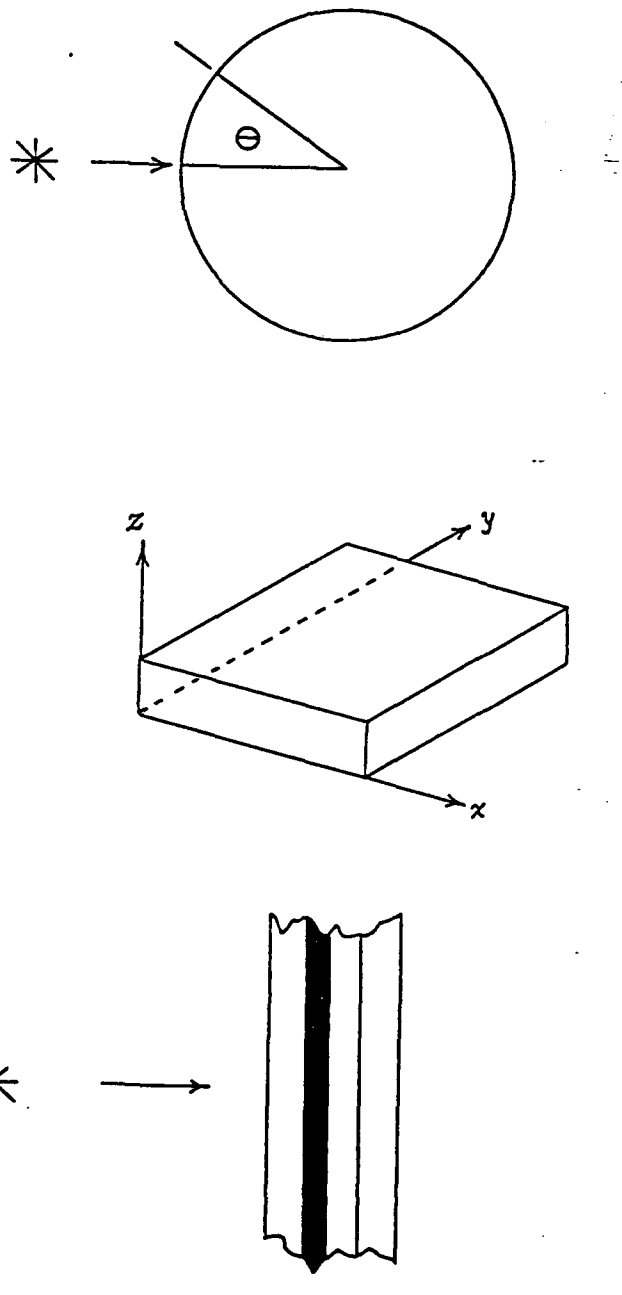

Figure 2.0-13. Thermal Models

Energy Balance:

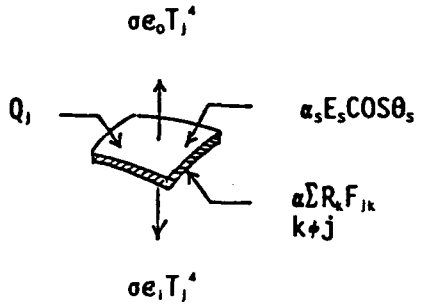

$$T_j^4 = \frac{(1-e_i)\alpha_s E_s \cos\theta_s + (1-e_i)Q_j + e_i R_j}{\sigma(e_o+e_i - e_o e_i)}$$

$$R_j = \frac{e_i \alpha_s E_s \cos\theta_s + e_i Q_j}{(e_o+e_i)} + \frac{e_o+e_i-e_o e_i}{(e_o+e_i)} \sum_{k \neq j} R_k F_{jk}$$

where

T_j ≡ Temperature
R_j ≡ Radiosity
α_s ≡ Solar Absorptivity
e_k ≡ Emissivities
E_s ≡ Solar Constant
θ_s ≡ Sun Angle
Q_j ≡ Earthshine
σ ≡ Stefan-Boltzmann Constant

Figure 2.0-14. Thermal Energy Balance on an Element

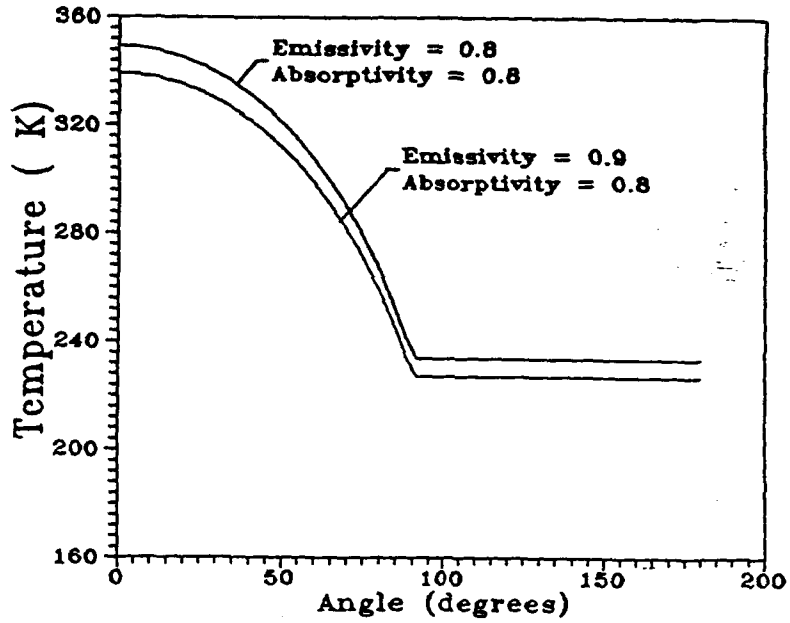

Figure 2.0-15. Thermal Profile Over Spherical Array

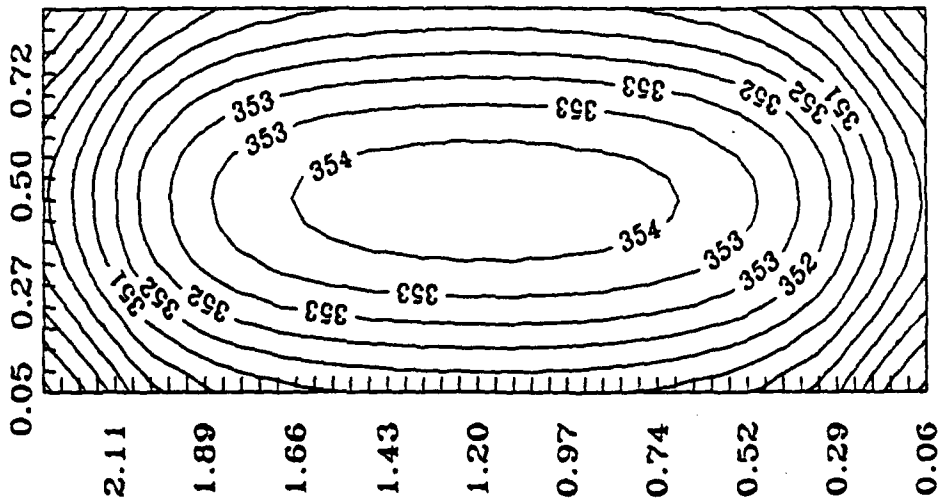

Figure 2.0-16. Thermal Contours Over Pillow-Type Solar Array

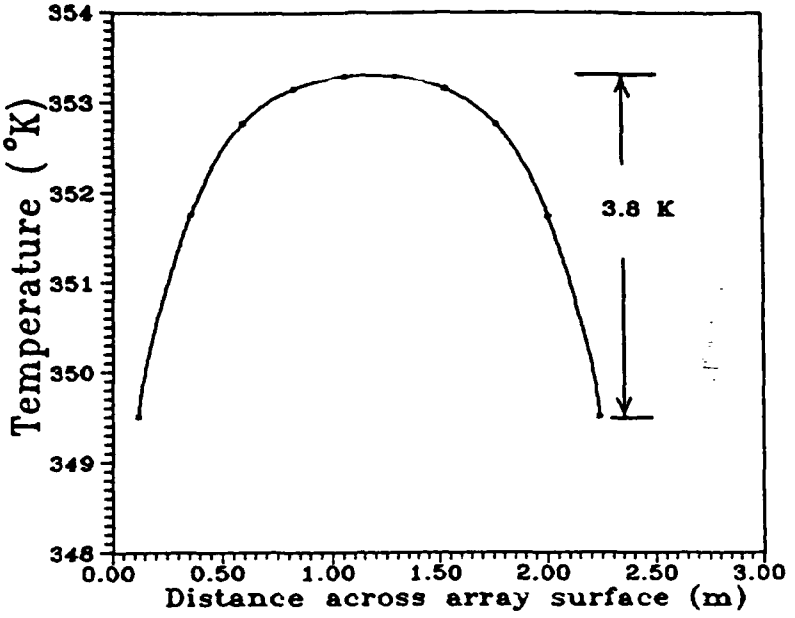

Figure 2.0-17. Thermal Profile Over Pillow-Type Array Facing Sun

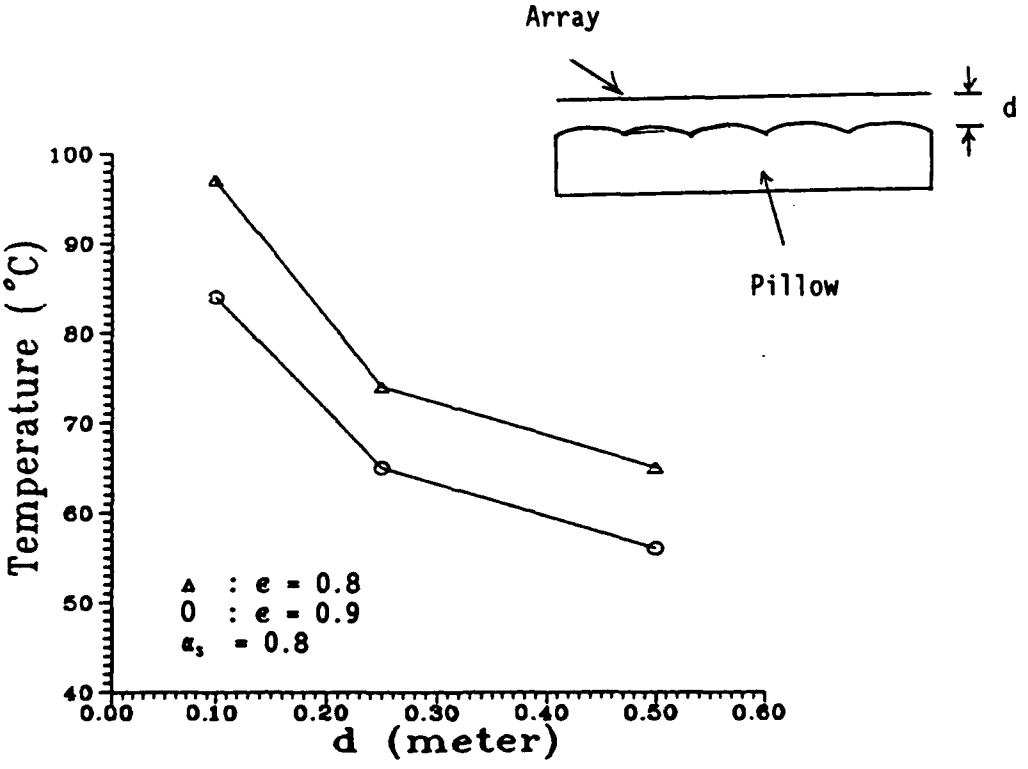

Figure 2.0-18. Array Temperature vs. Array-Pillow Distance

For the tubular-type ITSAT, a one dimensional model is used. This is shown in Figure 2.0-19. The temperature of the configuration is a function of the 1/4th power of the ratio (α_s/ϵ). If we take $\alpha_s \approx \epsilon$ then the temperature is about 57C.

In all calculations, the absorptivity is taken as $\alpha_s = 0.8$ and the emissivities (external and internal) are taken as $\epsilon_i = \epsilon_e = 0.9$.

2.6.1.2 TEMPERATURES UNDER ECLIPSE - Table 2.0-8 shows the temperatures under eclipse of the three different ITSAT configurations for three different orbits. These are worst case temperatures and the only power incident on the array is assumed to be that due to earthshine.

TABLE 2.0-8. TEMPERATURES UNDER ECLIPSE

	SPHERICAL		TUBULAR	PILLOW		
ORBIT	Tmax	Tmin		Tmax	Tmin	Tave
GEO	-178 C	-210 C	-181 C	-178 C	-214 C	-178 C
MOLNIYA	-115 C	-167 C	-119 C	-113 C	-175 C	-178 C
LEO	- 46 C	-121 C	-52 C	-43 C	-131 C	-43 C

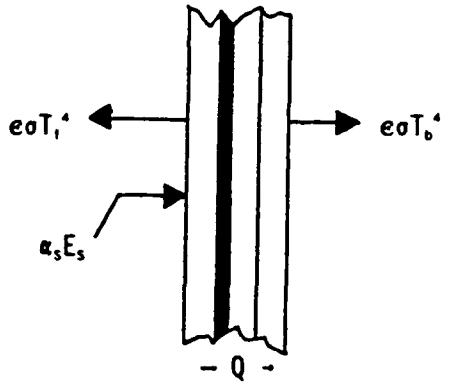

$$k_{eff} = \frac{L}{\sum_{i=1}^{4} li/ki}$$

$$\theta_{TH} = 2.4 \times 10^{-4} \text{ °K/Watt}$$

$$Tmax = 330.5 \left| \frac{\alpha_s}{\epsilon} \right|^{1/4}$$

Figure 2.0-19. One-Dimensional Model for Tubular-Type Solar Array

2.6.2 Temperature Effects

Tubular Configuration (Drawing 21002 Appendix 2) - The array is suspended by its four corners and has excellent heat rejection off the backside. It experiences a high temperature of 57°C, which results in a power degradation of only -4% total. The tubular structure is exposed to the sunlight and will undergo a bending due to the temperature gradient across the diameter of the tube. The aluminum-rigidized tube, used on the 200 watt designs, is covered on the sun side with white-dyed kapton to improve emissivity. Under worst case conditions, it experiences approximately 3.5° of bend along the array length, which results in only 0.1% power degradation. The Kevlar/UV-cured resin tube, used on the larger arrays, cannot be blocked by a white cover, but experiences only approximately 1.0° bend due to the thermal stiffness of Kevlar. The bending losses are, therefore, neglected.

Pillow Configuration (Drawing 21000 Appendix 2) - The 200 watt array is tied to the top of the aluminum-rigidized pillow, which reduces its backside heat rejection. The array experiences a high of 80°C, which results in a power degradation of only -9% total. The pillow structure must stay free of wrinkles in order to maintain its structural integrity. Therefore, the array is used to shade the pillow topside to minimize thermal gradients between the frontside and backside. Standoffs are used to prevent the array from touching the pillow, and extra material must be added to shade the pillow edges.

Spherical Configuration (Drawing 21001 Appendix 2) - Each 200 watt subarray is attached to the surface of the aluminum-rigidized sphere, which reduces its backside heat rejection. A subarray experiences a high of 76°C, which results in a power degradation of only -8%. The aluminum sphere underneath the subarrays is allowed to deform (bulge), but must be protected from local wrinkling. Therefore, each subarray's corners are held to the sphere by entensible ties, which allow relative expansion between the subarray and sphere surfaces, but keep the subarray touching the sphere to prevent thermal gradients between the exposed and covered portions of the sphere.

Make-Up Gas Systems - Thermal extremes affect the selection of make-up gas, which must not liquify or freeze in the cold of eclipse. This is discussed in Section 2.9.1.

2.7 BASIC AMORPHOUS SILICON ARRAY ELEMENTS

The most basic element of the array is the subcell. The manufacturing process turns out a continuous 3.625" wide strip of .75" long subcells. When cut to length, the result is a 1.2V cell, which is then connected to other cells in series and parallel to produce an array of the desired power, voltage, and dimensions.

The specified voltage is 32V. 27 cells of 1.2 volt each are connected in series to get that voltage. This arrangement is used in all of the arrays considered.

The power requirement is satisfied by varying the number of subcells in a cell (length of strip to cutoff) and the number of parallel circuits. Since both

of these parameters are discrete, array power as designed cannot in general match the specification exactly; i.e. 1028W designed vs. 1000W specified. When calculating array power, the distinction must be drawn between active area and actual area, which includes bussbars, hinges, and edge supports. The basic power equation used is:

(1353 w/m^2 incident sunlight) X (5% efficiency) X (active area) X (rad/therm degradation) (w = watt; rad = radiation; m = meter)
= power output, end of life

The 5% efficiency number is conservative, as efficiencies as high as 5.5% have been quoted for amorphous silicon. Active area is for two arrays in the case of planar arrays, and is effective cross-sectional area for the spherical configuration.

The basic rule in packaging the solar cells is not to have folds in the active area. Rolling to a 3 cm. minimum radius is acceptable. For these reasons flexible hinges are used throughout, which allow folding, then rolling. The hinges also allow panel-to-panel movement to accommodate differing radii within rolled up layers of sheets. All inflatable structures are encased to prevent handling damage prior to and during launch. To prevent premature inflation due to residual gases, vent systems are provided.

Each array of cells is on a stainless steel substrate etched to ~1.0 mil thickness. These cells will be connected, then laminated to a 1 mil kapton sheet. The array front side is coated with 1.7 mils of silicone rubber for the LEO and GEO orbits, giving a minimum array thickness of 3.7 mils. Minimum density is approximately 312.5 g/m^2. If more radiation protection is needed, silicone rubber is added to both sides. Some array cells have been produced on kapton substrates, but these are not baselined for this study due to uncertainties about efficiency and availability.

An example array design is shown in Figure 2.0-20.

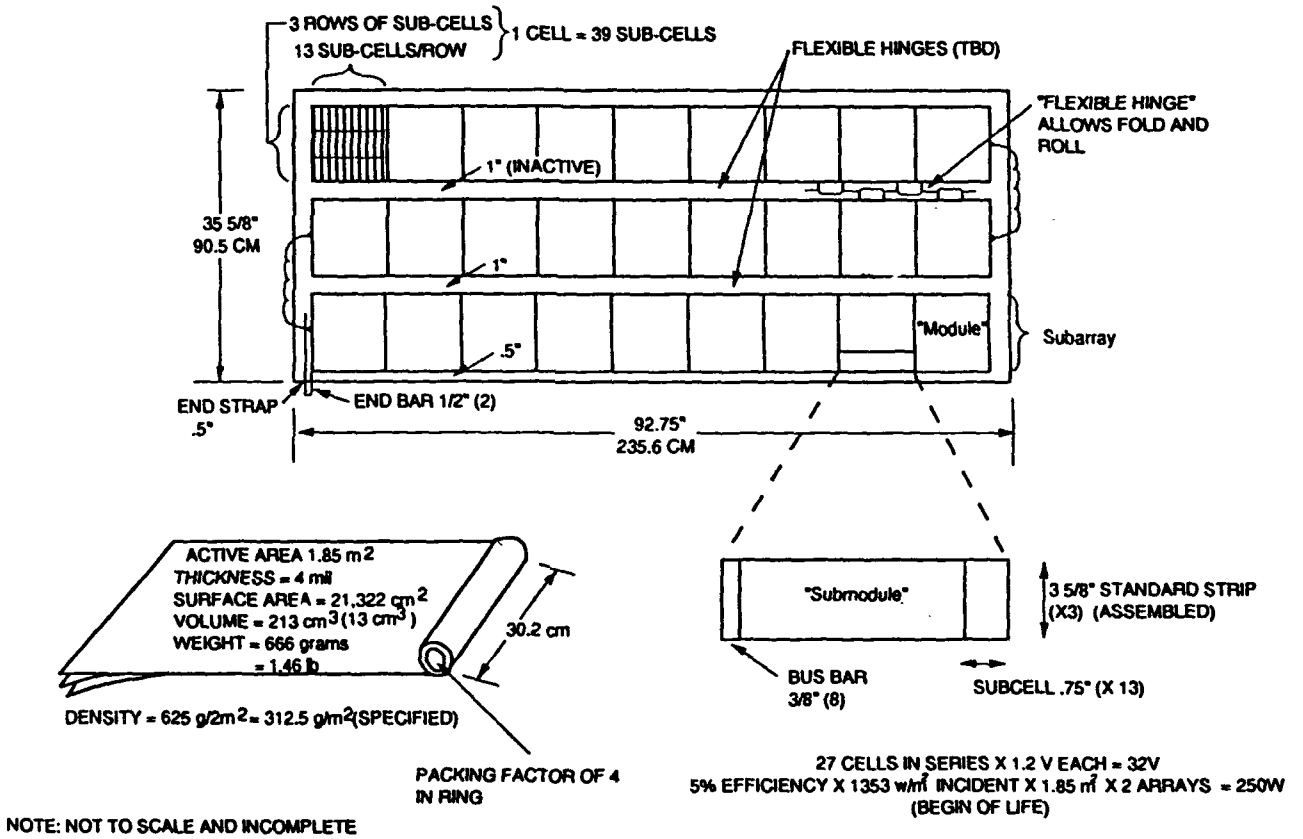

Figure 2.0-20. 200 Watt LEO/GEO Array Design

2.8 POWER/SIGNAL TRANSFER

Flexible flat ribbon cables are used to transfer array power and signals across the rotating drive arms. A one inch wide, four mil thick ribbon can carry 16 amps, which is adequate for the 200 watt systems. More cables are used for

larger arrays. The cables are wound around the drive arm as shown in Figure 2.0-21. There are two cables for each array, one positive and one negative, counterwound to balance torques. This allows maximum travel of 360°, so the arrays must be unwound and returned to their original position while in eclipse.

Slip rings which do not require unwinding were not selected because of their weight.

2-axis systems are discussed in Sections 2.10.14 and 2.10.15.

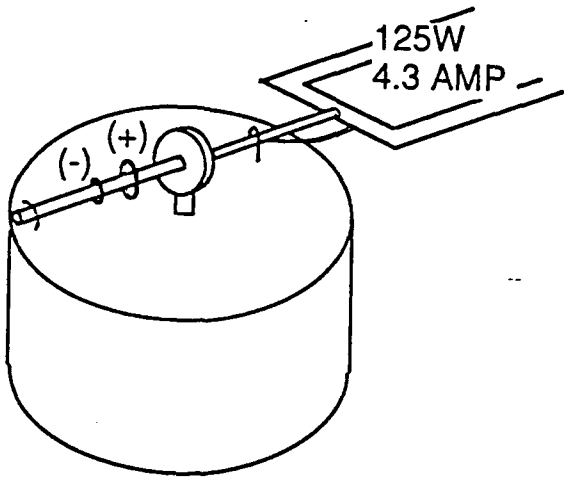

Figure 2.0-21 200 Watt Power/Signal Transfer

2.9 STRUCTURE MATERIALS

2.9.1 Non-Rigidized

Because of the atomic oxygen and debris environments, a baseline thickness of 2 mils was selected for the kapton structural elements. Kapton is also resistant to the radiation and thermal environments, but is unsuitable as an array covering because of its gold color which reduces transmitter power.

The selection of inflatant gases depends heavily on three criteria: 1) low molecular weight (M) to reduce mass leakage; 2) low stowage tank weight; and 3) at the inflation pressure, the gas must not condense at eclipse temperature. Outgassing is also of concern, especially for water vapor.

The gases considered were as follows: (R - gas constant)

GAS	M	R/M	Freezing Temp.@14.7psi, °C
Nitrogen	28	30.11	-210
Water	18	47.05	- 0
ammonia	17	50.44	- 77
CO_2	44	19.51	- 78

The low temperatures in eclipse depend on material and configuration, but are generally of this magnitude:

LEO:	-106°C
Molniya:	-156°C
GEO:	-203°C

Inflation pressures required are:

200 watt tubular:	.12 psi
200 watt sphere:	.012 psi
200 watt pillow:	.0012 psi

Water and ammonia, both of which are superior to nitrogen in terms of R/M, could be stored as liquids in a lightweight tank. Both gases, however, would liquify or freeze inside the inflatable during eclipse. CO_2 would also liquify or freeze inside the inflatable during eclipse and, in addition, is inferior to nitrogen on a molecular weight basis.

Nitrogen must be stored as a gas under high pressure, and so requires a relatively heavy storage tank. However, the eclipse requirement forces us to select it as the gas for pressurization.

2.9.2 Rigidized

The 200 watt concepts are aluminum-rigidized; the larger arrays use tubular structures of Kevlar with UV-cured resin. Another rigidization concept studied was Kevlar with a water gel matrix.

2.9.2.1 *Aluminum Laminate*

L'Garde has studied this concept and has test results, documented in Reference 2.0-9. This material is a lamination of 1/4 mil mylar, 3 to 4 mils aluminum, 1/4 mil mylar. The aluminum thickness is limited by packaging ability. The concept is to deploy the aluminum structure, e.g., a 4" diameter tube, with an initial inflation pressure of 7 to 14 psi. This will remove the folding wrinkles, leaving a thin-walled rigid aluminum tube. The gas is permitted to escape. Accordion-folding is best to reduce folding wrinkles and avoid pressure buildup during inflation. Tubes of this thickness to diameter ratio tend to buckle instead of fracturing.

The results of Reference 2.0-9 were used to calculate the stiffness, $E = 3.7 \times 10^6$ The density was taken at .098 lb/in^3.

This technique is simple, has no special storage requirements, and has no outgassing due to curing. However, our analysis has shown that the limitation on material thickness limits application to the small, 200 watt arrays.

2.9.2.2 UV-Cured Resin / Kevlar - This material, documented in References 2.0-10 and 2.0-11, consists of Kevlar, pre-impregnated with a resin which cures upon exposure to ultraviolet light. The pre-impregnated Kevlar must be encapsulated to avoid sticking to itself while stowed, to allow initial inflation, and to regulate curing and outgassing. Each torus side must be pointed to the sun to cure.

In contrast with the aluminum-rigidized material, this material can be very thick and yet fold easily for stowage. In fact, it is easier to manufacture in higher thicknesses. This makes it suitable for the larger arrays, as will be shown later. Further development would have to be done on this material to investigate handling, outgassing, curing, and composite structural characteristics.

2.9.2.3 Water Gel Matrix/Kevlar - L'Garde has studied this concept and has test results documented in Reference 2.0-11. The material consists of Kevlar, pre-impregnated with a water-based gel. Once in space and inflated, the water simply evaporates from the gel, leaving a rigid matrix.

Difficulties associated with the use of this material include 1) possibility of premature rigidization during launch, 2) how to allow the water to leave the matrix in a slow and controlled manner, and 3) outgassing. For these reasons, it was decided not to use this material in the conceptual designs.

2.10 POINT DESIGNS

There are 12 point designs, of which 4 are "extrapolated" (not shown), plus 4 additional designs due to the contractual modification to study 2-axis systems on STEP and Techstars. In addition, a 1000 watt LEO/GEO design was "extrapolated" to compare the efficiency of large arrays to small ones on an equal radiation basis. Further, both make-up gas and rigidizable systems were investigated for the 200 watt GEO and LEO pillow, sphere, and tube. Listed in order, the designs are:

Point Design 1		200 watts	Spherical	740km polar(LEO)	3 year life
Point Design 2		200 watts	Pillow	740km polar(LEO)	3 year life
Point Design 3		200 watts	Tubular	740km polar(LEO)	3 year life
Point Design 4	(extrap)	200 watts	Spherical	6 hour Molniya	3 year life
Design 4 Mod	STEP	200 watts	Tubular	6 hour Molniya	3 year life
Point Design 5	(extrap)	200 watts	Pillow	6 hour Molniya	3 year life
Design 5 Mod	Techstars	200 watts	Tubular	6 hour Molniya	3 year life
Point Design 6		200 watts	Tubular	6 hour Molniya	3 year life
Point Design 7	(extrap)	200 watts	Spherical	GEO	3 year life
Design 7 Mod	STEP	200 watts	Tubular	GEO	3 year life
Point Design 8	(extrap)	200 watts	Pillow	GEO	3 year life
Design 8 Mod	Techstars	200 watts	Tubular	GEO	3 year life
Point Design 9		200 watts	Tubular	GEO	3 year life
Point Design 10		1000 watts	Tubular	10000km, 60°	1 year life
Point Design 11		5000 watts	Tubular	3000km, 0°	1 year life
Point Design 12		5000 watts	Tubular	LEO-GEO transfer	1 year life
L'Garde extra	(extrap)	1000 watts	Tubular	LEO/GEO	3 year life

In this report, the first 9 point designs are discussed in a different order. All 3 tubular designs are first, then all 3 pillows, then all 3 spheres. The contract modifications are discussed last of all.

2.10.1 POINT DESIGN 3 - 200 WATT, 3 YEAR, LEO, TUBULAR

2.10.1.1 Array Sizing for LEO Radiation - The results of the radiation studies indicate that for the LEO orbit, an array with 1.7 mils of silicone rubber on top will degrade 20% over 3 years. This includes thermal efficiency losses. The backside stainless steel substrate is sufficient, and does not need additional shielding. The active area necessary is:

200w/(.8 rad/therm degrade X .05 efficiency X 1353w/m^2 incident) = 3.7m^2 active area

3.7m^2 tot / 2 = 1.85m^2 active area necessary per array

With bussbars and hinges, this corresponds to two 35.625" X 92.75" arrays, each weighing 666g (without structure), laid out as shown in Figure 2.0-20. There are 3 parallel circuits per array, and 13 subcells per cell.

2.10.1.2 Aluminum-Rigidized - Drawing 21002 (Appendix 2) is a drawing of this concept. The silicone rubber on the front and stainless steel on the back provide atomic oxygen protection for the array itself. The aluminum torus structure is also resistant to atomic oxygen.

2.10.1.2.1 Tube Sizing for On-Orbit Loads - The 'torusbend' program (Appendix 1) results are as follows:

Aluminum-Rigidized, 200 Watt, LEO/GEO

diameter	total thickness	weight(1 side tot)	load stress	critical stress	delta
3.00 inches	.0030 inch	2.17 lbs	169.1 psi	277.5 psi	108.4 psi
3.50	.0030	2.29	133.6	275.0	141.5
4.00	.0030	2.42	109.6	224.5	114.9
4.00	.0035	2.63	101.5	286.5	185.0
4.50	.0035	2.85	86.2	236.8	150.6
5.00	.0035	3.01	74.7	200.9	126.1
5.50	.0035	3.20	65.9	169.1	103.2

The 4" diameter, 3.5 mil thick tube is not the lightest but was selected because we've had experience with this design and it provides a significant margin of safety (185.0 psi) between the load stress and the critical stress.

2.10.1.2.2 Packaging and Deployment Techniques - From the deployed position, the array is accordion-folded using its two long flexible hinges and the short tube members are accordion folded in thirds. The long tube members, one on each side of the folded array, are then accordion-folded while the array is rolled in toward the spacecraft. This is possible because the array ties are allowed to twist or swivel. The outboard ties are extra long to allow the array roll to clear the outboard tube member.

The packaged array and torus are 25 inches long and 4 inches diameter (one side). The system packaged height is 5.5 inches.

The total system weight is 11.17 lbs, giving an efficiency of 39 watts/kg. Only 47% of the total array weight is array plus torus, indicating that larger

arrays in the same orbit should have greater efficiency due to fixed motor, etc. weights.

2.10.1.2.3 Launch Loads - The maximum Delta II axial acceleration of 12 g's places 51 ft-lbs of moment on each drive arm. This corresponds to a load stress of 406 psi. The extendible 1/32" thick, 2" diameter aluminum drive arm would fail due to material properties before it would fail in buckling. The compressive failure stress of aluminum is approximately 35,000 psi, so the loads can be handled without the need for external supports.

2.10.1.3 Make-Up Gas

Using a 6 inch diameter 2 mil kapton tube, the maximum compressive load stress due to 1 ft/sec^2 axial acceleration with a dynamic/safety factor of 2 is 88.5 psi. This requires .12 psi. of inflatant pressure to resist wrinkling. The array and torus weigh only 2.25 lb (one side). However, the inflatant necessary over three years in GEO is 1515 lbs each side using the choked flow model. The loss at LEO would be 3.5 times worse. No drawing was made of this design.

This demonstrates conclusively that we must rigidize if we wish to achieve 3 years in a 200 watt torus configuration.

2.10.2 Point Design 9 - 200 Watt, 3 Year, GEO, Tubular

2.10.2.1 Equivalence With LEO Design - Drawing 21007 (Appendix 2) is a drawing of this concept. The radiation environment at GEO is equivalent to that at LEO. The atomic oxygen environment is much worse at LEO and the aluminum-rigidized material does not need any special protection. Also, the radiation shielding doubles as atomic oxygen protection. Therefore, the aluminum-rigidized LEO system will work at GEO without any modification.

2.10.3 Point Design 6 - 200 Watt, 3 Year, Molniya, Tubular

2.10.3.1 Array Sizing for Molniya Radiation - The results of the radiation studies indicate that for the Molniya orbit, an array with 30 mils of silicone rubber on top and 17.5 mils of silicone rubber added to the backside will degrade to 41% over 3 years. This includes thermal efficiency losses. The active area necessary is:

200w/(.41 rad/therm degrade X .05 efficiency X 1353w/m^2 incident) = 7.2m^2 active area

7.2m^2 tot / 2 = 3.6m^2 active area necessary per array

Using 13 subcells per cell and 6 parallel circuits per array, the power at end of life is 200.7 watts. With bussbars and hinges, this corresponds to two 71.25" X 92.75" arrays, each weighing 14.28 lbs (without structure).

2.10.3.2 Aluminum-Rigidized - Drawing 21007 (Appendix 2) is a drawing of this concept. The silicone rubber on the front and back of the array protect it from atomic oxygen. The aluminum torus structure is also resistant to atomic oxygen.

2.10.3.2.1 Tube Sizing for On-Orbit Loads - The 'torusbend' program (Appendix 1) results are as follows:

Aluminum-Rigidized, 200 Watt, Molniya

diameter	total thickness	weight(1 side tot)	load stress	critical stress	delta
3.00 inches	.0055 inch	15.93 lbs	631.9 psi	813.3 psi	181.5 psi
3.50	.0050	16.03	518.5	658.6	140.1
4.00	.0050	16.30	407.3	510.6	103.3
4.50	.0050	16.56	330.2	432.9	102.7
5.00	.0045	16.56	299.9	301.8	1.9
5.50	.0050	17.10	232.5	307.1	74.6
6.00	.0045	17.05	218.5	224.5	6.0

The 5" diameter, 4.5 mil thick tube was selected to minimize thickness for foldability.

2.10.3.2.2 Packaging and Deployment Techniques - From the deployed position, the array is accordion-folded using its four long flexible hinges. The long tube members, both on one side of the folded array, are then accordion-folded while the array is rolled in toward the spacecraft.

The packaged array and torus are 25 inches long and 9 inches diameter (one side). The system packaged height is 9.5 inches.

The total system weight is 51.8 lbs, giving an efficiency of 8.5 watts/kg.

2.10.3.2.3 Launch Loads - The maximum Delta II axial acceleration of 12 g's places 300 ft-lbs of moment on each drive arm. This corresponds to a load stress of 2400 psi. The extendible 1/32" thick, 2" diameter aluminum drive arm would fail due to material properties before it would fail in buckling. The compressive failure stress of aluminum is approximately 35,000 psi, so the loads can be handled without the need for external supports.

2.10.4 Point Design 1 - 200 Watt, 3 Year, LEO, Pillow

It is necessary to somehow connect the top and bottom planes of the inflatable in order to prevent it from taking a spherical shape. A mattress design was selected because of the low weight of the inner-pillow ties (Figure 2.0-22). The array itself is the same as the 200 watt LEO/GEO array.

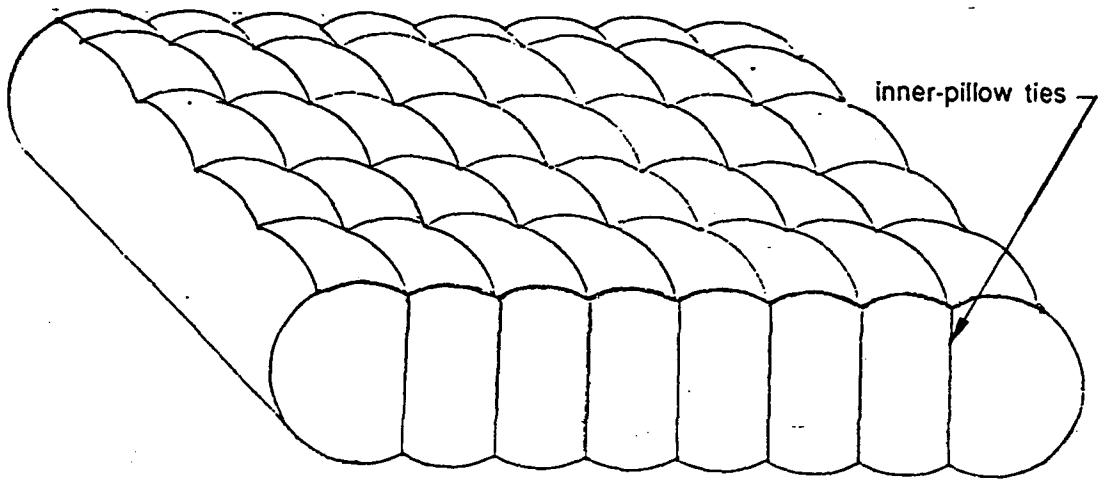

Figure 2.0-22 Mattress Shaped Pillow Structure Concept

2.10.4.1 Array Tied to Top vs. Array Integral - Two basic approaches were examined. In the first, the array is tied to the top of a pillow structure. In the second, the array itself forms the top side of the inflatable pillow in order to reduce total material area. The first approach was selected for these reasons:

1. The integral pillow would take on the shape of a mattress top, wrinkling it. This may damage the array.

2. The shape of the integral array would cause ~13% power loss due to non-perpendicular sun incidence. To compensate for this, the array would have to be made ~13% larger, offsetting the advantage of saving material area and weight by making the array the top pillow surface. It was found that equal weight could be achieved using the first concept.

3. The first concept is cheaper due to less array area.

2.10.4.2 Aluminum-Rigidized - Drawing 21004 (Appendix 2) is a drawing of this concept. The silicone rubber and stainless steel on the array provide atomic oxygen and radiation protection. The aluminum pillow structure is also resistant to atomic oxygen.

The pillow structure is preformed to shape, and must stay free of wrinkles in order to maintain its structural integrity. Therefore, the array is used to shade the pillow topside to minimize thermal gradients between the frontside and

backside. Standoffs are used to prevent the array from touching the pillow, and extra material is added to shade the pillow edges.

2.10.4.2.1 Pillow Sizing for On-Orbit Loads - The structural behavior of a pre-formed "waffle-iron" shaped thin pillow with internal ties is difficult to model and analyze. For the purposes of this conceptual study, the 'torusbend' program was modified to roughly determine load stresses and critical stresses in a pillow, and the results are:

200W Aluminum-Rigidized Pillow, LEO/GEO

pillow depth	total thickness	weight(1 side tot)	load stress	critical stress	delta
4.00 inches	.0035 inch	5.58 lbs	53.9 psi	286.5 psi	232.6 psi
5.00	.0035	5.70	44.0	200.9	156.9
6.00	.0035	5.83	37.3	148.0	110.7
7.00	.0035	5.96	32.6	111.4	78.8
8.00	.0035	6.09	29.0	92.5	63.5

The load stresses are lower than that of the tubular designs because they are spread out over a larger cross-sectional area. The results indicate that the pillow should easily be capable of handling the stationkeeping loads. The minimum realistic depth was considered to be 6 inches, and the 3.5 mil thickness was chosen because of experience with this material.

2.10.4.2.2 Packaging and Deployment Techniques - From the deployed position, the array is accordion-folded using its two long flexible hinges, then rolled in toward the spacecraft. The pillow structure is folded and rolled in with it.

The packaged array and pillow are 25 inches long and 6 inches diameter (one side). The system packaged height is 7 inches.

The total system weight is 38.4 lbs, giving an efficiency of 11.5 watts/kg.

2.10.4.2.3 Launch Loads - The maximum Delta II axial acceleration of 12 g's places 175 ft-lbs of moment on each drive arm. This corresponds to a load stress of 1400 psi. The extendible 1/32" thick, 2" diameter aluminum drive arm would fail due to material properties before it would fail in buckling. The compressive failure stress of aluminum is approximately 35,000 psi, so the loads can be handled without the need for external supports.

2.10.5 Point Design 8 - 200 Watt, 3 Year, GEO, Pillow (Extrapolated)

2.10.5.1 Equivalence With LEO Design - The radiation environment at GEO is equivalent to that at LEO. The atomic oxygen environment is much worse at LEO, but the aluminum-rigidized material does not need any special protection, and the radiation shielding doubles as atomic oxygen protection. Therefore, the aluminum-rigidized LEO system will work at GEO without any modification.

2.10.5.2 Make-Up Gas - Micrometeor and debris damage is ~3.5 times less severe at GEO than at LEO. The GEO orbit was therefore selected to attempt a feasible make-up gas pillow design. Drawing 21000 (Appendix 2) is a drawing of this

concept. The pillow is made of flat 2 mil kapton sheets, and the make-up gas tanks are located in the drive arms. Nitrogen is the inflatant.

The deeper the pillow, the lower the pressure necessary to resist compressive wrinkling due to stationkeeping accelerations. However, there is a limit to pillow thickness and pressure due to the array pull-out requirement. Pillow depth was traded vs. weight and the results are:

Each Array Paddle:

Pillow Depth, inches	Pressure, psi	Make-Up Gas Weight, lbs
6	.0153	122.0
9	.0071	62.5
17	.0028	31.3
30	.0012	20.4

Depths beyond 30 inches do not decrease the weight because of the array pull-out requirement , so 30 inches was selected. The steel tanks required to store the nitrogen gas weigh 33 lbs each. The total system weight is 119.6 lbs, giving an efficiency of 3.7 watt/kg. The packaged payload length penalty is 13.5 inches.

The tanks and make-up gas comprise 89% of the total weight, which explains the low efficiency. The gas loss at LEO would be ~3.5 times worse. Rigidization is obviously superior. Nonetheless, amongst make-up gas systems, the pillow configuration was found to weigh the least.

2.10.6 Point Design 5 - 200 Watt, 3 Year, Molniya, Pillow (Extrapolated)

This design is similar to the LEO pillow except that the array is the same as the 200 watt tubular Molniya array, and the pillow is therefore larger. This is due to the radiation environment in the Molniya orbit. No drawing was made of this concept.

2.10.6.1 Aluminum-Rigidized

The silicone rubber and stainless steel on the array provide atomic oxygen and radiation protection. The aluminum pillow structure is also resistant to atomic oxygen.

The pillow structure is preformed to shape, and must stay free of wrinkles in order to maintain its structural integrity. Therefore, the array is used to shade the pillow topside to minimize thermal gradients between the frontside and backside. Standoffs are used to prevent the array from touching the pillow, and extra material is added to shade the pillow edges.

2.10.6.1.1 Pillow Sizing for On-Orbit Loads - The 'torusbend' program was modified to roughly determine load stresses and critical stresses in a pillow, and the results are:

200W Aluminum-Rigidized Pillow, Molniya

pillow depth	total thickness	weight(1 side tot)	load stress	critical stress	delta
4.00 inches	.0035 inch	22.12 lbs	108.9 psi	286.5 psi	117.6 psi
5.00	.0035	22.28	87.8	200.9	113.0
6.00	.0035	22.45	73.8	148.0	74.2
7.00	.0035	22.61	63.7	111.4	47.6
8.00	.0035	22.78	56.2	92.5	36.3

The results indicate that the pillow should be capable of handling the stationkeeping loads. The minimum realistic depth was considered to be 6 inches, and the 3.5 mil thickness was chosen because of experience with this material.

2.10.6.1.2 Packaging and Deployment Techniques - From the deployed position, the array is accordion-folded using its four long flexible hinges, then rolled in toward the spacecraft. The pillow structure is folded and rolled in with it.

The packaged array and pillow are 25 inches long and 11 inches diameter (one side). The system packaged height penalty is 11.5 inches.

The total system weight is ~82 lbs, giving an efficiency of 5.4 watts/kg.

2.10.6.1.3 Launch Loads - The maximum Delta II axial acceleration of 12 g's places 375 ft-lbs of moment on each drive arm. This corresponds to a load stress of 3000 psi. The extendible 1/32" thick, 2" diameter aluminum drive arm would fail due to material properties before it would fail in buckling. The compressive failure stress of aluminum is approximately 35,000 psi, so the loads can be handled without the need for external supports.

2.10.7 Point Design 2 - 200 Watt, 3 Year, LEO, Spherical

2.10.7.1 Array Sizing for Unequal Solar Incidence, LEO Radiation - The spherical concept does not require active pointing. The sun always falls on it no matter what the spacecraft orientation. However, the solar incidence angle varies across the surface of the sphere, and there are cosine losses as a result. Basically, the sphere must be sized as if the disc area receives normal incidence. This means that necessary solar array area calculated as before must be multiplied by four to get the sphere or exposed array surface area.

The results of the radiation studies indicate that for the LEO orbit, an array with 1.7 mils of silicone rubber on top will degrade 20% over 3 years. This includes thermal efficiency losses. The backside stainless steel substrate is sufficient, and does not need additional shielding. The array area must therefore also be multiplied by a factor of 1.2.

Incidence varies across the surface, so it is desirable to group a single series circuit of solar cells as closely to each other as possible. Blocking diodes are used to bypass dark cells, but this only works if a small amount of the circuit is shaded. Therefore, 31 patches of nearly square "subarrays" are placed on the sphere surface. Each subarray consists of a complete series circuit of 27 1.2V cells, 10 subcells per cell. Drawings 21001 and 21003 (Appendix 2) depict the spherical configuration.

Subarrays must be arranged on the sphere surface in such a way as to allow an equal number of subarrays to be illuminated at any expected sun angle. The geometry is further complicated by spacecraft shadowing of the sphere. A geodesic arrangement was selected which allows for 15 to 16 (average 15.5) subcells to be illuminated on any given orbit.

2.10.7.2 Aluminum-Rigidized - Drawing 21003 (Appendix 2) is a drawing of this concept. The silicone rubber and stainless steel on the array provide atomic oxygen and radiation protection. The aluminum sphere structure is also resistant to atomic oxygen.

The aluminum sphere underneath the subarrays is made of gore panels. It is allowed to deform (bulge), but must be protected from local wrinkling. Therefore, each subarray's corners are held to the sphere by entensible ties, which allow relative expansion between the subarray and sphere surfaces, but keep the subarray touching the sphere to prevent thermal gradients between the exposed and covered portions of the sphere.

The sphere is 140 inches in diameter and 3.5 mils thick. It uses the entire 46 inch diameter payload aft bulkhead as a stowage canister and structural interface. This is best from both a packaging and structural standpoint.

2.10.7.2.1 Design for On-Orbit Loads - It is difficult to model and analyze the structural behavior of a truncated, cantilevered, gore-paneled sphere with panels tied to the surface subjected to bending moment. For the purposes of this conceptual study, the tangential stress at the compressive interface with the vehicle was trigono- metrically resolved. Considering a great circle of the sphere touching the compressive interface with the vehicle as a short cylinder (a seam), the data was extrapolated to determine what seam width (beam length) would be necessary to resist buckling. This is a conservative approach, as a cantilevered hemisphere could take much more load than a short cantilevered cylinder. The stationkeeping acceleration creates a 21 psi compressive stress in the 3.5 mil thick flat seam. The seam must be 2.2 inches wide to resist buckling, which is considered reasonable.

2.10.7.2.2 Packaging and Deployment Techniques - From the deployed position, the sphere is folded and packed into the cylindrical aft canister. Each subarray is capable of being folded, but as much effort as possible is made to lay each flat and spread out in the canister.

The system packaged height penalty is 3.5 inches.

The total system weight is 61.7 lbs, giving an efficiency of 7.1 watts/kg.

2.10.7.2.3 Launch Loads - Because the array is packaged in a disc in the aft end, launch loads are not expected to be a problem. There are no drive arms or motor mounts to consider.

2.10.8 Point Design 7 - 200 Watt, 3 Year, GEO, Spherical (Extrapolated)

2.10.8.1 Equivalence With LEO Design - The radiation environment at GEO is equivalent to that at LEO. The atomic oxygen environment is much worse at LEO,

but the aluminum-rigidized material does not need any special protection, and the radiation shielding doubles as atomic oxygen protection. Therefore, the aluminum-rigidized LEO system will work at GEO without any modification.

2.10.8.2 Make-Up Gas - Micrometeor and debris damage is ~3.5 times less severe at GEO than at LEO. The GEO orbit was therefore selected to attempt a feasible make-up gas spherical design. Drawing 21001 (Appendix 2) is a drawing of this concept.

The 140 inch diameter geodesic sphere consists of irregular pentagonal panels made of 2 mil kapton with one square subarray in the middle. It uses the entire 46 inch diameter payload aft bulkhead as a stowage canister and structural interface. Nitrogen is the inflatant.

A square unrestrained "fat pillow" was considered because it would be simpler to manufacture, but was rejected due to the weight of the 'dogear' corners.

The pressure necessary to resist the stationkeeping acceleration is .021 psi., which is also sufficient for the array pull-out requirement. This will require 284 lbs. of make-up gas. The steel tank required to store the nitrogen gas weighs 460 lbs. The spherical array itself weighs only 15.2 lbs.

The total system weight is 777 lbs, giving an efficiency of 0.6 watt/kg. The packaged payload length penalty is 12 inches.

The tanks and make-up gas comprise 96% of the total weight, which explains the low efficiency. The gas loss at LEO would be ~3.5 times worse. Rigidization is obviously superior.

2.10.9 Point Design 4 - 200 Watt, 3 Year, Molniya, Spherical (Extrapolated)

This design is similar to the LEO sphere except that the subarrays are shielded and sized for Molniya radiation, and the sphere is therefore twice as large. No drawing was made of this concept.

2.10.9.1 Array Sizing for Unequal Solar Incidence, Molniya Radiation - The results of the radiation studies indicate that for the Molniya orbit, an array with 30 mils of silicone rubber on top and 17.5 mils of silicone rubber added to the backside will degrade to 41% over 3 years. This includes thermal efficiency losses.

The sphere is 280 inches in diameter and has 61 subarrays placed on the surface. Each subarray consists of a complete series circuit of 27 1.2V cells, 10 subcells per cell. A geodesic arrangement was selected, which allows for 30 to 31 (average 30.5) subcells to be illuminated on any given orbit. Each subarray's corners are held to the sphere by entensible ties.

2.10.9.2 Aluminum-Rigidized - The silicone rubber and stainless steel on the array provide atomic oxygen and radiation protection. The aluminum sphere structure is also resistant to atomic oxygen. The entire 46 inch diameter payload aft bulkhead is used as a stowage canister and structural interface.

2.10.9.2.1 Design for On-Orbit Loads - Using an analysis similar to that described in section 2.10.7.2.1, the 3.5 mil thickness was deemed adequate to handle the stationkeeping loads.

2.10.9.2.2 Packaging and Deployment Techniques - From the deployed position, the sphere is folded and packed into the cylindrical aft canister. Each subarray is capable of being folded, but as much effort as possible is made to lay each flat and spread out in the canister.

The system packaged height penalty is 10 inches.

The total system weight is ~204 lbs, giving an efficiency of 2.2 watts/kg.

2.10.9.2.3 Launch Loads - Because the array is packaged in a disc in the aft end, launch loads are not expected to be a problem. There are no drive arms or motor mounts to consider.

2.10.10 Point Design 10 - 1000 Watt, 1 Year, 10000 km, 60° - The rigidized tubular concept was selected for the larger arrays because of its superior efficiency and simple structure.

2.10.10.1 Array Sizing for 10000 km Radiation - The results of the radiation studies indicate that for the 10000 km. orbit, an array with 30 mils of silicone rubber on top will degrade to 45.5% over 1 year. This includes thermal efficiency losses. The stainless steel substrate requires an additional 17.5 mils of silicone rubber on the backside. The active area necessary is:

1000w/(.455 rad/therm degrade X .05 efficiency X 1353w/m^2 incident) = 32.5m^2 (active)
32.5m^2 tot / 2 = 16.3m^2 active area necessary per array

Using 8 subarrays per paddle, 3 parallel circuits per subarray, and 15 subcells per cell, the actual power is 1028 watts (EOL). With bussbars and hinges, this corresponds to two 212.5" X 142.5" arrays, each weighing 65.44 lbs. (without structure).

2.10.10.2 Kevlar/UV-Resin Rigidized - Drawing 21005 (Appendix 2) is a drawing of this concept.

2.10.10.2.1 Tube Sizing for On-Orbit Loads - An attempt was made to use aluminum-rigidized material, but the thickness required was too great. Using steel and multiple bundled tubes did not work either. Therefore, Kevlar with UV-cured resin is baselined, and the 'torusbend' program results are as follows:

Kevlar/UV Resin Rigidized, 1000W,10000 km

diameter	total thickness	weight(1 side tot)	load stress	critical stress	delta
4.25 inches	.0190 inch	74.84 lbs	965.7 psi	983.8 psi	18.0 psi
4.50	.0185	75.15	889.3	912.6	23.3
4.75	.0180	75.42	824.4	837.4	13.0
5.00	.0180	75.96	750.6	786.9	36.2
5.25	.0175	76.20	703.5	706.0	2.5
5.50	.0175	76.73	646.6	654.0	7.4
5.75	.0175	77.25	596.7	602.0	5.3
6.00	.0180	78.14	540.0	584.7	44.6
8.00	.0170	81.61	341.0	352.6	11.6

The 5" diameter, 18 mil thick tube was selected.

2.10.10.2.2 Packaging and Deployment Techniques - From the deployed position, the array is accordion-folded using its flexible hinges, and the tube members are folded in. The pre-impregnated Kevlar is encapsulated to avoid sticking to itself while stowed, to allow initial inflation, and to regulate curing and outgassing. Each torus side must be pointed to the sun to cure.

The packaged array and torus are 48 inches long and 16 inches diameter (one side). The stowage canisters are oriented vertically in the Delta II launch vehicle, and are extended using the mechanism shown in the drawing (21005). The system packaged height penalty is 48 inches.

The total system weight is 238.5 lbs, giving an efficiency of 9.2 watts/kg. The reason for this low efficiency is the orbit specified, which requires array oversizing and heavy shielding from radiation.

2.10.10.2.3 Launch Loads - The stowage canisters are oriented vertically, so the maximum Delta II axial acceleration of 12 g's puts the support members in compression with 2862 pounds of force. The compressive failure stress of aluminum is approximately 35,000 psi, so the loads can be handled if only .1 in^2 of cross-sectional material area is available, which it is.

2.10.11 Point Design 11 - 2500 Watt, 1 Year, 3000 km, Equatorial

2.10.11.1 Array Sizing for 3000 km Radiation - The results of the radiation studies indicate that for the 3000 km. orbit, an array with 150 mils of silicone rubber on top will degrade to 45% over 1 year. This includes thermal efficiency losses. The stainless steel substrate requires an additional 137.5 mils of silicone rubber on the backside. The active area necessary is:

2500w/(.45 rad/therm degrade X .05 efficiency X 1353w/m^2 incident) = 82.2m^2 (active) 82.2m^2 tot / 2 = 41.1m^2 active area necessary per array

Using 21 subarrays per paddle, 3 parallel circuits per subarray, and 14 subcells per cell, the actual power is 2491 watts (EOL). With bussbars and hinges, this corresponds to two 298.5" X 249.4" arrays, each weighing 806.4 lbs. (without structure).

2.10.11.2 Kevlar/UV-Resin Rigidized - Drawing 21006 (Appendix 2) is a drawing of this concept.

2.10.11.2.1 Tube Sizing for On-Orbit Loads - The 'torusbend' program results are as follows:

Kevlar/UV Resin Rigidized, 2500W, 3000 km

diameter	total thickness	weight(1 side tot)	load stress	critical stress	delta
9.00 inches	.0580 inch	901.05 lbs	1223.6 psi	1233.2 psi	9.6 psi
9.50	.0550	901.31	1159.8	1169.3	9.5
10.00	.0460	890.10	1235.4	1242.3	6.9
10.50	.0450	892.53	1151.1	1171.0	19.9
11.00	.0440	894.78	1077.8	1096.5	18.7
14.00	.0420	914.90	723.9	724.0	.1

The 10" diameter, 46 mil thick tube was selected.

2.10.11.2.2 Packaging and Deployment Techniques - From the deployed position, the array is accordion-folded using its flexible hinges, and the tube members are folded in. The pre-impregnated Kevlar is encapsulated to avoid sticking to itself while stowed, to allow initial inflation, and to regulate curing and outgassing. Each torus side must be pointed to the sun to cure.

The packaged array and torus are 83 inches long and 38 inches diameter (one side). The stowage canisters are oriented vertically in the 86 inch diameter section of the Delta II launch vehicle, and are extended using the mechanism shown in drawing 21006. The system packaged height penalty is 98 inches.

The total system weight is 2129 lbs, giving an efficiency of 2.6 watts/kg. The reason for this low efficiency is the orbit specified, which requires array oversizing and heavy shielding from radiation.

2.10.11.2.3 Launch Loads - The stowage canisters are oriented vertically, so the maximum Delta II axial acceleration of 12 g's puts the support members in compression with 25,548 pounds of force. The compressive failure stress of aluminum is approximately 35,000 psi, so the loads can be handled if only .75 in^2 °f cross-sectional material area is available, which it is.

2.10.12 Point Design 12 - 5000 Watt, 1 Year, LEO to GEO Transfer

2.10.12.1 Array Sizing for LEO/GEO Transfer Radiation - The results of the radiation studies indicate that for this mission, an array with 50 mils of silicone rubber on top will degrade to 34% over 1 year. This includes thermal efficiency losses. The stainless steel substrate requires an additional 37.5 mils of silicone rubber on the backside. The active area necessary is:

5000w/(.34 rad/therm degrade X .05 efficiency X 1353w/m^2 incident) = 217.7m^2 (active) 217.7m^2 tot / 2 = 108.8m^2 active area necessary per array

Using 55 subarrays per paddle, 3 parallel circuits per subarray, and 14 subcells per cell, the actual power is 5033 watts (EOL). With bussbars and hinges, this corresponds to two 497.5" X 391.9" arrays, each weighing 701.5 lbs. (without structure).

2.10.12.2 Kevlar/UV-Resin Rigidized - Drawing 21009 (Appendix 2) is a drawing of this concept.

2.10.12.2.1 Tube Sizing for On-Orbit Loads - The 'torusbend' program results are as follows:

Contraves Kevlar/UV-Cured Resin, 5000W

diameter	total thickness	weight(1 side tot)	load stress	critical stress	delta
10.00 inches	.0740 inch	917.14 lbs	1296.6 psi	1306.1 psi	9.6 psi
10.50	.0700	915.92	1241.2	1252.0	10.8
11.00	.0670	916.74	1182.9	1200.4	17.5
11.50	.0640	916.69	1133.3	1143.9	10.6
12.00	.0620	919.26	1078.2	1093.5	15.3
12.50	.0600	921.26	1029.9	1039.7	9.8
13.00	.0590	926.49	974.9	996.0	21.1
13.50	.0580	931.43	925.6	950.8	25.2
14.00	.0570	936.09	881.2	904.0	22.7

The 11" diameter, 67 mil thick tube was selected.

2.10.12.2.2 Packaging and Deployment Techniques - From the deployed position, the array is accordion-folded using its flexible hinges, and the tube members are folded in. The pre-impregnated Kevlar is encapsulated to avoid sticking to itself while stowed, to allow initial inflation, and to regulate curing and outgassing. Each torus side must be pointed to the sun to cure.

The panels are packaged together into a canister 83 inches long and 38 inches in diameter. The stowage canister is oriented vertically in the 86 inch diameter section of the Delta II launch vehicle, and the paddles are extended using the mechanism shown in drawing 21009. The system packaged height penalty is 78 inches.

The total system weight is 1910.6 lbs, giving an efficiency of 5.8 watts/kg. The reason for this low efficiency is the mission specified, which requires array oversizing and heavy shielding from radiation.

2.10.12.2.3 Launch Loads - The stowage canisters are oriented vertically, so the maximum Delta II axial acceleration of 12 g's puts the support members in compression with 22,927 pounds of force. The compressive failure stress of aluminum is approximately 35,000 psi, so the loads can be handled if only .7 in^2 of cross-sectional material area is available, which it is.

2.10.13 1000 Watt, 3 Year, LEO, Tubular (Extrapolated)

This analysis was done in order to examine the efficiency advantage of high output arrays not subject to large radiation burdens.

The results of the radiation studies indicate that for the LEO orbit, an array with 1.7 mils of silicone rubber on top will degrade 20% over 3 years. This includes thermal efficiency losses. The backside stainless steel substrate is sufficient, and does not need additional shielding. The radiation shielding doubles as atomic oxygen shielding. The active area necessary is:

1000w/(.8 rad/therm degrade X .05 efficiency X 1353w/m^2 incident) = 18.5m^2 active area

18.5m^2 tot / 2 = 9.24m^2 active area necessary per array paddle

page 26

Using 6 subarrays per paddle, 3 parallel circuits per subarray, and 11 subcells per cell, the actual power is 994 watts (EOL). With bussbars and hinges, this corresponds to two 106.875" X 158.5" arrays, each weighing 7.5 lbs. (without structure).

Using Kevlar with UV-cured resin as the torus material, assuming it is encapsulated in an atomic oxygen resistant material such as kapton, the 'torusbend' program results are as follows:

Contraves Kevlar/UV-Cured Resin, 1000W, LEO

diameter	total thickness	weight(1 side tot)	load stress	critical stress	delta
3.00 inches	.0085 inch	9.73 lbs	417.3 psi	513.3 psi	96.0 psi
3.50	.0085	10.11	320.1	332.1	12.1
4.00	.0085	10.49	255.6	282.7	27.1
4.50	.0085	10.88	210.5	233.3	22.8
5.00	.0085	11.27	177.5	183.9	6.4
6.00	.0080	11.78	138.5	158.0	19.5
7.00	.0080	12.53	109.4	122.3	12.9
Aluminum-Rigidized:					
4.00	.0055	11.06	415.3	488.4	73.1
5.00	.0055	11.97	291.1	333.0	41.9
6.00	.0050	12.39	232.7	259.0	26.3
7.00	.0050	13.25	184.8	207.2	22.4

The aluminum-rigidized material could not be made thick enough to be practical. The 4" diameter, 8.5 mil thick Kevlar tube was selected.

The system packaged height penalty is ~10 inches.

The total system weight is ~31 lbs, giving an efficiency of ~70 watts/kg. This demonstrates that larger arrays have greater efficiency.

2.10.14 Contract Modification of Point Design 4-200 Watt, 3 Year, Molniya, Tubular Attached to a STEP-Type Satellite Bus

This design was undertaken to investigate 2-axis pointing, packaging, and deployment of 200 watt solar arrays attached to a non-generic spacecraft. Drawing 21011 (Appendix 2) is a drawing of this concept.

2.10.14.1 Array Used - This application is equivalent structurally and environmentally to Point Design 6 (Section 2.10.3). Therefore, the same array and torus are used, adapted to a different drive system. The array has 30 mils of silicone rubber on top and 17.5 mils of silicone rubber added to the backside. Using 13 subcells per cell and 6 parallel circuits per array, the power at end of life is 200.7 watts. With bussbars and hinges, this corresponds to two 71.25" x 92.75" arrays, each weighing 14.28 lbs (without structure). The torus is rigidized aluminum, 5 inches in diameter, 4.5 mils thick, and each weighs 2.8 lbs.

2.10.14.2 STEP Satellite - The "STEP" modular spacecraft (Figure 2.10-23 and Ref. 2.0-22) is a 12 sided polygon, 38 inches in diameters, 11.5 inches long, weighing 188 pounds. This core vehicle is stackable to accommodate payloads on the front end and orbit insertion systems on the aft end. The aft interface consists of a 22" Marman ring and/or an expendable truss structure. STEP is 3-axis stabilized in this application, and it is launched on Pegasus.

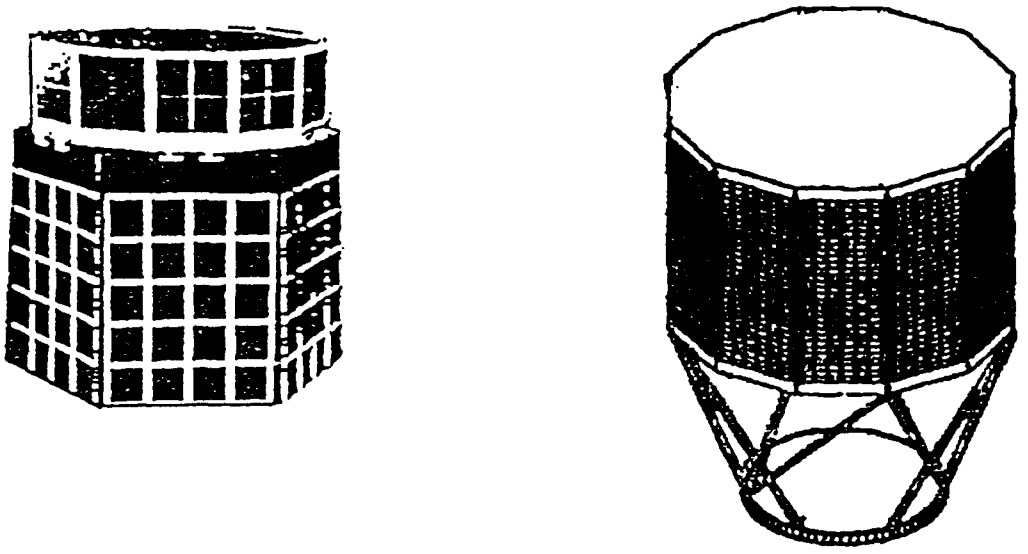

Figure 2.0-23. STEP Satellite with Representative Payloads and AFT OIS Truss

2.10.14.3 Pointing, Packaging and Deployment - With only four inches of space between the 19 inch radius STEP core module and the 23 inch radius Pegasus payload bay, the arrays cannot be side-mounted. This leads to an aft-mount system. The drive arms telescope outward, as before, to a diameter sufficient to clear any 46 inch diameter payloads which may be stacked to the STEP forward bulkhead.

A 2-axis pointing system is needed because STEP is 3-axis stabilized and cannot be rotated about its z-axis to suit solar array pointing needs. This is accomplished by placing an inboard drive motor at the mounting base of the point design 6 system. This motor effectively replaces the spacecraft yawing function. This motor will sweep the arrays around the spacecraft sides ±50° worst case, leaving room for any side-mounted radiators, antennas, jets, etc. There are flex ribbon power transfer cables across each drive.

From the deployed position, the array is accordion-folded using its four flexible hinges. The long tube members, both on one side of the folded array, are then accordion-folded while the array is rolled in toward the spacecraft.

The packaged array and torus are 25 inches long and 9 inches diameters (one side). The system packed height penalty is 10.0 inches. An expendable truss system which accommodates the aft-mounts solar array is shown in the drawing.

The total solar array system weight is 52.3 lbs, giving an efficiency of 8.4 watts/kg.

2.10.14.4 Launch Loads - The maximum Delta II axial acceleration of 12 g's places 300 ft-lbs of moment on each drive arm. This corresponds to a load stress of 2400 psi. The extendable 1/32" thick, 2" diameter aluminum drive arm would fail due to material properties before it would fail in buckling. The

compressive failure stress of aluminum is approximately 35,000 psi, so the loads can be handled without the need for external supports. The inboard drive motor must be spec'd to handle this axial load.

2.10.15 Contract Modification of Point Design 5 - 200 Watt, 3 Year, Molniya, Tubular Attached to a TECHSTARS-Type Satellite Bus

This design was undertaken to investigate 2-axis pointing, packaging, and deployment of 200 watt solar arrays attached to a non-generic spacecraft. Drawing 21013 (Appendix 2) is a drawing of this concept.

2.10.15.1 Array Used - This application is equivalent structurally and environmentally to Point Design 6 (Section 2.10.3). Therefore, the same array and torus are used, adapted to a different drive system. The array has 30 mils of silicone rubber on top and 17.5 mils of silicone rubber added to the backside. Using 13 subcells per cell and 6 parallel circuits per array, the power at end of life is 200.7 watts. With bussbars and hinges, this corresponds to two 71.25" x 92.75" arrays, each weighing 14.28 lbs (without structure). The torus is rigidized aluminum, 5 inches in diameter, 4.5 mils thick, and each weighs 2.8 lbs.

2.10.15.2 TECHSTARS Satellite - The Techstars "Tie-Fighter" spacecraft (Figure 2.0-24 and Ref. 2.0-12) is 66 cm long by 72 cm wide by 46 cm high, and weights 120-200 pounds. This bus accommodates payloads underneath and has provisions for side-mounting solar arrays. It is 3-axis stabilized in this application, and it is launched on Pegasus.

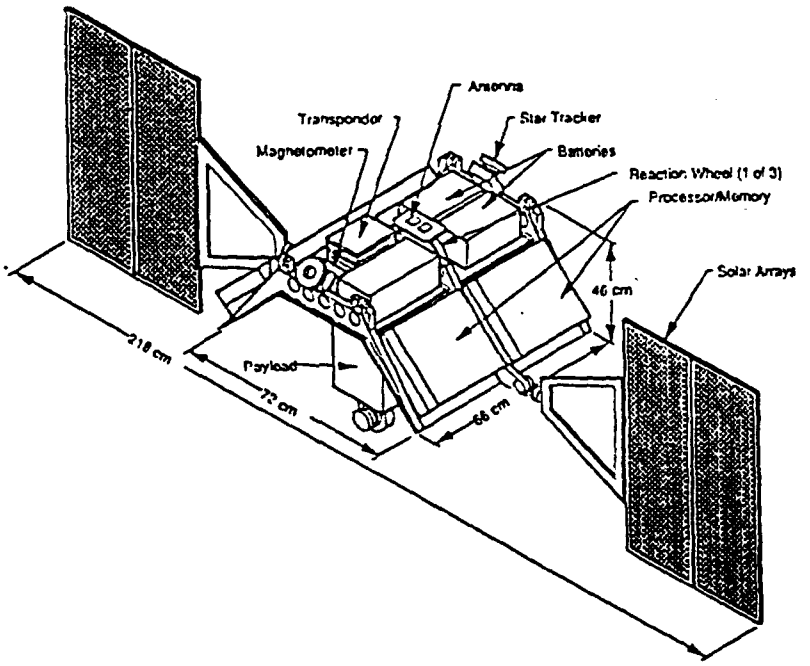

Figure 2.0-24. Techstars Satellite with Representative Payload and Planar Solar Arrays

2.10.15.3 Pointing, Packaging and Deployment - The Techstars configuration leaves ample room for side mounted arrays. The arrays are folded over onto the sides of the spacecraft while stowed.

A 2-axis pointing system is needed because Techstars is 3-axis stabilized and cannot be rotated to suit solar array pointing needs. This is accomplished by using and elevation drive inboard, and an azimuth drive outboard, on each array. The drive arms must be long enough to avoid spacecraft shadowing of the arrays in high beta angle conditions. The azimuth motor is located at the outboard end of the drive arm, instead of inboard, to facilitate more compact stowage. The elevation drive motor is used to unstow the array away from the spacecraft side before deployment. There are flex ribbon power transfer cables across each drive.

From the deployed position, the array is accordion-folded using its four long flexible hinges. The long tube members, both on one side of the folded array, and then accordion-folded while the array is rolled in toward the spacecraft.

The packaged array and torus are 25 inches long and 9 inches diameter (one side). The system packaged height penalty is 9.5 inches.

The total solar array system weight is 52.8 lbs, giving an efficiency of 8.3 watts/kg.

2.10.15.4 Launch Loads - The array canisters are attached to the sides of the spacecraft via pylons, giving a very strong arrangement for launch. The axial launch loads will not be a problem.

2.10.16 Contract Modification of Point Design 7 - 200 Watt, 3 Year, GEO Tubular Attached to a STEP-Type Satellite Bus

This design was undertaken to investigate 2-axis pointing, packaging, and deployment of 200 watt solar arrays attached to a non-generic spacecraft. Drawing 21010 (Appendix 2) is a drawing of this concept.

2.10.16.1 Array Used - This application is equivalent structurally and environmentally to Point Design 9 (Section 2.10.2). Therefore, the same array and torus are used, adapted to a different drive system. The array has 1.7 mils of silicone rubber on top. Using 13 subcells per cell and 3 parallel circuits per array, the power at end of life is 200.0 watts. With bussbars and hinges, this corresponds to two 35.625" x 92.75" arrays, each weighing 1.47 lbs (without structure). The torus is rigidized aluminum, 4 inches in diameter, 3.5 mils thick, and each weighs 1.16 lbs. This system would also be appropriate at LEO.

2.10.16.2 Pointing, Packaging and Deployment - With only four inches of space between the 19 inch radius STEP core module and the 23 inch radius Pegasus payload bay, the arrays cannot be side-mounted. This leads to an aft-mount system. The drive arms telescope outward, as before, to a diameter sufficient to clear any 46 inch diameter payloads which may be stacked to the STEP forward bulkhead.

A 2-axis pointing system is needed because STEP is 3-axis stabilized and cannot be rotated about its z-axis to suit solar array pointing needs. This is accomplished by placing an inboard drive motor at the mounting base of the point design 6 system. This motor effectively replaces the spacecraft yawing function.

This motor will sweep the arrays around the spacecraft sides ±50° worst case, leaving room for any side-mounted radiators, antennas, jets, etc. Actually, only ±29° is needed for the GEO orbit, but the Molniya travel is baselined. There are flex ribbon power transfer cables across each drive.

From the deployed position, the array is accordion-folded using its two flexible hinges. The long tube members, one on each side of the folded array, are then accordion-folded while the array is rolled in toward the spacecraft.

The packaged array and torus are 25 inches long and 4 inches diameters (one side). The system packed height penalty is 7.5 inches. An expendable truss system which accommodates the aft-mounts solar array is shown in the drawing.

The total solar array system weight is 11.42 lbs, giving an efficiency of 38.5 watts/kg.

2.10.16.3 Launch Loads - The maximum Delta II axial acceleration of 12 g's places 51 ft-lbs of moment on each drive arm. This corresponds to a load stress of 406 psi. The extendible 1/32" thick, 2" diameter aluminum drive arm would fail due to material properties before it would fail in buckling. The compressive failure stress of aluminum is approximately 35,000 psi, so the loads can be handled without the need for external supports. The inboard drive motor must be spec'd to handle this axial load.

2.10.17 Contract Modification of Point Design 8 - 200 Watt, 3 Year GEO Tubular Attached to a TECHSTARS-Type Satellite Bus

This design was undertaken to investigate 2-axis pointing, packaging, and deployment of 200 watt solar arrays attached to a non-generic spacecraft. Drawing 21012 (Appendix 2) is a drawing of this concept.

2.10.17.1 Array Used - This application is equivalent structurally and environmentally to Point Design 9 (Section 2.10.2). Therefore, the same array and torus are used, adapted to a different drive system. The array has 1.7 mils of silicone rubber on top. Using 13 subcells per cell and 3 parallel circuits per array, the power at end of life is 200.0 watts. With bussbars and hinges, this corresponds to two 35.625" x 92.75" arrays, each weighing 1.47 lbs (without structure). The torus is rigidized aluminum, 4 inches in diameter, 3.5 mils thick, and each weighs 1.16 lbs. This system would also be appropriate at LEO.

2.10.17.2 Pointing, Packaging and Deployment - The Techstars configuration leaves ample room for side mounted arrays. The arrays are folded over onto the sides of the spacecraft while stowed.

A 2-axis pointing system is needed because Techstars is 3-axis stabilized and cannot be rotated to suit solar array pointing needs. This is accomplished by using and elevation drive inboard, and an azimuth drive outboard, on each array. The drive arms must be long enough to avoid spacecraft shadowing of the arrays in high beta angle conditions. The azimuth motor is located at the outboard end of the drive arm, instead of inboard, to facilitate more compact stowage. The elevation drive motor is used to unstow the array away from the

spacecraft side before deployment. There are flex ribbon power transfer cables across each drive.

From the deployed position, the array is accordion-folded using its two long flexible hinges. The long tube members, one on each side of the folded array, and then accordion-folded while the array is rolled in toward the spacecraft.

The packaged array and torus are 25 inches long and 4 inches diameter (one side). The system packaged height penalty is 5.0 inches.

The total solar array system weight is 12.42 lbs, giving an efficiency of 35.4 watts/kg.

2.10.17.3 Launch Loads - The array canisters are attached to the sides of the spacecraft via pylons, giving a very strong arrangement for launch. The axial launch loads will not be a problem.

2.11 COMPARISONS AND RECOMMENDATIONS

Efficiencies of the various configurations are summarized in Figure 2.0-25.

Power/Config	Orbit					
	LEO	Molniya	3000Km	10,000Km	LEO/GEO Xfer	GEO
Make-Up Gas:						
200W, Pillow	1.0					3.7
200W, Sphere	.2					.6
200W,Tube	- -					- -
Rigidized:						
200W,Tube						
46" P/L	39 [3]	8.5 [6]				39 [9]
STEP	38.5	8.4 [4M]				38.5 [7M]
Techstars	35.4	8.3 [5M]				35.4 [8M]
200W,Pillow	11.5 [2]	5.4 [5]				11.5 [8]
200W,Sphere	7.1 [1]	2.2 [4]				7.1 [7]
1000W,Tube	70			9.2 [10]		70
2500W,Tube			2.6 [11]			
5000W,Tube					5.8 [12]	

NOTE: Numbers in brackets [] are point design numbers; "M" refers to contract modification.

Figure 2.0-25. Efficiencies (watts/kg) vs. Power, Configuration and Orbit

From these results, we can make some conclusions:

Among make-up gas systems, the pillow configuration is best.

Rigidizable systems are much better than make-up gas systems.

Among rigidizable systems, the tubular torus configuration is best.

Orbit selection has a strong effect on efficiency due to radiation. The safest orbits are LEO and GEO.

Higher wattage arrays are more efficient than smaller arrays in the same orbit.

The best large array examined is the 1000 watt, LEO/GEO, rigidized, tubular system. It achieves 70 watts/kg, nearing the 100 watts/kg goal. Larger arrays would certainly be even more efficient.

The best 200 watt array examined is the LEO/GEO, rigidized, tubular system. It achieves 39 watts/kg.

2.12 COST

The following cost summary presents total cost estimates for the 12 point designs and the additional STEP and Techstars satellite configurations.

The designs presented are for rigidized configurations. The costing assumes that the processes to be used for fabrication and space deployment are well understood and developed. Additionally the array material costs have been taken from quotations from Dr. J. Hanak. It is anticipated that as the cell technology progresses, this cost will drop significantly.

The costs presented are for generation of fabrication drawings from an existing design, hardware purchases, fabrication and assembly, testing and documentation of an engineering prototype solar array. It is anticipated that this array will be flight weight.

The cost data is presented in two forms: 1) A summary table, Table 2.0-9 presenting the point designs addressed, output power expected at the end of a 3 year life and respective prototype costs. 2) Three summary graphs, Figure 2.0-26 presenting all of the designs, Figure 2.0-27 presenting only the 200 Watt designs, (each graph showing total ROM cost, array material cost and labor cost) and Figure 2.0-28 presents total system cost in increasing order of point design and $/Watt cost for each design.

Some of the important points are:

a) As the arrays get larger the array material is the major cost.

b) As the technology advances the array material cost will significantly decrease.

c) The labor cost is shown for only one unit, as the quantity is increased a significant savings can be realized (i.e. tooling costs and other factors can be amortized over a selected quantity).

d) The most economical designs are point designs 2, 3, 8, and 9.

TABLE 2.0-9. 12 POINT DESIGN PROTOTYPE COST SUMMARY

Point Designs	Power (W) 1	Description	Orbit	System Cost	Array Cost	Other Material	Labor Cost	$/Watt	Watt/Kg
1	200	Rigidized Sphere	LEO	$956,349	$413,600	$67,000	$475,749	$4,782	7.1
2	200	Rigidized Pillow	LEO	$523,873	$100,000	$66,600	$357,273	$2,619	11.5
3	200	Rigidized Tubular	LEO	$523,873	$100,000	$66,600	$357,273	$2,619	39.0
4	200	Rigidized Sphere	Molniya	$1,532,930	$827,200	$67,000	$638,730	$7,665	2.2
5	200	Rigidized Pillow	Molniya	$656,587	$195,200	$66,600	$394,787	$3,283	5.4
6	200	Rigidized Tubular	Molniya	$656,587	$195,200	$66,600	$394,787	$3,283	8.5
7	200	Rigidized Sphere	GEO	$956,349	$413,600	$67,000	$475,749	$4,782	7.1
8	200	Rigidized Pillow	GEO	$523,873	$100,000	$66,600	$357,273	$2,619	11.5
9	200	Rigidized Tubular	GEO	$523,873	$100,000	$66,600	$357,273	$2,619	39.0
10	1000	Rigidized Tubular	10000 KM	$1,639,395	$889,200	$77,600	$672,595	$1,639	70.0
11	2500	Rigidized Tubular	3000 KM	$3,192,125	$1,944,600	$86,600	$1,158,925	$1,277	2.6
12	5000	Rigidized Tubular	LEO/GEO Xfer	$7,662,159	$5,147,100	$92,600	$2,422,459	$1,532	5.8
Step GEO	200	Rigidized Tubular	GEO	$543,170	$100,000	$70,000	$373,170	$2,716	38.5
Step Molniya	200	Rigidized Tubular	Molniya	$683,162	$195,200	$70,000	$417,962	$3,416	8.4
Techstars GEO	200	Rigidized Tubular	GEO	$543,170	$100,000	$70,000	$373,170	$2,716	35.4
Techstars Molniya	200	Rigidized Tubular	Molniya	$683,162	$195,200	$70,000	$417,962	$3,416	8.3

1. Estimated end-of-life output power at designated orbit.

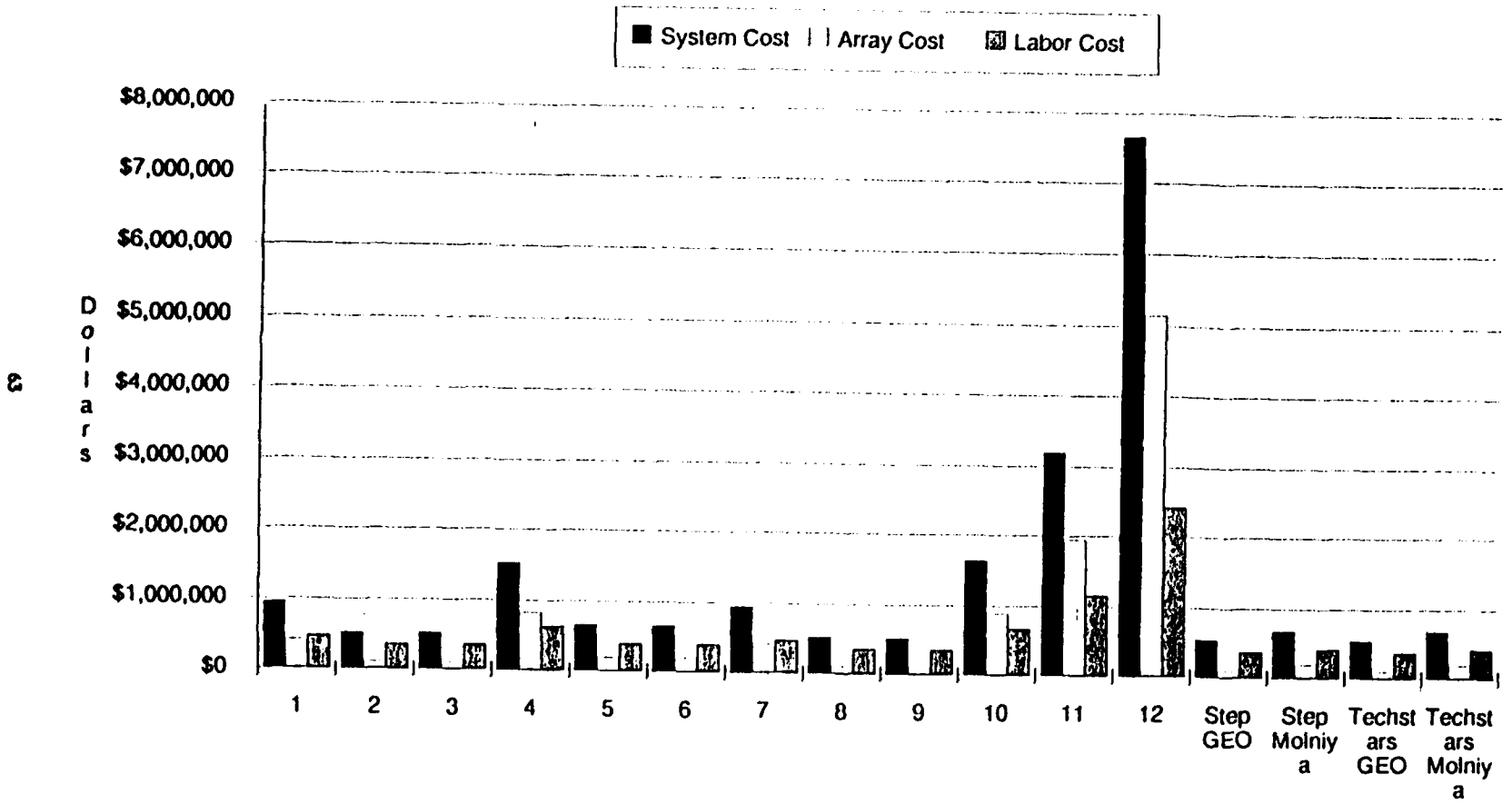

Figure 2.0-26. 12 Point Design Prototype Cost Summary Chart

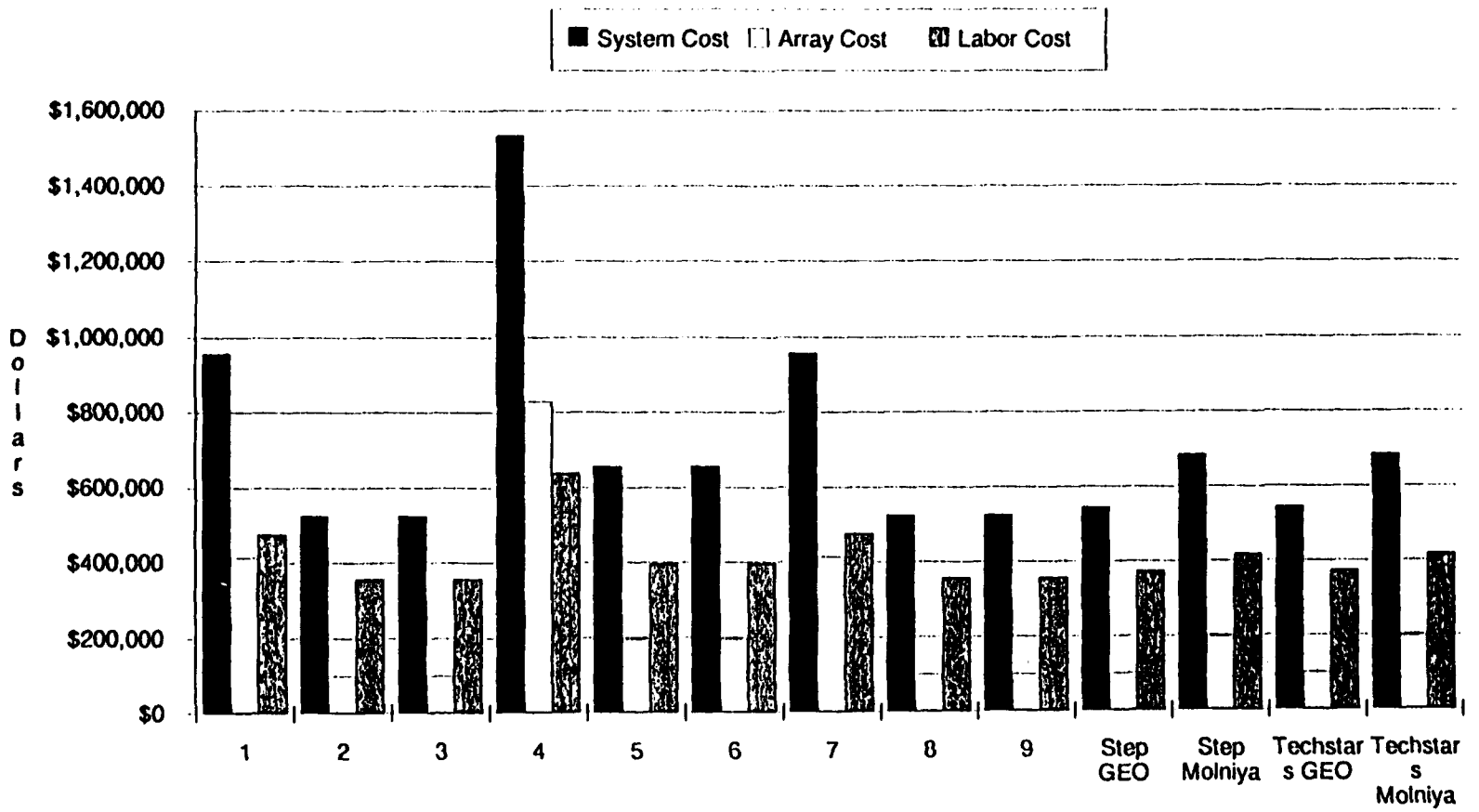

Figure 2.0-27. 200 Watt Designs Cost Summary

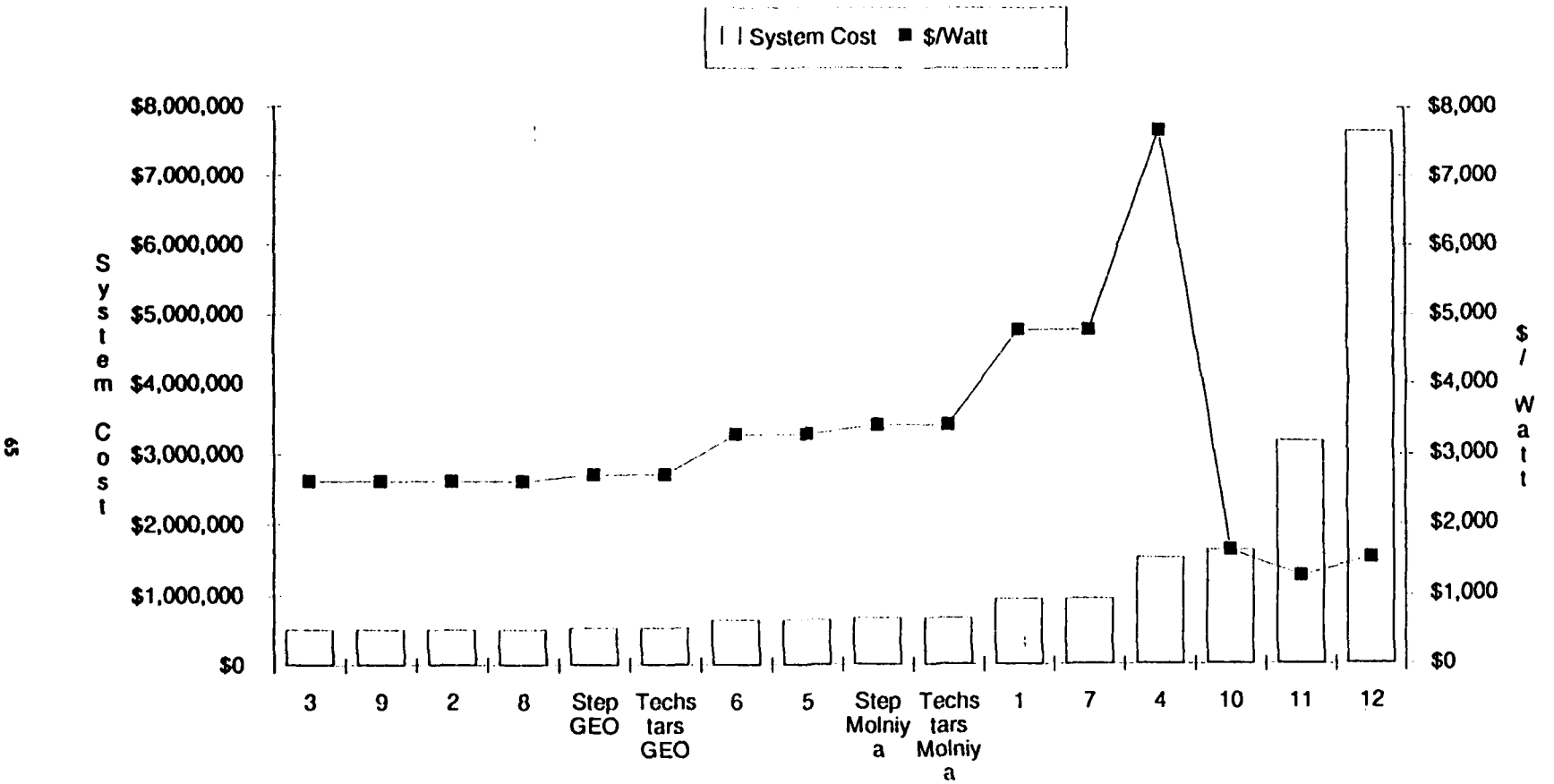

Figure 2.0-28. ITSAT System Cost and $/Watt Cost vs. Point Design

3.0 DESIGN

As a result of the concept study described in Section 2.0, L'Garde was directed to design a prototype solar array system for testing of packaging, deployment and functional characteristics with the following conceptual design parameters:

- Array Configuration: Self-rigidizing tubular type
- Deployed Solar Cell Area Per Panel: Approximately two square meters
- Orbit: 740 kilometers altitude at 90 degrees inclination
- Inflatable Solar Array Design Life: Three years
- Satellite Interface Requirements: Two axis pointing & tracking, TECHSTAR bus
- On-Orbit Acceleration Load: Maximum 0.03 G in any direction
- Launch Environment: Worst case combination of Pegasus, Taurus and Delta 2

The prototype unit was not required to contain the pointing system since this was not required for evaluation of packaging and deployment. The prototype configuration is shown in Figure 3.0-1 and consists of two major components; the solar array and the rigidized structure.

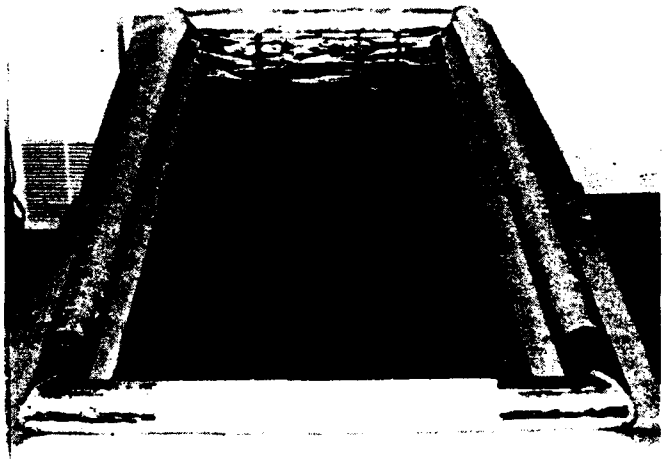

0671

Figure 3.0-1. Prototype Unit

3.1 DESIGN CONSIDERATIONS: SOLAR CELL CHOICE

Numerous different types of solar cells had been considered for comparison in the process of choosing amorphous silicon as the baseline in the proposal. The overall matrix included the following:

- Thin crystalline silicon (Cryst-Si)
- Gallium arsenide on germanium (GaAs/Ge)
- Cleft gallium arsenide (Cleft GaAs)
- Copper indium diselenide (CIS)
- Amorphous silicon (aSi)

Major sources of the above are listed in Table 3.0-1. Each type of cell has distinct advantages and disadvantages. For example, the processes for fabricating crystalline silicon and GaAs/Ge solar cells are considered more mature technologies. As such, the cell behaviors are well understood and predictable, their manufacture is relatively routine, there has been thorough radiation and other qualification testing and they have been flown in space. Crystalline silicon, usually 8 to 12 mils thick, can now be readily etched to 2.0 mils to save weight. The overall thickness of GaAs/Ge, also formerly 8 mils, has been reduced to 3.5 mils for the same reason.

TABLE 3.0-1. CELL SOURCES

CELL	SOURCES
aSi	Apogee Solarex Iowa Thin Films Sanyo
CIS	ISET Boeing Siemens Martin Marietta
GaAs/Ge	ASEC
Cleft GaAs	Kopin
Crystalline-Si	Spectrolab ASEC

3.1.1 Thin Crystalline Si

A cross-section of the thin crystalline solar cell is shown in Figure 3.0-2. The basic silicon p-type wafer is sliced from a crystalline ingot and then chemically etched to the finished thickness. An n-type junction is then diffused into the top surface which may be either textured or polished. Two Anti-Reflection (AR) coatings are added followed by a three layer metal system to form an upper contact.

The Back Surface is boron diffused to create a small Field (BSF) to sweep free carriers back toward the junction for additional collection. A Back Surface Reflector (BSR) made of evaporated Al is also added to redirect photons into the silicon mass that ordinarily would have been lost. The triple layer back contact is similar to the front. Overall efficiency is 13.8%. Because of the costly crystal growth and the wasteful sawing and etching operations, the production of such thin silicon solar cells is inherently expensive.

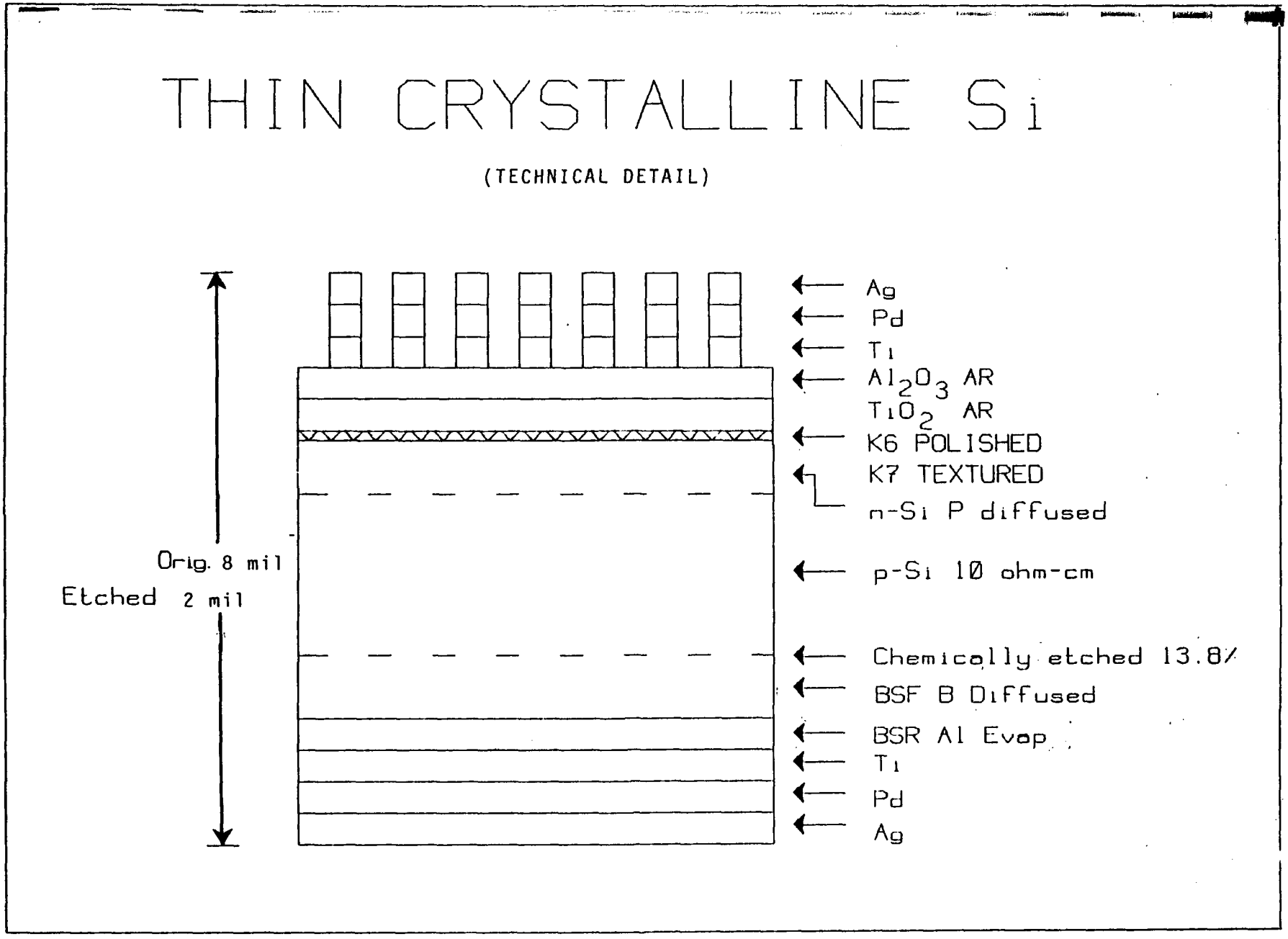

Figure 3.0-2. Thin Crystalline Si Solar Cell

3.1.2 Gallium Arsenide on Germanium

An overview of the GaAs/Ge cell is shown in Figure 3.0-3, while more technical details of its window and metalization systems are shown in Figure 3.0-4.

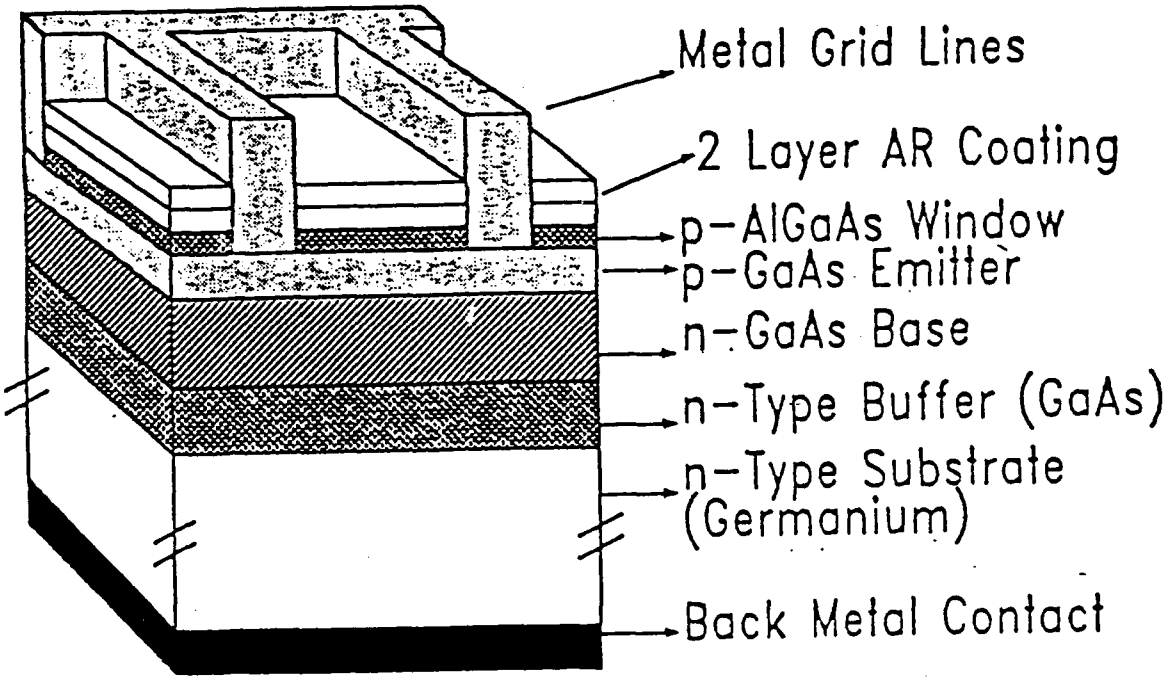

Figure 3.0-3. GaAs/Ge Solar Cell Cross-Section Schematic

As with thin silicon, the GaAs/Ge process starts with an expensive single crystal, this time germanium, which is then cut and further processed. In this case, however, layers are not diffused into but grown onto the Ge surface by a high tech metal organic chemical vapor deposition (MOCVD) technique. In this manner buffer, base, emitter and Al GaAs window layers are grown. The uppermost surface is then AR-coated before both sides are metallized.

GaAs/Ge is considerably more efficient, 18.5%, compared to thin crystalline Si. However, it is also more expensive, approximately 60% higher. The cost of a square centimeter of GaAs/Ge is $12.59 compared to $7.92 for silicon.

Both these types of solar cells are susceptible to radiation damage, Si more so than GaAs/Ge. As a result, cover glasses are required, which add to the weight.

Cell blankets can be made using either cell type in which the overall array exhibits some flexibility. However, the cells themselves are inflexible and, whether covered with glass or not, tend to be relatively fragile and brittle.

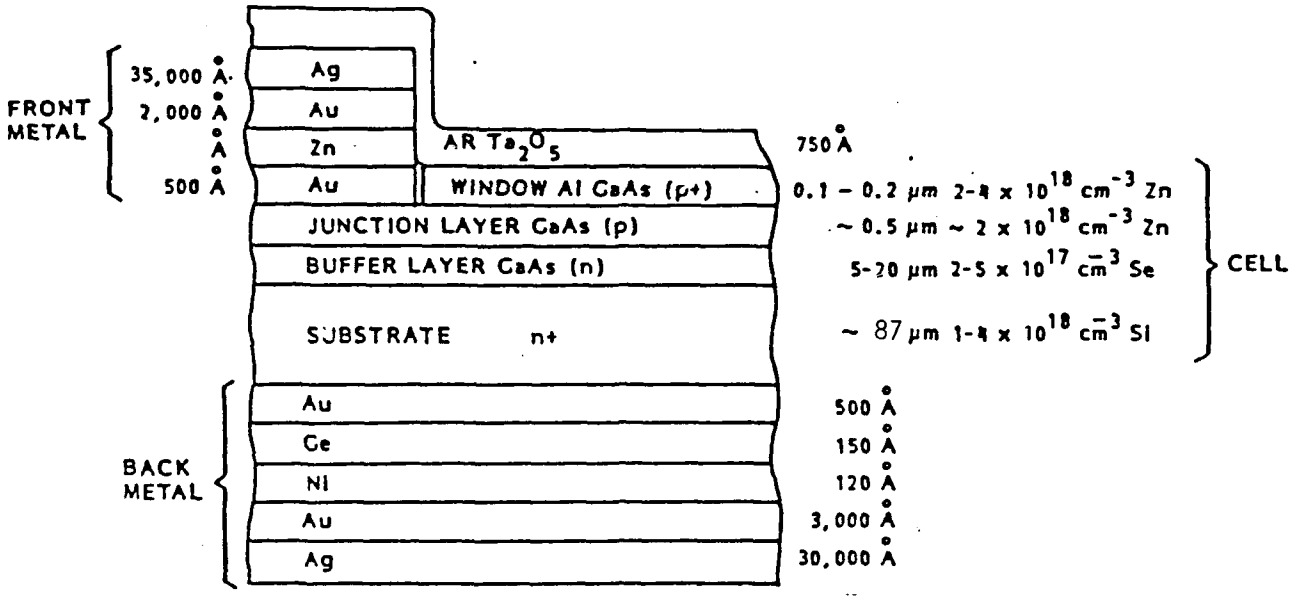

NOTES:

(1) NOT TO SCALE

(2) GRID LINES

- AuZnAu, 10 μm WIDE
- Ag, 15-18 μm WIDE

Not to Scale

Figure 3.0-4. GaAs/Ge Solar Cross-Section Schematic

3.1.3 Cleft GaAs

The Cleft GaAs solar cell is still under development. In other words, it is an experimental cell in which the final design configuration and behavior are still unknown. However, it holds much promise in that it is potentially very light weight while generating power at high efficiency, 18.5%.

A cross-section of the device is shown in the exploding diagram of Figure 3.0-5. Here the upper GaAs solar cell has been mechanically separated or "cleft" from the reusable n-GaAs base substrate on which it had been grown.

The technology is similar to GaAs/Ge except for three differences:

1. The original crystal substrate upon which the critical cell layers are grown by MOCVD consists of GaAs instead of Ge.

2. A thin, porous silicon nitride (SiN) or (SiO_2) layer is deposited on this substrate before initiation of growth. The subsequent GaAs layers then nucleate onto the substrate through the microscopic holes in the thin, weakly adhered film.

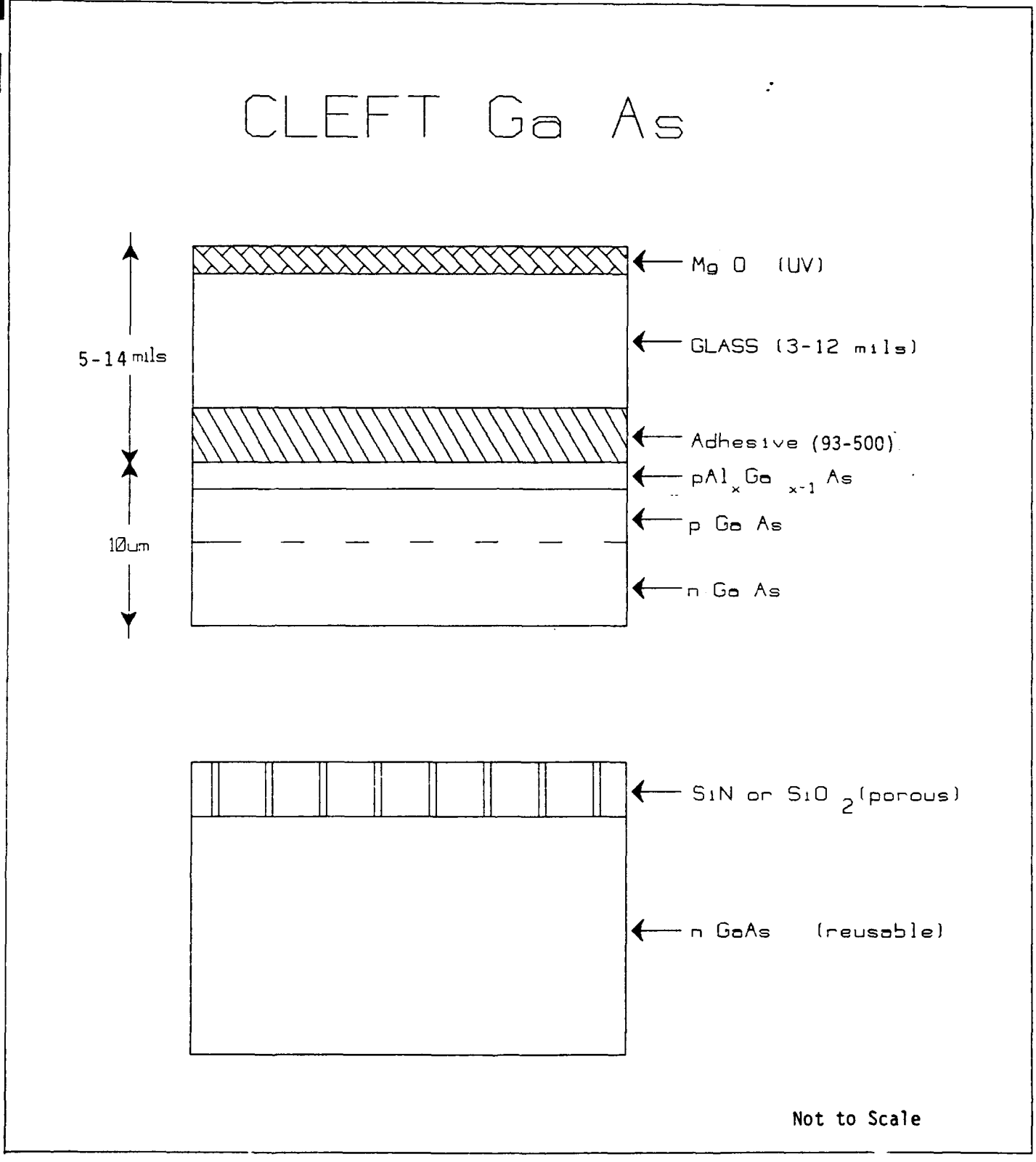

Figure 3.0-5. Cleft GaAs Solar Cell

3. After growth is complete a cover glass superstrate (rather than a substrate) is attached to the top of the cell and the active layers are cleft from the lower reusable crystal.

The resulting cell is extremely thin, ~10μm, but the relatively heavy glass superstrate must remain attached in order to facilitate handling. However, this superstrate can serve as a radiation protection which would have been necessary regardless. Thus, compared to the cross-section of GaAs/Ge described previously, the 3.5 mil Ge substrate has been completely eliminated resulting in an array with potentially higher power densities.

Significantly, cleft GaAs cells are not available in quantity. Research (as opposed to production) specimens at approximately $100 per square centimeter are available but in extremely limited quantities.

Like crystalline Si and GaAs/Ge cells, rigid cleft GaAs cells can be glued to a thin blanket substrate resulting in some flexibility, but cells and covers are still susceptible to handling, packaging and deployment damage.

3.1.4 Copper Indium Diselenide

CIS solar cells are also developmental. Compared to both GaAs types they are only medium powered (approximately 10-11%). However, they have much more potential of eventually being low cost, light weight, and extraordinarily flexible. In addition, preliminary radiation testing seems to indicate only minimal degradation suggesting the possible elimination of encapsulation for some missions. The cross-section of the cell is shown in Figure 3.0-6. CIS technology is relatively low cost and simple: no crystal, no kerf loss due to cutting and no expensive MOCVD process. Instead, straight forward evaporation or sputtering methods are used to deposit $CuInSe_2$ and CdS layers onto a genuinely flexible metal foil (i.e., 1 mil of Ti). Total thickness of the active material of the cell is negligible.

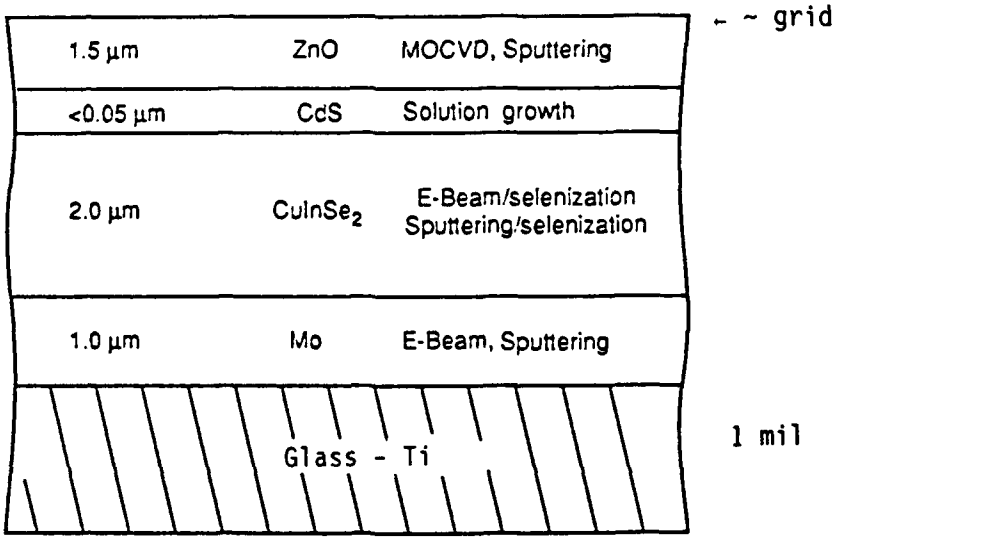

Figure 3.0-6. CIS Solar Cell Cross-Section Schematic

Another advantage is the possible interconnection of cells into modules by monolithic rather than cumbersome manual processes.

Disadvantages are that space CIS cells are not presently available, although preliminary work, funded internally, is underway at both Boeing and Martin Marietta. Capability is infantile, the firm with the highest potential of being a serious producer, International Solar Electric Technology (ISET), cannot presently fabricate them at any cost, and is seeking large infusions of development - rather than production - funding.

3.1.5 Amorphous Si

Amorphous Si has many of the advantages of CIS. Although low powered it has the potential of being very inexpensive, extremely light and thoroughly flexible. It too is deposited onto metal foils by a simple technique and is monolithically interconnectable.

An apparent distinct advantage is that the technology already exists. But an in-depth review of the literature substantiates that the vast body of data focuses only on terrestrial applications. Proven commercial amorphous arrays are routinely fabricated only for earth-bound systems. None have been flown in space.

However, Government interest with respect to amorphous silicon for space applications is growing.

3.2 AMORPHOUS SILICON PRELIMINARY DESIGN

Based on the review of the solar cell information outlined above, amorphous silicon was chosen as a viable candidate to incorporate with other elements of the ITSAT system to demonstrate proof-of-principle as required in Phase 1. As a result, individual amorphous silicon cells were integrated into a flexible blanket array. This system was successfully used in the prototype unit packaging and deployment tests.

3.2.1 Preliminary Design Requirements

The basic requirements (per panel) were as follows (Ref. 3.0-1):

Minimum BOL Power:	125W @ AM0; 100W @ AM1.5*
Minimum EOL Power:	100W @ AM0
Life; Orbit:	3 years; LEO/GEO
Nominal Operating Voltage:	32V
Approximate Dimensions:	0.9m X 2.4m
Maximum Density:	312.5 g/m^2
Maximum Packaged OD:	4 in.

* Power was measured under local terrestrial sunlight, then correlated to the terrestrial standard AM1.5 (Ref. 3.0-2). Extrapolation to space (AM0) was accomplished by multiplying by 1.25. This factor is conservative, as the factor quoted in Ref. 3.0-3, p.7 is 1.28.

The preliminary design, documented in Ref. 3.0-1 is shown in Figure 3.0-7: Twenty-seven cells of 1.2 volt each were connected in series to get the specified voltage of 32V. The power requirement was satisfied by selecting 13 subcells per

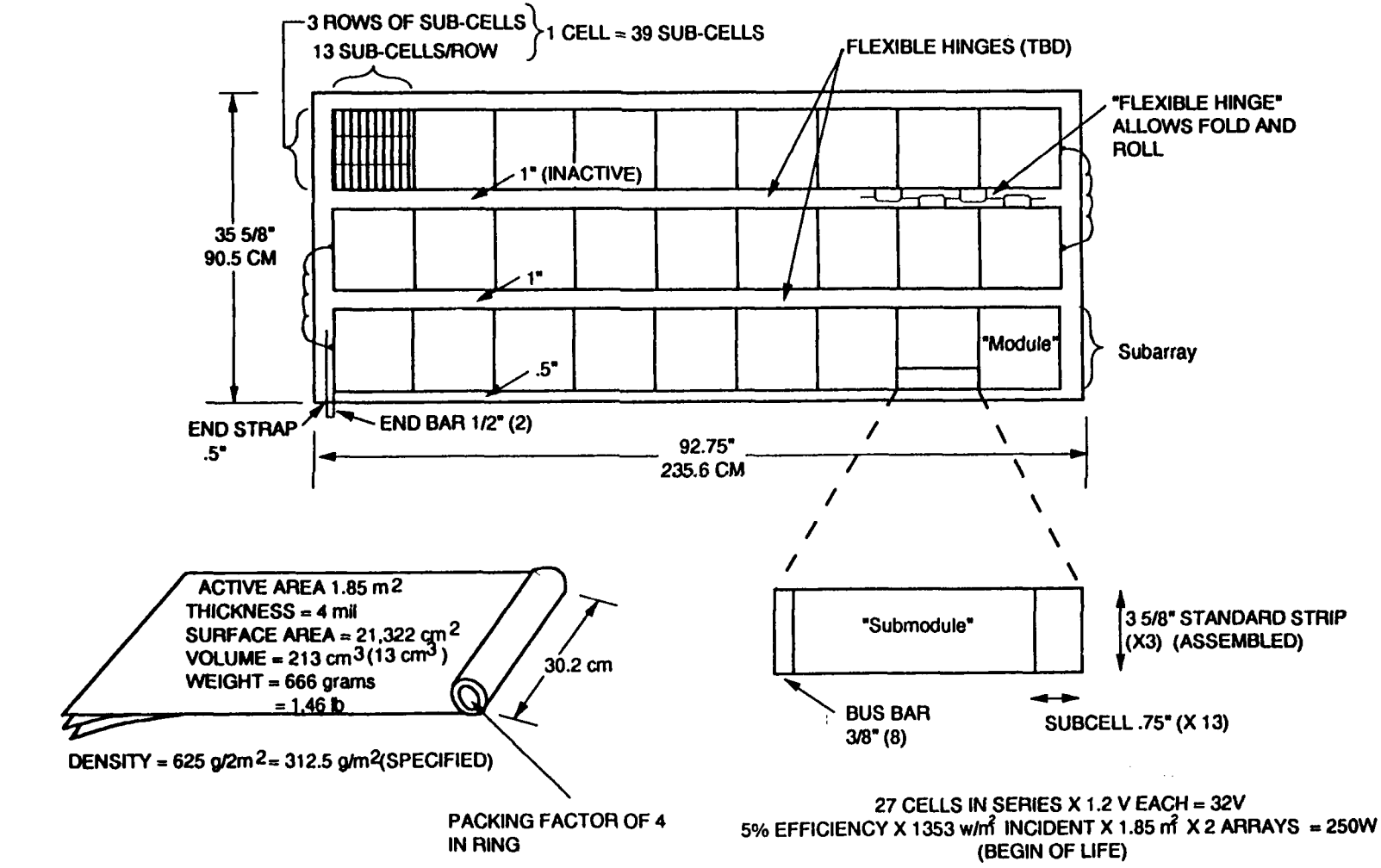

NOTE: NOT TO SCALE AND INCOMPLETE

TI 715
VU-60-BD-026

Figure 3.0-7. Array Preliminary Design

cell and 3 parallel circuits. When calculating array power, the distinction was drawn between active area and actual area, which includes bussbars, hinges, and edge supports. Approximate active area is 1.85 m^2. The basic power equation used was:

(1353 w/m^2 incident sunlight) X (5% efficiency) X (active area) X (degradation factor)

= power output, end of life

The incident sunlight power in space is quoted in Ref. 3.0-4, p. 2.4-2, while the array efficiency was estimated by the supplier based on experience with a previous array (Ref 3.0-5).

The degradation is due to temperature, particle radiation damage, Staebler-Wronski loss, encapsulant darkening due to UV, and mechanical damage. All factors but the lattermost are estimated based on aSi technology reports. Mechanical degradation was tested in the packaging/deployment tests, with the goal of zero loss. The total degradation was initially estimated by the supplier as 20% over the 3 year life, 17% by the Staebler-Wronski effect, and 3% by radiation (Ref. 3.0-6). These contributions were later revised, but the result was still ~22%. A suitable non- darkening encapsulant is presently a development issue, as will be discussed later.

3.2.2 aSi Tandem Cell Structure

The cell structure selected was a stacked "tandem" cell, shown in Figure 3.0-8. This structure was expected to exhibit less degradation due to Staebler-Wronski effect and radiation (Ref. 3.0-7). The current passes vertically through the stacked cells, putting them in series. The combination of two 0.6V cells therefore produces 1.2V. The thin upper cell acts as a filter, absorbing and converting the lower energy photons while passing the rest on to the thicker lower layer. Cell thicknesses are selected to match currents. This scheme provides for a higher conversion efficiency.

Unlike crystalline silicon, amorphous silicon has irregular atomic arrangements. Interactions between photons and silicon atoms occurs more frequently, so that much more light is absorbed and, therefore, the cell structure itself can be made extremely thin, approximately 1 micron total. This allows for a flexible cell, and the potential for low cost due to low material cost. Also, it can be deposited like a coating on the substrate, whereas crystalline cells must be cut from a silicon wafer and individually bonded to the substrate.

The substrate was 1 mil of stainless steel, thinned down from 8 mils. The top and bottom encapsulation were 1.6 mils of mylar each, including adhesive. The top layer was textured to reduce reflection losses and trap light. The encapsulants chosen were not space-qualified, per Phase 1 Statement Of Work. These three layers essentially constituted the entire thickness, making for a 4.2 mil thick array.

The stainless substrate acted as the lower electrode. The upper electrode consisted of a transparent Indium-Tin-Oxide (ITO) layer covering the entire array, with a screen-printed silver collection grid connected to tinned copper bussbars.

In the course of testing it was found that the primary failure mechanism in thin film arrays was a drain or short developing between the top (+)

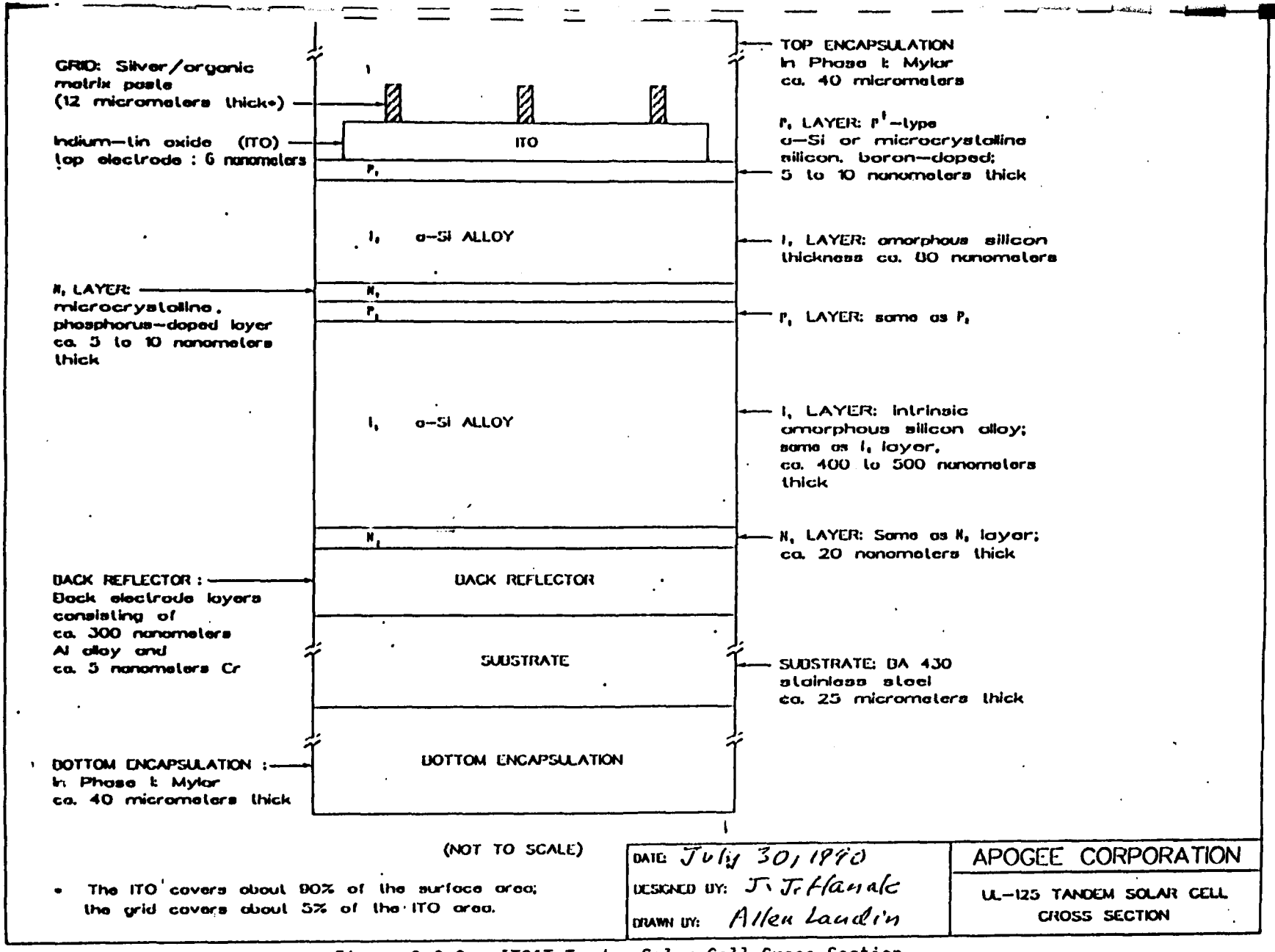

Figure 3.0-8. ITSAT Tandem Solar Cell Cross-Section

transparent electrode and the bottom (-) electrode. Some "shunt resistance" is pre-existing in the array due to manufacturing and fabrication imperfections and the thin nature of the cells. The high incident solar power stresses any potential shorts. This usually results in the shorts burning themselves out, like overloaded fuses, and may actually improve array performance. However, it may result in a local high shunt current condition, particularly if a bussbar is over the active area, which could cause high local temperatures and further damage the array, causing a visible discoloration.

3.2.3 Thermal Losses

Since the array is suspended by its four corners and has excellent heat rejection off the backside, in space it is expected to experience a high temperature of 57°C, which will result in a power degradation of 3.8% over a 3 year mission (Ref. 3.0-8, Fig. 5).

3.2.4 Staebler-Wronski Loss

The Staebler-Wronski loss is peculiar to amorphous silicon, and is thought to be due to the weak silicon-silicon bonds. Figure 3.0-9 shows data for modules tested outdoors by SERI. The irregularities are due to terrestrial environment variations. The stabilized loss is 10%-12% for ITSAT-type modules. This loss occurs over the first 1-3 months of continuous exposure, but levels out after that. Tandem cells are much better than single cells, which lose ~20%.

3.2.5 Radiation Damage

The array is on a 1 mil stainless steel substrate, which provides an equivalent of 2.1 mils glass radiation protection. With 1.6 mils of silicone rubber (a possible substitute for the Mylar) on each side, the total equivalent glass shield thickness is 1.7 mils on each side of the array.

The 1 MeV equivalent electron fluence from trapped electrons and protons combined in a 740 km., 90° circular orbit over 3 years with a finite backshield was calculated as $3.7X10^{14}/cm^2$ using data supplied by PL, Figure 3.0-10 (see also Ref. 3.0-9 p. 6-47). The radiation damage was then calculated from a curve supplied by Apogee, Figure 3.0-11. The radiation loss was estimated to be ~7%, bringing the total thermal/Staebler-Wronski/radiation degradation to ~22%.

It should be noted, however, that at present, the radiation damage factor for aSi with an encapsulant as a function of particle energy and backshielding is not well known, and there are many conflicting claims. A study is currently being conducted at JPL to quantify the radiation effects on both aSi and CIS.

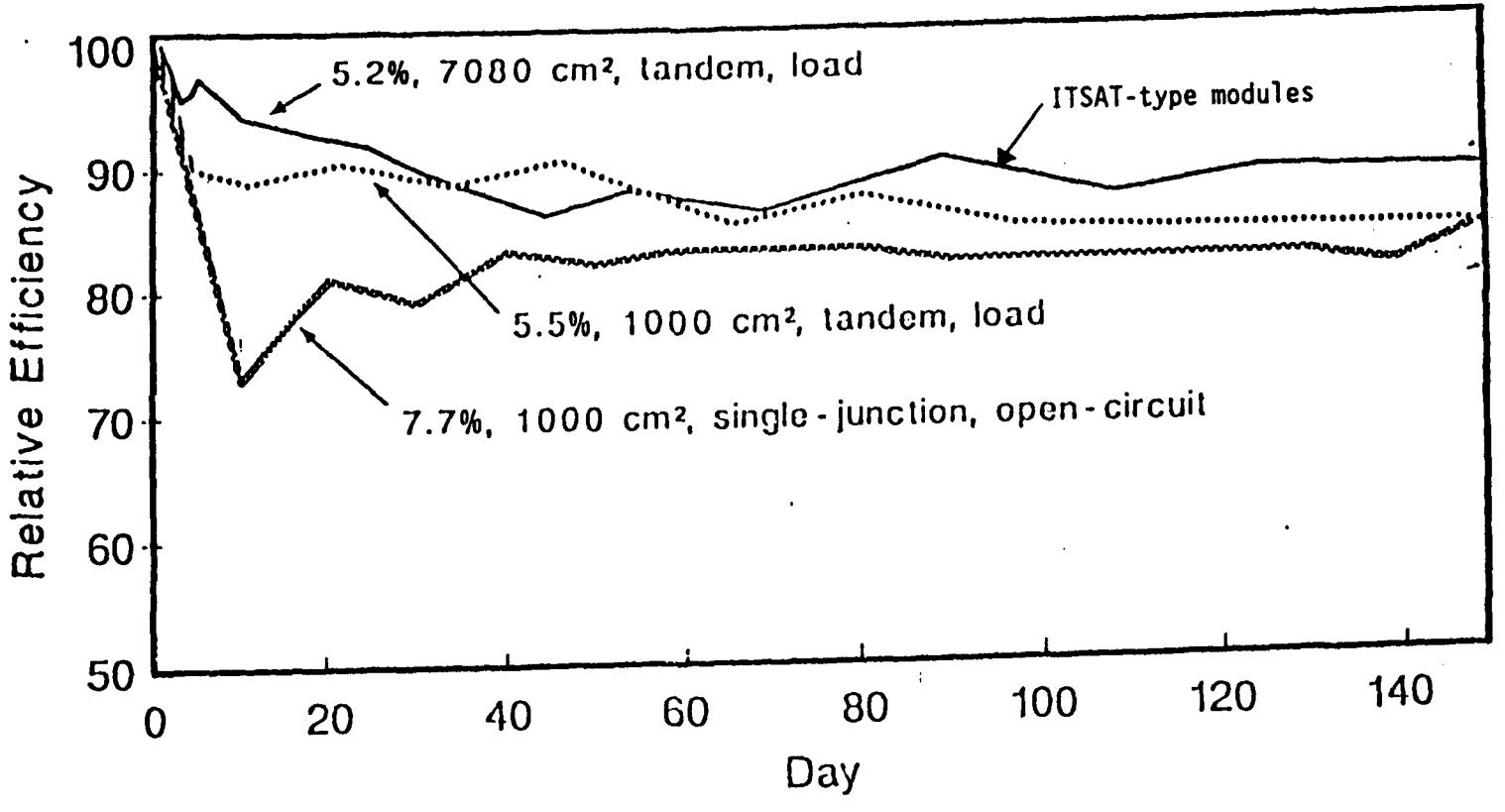

Figure 3..0-9. Staebler-Wronski Loss

		shielding	0	25.4	76.4	152	305	509	764	1524
Low orbit	case 1,2,3									
altitude	inclination									
740	90									
combined electron/proton		fluence/yr	1.32E+15	7.46E+13	3.66E+13	2.24E+13	1.35E+13	9.34E+12	7.38E+12	5.30E+12
Mid orbit	case 11									
altitude	inclination									
3000	0									
combined electron/proton		fluence/yr	7.18E+16	5.88E+16	4.68E+16	3.76E+16	2.56E+16	1.46E+16	9.13E+15	3.85E+15
High orbit	case 10									
altitude	inclination									
10000	60									
combined electron/proton		fluence/yr	1.10E+19	6.64E+17	1.31E+17	2.90E+16	3.82E+15	9.13E+14	3.10E+14	5.83E+13
6hr Molniya	case 4,5,6									
altitude	inclination									
516/20287	63.4349									
combined electron/proton		fluence/yr	5.82E+18	1.58E+17	3.57E+16	1.15E+16	3.20E+15	1.13E+15	5.24E+14	1.52E+14
Orbit transfer	case 12									
from 300km 28 deg										
to 35794km 0 deg										
combined electron/proton		fluence/yr	8.10E+18	5.00E+17	1.40E+17	5.50E+16	1.80E+16	6.80E+15	3.20E+15	9.70E+14
Geo orbit	case 7,8,9									
altitude	inclination									
35794	0									
combined electron/proton		fluence/yr	5.30E+17	7.51E+13	6.19E+13	4.96E+13	3.44E+13	2.30E+13	1.47E+13	4.69E+12

Figure 3.0-10. Fluences vs. Orbit and Shield Thickness

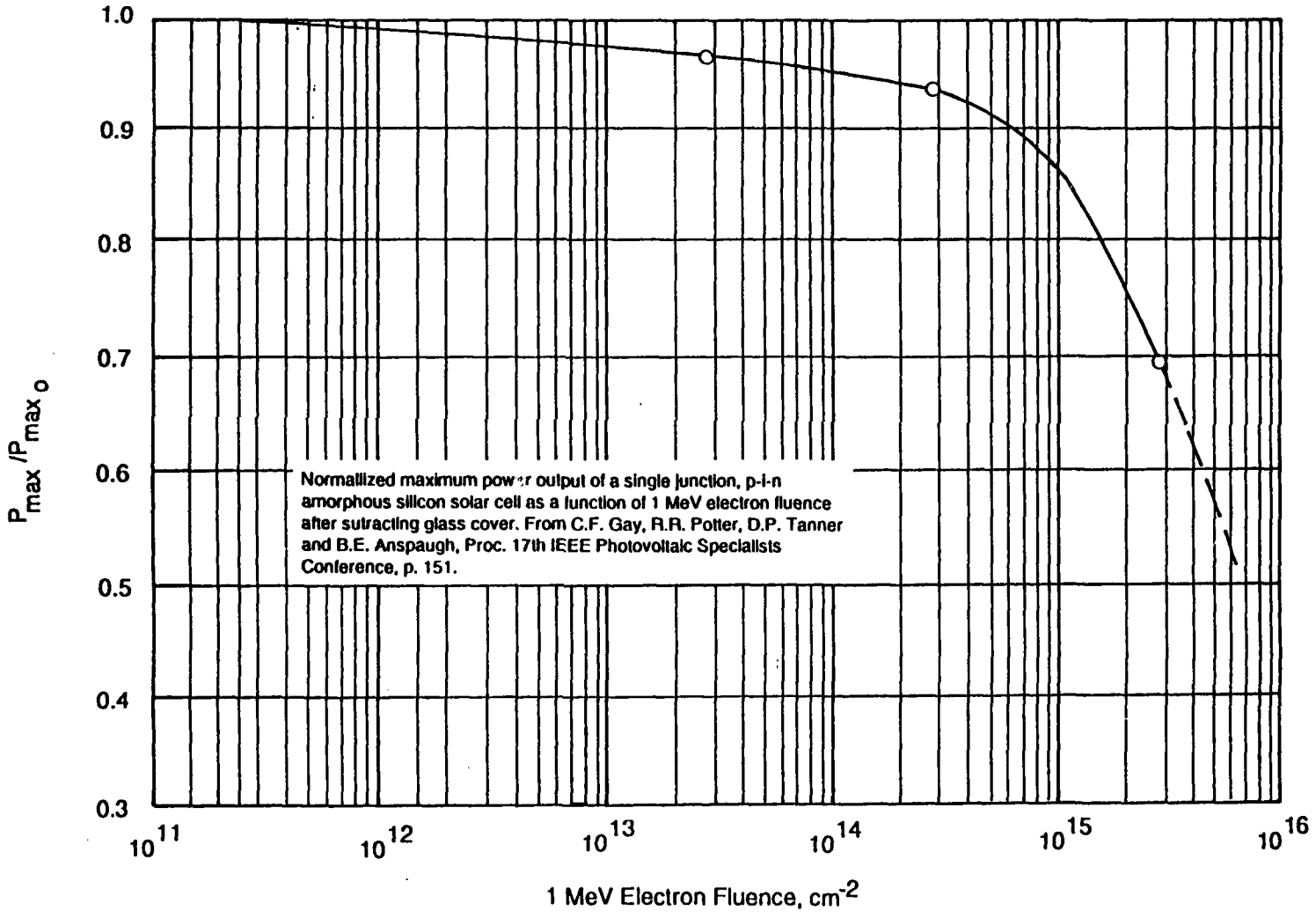

Figure 3.0-11. Power Degradation vs. Fluence

3.2.6 Encapsulation

The array requires a flexible encapsulant that will be a radiation shield, remain transparent in the UV environment, resist atomic oxygen, and withstand thermal cycling. Additionally, it is desirable for the material to be directly and inexpensively applied without the use of adhesives.

During the 1950's and 1960's, Lockheed developed spray-on coatings, but their properties remained proprietary. FEP-Teflon covers were later developed by NASA Lewis, but the material became yellowish under UV, and was made brittle under prolonged exposure to 60°C temperatures (Ref. 3.0-4, p. 4.6-1).

UV radiation is much more severe in space than on earth, where the ozone layer acts as a shield. There are two common approaches to protecting a polymer from UV damage. One is to put a coating of UV absorbing material on top; the other is to put additives in the polymer to stabilize it. Additionally, particle radiation can also damage the cover, and the combined effect is usually worse.

Atomic oxygen is the subject of ongoing studies. A promising approach is to sputter a thin layer of silicon dioxide on the surface, although microcracks and pinholes would have to be dealt with. If a silicone rubber is used as the encapsulant, it may form its own SiO_2 layer.

Polyimides are known to be very stable and resistant to atomic oxygen, but the common form, Kapton, is dark. Ref. 3.0-10 reports on the possibility of producing a clear polyimide.

Another issue with the array laminate is thermal cycling if the layers have different coefficients of linear thermal expansion. The fact that this array is so thin significantly eases this problem.

At present, no suitable encapsulant exists. The development of such an encapsulant must take into account all of the above issues.

3.2.7 Array Construction

The array was fabricated by Apogee using a manual technique very similar to that used to build the Sovonics "UL-200" array (Ref. 3.0-5, Fig. 1).

The stock material was manufactured by Sovonics, the cells being deposited by plasma decomposition onto 8 mil stainless steel substrates using silane as the feed gas. Thirty "slabs" of cells were bought for ~$200 each. The subsequent array thinning and fabrication was the largest cost item. This step is commonly the most expensive for all types of arrays.

Each slab was ~14" X 50", and the current collection electrodes were already screen printed onto the patterned cells (Ref. 3.0-11). Of the original 30 slabs, 10 were tested under low light and judged to be inadequate. The remaining slabs were cut into (60) 10-1/2" X 10-7/8" "modules" consisting of 3 rows of cells. This required some topographical mapping, as bad cells had to be avoided (Ref. 3.0-12). In all, 41 were perfect; 27 were needed to make an array. Occasionally it was possible to remove shorts by application of reverse bias

voltage. Some cells were then tested in direct sunlight to verify conversion efficiency. Low light testing had to be done frequently throughout fabrication due to the sensitivity of the cells to frequent handling.

The collection grid was then connected in series rows to tinned copper bussbars by silver paste. These bussbars are over active areas. The modules were then etched on each end and bussbars applied. Nine modules were connected in series to form a sub-array. Some shorted cells were found in the sub-arrays and were disconnected from the grid. Each sub-array was then laminated to its top encapsulant.

The next step was to thin the sub-array backside from 8 mils to 1 mil by chemical milling. On some trial runs, it was found that the roller force was breaking bussbars once the stainless steel was near 1 mil. This necessitated not thinning fully down to 1 mil.

Once thinned, the backside encapsulation was applied, bypass diodes were added, flexible hinges were added, and attachment grommets were fastened at the corners and sides using a monofilament line around the perimeter, to which the array was taped and the grommets were fastened.

3.2.8 Bypass Diodes

When a portion of the array is shadowed (or if cell currents are mismatched), the darkened cells are put under reverse bias which can damage them. Also, the current must go through the cells in series, and darkened cells have high resistance. Bypass diodes are therefore needed to protect the cells and to prevent power loss due to darkened cell resistance.

Originally, special flat diodes were envisioned for the array to assist in packaging, but these were not available in sufficient capacity, so standard barrel diodes were used. These were soldered through holes in the top encapsulant. In this manner each module is bypassed.

For future applications, it may be possible to use one of the solar cells itself as a bypass diode, reducing cost and complexity. (Ref. 3.0-13).

3.2.9 Flexible Hinges

The basic rule in packaging the solar cells is not to have folds in the active area. For these reasons two flexible hinges are used along the array length, which allow for first folding the three array strips accordion-style, and then rolling in toward the spacecraft (Ref. 3.0-14). The hinges also allow panel-to- panel movement to accommodate differing radii within the rolled up layers of sheets.

The hinge loops were made by simply folding over pieces of Mylar. One hinge line was made of monofilament, while the other is a wire which also serves to carry the array current back to the spacecraft end of the array. The hinge concept is shown in Figure 3.0-12.

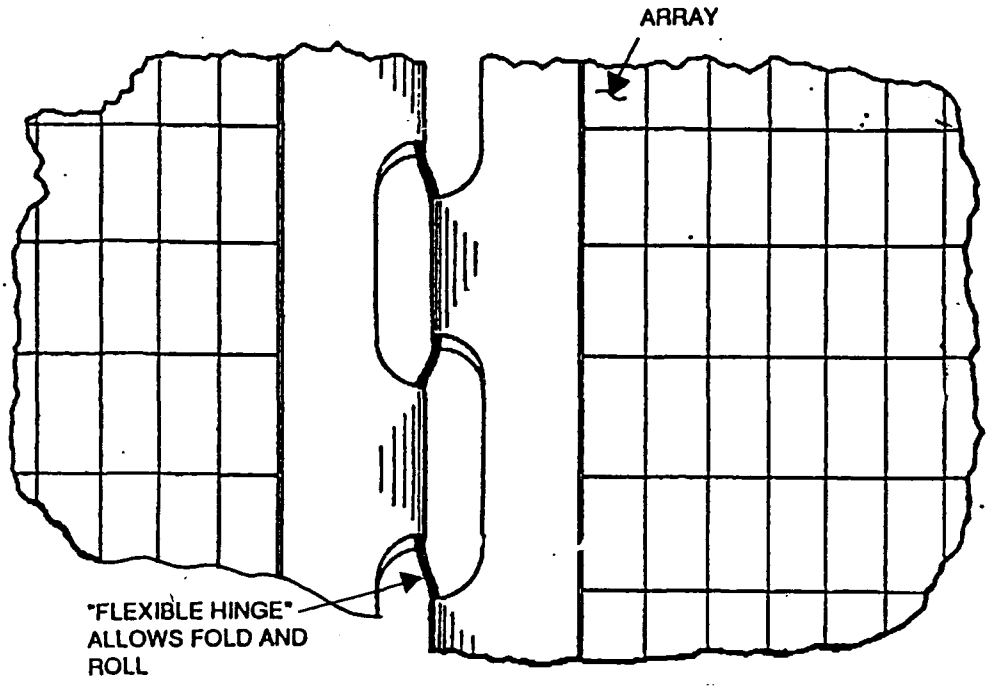

Figure 3.0-12. Array Hinge Concept

3.3 AMORPHOUS SILICON DESIGN LIMITATIONS

Early testing and analysis (described in later sections of this report) concluded that a similarly manufactured blanket array incorporating amorphous silicon cells will not be the recommended choice for later program phases. Highlights of the limitations is as follows:

1. Beginning of Life (BOL) Power: BOL power was expected to be 100w at AM1.5. Actual L'Garde testing confirmed that the array generated only 93w.

2. End of Life (EOL) Power: Because of such low BOL power, the critical EOL requirement of 100w AMO after 3 years in either LEO or GEO cannot be achieved.

3. Excessive Photon Degradation: Limited Staebler-Wronski degradation (17%) was expected over the entire 3 year space mission. However, new data suggests that loss of power for aSi cells can be much more severe. Figure 3.0-13 shows 27% degradation after only 505 hours (21 days) of AMO exposure in a benign (25°C) terrestrial test environment. This data is critical but came late. This test was performed one month ago at JPL upon amorphous cells similar but not identical to those used as the L'Garde prototype array.

4. Unknown Radiation Effects: Early aSi industry tests suggested superior radiation performance by amorphous silicon. However, the anticipated definitive JPL tests needed are still far from completed. As a result, no EOL predictions can be made with confidence at this time.

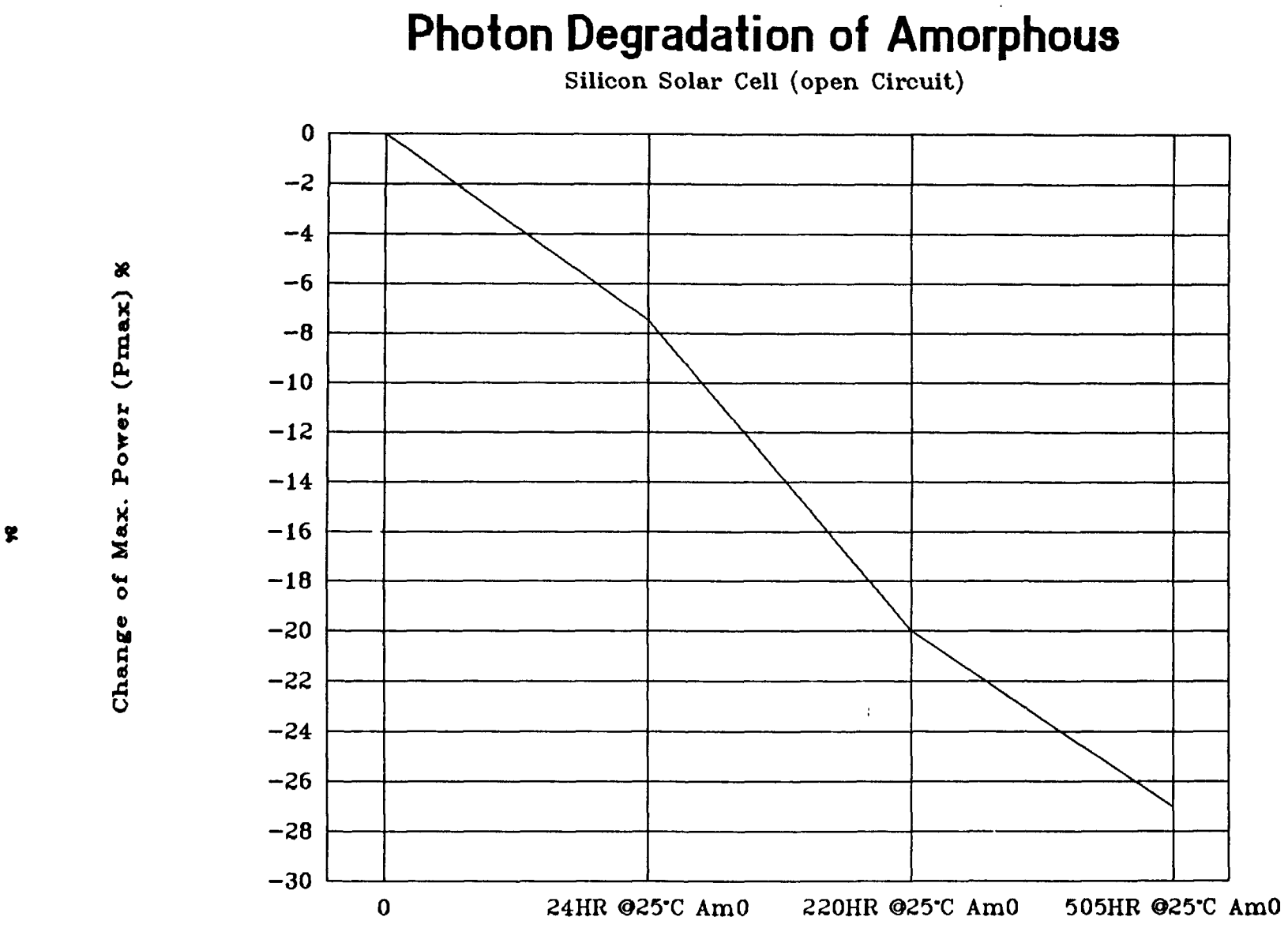

Figure 3.0-13. Photon Degradation of Amorphous Silicon Solar Cell
(NASA JPL 9/17/91: aSi Solarex Solar Cell - Courtesy B. Anspauce)

5. Qualification Testing: Likewise, numerous other tests (such as temperature cycling, high-temperature-low-vacuum dwell, etc.) essential to qualifying the cell and blanket materials for survival in space, were not completed for representative amorphous silicon solar cells as expected. Development of amorphous silicon is not proceeding rapidly enough to sufficiently minimize risk in achieving the specified goals of the ITSAT program. Although completing the required development through in-house experiments was seriously considered, such effort proved to be well beyond the scope of this program.

6. Unsuitable Blanket Materials: The use of mylar in the blanket substrate is not applicable to the space environment due to its known susceptibility to UV radiation. Other inherent components, such as the bypass diodes are also not space qualified.

Because of the above the Phase 1 program effort proceeded along two parallel paths.

A) L'Garde continued the use of the aSi solar array, but only for Phase I prototype system analysis. The amorphous array, although not flight hardware, remained a fully suitable Phase 1 article for ITSAT integration and testing. First, its size met specifications. Second, the blanket materials, although far from ideal for actual space application, were almost identical in thickness and flexibility to the material (kapton) most commonly used in deployed blanket arrays. Third, the array was populated with actual powered solar cells that could be monitored visually, mechanically and electrically before and after folding, packaging and deployment operations. Fourth, the cells and cell modules themselves were similar to other thin solar cell technologies (i.e., CIS) that were still under consideration for the recommended design.

Indeed, use of this prototype blanket throughout Phase I has led to improved handling techniques, the identification of "Z" fold advantages and disadvantages and the need to include light weight restraining guides to prevent large out of plane excursions of the torus during deployment that can put excessive or misdirected stresses on the array blanket.

B) L'Garde continued the detailed trade-off studies and predictions for cell-blanket arrays for specific missions in well-defined space environments. The goal was the identification of components and a design suitable for recommendation for Phase 2 and Phase 3 of the ITSAT Program as stipulated in Task 4.1.5 of the Statement of Work.

3.4 ALTERNATE DESIGN FLIGHT PREDICTIONS

Path B, described immediately above, entailed detailed flight predictions based on the two missions outlined in Table 3.0-2. As shown, LEO and GEO orbits have considerably different radiation and thermal environments expected to affect BOL and EOL of the cells under study differently. The matrix of cells was thin crystalline silicon, GaAs/Ge, cleft GaAs and CIS.

TABLE 3.0-2. MISSION SPECIFICATIONS

ORBIT	LEO	GEO
Altitude(km)	740	35,794
Orientation	Polar(90°)	Equator(0°)
E O L Power(w)*	100–200	100–200
Duration (yr.)	3.0	3.0
Orbit Duration	100 min	24 hr
Eclipse Duration	34 min	1.2 hr
Eclipse Cycles/3yrs	15,330	264
Temperature Extremes °C	+80/–80°	+45/–170°

* per wing

3.4.1 Basic Blanket Dimensions

The basic overall blanket dimensions were fixed by the ongoing parallel torus design, development and testing program. Sides were 90.5 cm by 235.6 cm with 14 folds along the length to form 15 identical subpanels. The overall design is shown in Figure 3.0-14. The subpanel length and width were 90.5 cm and 15.7 cm respectively. The fold pattern allowed for flat stowage within the launch vehicle cavity without the complication of additional folding into a Z pattern which was shown to put stress onto the array during deployment. The 15.7 cm subpanel height coincides with the dimension of the 4 inch torus uninflated and flatted in stowage. The unit subpanel is shown in Figure 3.0-15.

The area of the entire blanket is 2.13m^2. This figure was chosen as the baseline array size under consideration in the design study. Four other blanket arrays studied in parallel were multiples of this basic unit. Thus, the total matrix consisted of the following array areas: 2.13, 4.26, 8.52, 17.04 and 34.08m^2.

3.4.2 Recommended Blanket Choice: APSA-TYPE

Parallel to solar cell selection, available blanket technologies have been carefully investigated. The most viable candidate is the blanket portion of the Advanced Photovoltaic Solar Array (APSA) system recently demonstrated by Dick Kurland of TRW (JPL Contract No. 957990-MODIO).

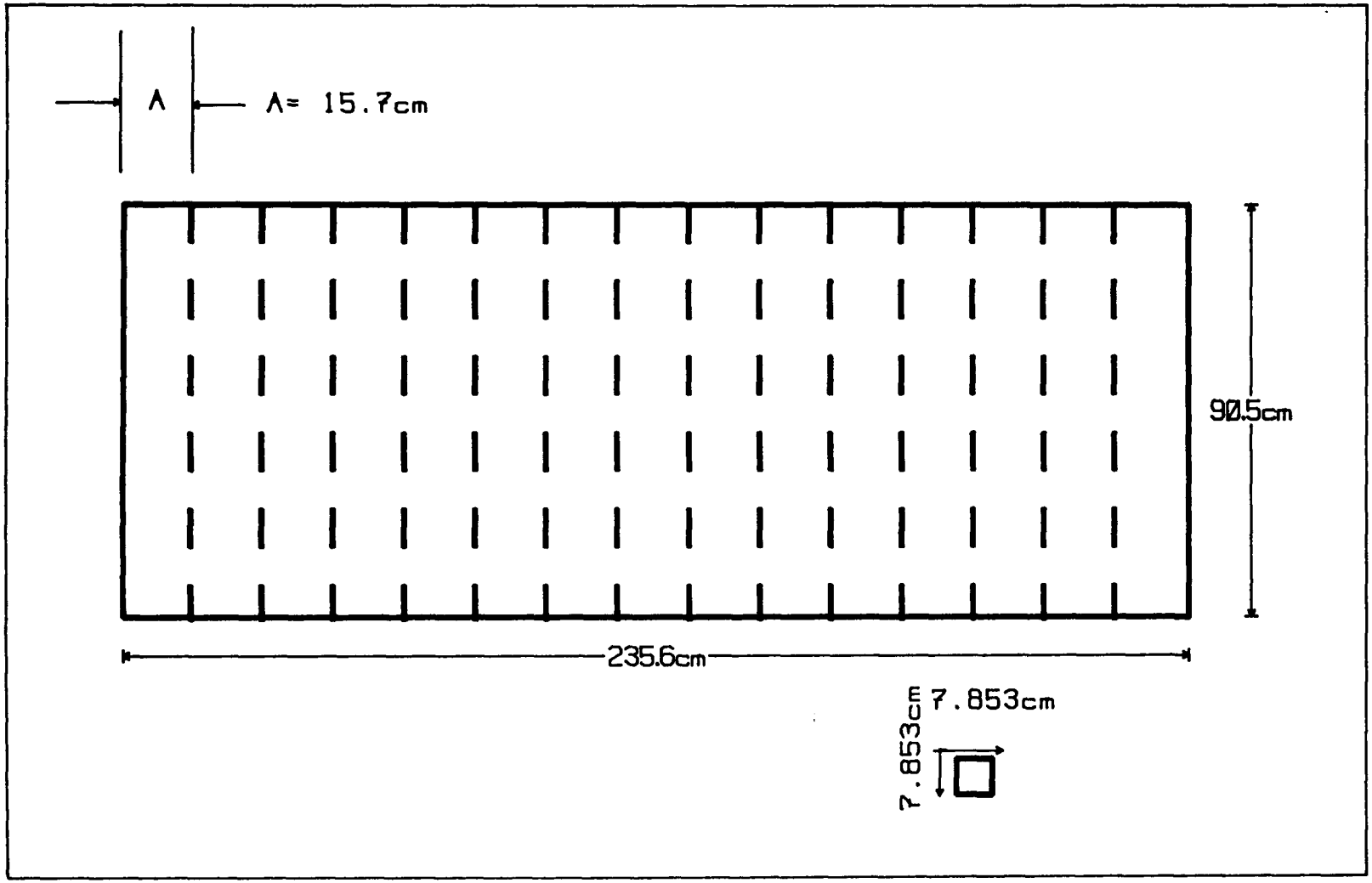

Figure 3.0-14. Total Panel (15 Sub-Panels)

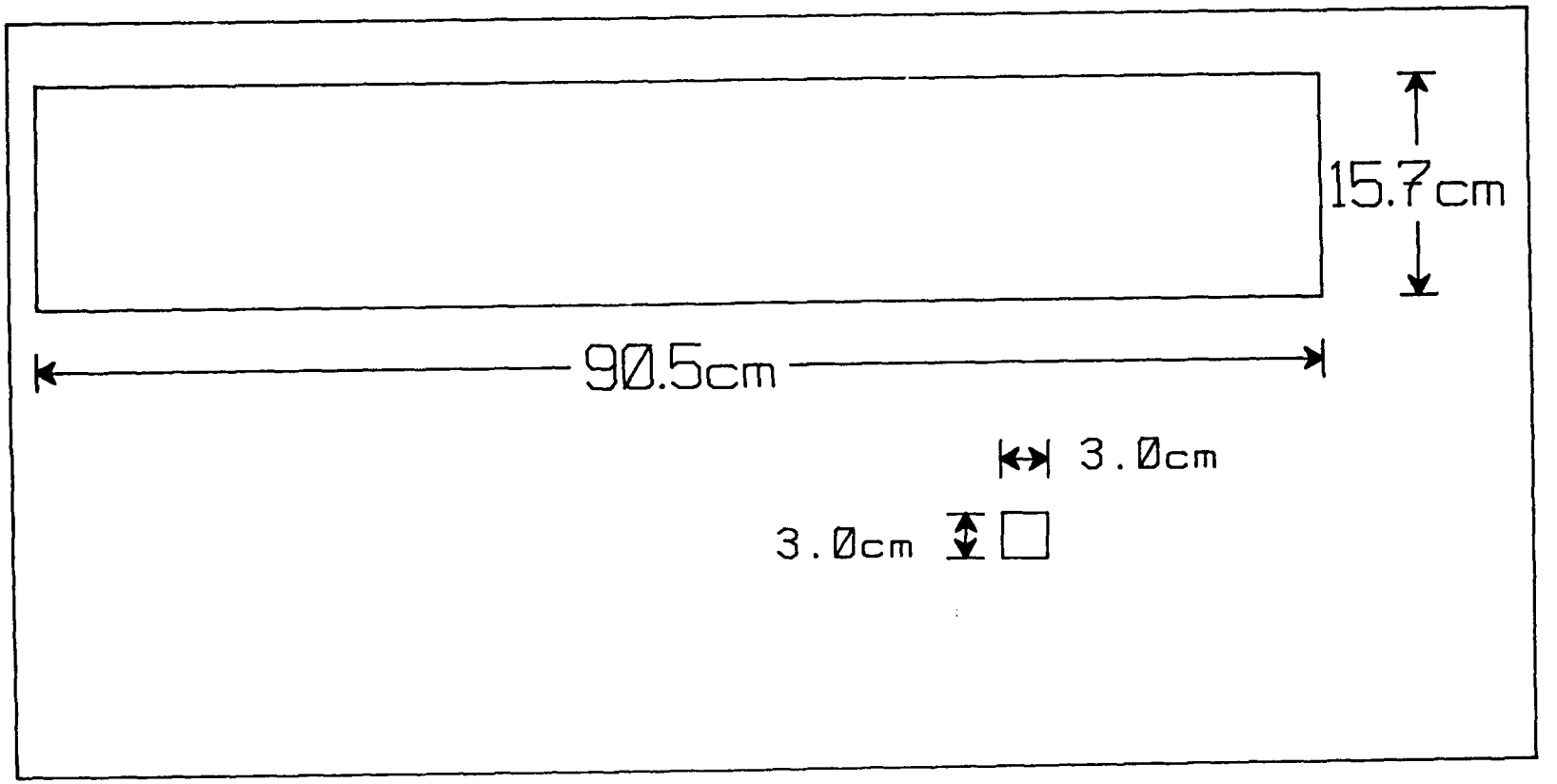

Figure 3.0-15. Sub-Panel (One of 15)

The overall system consisted of a single wing, 5.8 KW, flexible array folded into 40 large sub-panels. Overall area was 431.38 ft^2 populated with 28,800 thin crystalline Si solar cells with dimensions of 2cm x 5.7 cm. Total length was 606 in. folded accordion style and stowed during launch in a specially constructed compartment. The array was designed to be deployed in space by an 8.57 inch diameter mast.

Certainly the mast deployment method is of little use to the present L'Garde ITSAT system. However, the thoroughly space qualified and tested blanket array is especially relevant.

Its incorporation into the ITSAT design offers much leverage to the ongoing program in terms of cost, schedule and testing since the TRW array proved to be a highly successful advanced design. The APSA deployed system as a whole resulted in power densities of 138 w/kg.

Consequently, numerous visits were made to TRW to investigate applicability and critical issues. These design reviews proved that the APSA-type blanket is indeed readily compatible as a flexible substrate to each of the four types of solar cells under study. In addition, TRW is both capable and willing to fabricate the array for the ITSAT configuration.

Assuming an APSA-type blanket as the array substrate, system weight and power figures were calculated using L'Garde's inflatable torus deployment design for each of the four types of solar cells under study.

3.4.3 Packing Factors

A major consideration in power predictions is determination of the packing factor - how much loss results from dead space between and around the active area of solar cells. In calculating this figure, 2cm x 4 cm solar cells were assumed for all candidates with standard 30 mil spaces. In addition, 0.4 inch borders were assumed around the body of cells centered in each of the array's 15 subpanels (Figure 3.0-15) for all but the CIS cells. These, being thinner than the others, are expected to tolerate borders half this width.

In each case the active area was further reduced by the allocation of an inch of blanket material along its length to accommodate the electrical harness.

Based on these considerations, the overall packing factor for crystalline Si, GaAs/Ge and cleft GaAs was determined to be 0.8424, while for CIS it was 0.9430. These and other results are tabulated in Tables 3.0-3 and 3.0-4.

3.4.4 Assembly Losses Factor

Assembly losses are due to power degradation as a result of installation mismatch, diode drop and harness configuration. Each is fairly small and independent of solar cell type, yet the total impacts BOL and EOL. An assembly losses factor of .943 resulted from design analyses.

TABLE 3.0-3. CELL TRADEOFFS:BOL POWER DENSITY

	Cell Efficiency n %	Packing Factor %/100	Assembly Losses* Factor %/100	Orbit	Temp. Factor %/100	B O L array n %/100	Solar Constant w/sq.m	B O L Power Density w/sq.m
Thin Crystal Si	13.8	0.842	.943	GEO	.975	10.64	1353	144.64
				LEO	.800	8.77	1353	118.66
GaAs/Ge	18.5	0.842	.943	GEO	.950	13.96	1353	188.88
				LEO	.863	12.68	1353	171.56
Cleft GaAs	18.5	0.842	.943	GEO	.950	13.96	1353	188.88
				LEO	.863	12.68	1353	171.56
CIS	11.0	0.943	.943	GEO	.981	9.60	1353	129.89
				LEO	.844	8.26	1353	111.76

* Installation mismatch,Diode drop,and Harness losses

TABLE 3.0-4. CELL TRADEOFFS:EOL (3 YEARS) POWER DENSITY

	Cell Efficiency n %	Packing Factor %/100	Assembly Factor %/100	Orbit	Combined* Losses Factor %/100	Temp. Factor %/100	Radiation Factor %/100	E O L Array n %/100	Solar Constant w/sq.m	E O L Power Density w/sq.m
Thin Cryst Si	13.8	0.842	.943	GEO	.983	.935	.962	9.69	1353	131.11
				LEO	.983	.760	.892	7.30	1353	98.77
GaAs/Ge	18.5	0.842	.943	GEO	.983	.930	.960	12.90	1353	174.54
				LEO	.983	.843	.901	10.97	1353	148.42
Cleft GaAs	18.5	0.842	.943	GEO	.983	.930	.948	12.74	1353	172.37
				LEO	.983	.843	.852	10.38	1353	140.44
CIS	11.0	0.943	.943	GEO	.988	.973	.990	9.31	1353	125.96
				LEO	.988	.836	.990	8.00	1353	108.24

* UV,Temperature Cycle Fatigue,Cover Darkening and Adhesion Darkening

3.4.5 Temperature Factor

Each type of solar cell operates at a different temperature in space due to variations in its absorptivity and emissivity. Orbit is critical: LEO temperatures exceed GEO as a result of the contribution of heat radiated from the earth's surface.

A table of the estimated operating temperatures of the four solar cell types is given in Table 3.0-5. In each case EOL exceeds BOL due to lower power after three years as a function of radiation. Since a degraded solar cell cannot off-load electrical energy as efficiently, there is a greater generation of heat.

TABLE 3.0-5. OPERATING TEMPERATURES

	GEO		LEO		
Solar Cell	BOL °C	EOL °C	BOL °C	EOL °C	K (%/°C)
Si	33	41	68	76	0.50
GaAs/Ge	48	56	83	91	0.25
Cleft GaAs	48	56	83	91	0.25
CIS	33	35	68	70	0.39

The temperature degradation factor, TF, is computed using the value of each cell's temperature coefficient, K, which is the measure of loss in maximum power per °C (%/°C). The computation is as follows:

$$TF = 1 - [K\ (T_{op} - T_{REF})]$$

where T_{op} is the operating temperature in °C and T_{REF} is 28°C, the reference temperature at which solar cells are tested.

BOL and EOL temperature degradation factors are shown in the appropriate columns of Tables 3.0-3 and 3.0-4.

3.4.6 Radiation Losses

Radiation losses result from continuous omnidirectional proton and electron bombardment in the space environment. However, such bombardment is attenuated by the presence of any shielding materials on front and back surfaces. In general, the thicker and more massive the material, the greater the shielding effect. For this reason, cover glasses of various thicknesses are routinely

added to the cell's front surfaces, depending on the environment and the desired EOL (within limits).

Specifically in this study, the silicon cells were assumed to have 2 mil glasses while CIS, far superior in radiation hardness, had none. Both GaAs type cells, Ge and cleft, were fitted with 3 mil covers. Front electron and proton fluences were then calculated. The shielding effects of the blanket components protecting the back side were next determined for both electrons and protons.

Finally, the overall effect on P_{MAX} from the four radiation components was determined by comparison with known, calibrated power loss behavior for the particular type of cell under consideration.

The resulting radiation degradation factors are shown in Tables 3.0-3 and 3.0-4.

3.4.7 EOL Combined Losses

An additional loss factor is included in Table 3.0-4 to account for change due to UV exposure, fatigue from temperature cycling and attenuated transmission resulting from cover and adhesion darkening. The combined value for these effects is smaller for CIS since the cell was assumed to have no cover.

3.4.8 BOL/EOL Predictions

By means of Tables 3.0-4 and 3.0-5, the BOL and EOL powers in terms of watts per unit area were readily determined. Total system power was then calculated for the five different torus deployment systems, each distinguished by the different array area defined in Section 3.4.1.

BOL and EOL predictions for the five systems are tabulated in Table 3.0-6.

3.5 SYSTEM POWER DENSITIES VERSUS TOTAL ARRAY POWER

Areal densities in kilograms per unit array area were next calculated for each of the three subcomponents of the entire system:

a) solar cell stack
b) blanket stack
c) torus weight and deployment system

The sum of these yielded the system areal density for each solar cell type for each of the five array-torus deployment systems.

Results were plotted in Figures 3.0-16 and 3.0-17 for BOL GEO. Although the highest power densities were achieved by the immature cell technologies, cleft GaAs and CIS, values for thin crystalline Si are still very high compared to conventional technologies. BOL LEO data of Figures 3.0-18 and 3.0-19 mimic this observation.

TABLE 3.0-6. BOL/EOL POWER PREDICTIONS

TORUS DESIGN		System 1 (2.13m²)	System 2 (4.26m²)	System 3 (8.52m²)	System 4 (17.04m²)	System 5 (34.08m²)
B O L						
Cryst Si	GEO	308	616	1232	2468	4929
	LEO	253	506	1011	2022	4044
GaAs/Ge	GEO	402	805	1609	3219	6437
	LEO	365	731	1462	2923	5847
Cleft GaAs	GEO	402	805	1609	3219	6437
	LEO	365	731	1462	2923	5847
CIS	GEO	277	553	1107	2213	4427
	LEO	238	476	952	1904	3809
E O L						
Cryst Si	GEO	279	559	1117	2234	4468
	LEO	210	421	842	1683	3361
GaAs/Ge	GEO	372	744	1487	2974	5948
	LEO	316	632	1265	2529	5058
Cleft GaAs	GEO	367	734	1469	2937	5874
	LEO	299	598	1197	2392	4786
CIS	GEO	268	537	1073	2146	4293
	LEO	231	461	922	1844	3689

(All unlabeled values are in watts)

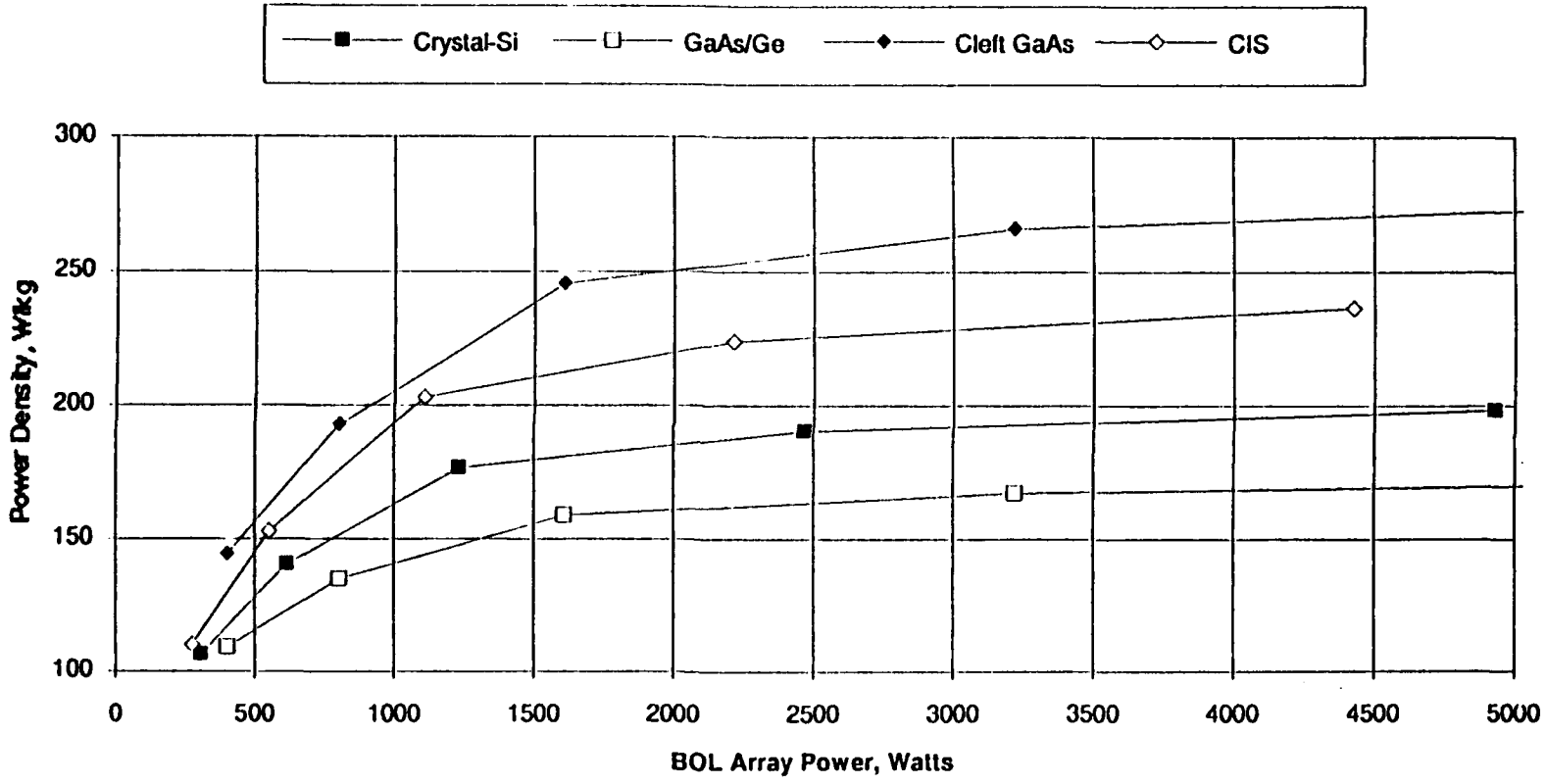

Figure 3.0-16. BOL Power Density vs Deployed Array Power, APSA-Type Flexible Blanket/Torus Deployed, 3 Year GEO

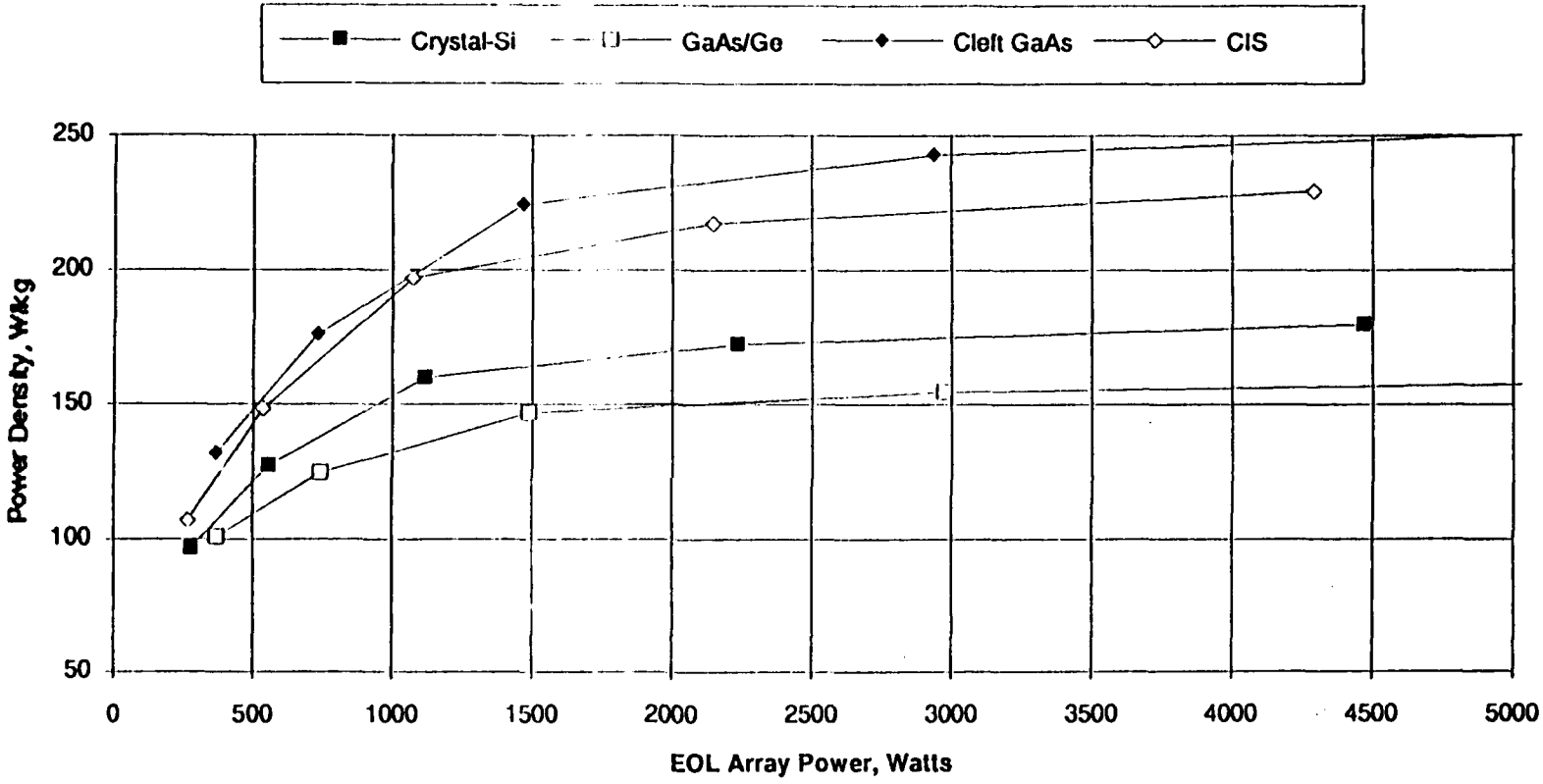

Figure 3.0-17. EOL Density vs Deployed Array Power, APSA-Type Flexible Blanket/Torus Deployed, 3 Year GEO

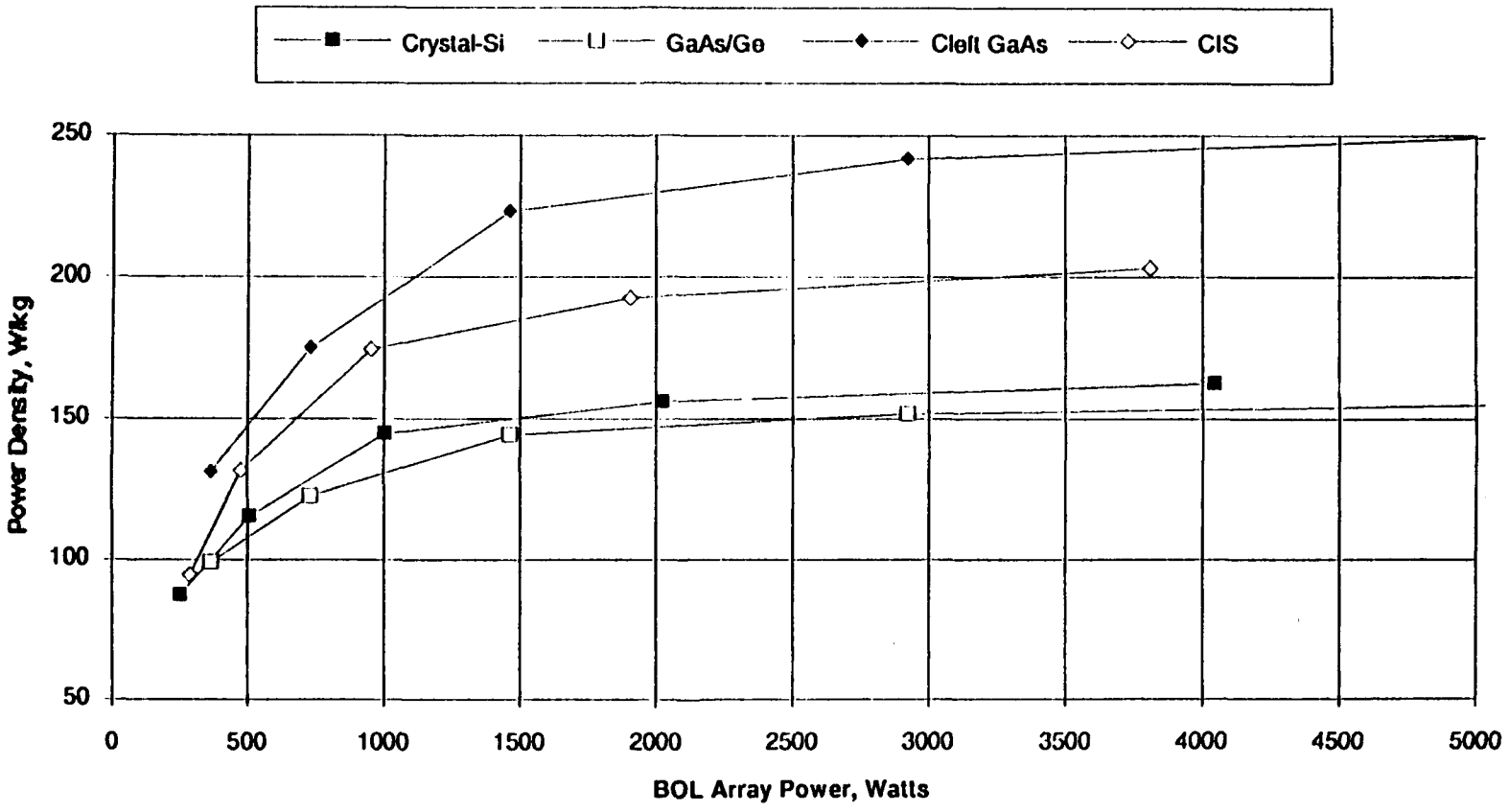

Figure 3.0-18. BOL Power Density vs Deployed Array Power, APSA-Type Flexible Blanket/Torus Deployed, 3 Year LEO

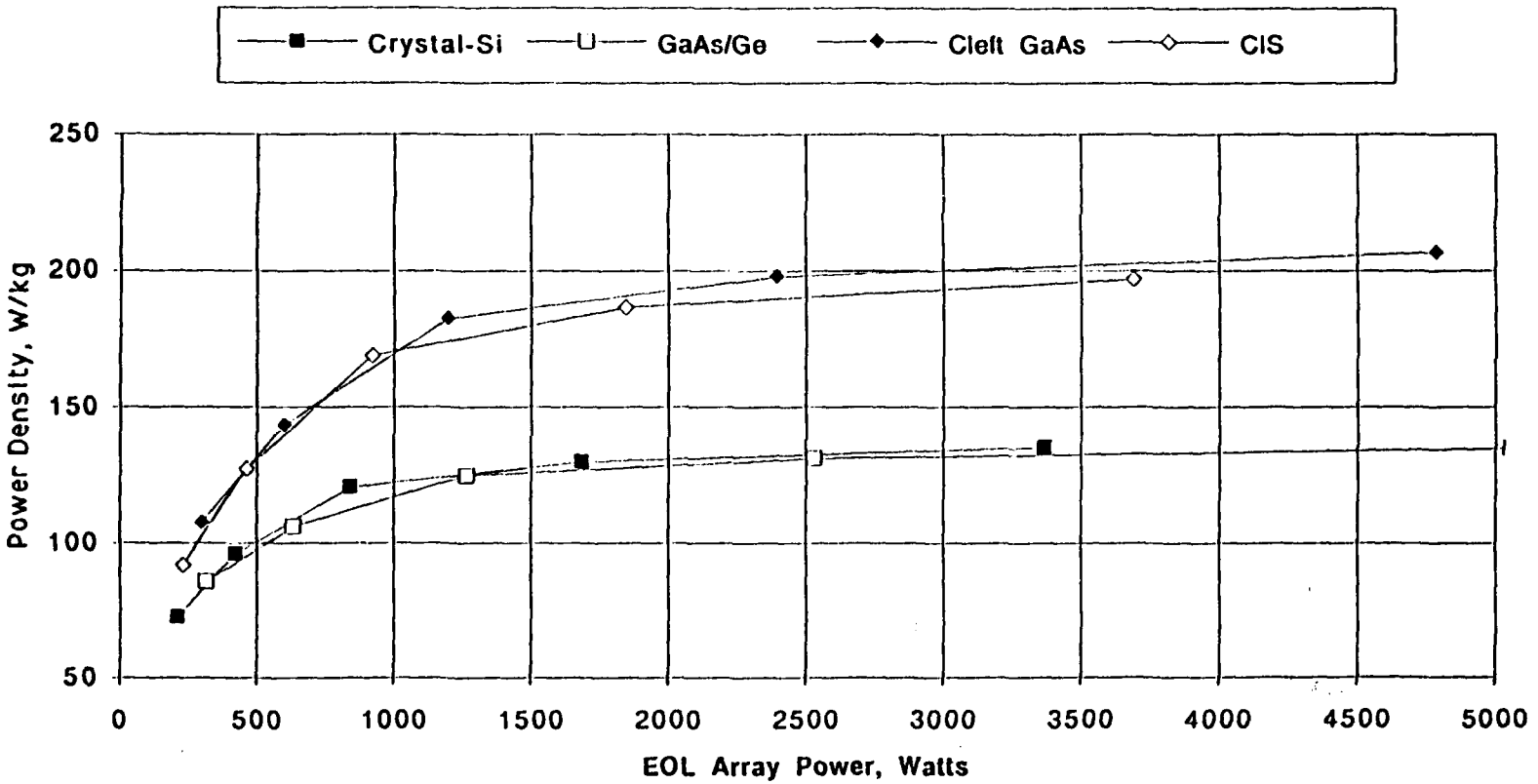

Figure 3.0-19. EOL Density vs Deployed Array Power, APSA-Type Flexible Blanket/Torus Deployed, 3 Year LEO

3.6 DEPLOYMENT COMPARISON

The BOL geosynchronous power density in watts per kilogram was compared for four distinct state-of-the-art deployment systems: ITSAT, BI-STEM, ASTROMAST and DSCS III. In all cases, thin crystalline Si solar cells were used. The first three assumed these cells to be fabricated in an APSA-type blanket as recommended in Section 3.4.2. The fourth used the identical geometrical and power layout on a standard, rigid panel constructed of a half inch honeycomb core, 8 mil Al facesheets, and conventional adhesives. This deployment comparison is summarized in Table 3.0-7. Of these, ITSAT has already been adequately described. A brief outline of the three other methods is in order.

TABLE 3.0-7. DEPLOYMENT SYSTEM COMPARISON

Deployment System	Array Substrate	Solar Cells
ITSAT	Flexible:APSA Blanket	Thin Crystalline Si
BI-STEM	Flexible:APSA Blanket	Thin Crystalline Si
ASTROMAST	Flexible:APSA Blanket	Thin Crystalline Si
DSCS III	Rigid:Al Honeycomb	Thin Crystalline Si

BI-STEM consists of two rolls of preformed, springy material, stainless steel or beryllium copper, that are stored flat on two rollers but curl longitudinally when the rollers are activated and the material unravels. The two curls, one inside the other for extra strength, then form an extendable hollow rod which deploys the flexible array to which it is attached. The system is applicable only for lightweight panels to a limited extension (approximately 8 meters). Major contributors to weight are the activator motor and gears, the bistem material and the array's storage container.

ASTROMAST is a heavier, single, extendable, usually telescopic shaft that is motor driven to deploy the attached blanket. It is similar in concept to the single shaft used to extend a projector screen. Components of weight are mast, motor, stowage container and related hardware.

DSCS III is representative of a latch and spring deployment scheme routinely used for conventional smaller rigid arrays. Typically, such systems are not light. Specifically, DSCS III involved 11.0 kilograms of hardware to deploy a 1.0 kilowatt array. An advantage is that folded rigid arrays require no stowage container during launch. The disadvantage is that a relatively massive array substrate is required. Contrary to the 1000 watt DSCS III design,

the arrays deployed in this comparison study varied from 308 to 4,929 watts. To accommodate these different sizes, a weighted scaling formula was used to extrapolate from the original DSCS weight and watt configuration.

Results are shown in Figure 3.0-20 and demonstrate that ITSAT is significantly superior to all other deployment methods in all ranges. Power densities for the smallest arrays, 308 watts, were 390% better than DSCS and 28% better than BI-STEM. For a 1232 watt panel, these figures were 447% and 49% respectively. Significantly, the ITSAT design remains distinctly superior even at higher powers. At 4929 watts, the power density was 68% greater than the ASTROMAST design and 44% better than the TRW APSA mast-deployed blanket system.

Other significant figures of merit are included in Figure 3.0-20 for further comparison. These are averaged state-of-the-art power densities for numerous other satellite systems presently in use. The data is reconfigured in Table 3.0-8 for clarity. In general, rigidly deployed arrays result in power densities in the 40's, while for flexible systems, the figure is roughly 60. The recent highly successful TRW mast-deployed APSA system was considered a technological breakthrough at 138 watts/kg. However, it is applicable only to large solar arrays. The ITSAT design at 106 to 198 watts/kg is significantly better for all array sizes.

3.7 PHASE 2 AND 3 RECOMMENDED ARRAY DESIGN

Based upon the detailed study described in this section, the best ITSAT system choice is the thin crystalline silicon solar cells incorporated in a flexible kapton APSA-type blanket.

Although cleft GaAs and CIS exhibit definite promise, it is clear they are presently clearly developmental cells that cannot mature and be qualified in sufficient time for incorporation into Phase 2 and 3 of the ITSAT program. The recommendation of the thin crystalline Si/APSA-type blanket array system is based on the following key criteria:

1) fully developed cell and blanket technologies
2) fully qualified cell and blanket materials
3) high efficiency
4) light weight
5) high BOL/EOL power in both LEO and GEO
6) superior power density
7) maximum program leverage
8) proven, experienced cell fabricator
9) willing blanket fabricator
10) available technology: cells and blanket material in production quantity
11) best schedule
12) lowest price

In short, it best meets all technical and administrative program requirements.

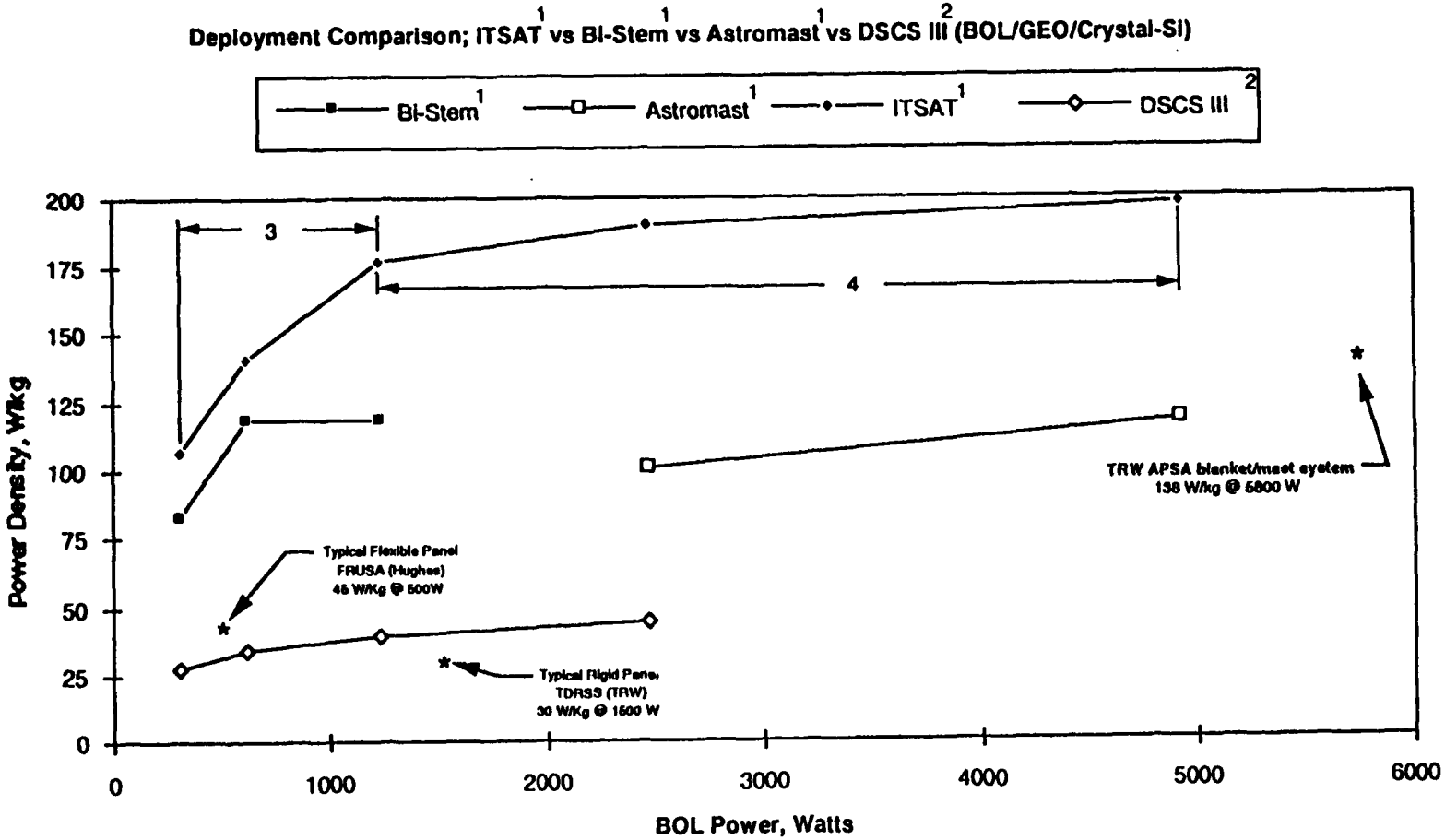

1. L'Garde flexible blanket design.
2. Rigid panel design.
3. ITSAT Based on Aluminum Laminate.
4. ITSAT Based on U-V cured resin structure.

Figure 3.0-20. Deployment Comparison, ITSAT vs Bi-Stem vs Astromast vs DSCS III (BOL/GEO/Crystal-Si) Single Panel

TABLE 3.0-8. STATE-OF-THE-ART POWER DENSITIES

Type	Array Size (kw)	Power Density (Watts/KG)
ITSAT	0.3–5.0	106 – 198
RIGID	generally ≥ 1.0	43
FLEXIBLE	generally ≥ 1.0	60
APSA (TRW)	≥ 5.8	138*

** Demonstrated in design only ; not flown*

3.8 ARRAY FABRICATION DESIGN SPECIFICATION

In light of the results of this design study, attention is being focused on developing an array fabrication design specification. Dimensions, fold pattern and subpanel areas were previously described in Section 3.4.1. The cell of choice is 2.2mil 10 ohm-cm polished silicon, 13.8% efficient. It will have a boron diffused back surface field and an aluminum back surface reflector. The original source will be Spectrolab, where this type of cell is generally referred to as a K6 3/4. Initial solar cell dimensions of 2 x 5.68 cm will be considered although sizing might be varied somewhat to achieve the .8424 maximum packing factor described in the design predictions of Section 3.4.3.

Cell cover will be 2 mil CMX Cerium oxide doped borosilicate, preferably edge etched, with UV and AR coatings.

Cover adhesive will be DC 93-500, 1.5 mils, while cell to substrate adhesive will be CV1-1142, 2 mils. The substrate material will be 2 mil carbon-loaded kapton. This cell assembly-blanket arrangement is shown in Figure 3.0-21.

Interconnects will be shallow 2 in-plane rounded box loop design consisting of 1 mil silver plated invar.

3.8.1 ITSAT System Design Flexibility

The possible future advantage of the CIS and cleft GaAs technologies revealed by this design review cannot be ignored. Of the two, CIS has the more potential due to the probability of cells achieving lower cost, lighter weight, greater radiation hardness and monolithic integration. Full development, however, is still at least 2 years away - well beyond the scope of this immediate program unless there is an extraordinary infusion of development funding. Boeing and Martin Marietta, for example, have ongoing IR&D programs that might accelerate in-house CIS capability considerably.

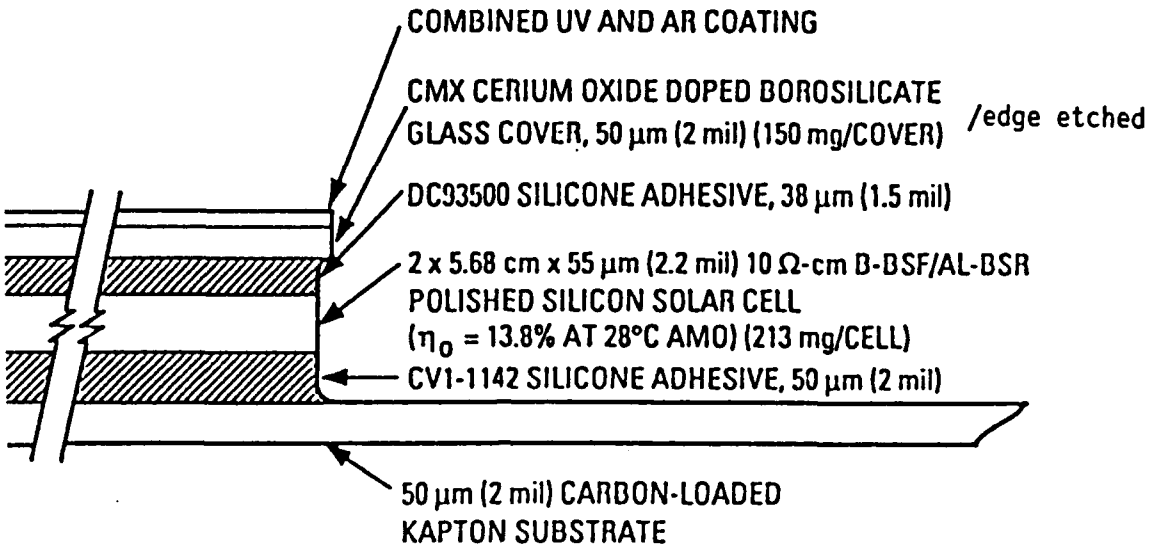

Figure 3.0-21. Recommended Cell Assembly-Blanket Arrangement

To take advantage of any such future sudden breakthroughs, an important criterion of the basic ITSAT solar array design is flexibility to allow for the interchange of the thin crystalline silicon solar cells with those of either the cleft GaAs or CIS emerging technologies.

3.8.2 Array Population Options

The final layout and electrical diagram of individual cells on the kapton blanket is open to further consideration since the system has been purposely designed to supply a premium of area. This allows a choice of attractive options.

Consider, for example, the simplest ITSAT system with the 2.13m^2 array working area: even after generous allowances for all practical limiting factors (packing density, radiation losses, etc.), it results in a GEO BOL/EOL power of 308 w/279w per wing - well over program requirements. Some of the many choices are:

Option 1: The provision of additional power depending on cost and customer inclination.

Option 2: Coverage of unused array area with mass simulators.

Option 3: Timely inclusion of small experimental arrays of promising cells under development, for example CIS or cleft GaAs, depending on availability.

Each option will be fully explored with DARPA/ASTP.

3.9 STRUCTURE

The concept definition study showed it is impractical to develop a purely inflatable structure for long term space applications if the internal pressure requirement is above a few hundredths of a psi. As a result the selected structure is deployed by inflation and then rigidized. The structure is made up of thin walled tubular elements (The rectangular structure shown in Figure 3.0-1). The tubular elements are fabricated from a single layer of plastic-aluminum-plastic laminate with a total thickness of approximately .004 in. The material is thin enough to be packaged but when inflated and rigidized is capable of carrying significant loads in compression and bending.

The structure is pressurized to one or two psi to deploy it. The pressure is then raised sufficiently to strain the aluminum past it's yield point. This process removes all packaging wrinkles and results in a smooth thin walled tube. The pressure is then vented leaving a rigid structure not dependent on internal pressure.

3.9.1 Development of Aluminum-Plastic Laminate for Rigidizable Torus

The purpose of the plastic film on either side of the 3 mil aluminum is to assure a pressure tight structure during the rigidization process. If bare aluminum foil were to be folded and packaged as required by the torus, the foil would develop sufficient pin holes (one at every compound fold) to make inflation and rigidization unreliable. Once rigidized the presence of pin holes in the foil has no detrimental effect on the strength of the structure.

It is necessary to provide both an inner and outer layer of film because the sharp corners created by compound folds tends to tear the layer of film exposed to the sharp corner of the aluminum foil. The opposite layer of film then provides the required pressure integrity. During packaging sharp corners can occur on both sides of the foil, hence, the need for film on both sides. Tear resistance then becomes an important property of the plastic film. Apart from tear resistance of the plastic film there are other important criteria which should be taken into consideration to select the proper laminate for this particular application. These mainly are weight, volume, compression and bending strength. (Resistance to the space hazards was left to be addressed in Phase 2 of the program).

A matrix of 22 different aluminum/plastic laminates were developed and fabricated utilizing a good representation of various commercially available plastic films. These laminates were made by pressing 3 mil thick aluminum foil (type 1145-0) and plastic film in the hot press (≈ 350F and 30 psi pressure). Adhesives were used to bond the foil to the plastic.

Table 3.0-9 gives the laminate type and initial test data obtained on tear strength, areal density, compression failure (performed on small coupons) and modulus.

From the beginning of laminate development, we were aware that the best criteria to test these laminates (apart from tear strength) was testing of cylindrical tubes made from each laminate for compression and bending strength. This, however, was not done because of considerable time and money needed to fabricate test cylinders. Instead, a stepwise testing process was adopted for

TABLE 3.0-9. MATRIX OF NEW POLYMER FILM-ALUMINUM LAMINATES DEVELOPED AND TESTED

Laminate Type	Lam. #	Thickness Mils	Areal Density Oz./Y² (B)	Init.Tear Resist Pounds	Tear Strength X10⁻³,PPI(A)	A/B x 10³	Compression Failure (lbs.) MD	Compression Failure (lbs.) TD	Compression Failure PSI MD	Compression Failure PSI TD	Tensile Modulus PSI X10⁻³ MD	Tensile Modulus PSI X10⁻³ TD	Yield, PSI MD	Yield, PSI TD
TF-330-ALUM 3 ply (1)		5.6	7.78	1.97	3.5	45.0								
TF-330-ALUM 2 ply		4.3	6.84	1.71	3.98	58.2								
PECN-ALUM 3 ply (2)		5.8	7.92	3.71	6.40	80.8								
PECN-ALUM 2 ply		4.6	7.05	2.77	6.02	85.4								
AN-33-ALUM 2 ply (3)	5	7.1	7.915	5.51	7.76	98.0	3.29	5.17	371	583	590	-	400	800
AN-33-ALUM 2 ply	6	5.6	6.99	5.09	9.09	130.0	4.29	3.79	613	541	434	1,066	600	760
Dartek-C-101-ALUM 2 ply (4)		4.9	7.31	3.09	6.31	86.3								
Dartek-C-101-ALUM 3 ply		6.6	8.63	3.88	5.88	68.1								
Dartek-T-420-ALUM 3 ply (5)	9	5.6	7.84	5.51	9.84	125.5	4.04	3.33	577	476	390	1,056	650	400
Dartek-T-420-ALUM 2 ply	10	4.3	7.03	3.17	7.37	104.8	2.37	2.69	339	384	975	1,447	1800	1000
1/4 mil Mylar-ALUM 2 ply		3.4	6.57	1.11	3.27	49.8								
1/4 mil Mylar-ALUM 3 ply	12	4.3	7.02	2.30	5.35	76.2	4.24	3.24	789	603	800	1,209	1000	800
1/2 mil Mylar-ALUM		4.7	7.50	1.86	3.96	52.8								
1/2 mil Mylar-ALUM 2 ply		4.1	6.85	2.17	5.29	77.2								
1 mil Mylar-ALUM 3 ply	15	5.3	8.31	3.83	7.22	86.9	5.95	5.91	898	892	920	1,467	600	800
1 mil Mylar-ALUM 2 ply	16	4.3	7.25	4.73	11.00	151.7	3.92	5.79	729	1077	957	1,887	1000	3200
AN-19-ALUM 2 ply (6)	17	8.0	8.01	7.66	9.58	119.6	7.71	4.12	771	412	525	638	800	670
AN-19-ALUM 3 ply	18	10.9	9.67	12.63	11.59	119.9	9.63	7.04	517	707	240	473	400	600
TF-310-ALUM 3 ply (1)		5.3	7.72	2.40	4.53	58.7								
TF-310-ALUM 2 ply		4.3	6.99	2.12	5.05	72.2								
PCN-ALUM 2 ply		7.5	9.63	4.85	6.47	67.2								
GV Laminate-inhouse 2 ply		5.9	9.32	4.11	6.97	74.8								

1) TF-310 & 330: polyurethane film
2) PECN: polyethylene coated nylon film
3) AN-33: nylon reinforced 1/4 mil polyester film
4) Dartek C101: unoriented nylon film
5) Dartek T420: oriented nylon film
6) AN-19: nylon reinforced 1/2 mil polyvinyl fluoride film
7) PCN: polyurethane coated nylon ripstop
9) All laminate were made using aluminum foil type 1145-0 (MD and TD) Machine and Transverse Directions

initial screening of laminates in Table 3.0-9. Expensive tube testing was then only performed on potential candidates identified by the screening tests. The sequence was as follows:

Step 1: All laminates were initially tested for tear resistance, areal density and thickness. The 22 laminates thus were narrowed down to 9. These selected laminates were numbers 5, 6, 9, 10, 15, 16, 17 and 18. (See Lam. # column in Table 3.0-9).

Step 2: The 9 selected laminates were then tested for compression resistance (using small coupons) and modulus (as an indication of bending strength). The laminates were then ranked based on their tear, compression, yield resistance and strength. Figures 3.0-22 and 3.0-23 show a simple illustration of the way groups of laminates (close to each other) were placed in the same rank. Table 3.0-10 gives the results of the ranking process. Each group of laminates with corresponding properties close to each other were ranked and placed within the same group.

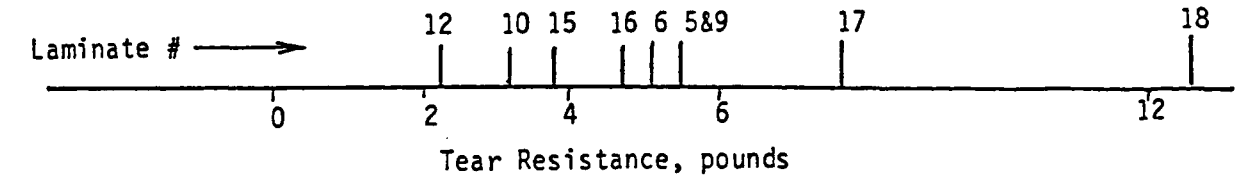

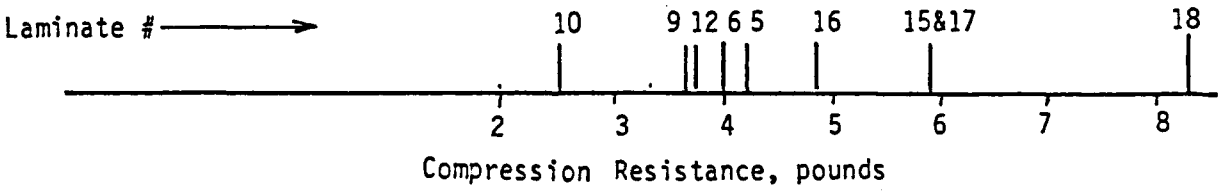

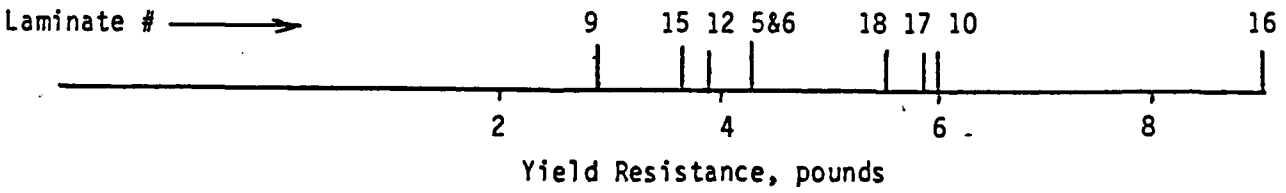

Figure 3.0-22. ITSAT Selected Laminate Candidates Based on Their Resistance

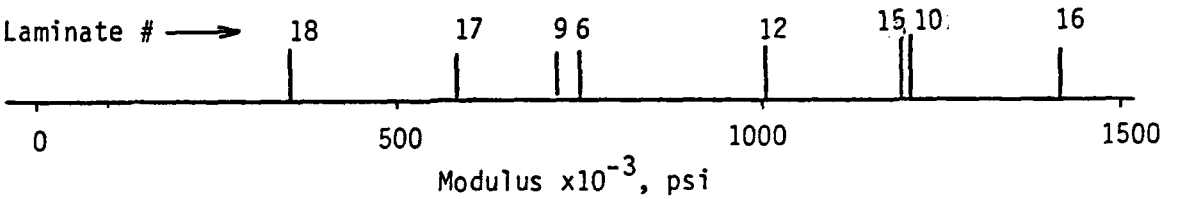

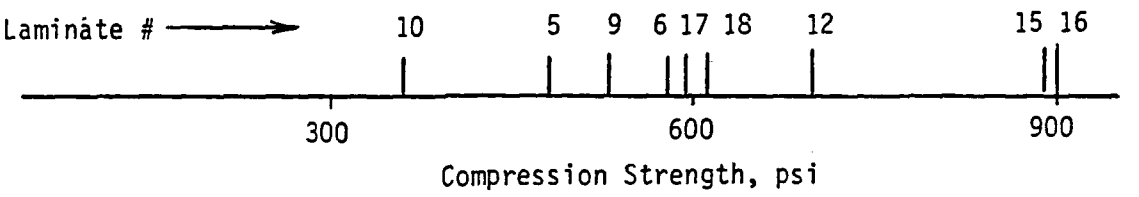

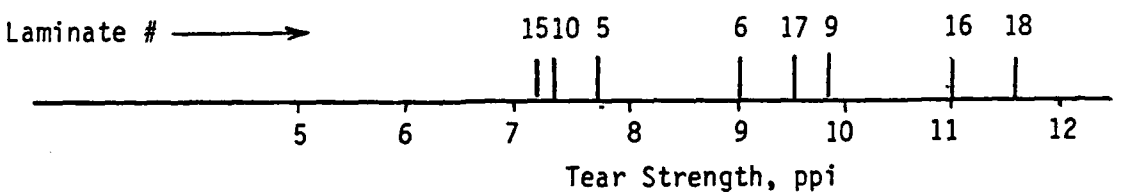

Figure 3.0-23. ITSAT Selected Laminate Candidates Based on Their Strength

TABLE 3.0-10. RANKING OF SELECTED LAMINATES

* Ranking Based on Resistance

	Tear (lbs)	Compression (lbs)	Yield (lbs)
Best	18	18	16
	17	15 & 17	10, 17 & 18
Worst	5, 6, 9 & 16	16 & 5	5 & 6

* Ranking Based on Strength

	Modulus psi	Compression psi	Tear ppi
Best	16	16 & 15	18 & 16
	10 & 15	12	9 & 17
Worst	12	18, 17 & 6	6

The two top laminates from each group (i.e. #'s 18, 17, 16 and 15) were selected for large scale compression testing on actual tubes.

These four laminates were further down selected by eliminating laminates #16 and 17 based on the following rational.

- Both #16 and #17 are 2 ply laminates. It was suggested that 2 ply laminates are considerably more prone to tear and puncture during packaging (because of the aluminum being covered on only one side).

- Laminate #15 was preferred to #16 because L'Garde had previous experience with a similar 3 ply laminate structure (i.e. Mylar-Al-Mylar) and L'Garde considered this an important plus.

Based on the above discussions laminates #18 and #15 were selected for further testing. Figure 3.0-24 gives the cross-section of these laminates.

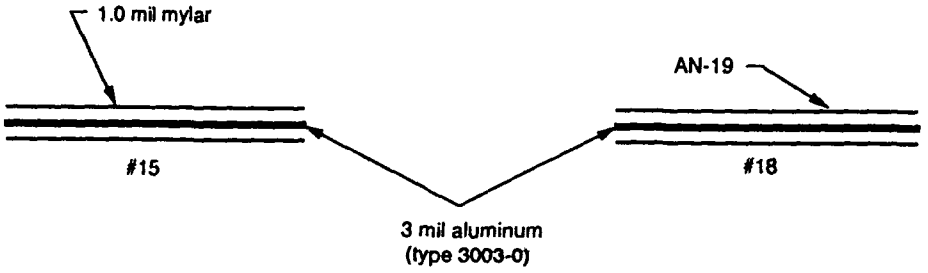

Figure 3.0-24. ITSAT Cross Section of Final Candidate Laminates

24" x 24" pieces of the selected laminates (i.e. #15 and #18) were fabricated using vacuum bagging methods. Cylindrical tubes of 3.5" diameter and 12" long were fabricated using adhesively-bonded double butt joint (1.0" wide) and then closed at both ends by an epoxy-bonded plastic cap. The tubes were then accordion folded, inflated and then rigidized under 15 psi pressure.

For comparison purposes 3 ply laminates of ¼ mil-Kapton-3 mil-Al-¼ mil Kapton, ¼ mil mylar-3 mil-Al-¼ mil Mylar, and bare 3 mil aluminum tubes were also made and tested.

All the laminates were made using 3 mil aluminum foil type 3003-0 which exhibited superior tear strength to that of type 1145-0. Table 3.0-11 compares the initial tear strength of various 3 mil aluminum foils, measured by ASTM D1004 test method.

The buckling strength of these tubes was measured on a tensile tester. Table 3.0-12 shows the results of compression testing of the tubes.

TABLE 3.0-11 INITIAL TEAR RESISTANCE OF DIFFERENT 3 MIL ALUMINUM FOILS, POUNDS

TYPE	1145 - 1419	1100-0	1145-0	3003-0
MD*	1.88	2.34	2.47	3.70
	2.77	2.28	2.38	3.27
TD*	3.13	2.26	2.56	3.49
	2.42	2.65	2.47	2.81

* MD: Machine Direction
TD: Transverse Direction

Figure 3.0-25 shows the relationship between displacement and compression force of tested tubes before they buckled. Figures 3.0-26a to 3.0-26d show typical accordion folded tubes during different stages of inflation/rigidization and compression testing before it buckles.

TABLE 3.0-12. BUCKLING STRENGTH OF CYLINDRICAL TUBES MADE OUT OF ALUMINUM-PLASTIC LAMINATES

(MEASURED: ON 3.5" x 12" TUBES AFTER ACCORDION FOLDINGS AND THEN UNFOLDING UNDER 15 PSI PRESSURE)

LAMINATE*	BUCKLING FORCE, POUNDS	DISPLACEMENT, MILS
1/4 KAPTON #1	41	81
1/4 KAPTON #2	47.5	77
1/4 KAPTON #3	15 - 16	96 (Pin Holes)
AN-19 #1	67	113
AN-19 #2	64	107
AN-19 #3	64	101
1.0 MYLAR #1	48.5	87
1/4 MYLAR #1	47.3	68
VIRGIN Al TYPE 3003-0	COULD NOT BE RIGIDIZED DUE TO BIG PIN HOLES EVEN AT PRESSURES ABOVE 15 PSI.	
VIRGIN Al TYPE 3003-0 BEFORE PACKAGING	52	75

* AN-19: Laminate #18 - See Table 3.2-1

1.0 Mylar: Laminate #15 - See Table 3.2-1

¼ Kapton: 3 ply Laminate of ¼ mil Kapton-Al-¼ mil Kapton

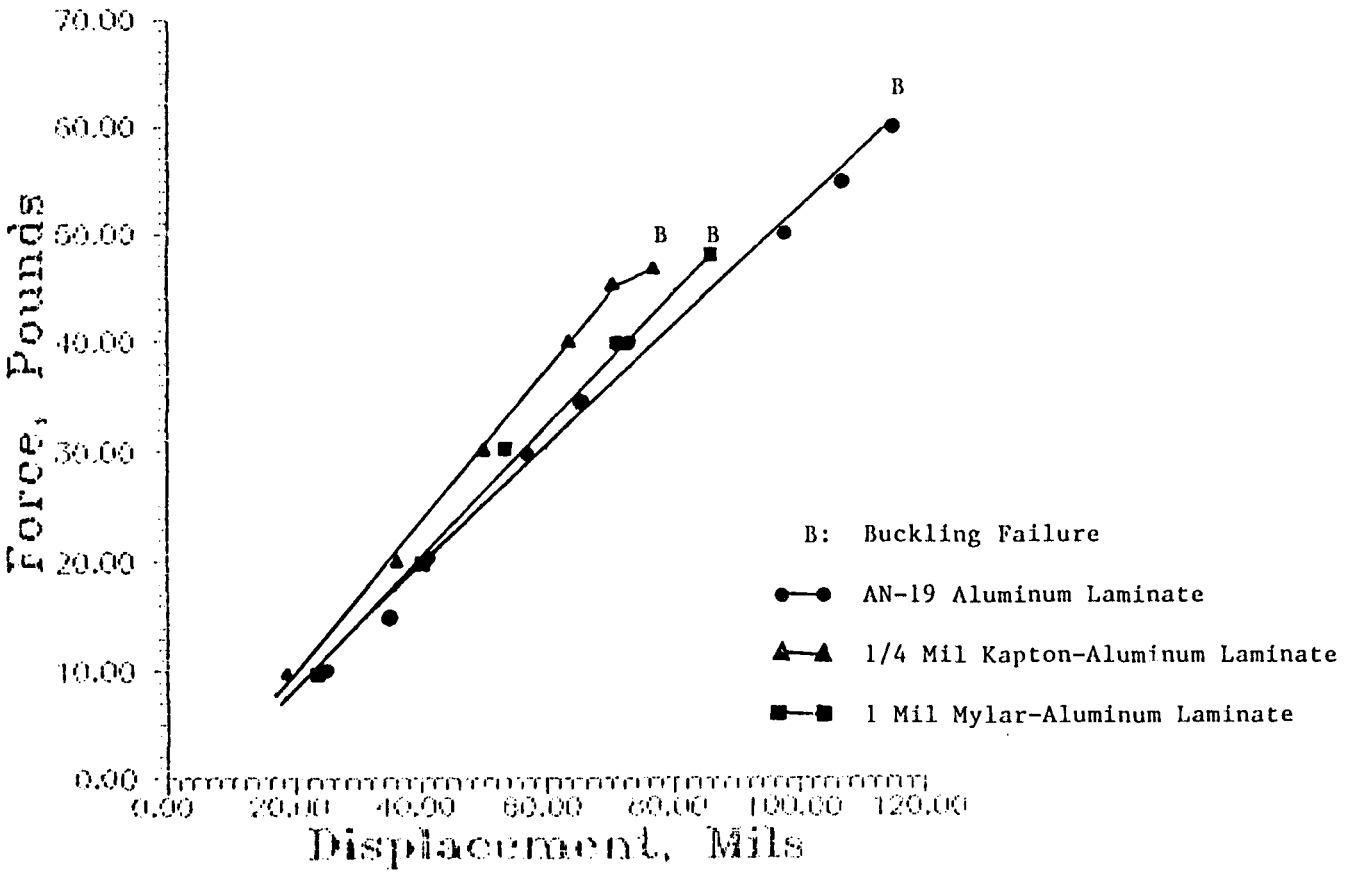

Figure 3.0-25. Buckling Strength of 3.5" x 12" Candidate Aluminum Laminates (After folding and unfolding)

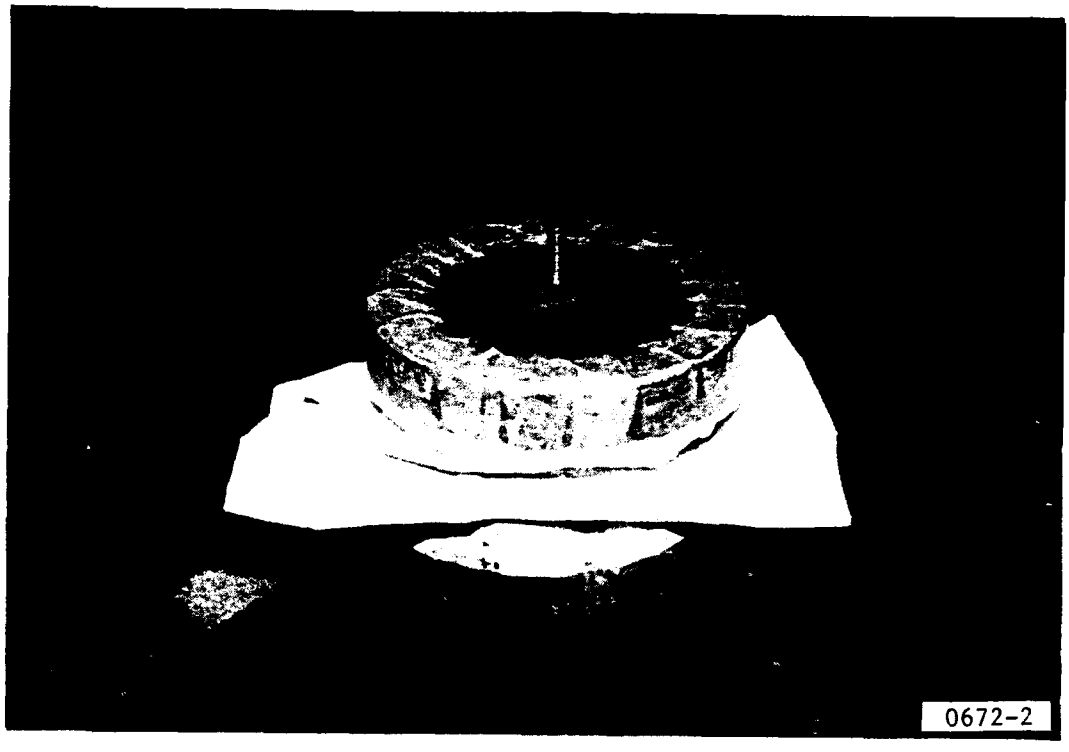

Figure 3.0-26a. A Typical Accordion Packaged Tube (Before Rigidization).

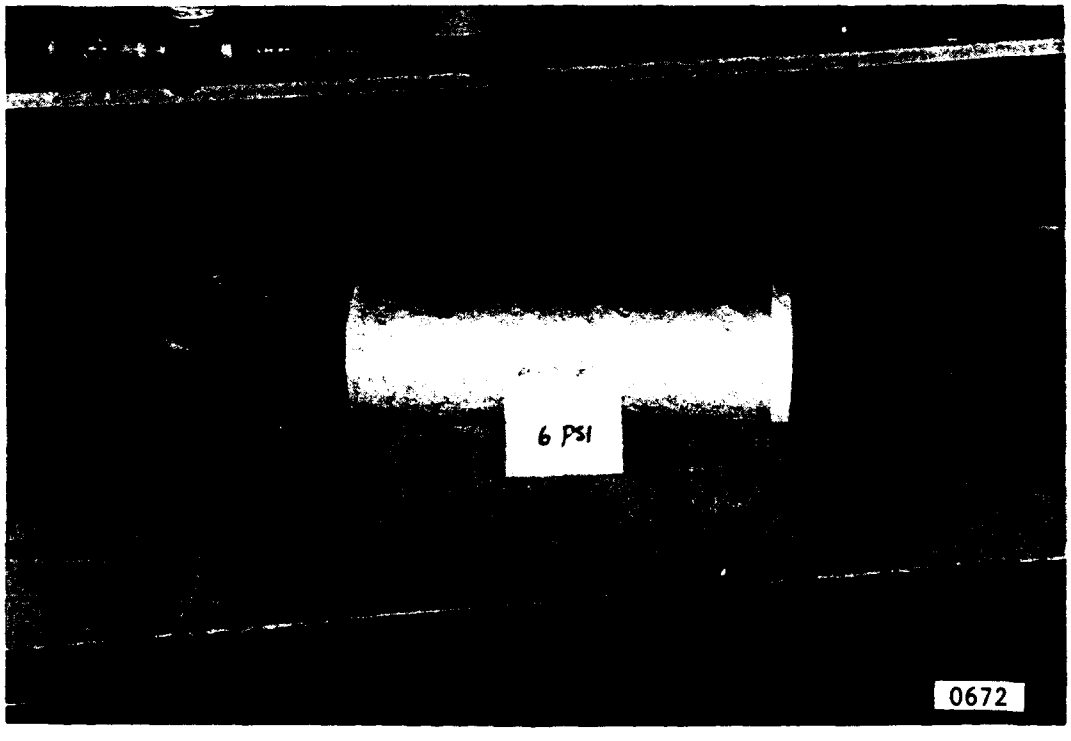

Figure 3.0-26b. Rigidized Tube (AN-19 Laminate) Under 6 psi Inflation Pressure

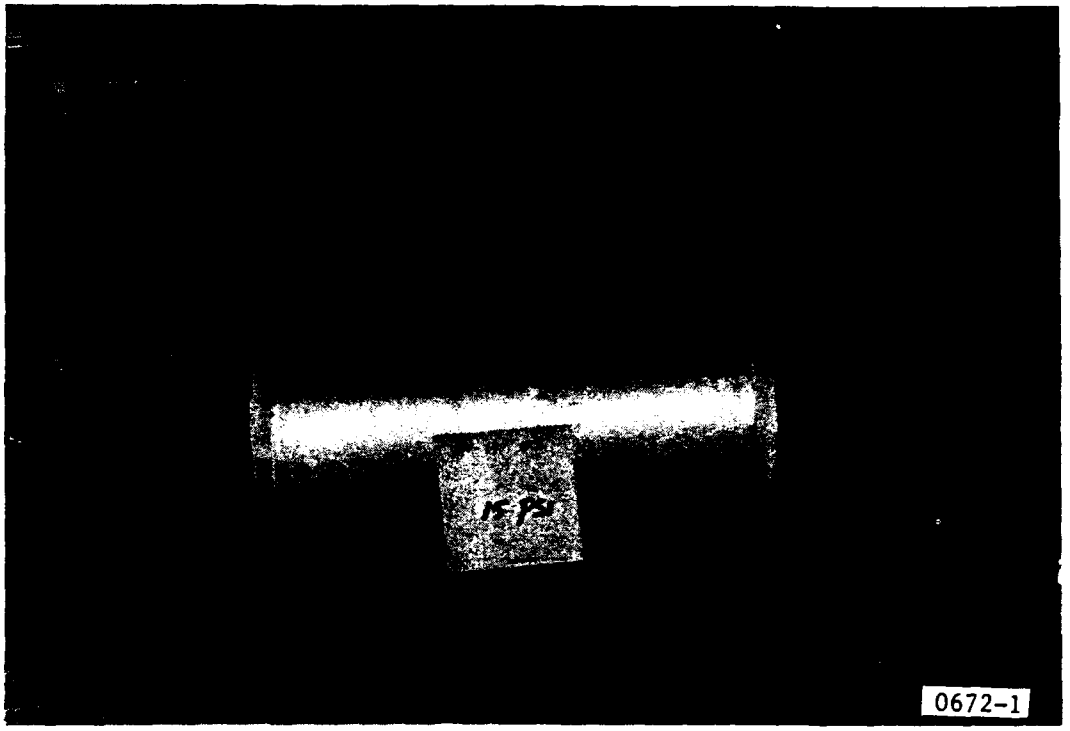

Figure 3.0-26c. Rigidized Tube (AN-19 Laminate) Under 15 psi Inflation Pressure

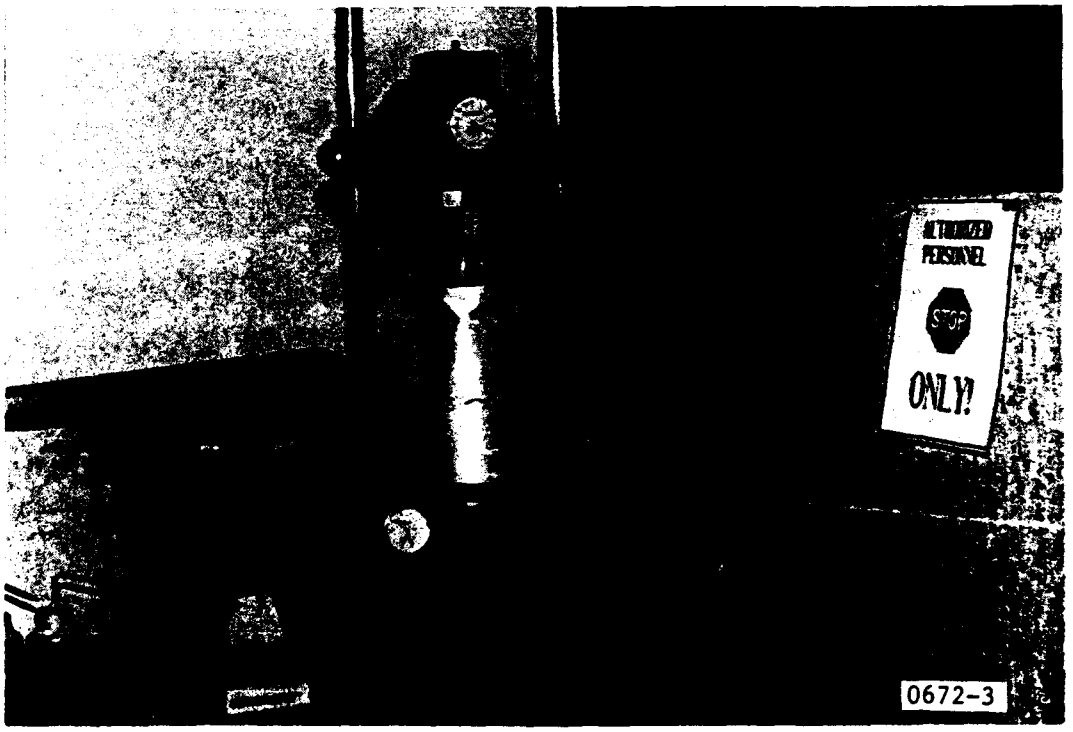

Figure 3.0-26d. Compression Testing of AN-19 Laminate After Rigidization - Buckling Failure at 64 Pounds

Based on the test data provided in Table 3.0-12 the laminate of choice in terms of tear strength and compression resistance is obvious, and that is a 3 ply laminate of AN-19. Aluminum.AN-19. AN-19 is a nylon-reinforced PVF film commercially available and made by ORCON Corp. The supplied film is already covered by a thin layer of adhesive which readily bonds to aluminum under the influence of heat and pressure.

3.9.2. Structural Analysis

The primary analytical technique used in the static and eigenvalue frequency analysis of the ITSAT is the finite element method (FEM). This is a computer-aided mathematical technique for obtaining approximate numerical solutions to the differential equations predicting the response of physical systems to external and internal influences. We have compared the results of this analytical tool against a substantial number of "verification problems" spanning linear and nonlinear static analysis, linear and nonlinear transient dynamic analysis, frequency and random vibration problems, and thermal and thermal-stress analyses. In particular, we have compared our FEM code with NASA's "Buckling of thin-walled circular cylinders" with very good agreement [3.0-15]. Of course, the predictions of analytical tools like the FEM must, in the final analysis, be tested by experimental results. As a preliminary test, we measured the natural frequency of the ITSAT (in plane oscillation) and it compared very well with our FEM calculations - 3.9 Hz (experiment) versus 3.761 Hz (FEM). The FEM technique has been shown to be a very reliable analytical tool when used by a competent analyst and any disagreement between experimental results and FEM predictions may be attributed more to (i) how accurate the values of material properties are, which for a large number of "new" materials are scarce or even nonexistent, (ii) how well the (continuous) physical domain is represented by the FEM geometrical model - is there enough elements and are they of the right element order in the right locations, etc., and (iii) are the boundary conditions used in the model the same as those imposed on the physical system in the laboratory. Furthermore, the analyst almost always has to assume that the materials in the model are perfect - no microscopic cracks in the cylinder for example. In principle at least, even these cracks may be included in the model but one ends up with a problem of great difficulty that may not be of any practical use anyway.

The first analysis run was on a corner elbow 6 inches long on a side. The material used for the initial analysis was aluminum. Figure 3.0-27 shows the finite element model used. The loading was a 5-panel nodal force at the inner corner. The model is constrained at the bottom caps as shown in Figure 3.0-28. Figures 3.0-29 and 3.0-30 show the maximum shear stress and the Von Mises equivalent stresses. As can be seen the stresses are below the yield strength of aluminum. The deflections for this particular load are of the order of 10^{-3} inch.

A finite element model of the torus-array assembly is shown in Figure 3.0-31. The array is discretized into 16 X 6 rectangular shell elements and the rectangular torus, into 1976 shell elements. The material properties used are that for 12 mil thick AN19 laminate for the torus material and stainless steel for the solar array. The loading imposed on the structure for modeling purposes is an in-plane acceleration of 1 foot/sec/sec - the expected loading the ITSAT will undergo once deployed. No attempt was made to model the inflation process.

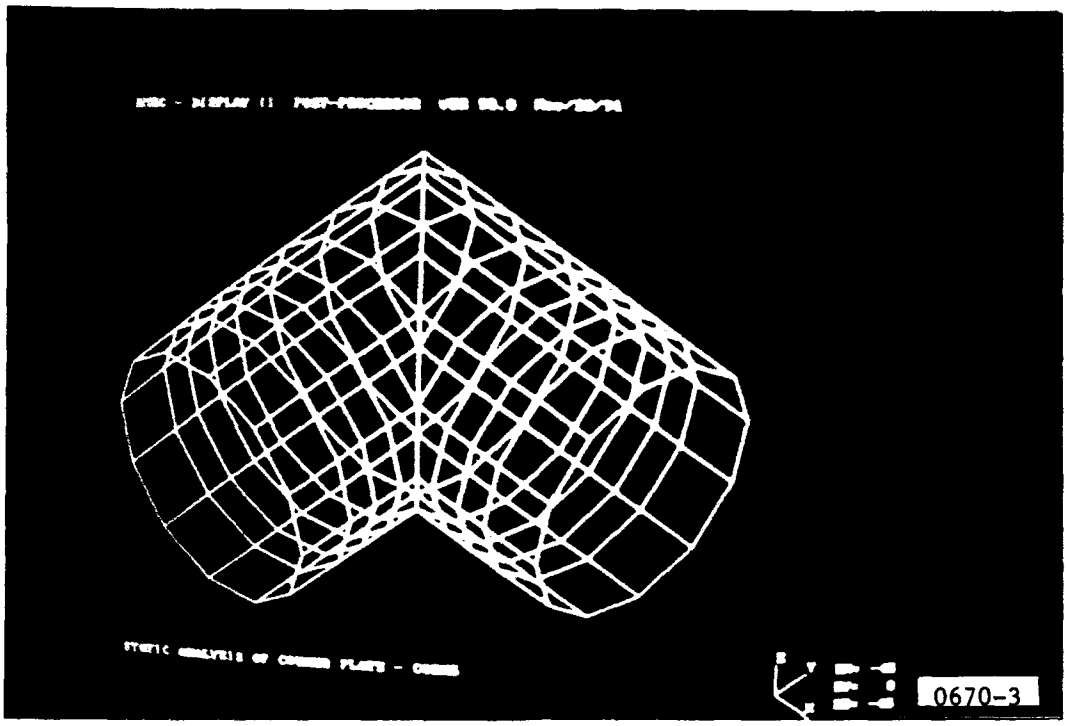

Figure 3.0-27. F.E. Model of Corner Elbow

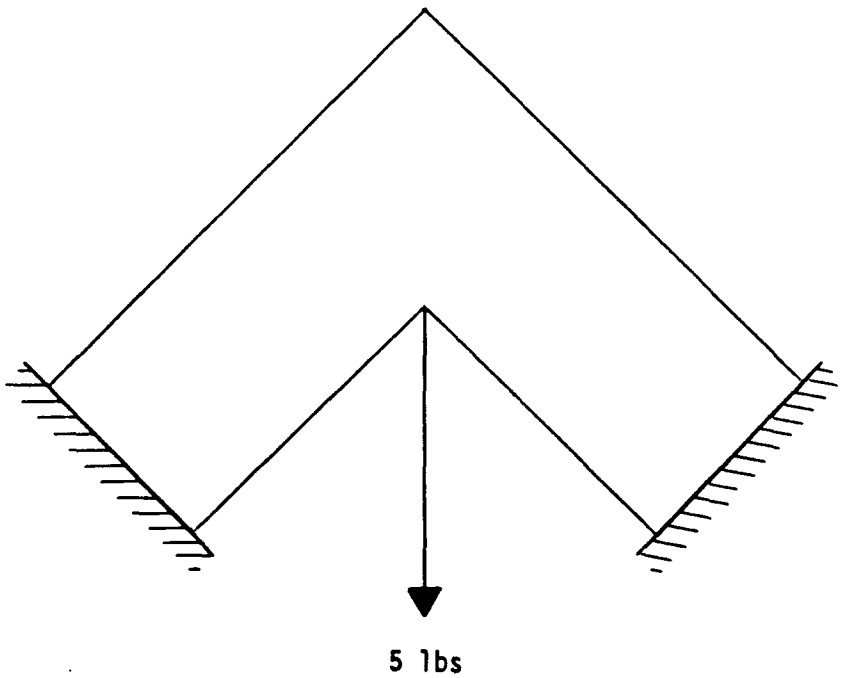

Figure 3.0-28. Loading on Corner Elbow

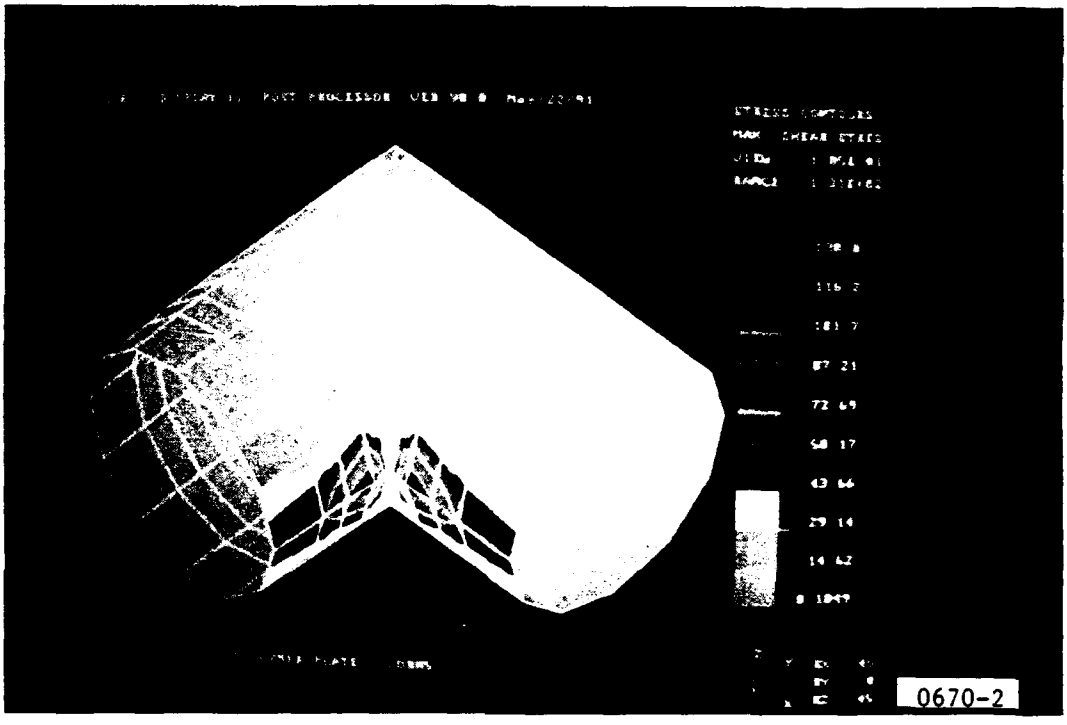

Figure 3.0-29. Maximum Shear Stresses

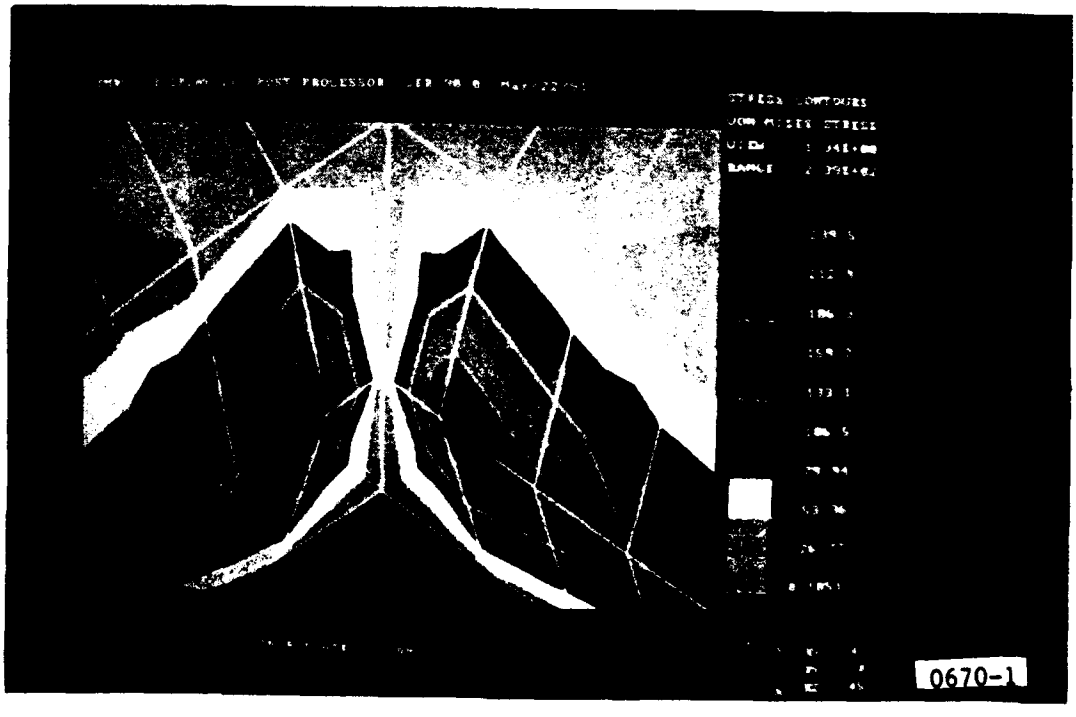

Figure 3.0-30. Von-Mises Equivalent Stresses

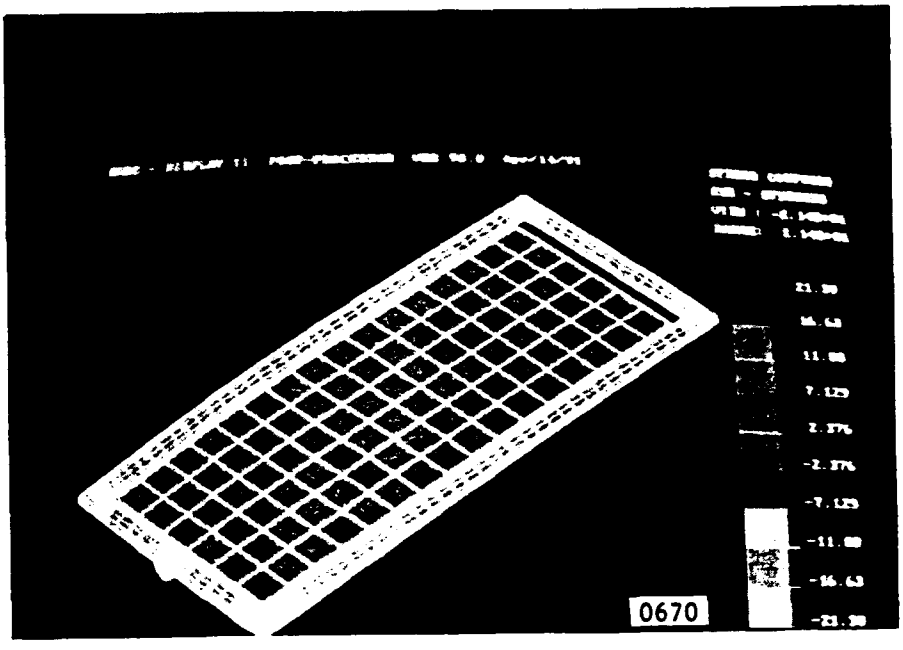

Figure 3.0-31. Finite Element Model of Inflatable Torus Solar Array

Table 3.0-13 shows the mass properties and the maximum stresses in the ITSAT. As can be seen, the maximum value of the stresses are below the yield strength of the materials as indicated in the table. It should be pointed out that the yield strength of the AN19 laminate was measured in L'Garde's laboratory using standard tension tests and the yield strengths quoted here were not "offset" as is commonly practiced [3.0-16]. Furthermore, it should also be noted that ductile materials are found experimentally to stress hydrostatically and have yield strengths greatly in excess of the values given by the simple tension tests. Hence, these values of yield strength for AN19 are very conservative.

Another FEM analysis was run which used for the loading, a transverse gravitational acceleration of 1 g and in-plane nodal forces at two adjacent corners (along a long arm). These will be the loadings on the ITSAT in the laboratory when it is tested. The purpose was to determine the values of the nodal forces that together with the 1 g transverse load will result in a stress distribution that "looks like" those experienced in space. Obviously, because the test is done under 1 g, the in-space conditions cannot be duplicated. However, this particular analysis established that the ITSAT should stand up against the "worst case" in-space loading of .03g. Figure 3.0-32 shows the relationship between the test load and the equivalent "g" load in space.

TABLE 3.0-13. PROPERTIES OF AN19 LAMINATE

Density:	10^{-4} lb-sec^2/in^4
Moduli:	Ex = 480,000 psi Ey = 480,000 psi
Thickness:	12 mils for torus 15 mils for corner elbows
Yield Strength:	Sy = 400 psi in machine direction Sy = 600 psi in transverse direction
Maximum Stress:	σ_{max} = 80 psi in tubular sections σ_{max} = 250 psi in corner elbow

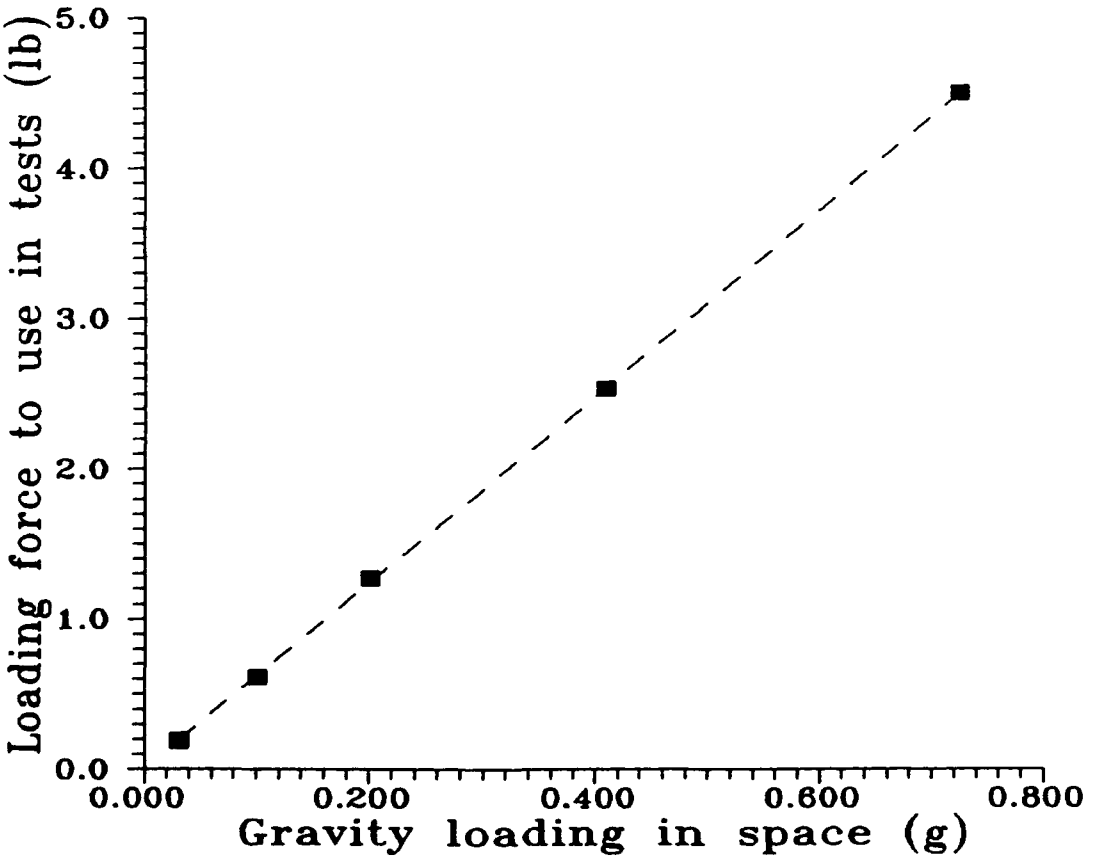

Figure 3.0-32. Gravity Loading in Space

3.10 PROTOTYPE CONFIGURATION

The prototype configuration is shown in Figure 3.0-1 and consists of the aSi array, the inflatable deployed rigidizable structure and a canister simulator.

The prototype torus was fabricated using the laminate described in 3.9.1. The four tubular members were constructed with the use of the two mandrels shown in Figure 3.0-33. The laminate material was "laid up" on the mandrels and the longitudinal butt joint formed. The tubes were then cut at a 45° angle at both ends using the mandrels to control the length and angle of cut. Index marks were then applied to the tubes using corresponding marks on the mandrel for their locations.

The corner joints were formed by installing the tubular members on the corner mandrel shown in Figure 3.0-34. The tubes were aligned using the index marks and joined using fabric tape. The joint was completed by laminating 2 mil aluminum to the corners over the splice areas and onto each tube member for a distance of ten inches. A single layer of tape was added over the splice area that contained the grommet for attachment of the solar array ties.

The canister half simulator was then bonded to the completed torus. The canister half also contained a small fitting for attachment of the completed test article to the test fixture.

The final step was to install the aSi solar array supplied by Apogee Corp. This was accomplished with four tension ties between the array corner and the grommets at each corner of the torus. These tension ties also contained swivels that allowed the array to unroll during deployment.

Figure 3.0-33. Tube Mandrels

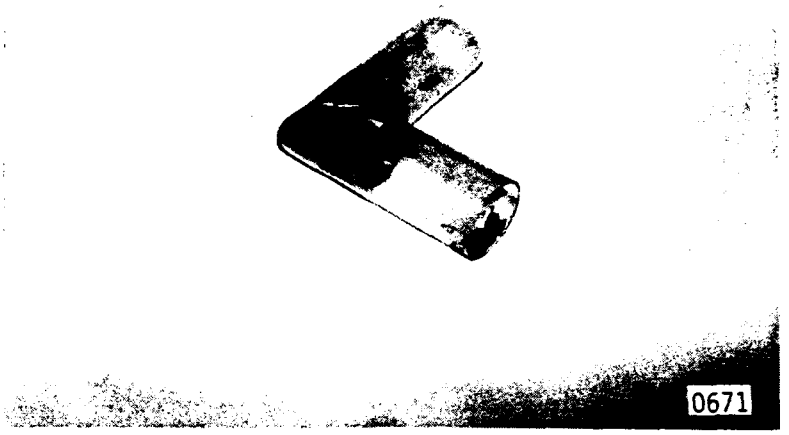

Figure 3.0-34. Elbow Mandrel

3.11 RELIABILITY

During the final quarterly review the question of deployment reliability was raised. The simplicity of an inflatably deployed structure provides considerable inherent reliability. There are no complex hinges, linkages, motors and latches required as with a typical mechanical system. Only a simple gas tank and control valves. Unfortunately, this inherent reliability has not yet been demonstrated by test.

The "one shot" nature of the aluminum laminate precludes repeated preflight testing of the flight structure. This is not the case for either the UV cured resin system or the water soluble gel system. Both of these types could be repeatedly deployed and repackaged for testing purposes with no degradation to the structure.

The aluminum laminate structure used in the PFRT concept must then be treated differently than the resin and gel systems or the normal mechanical deployment devices used with current rigidized crystalline silicon arrays. It must be treated as any other "one shot" device. That is, its reliability should be established by lot acceptance testing. The nature of the rigidized structure for the PFRT concept readily lends itself to this approach. A simple test can be devised that makes use of a reusable inflation system and a standard Personal Computer to control the solenoid metering valve. In this approach the reliability testing would consist of packaging and deploying a statistically significant number of tubes (approx. 100). This number of tests without a failure would result in a demonstrated reliability of .993. Because the tubes are extremely simple to fabricate and package, and the testing so straight forward using this approach to establishing the reliability of the structure would be very cost effective.

Deployment and functional tests of the solar array system conducted during the normal acceptance and preflight testing of a spacecraft could still be accomplished, however, the structure would not be rigidized, just inflated for deployment. As with all solar array deployment systems it would be advantageous to minimize the number of these preflight deployments.

4.0 TESTING

The following section describes testing performed on the ITSAT prototype assembly. The majority of testing was performed on the inflatable rigidizable torus structure. Several electrical tests were performed on the amorphous silicon solar array. Finally, system assembly packaging tests were performed characterizing inflation dynamics and effects to the solar array during and after deployment.

4.1 SYSTEM REQUIREMENTS

As a result of the concept definition study, a rigidizable torus was baselined for the structure. The aSi array was baselined for the ITSAT program during the proposal.

The ITSAT torus is required to handle 1 ft/sec^2 static acceleration, any direction. The original estimates of torus strength were based on extrapolations of data for long, thin tubes in pure bending. It was assumed that one long tube of the torus would take all the load in an in-plane acceleration because the lower solar array ties will not carry loads in compression. The torus structure is expected to be even stronger because some loads are transferred into the lower tube. Data extrapolations were used instead of theory because the theory shows much higher strength - it does not work well for high length/radius and radius/thickness ratios. The original data curves for the predictions are shown in Figure 4.0-1. The material selected was a laminate, of AN19, aluminum, AN19 which had a predicted safety factor of 4.94. A full study on various laminates is discussed in Section 3.2.

Design goals and actual system design were as follows:

	Design Goal	As Tested
System Weight:	3.75 lbs	4.75 lbs
Output Power:	125 W (AM 0)	93 W (AM 0)
Maximum G load:	1 ft/sec2	8 ft/sec2
Structure F/S:	Not Specified	8:1 Avg.

4.2 RIGIDIZABLE TUBE TEST RESULTS

Due to the particulars of the design, tubes were built to characterize the theory vs actual test data, to investigate effects of packaging on strength and to measure the natural frequency. The test set-up is shown in Figure 4.0-2. Since the torus design transfers all loads to the long tubes these data can be extrapolated to the torus design.

In the fabrication of bend test tube #1, difficulties were encountered removing the mandrel. This caused some damage to the tube. The tube was slowly pressurized for rigidization, but the seam began to fail at 9 psi (versus the target 13 psi). Since the failure was not catastrophic, the tube was still subjected to the bend tests. It was then repaired and the natural frequency measured.

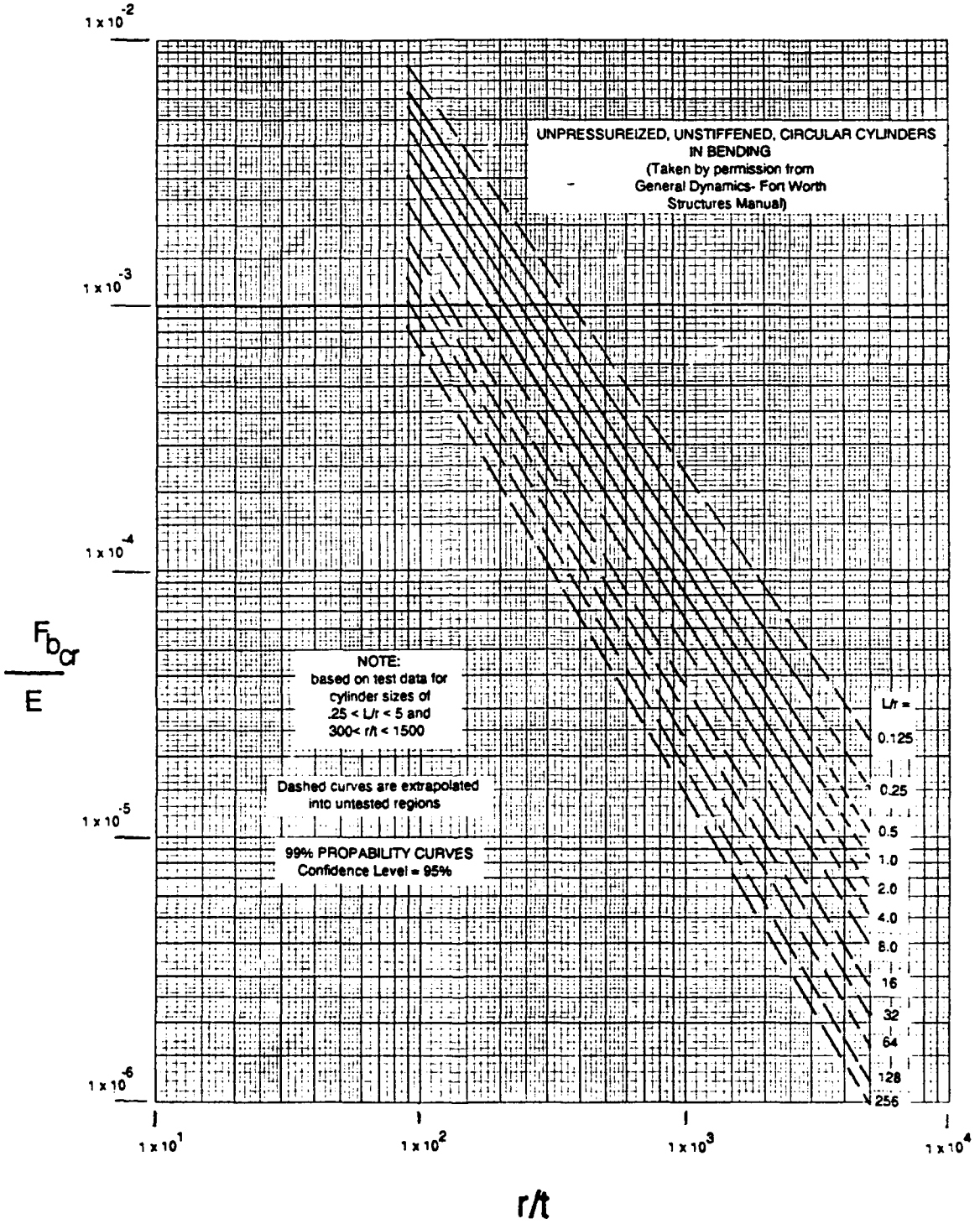

Figure 4.0-1. Buckling Loads for Unpressurized Cylinders

Once the first tube was built, it was found to be heavier than expected. The safety factors calculated below reflect this data. The actual weights are measured values in *italics*:

Torus Tube Weight/Length:	*.00745 lb/in*
Torus Tube Lengths:	2(108.75-4)+2(45.75-4) = 293 in
Total Tube Weight:	.00745X293 = 2.18 lb
Corner Weight, ea:	.155 lb
Total Torus Weight:	2.18 + .155X4 = *2.80 lb*
Array Blanket Weight:	*1.74 lb*
Total System Weight:	2.80 + 1.74 = 4.54 lb

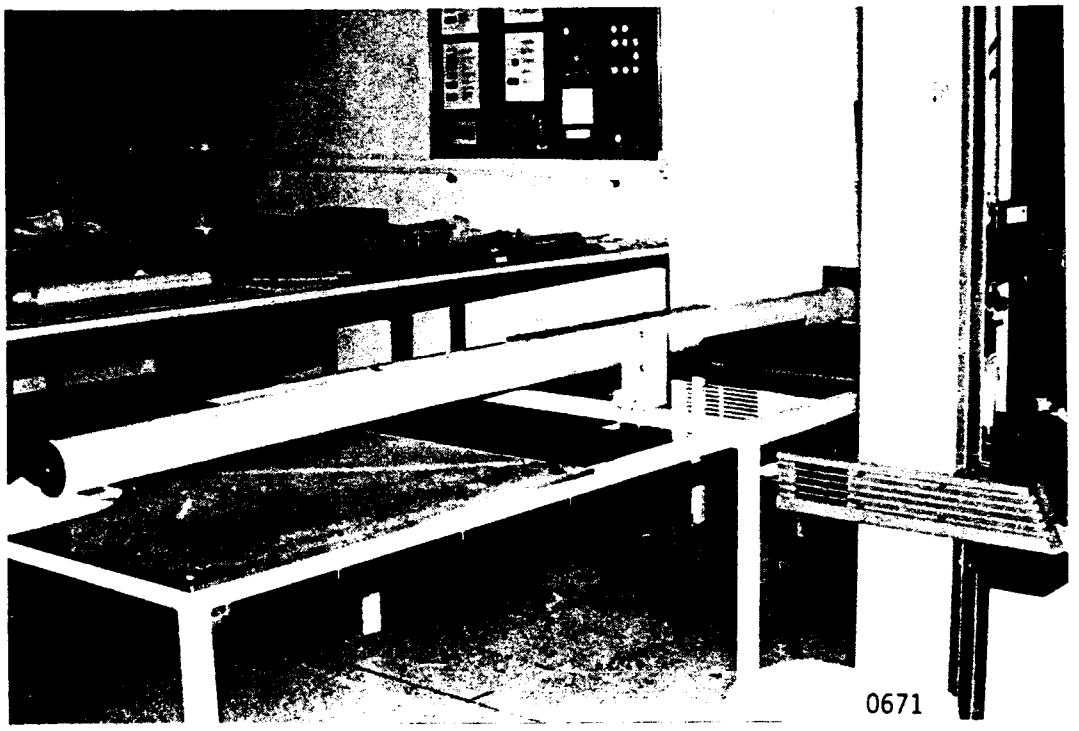

Figure 4.0-2. Tube Bend Test Configuration

4.2.1 Natural Frequency Test

The expected natural frequencies of the torus plus array, as calculated by finite element analysis, are:

	Predictions
Mode 1 (out of plane):	2.078 Hz
Mode 2 (in plane):	3.761 Hz
Mode 3:	4.921 Hz
Mode 4:	6.276 Hz
Mode 5:	9.093 Hz

As noted above, bend test tube #1 required repair. The leaking seam section on the tube was removed and replaced. However, this attempt to repair it was less than successful since it could not be pressurized above 11 psi. The tube was never packaged and used only to test for natural frequency (by video taping). The results were:

Start Time:	5.3 sec
End Time:	6.2 sec
Number of Cycles:	3.5
Frequency:	3.5/.9 = 3.9 Hz

This frequency probably represents the first (out of plane) mode. Note that the tested frequency is higher than expected. In any case, all frequencies are above 1-2 Hz, which is thought to be the lower limit for interference with the spacecraft attitude control system.

4.2.2 Structural Bending Tests

The structural testing conducted on bend test tube #1 was performed prior to repairing and prior to packaging it. In all tests, the nature of the failure was gentle, with the stress flattening out as strain increased. Failure was taken at the knee of the curve. The results are:

STATIC REQUIREMENT:

.031g Load Moment:	.031g X 4.54 lb X 108.75"/2 = 7.65 in-lb
.031g Test Load:	7.65 in-lb / 108.75" = .070 lb

PREDICTIONS:

Fbcr/E (predicted):	$4.3X10^{-4}$
E (measured on coupon):	$.5X10^{6}$ psi
Diameter; Thickness; Iz:	4"; 11 mils; 0.2717 in^4
Expected Failure Stress:	$4.3X10^{-4}$ X $.5X10^{6}$ = 215 psi
Expected Failure Moment:	Fbcr X Iz / r = 29.2 in-lb
Expected Failure Load:	29.2/108.75 = .268 lb

TEST DATA:

Tested Failure Load:	0.6 lb
Failure Location:	28" from fixed end

Bend test tube #2 experienced catastrophic seam failure at 8 psi. This necessitated shortening the tube to 84". Tests were done to correct the seam curing procedure, and changes were incorporated. The tube was then successfully pressurized to 13 psi. and tested. Note that this test was before packaging. The results were:

STATIC REQUIREMENT:

.031g Load Moment:	.031g X 4.54 lb X 108.75"/2 = 7.65 in-lb
.031g Test Load:	7.65 in-lb / 84" = .091 lb

PREDICTIONS:

Fbcr/E (predicted):	$4.7X10^{-4}$
E (measured on coupon):	$.5X10^{6}$ psi
Diameter; Thickness; Iz:	4"; 11 mils; $0.2717in^{4}$
Expected Failure Stress:	$4.7X10^{-4}$ X $.5X10^{6}$ = 235 psi
Expected Failure Moment:	Fbcr X Iz / r = 31.9 in-lb
Expected Failure Load:	31.9/84 = .380 lb

TEST DATA:

Tested Failure Load:	1.13 lb
Failure Location:	6" from fixed end

Bend test tube #2 was then packaged under vacuum in 3" accordion folds. The tube was then deployed under 1-3 psi., then pressurized to 13 psi, and then tested to investigate strength loss due to packaging. The results were:

TEST DATA:

Tested Failure Load:	0.9 lb
Failure Location:	6" from fixed end
Deflection @ Failure:	~0.7"

Bend test tube #2 was then repressurized without repackaging, but failed catastrophically at ~10 psi due to the AN-19/Al adhesive problem. The joint design has been modified by the addition of an additional layer of tape on the inner surface to eliminate this problem. In addition, we will not re-fold the tubes on the same lines.

The conclusions on the structural tests are as follows:

Safety Factor, Before Packaging:	1.13/.091 = 12.42
Safety Factor, After Packaging:	0.9/.091 = 9.89
Packaging Loss:	(1.13-.9)/1.13 = 20.4%
Equivalent E, Before Packaging:	$1.487X10^{6}$ psi

The equivalent E can be used as an empirical factor to use the data curves for other predictions. Test data was two to three times better than expected; ten times over requirement. Note that only data from the fully pressurized tube #2 was used.

In addition to the results listed above the following should be noted:

- The packaged length of the tube itself was 2" (full length 84").
- There was much leaking at the seam fold pints due to separation between the joint tape's lower layer of AN-19 and its aluminum layer which was solved by the addition of a layer of tape.
- During deployment the tube was bent approximately 14" out of the array plane, but was properly aligned upon full deployment.
- During deployment, the tube would "pop" as seams unfolded. This may be of concern for a spacecraft attitude control system. The popping can be eliminated by coating the inside to prevent excess adhesive from sticking to the inside walls.

- The tube took on a slight "banana" shape due to the seam, but relaxed when the tube was cantilevered to the structural test fixture. The difference was 1/8" over 84" of tube length. This slight curvature is not expected to affect the overall array performance, however, if later testing indicates there is a problem then an additional seam can be added 180°from the existing one to provide symmetry and eliminate the curvature.

4.3 TORUS TEST RESULTS

Two tori were built during this program. Both units were fabricated from laminate #18 (AN19-A1-AN19). The first unit S/N 001 was used primarily to develop the packaging technique and thus, was not suitable for post packaging structure testing.

Also, upon rigidization both tori exhibited warpage. This warpage is probably not enough to significantly affect the array performance but it was clearly an indication that something was not as planned. An examination of the tooling mandrels revealed the index marks on the corner mandrel that were used to align the tubes were slightly mislocated (approximately 0.01 inch). While this error was small it was sufficient to cause the tori to warp. The mandrels have been corrected to prevent this problem on any future tori.

4.3.1 Natural Frequency Test

Natural frequency tests were performed on each torus in the plane of the solar array. The results are shown below.

S/N 001	
Pre Packaging	1.63 Hz
S/N 002	
Pre Packaging	1.48 Hz
Post Inflation	1.33 Hz

Note: As mentioned earlier, S/N 001 was not rigidized following deployment due to the excessive packaging while developing the packaging methodology.

4.3.2 Structural Bending Tests

Structural bending tests were performed on both tori. These tests indicate that the torus is very stiff and will not fail due to structural effects during its life. Factors of safety on the order of 8:1 were realized.

The test set-up is shown in Figure 4.0-3. The torus was loaded using the tensiometer. The data is plotted load vs deflection until the curve begins to flatten (which indicates a failure). In all cases failure was in buckling. Table 4.0-1 presents the test data on S/N 001 and 002.

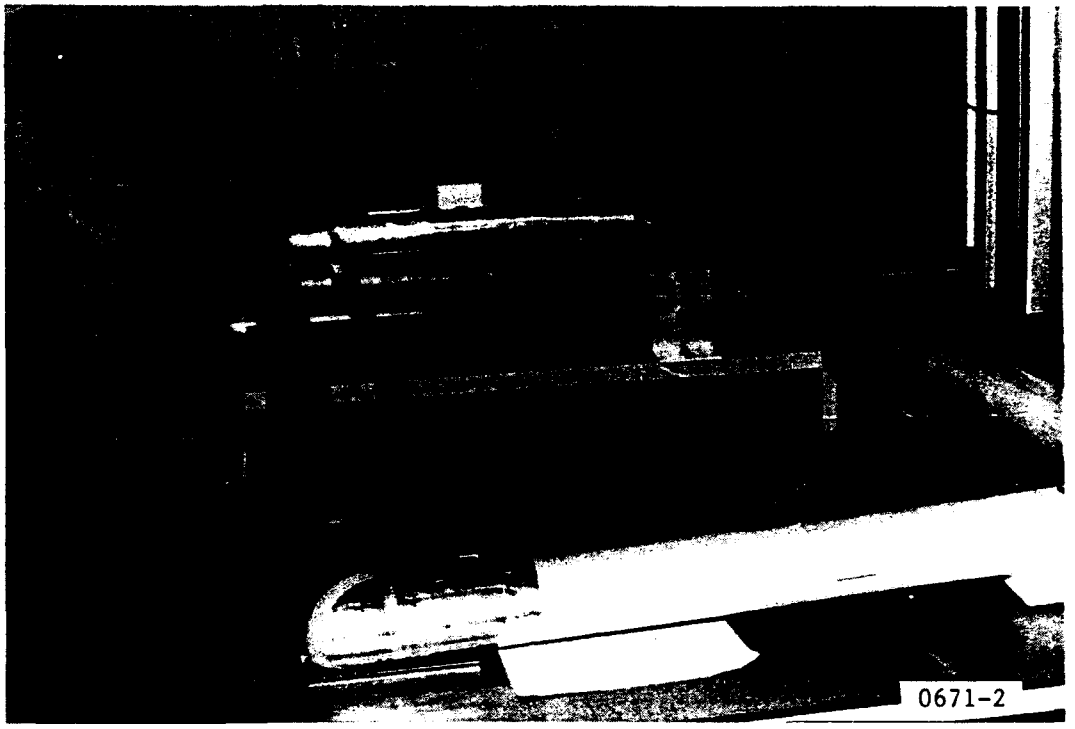

Figure 4.0-3. ITSAT Test Set-up

TABLE 4.0-1. TORUS TEST DATA SUMMARY

		S/N 002	
	S/N 001	Pre Packaging	Post Packaging
Torus/Array Assy Weight (lbs)	2.97	3.00	3.00
Load at Failure (lbs)	2.55	4.35	1.60
Type of Failure	Buckling	Buckling	Buckling
Zero G Load Capability	0.41	0.70	0.26
Margin of Safety	13.2	22.6	8.24

4.3.3 Packaging Tests

Several packaging methods were investigated. The first method flattened the torus "horizontally" and once flat it was folded accordion style while the solar array was rolled. The packaged system was stowed in the container. Figure 4.0-4 depicts this approach. As can be seen, the initial canister size is not quite large enough to contain the packaged array plus structure. The canister will require redesign. The new design will change the cross-section of the cylinder to an oval by the addition of a two inch straight segment to the top and bottom of the fixed canister half.

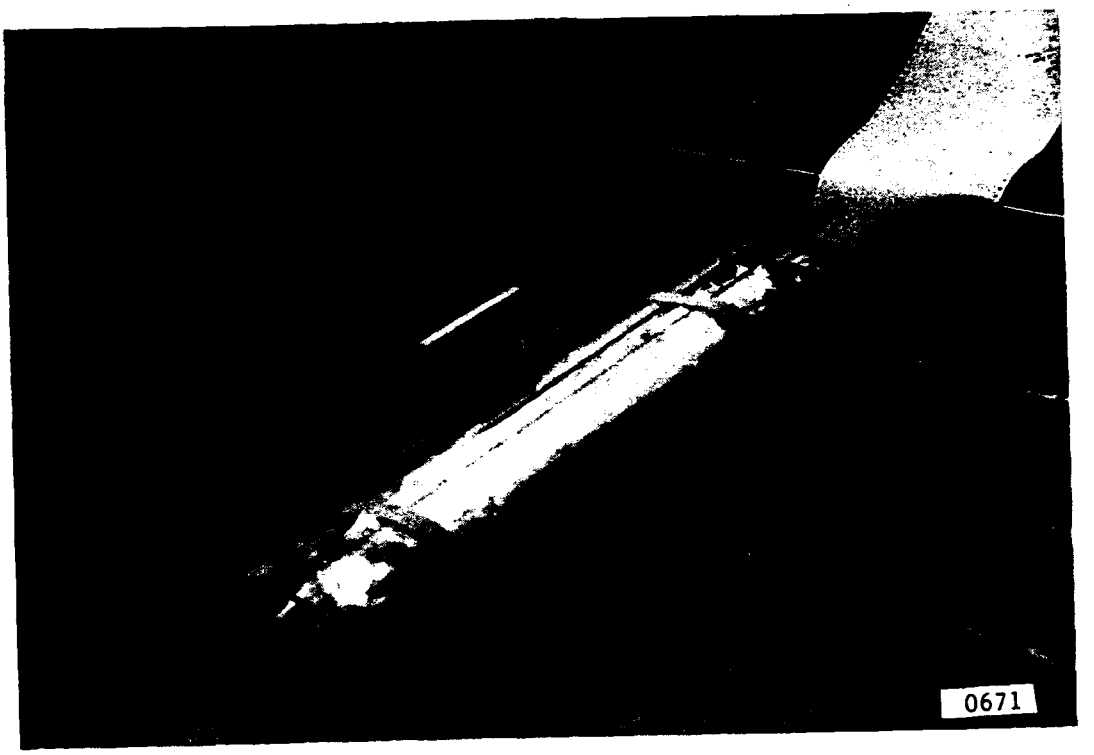

Figure 4.0-4. Packaged Array

When inflated, the solar array deployed properly. However, there were two problems. First the torus tubes did not deploy straight out as the array was deployed, but developed their full length prior to the array being fully extended. This resulted in the tubes developing significant bends. In the current configuration, the array was attached to the torus only at its four corners. It is clear that intermediate attachments between the tubes and arrays will be required to prevent the tubes from bending out of position.

Second, the torus corners failed at the inside junction of the tubes when inflated for rigidization. A second packaging method was developed in an effort to minimize the packaging stresses on the corners. This method consists of flattening the torus members in the "vertical" direction and then accordion folding them while rolling the solar array as with the first method (Figures 4.0-5 and 4.0-6). The advantage of the second method is that the corners are not folded completely flat. As a result the packaging efficiency is less than the first method. If the corners are folded completely flat in the second method, the packaged volume will be about the same as the first method but a different packaged shape results.

Prior to constructing the complete torus a prototype corner had been fabricated to evaluate the packaging capability. During the evaluation testing the corner had been able to be packaged flat (horizontal) with no adverse affects.

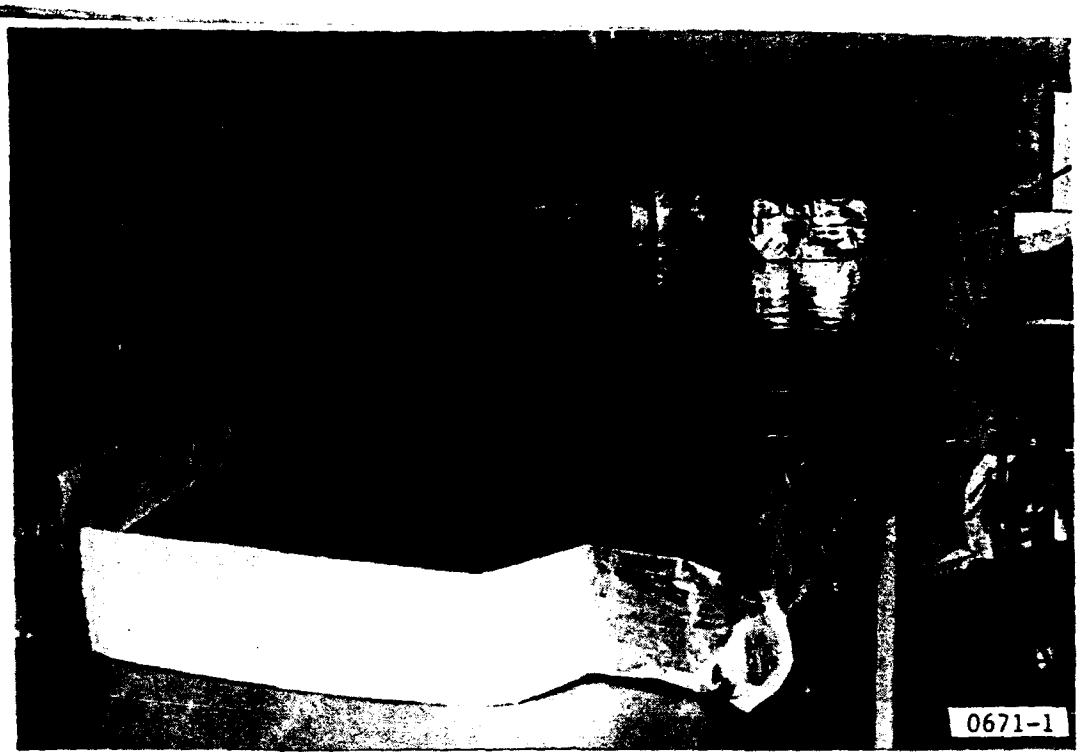

Figure 4.0-5. Alternate Packaging Method

Figure 4.0-6. Packaged System, Method 2

In order to understand why the complete torus corners failed after a single packaging, a study of construction and of the corner folding and packaging procedures was performed. The following observations were made:

1) A specific sequence must be followed when folding a torus because the closed loop can induce unnecessary stresses on the corner joints. It's best to fold the corners first thus reducing the circumference of the torus before collapsing the four legs.

2) Care in folding the corner so as not to unnecessarily stress the miter joint is desirable.

3) Wider strips of tape spanned the miter joint on the early elbow compared to the torus elbows.

4) Subtle differences in the folding for packaging and the fabrication can make a significant difference.

The lay-up procedures on these irregular shapes do not lend themselves to analysis, hence an iterative process of fabrication and test is required. These early iterations provide the education necessary to ultimately achieve consistency and reliability.

With the benefit of the information from the failure, another prototype corner was fabricated. This corner was folded such that it avoided the unnecessary stresses. It was then inflated and tested by applying a force to the root of the 90° angle, as would be done by an attachment to an array. The required force to sustain the .03g's is .12 lbs., and incipient squashing of the corner occurred at 26.5 lbs., a factor of safety of 221.

L'Garde feels confident that the level of knowledge achieved on this third iteration of the fabrication process is sufficient to fabricate, fold and package a complete rectangular torus.

As a result of this corner testing we can conclude that both packaging methods are acceptable since both resulted in successful deployment of the array and both will result in approximately the same packaged volume. The selected method will depend on which packaged form factor is more appropriate for the specific application.

4.4 AMORPHOUS SILICON SOLAR ARRAY TESTS

Both physical and electrical measurements were performed on the solar array.

4.4.1 Weight and Dimensions

The actual dimensions turned out to be 94.75" X 33.75" X ~4 mil thick which is very close to the preliminary design.

Due to bussbar problems encountered during thinning, the array could not be thinned as much as desired. This, along with higher actual bussbar, etc. weights than expected, resulted in the final weight being 787 grams (381 g/m^2 vs. the goal of 313 g/ m^2).

4.4.2 I-V Curve Test Procedure (Ref. 4.0-1)

The output of the array is specified at its maximum power point. In order to find this point, the entire I-V curve must be run. A variable resistor is used to sweep out the curve. The set-up is as follows:

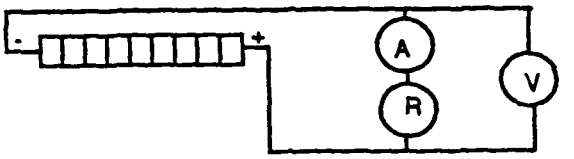

Accuracy of the testing is limited by fundamental difficulties in testing space arrays on earth. The atmosphere attenuates the incident solar radiation spectrally and non-linearly (Figure 4.0-7). Therefore, there is a specified terrestrial spectrum called "AM1.5", used as reference in testing.

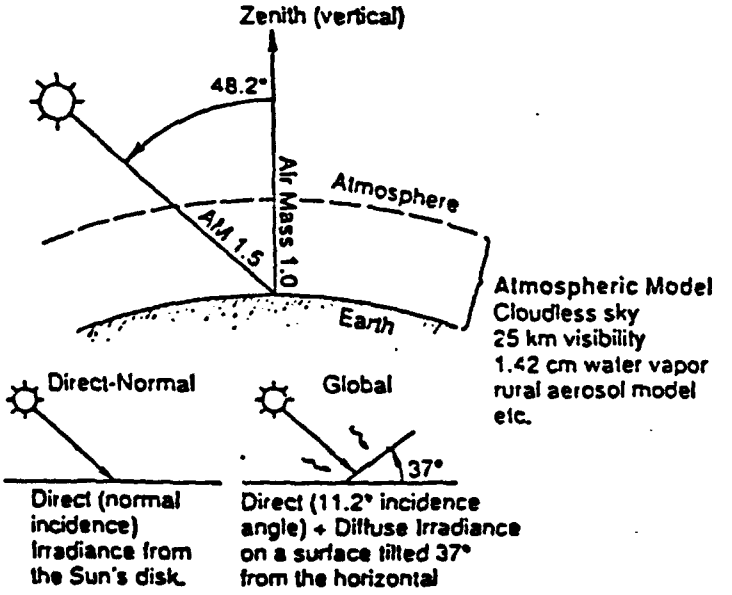

Figure 4.0-7. AM1.5 Conditions (Ref. 3.0-2)

The power output of a solar array in space is generally accepted as 1.25 times greater than AM1.5 (Ref. 3.0-3). It is difficult to compare the two due to differences in spectrums and differences in the spectral sensitivities of the various types of solar cells of interest (Figure 4.0-8).

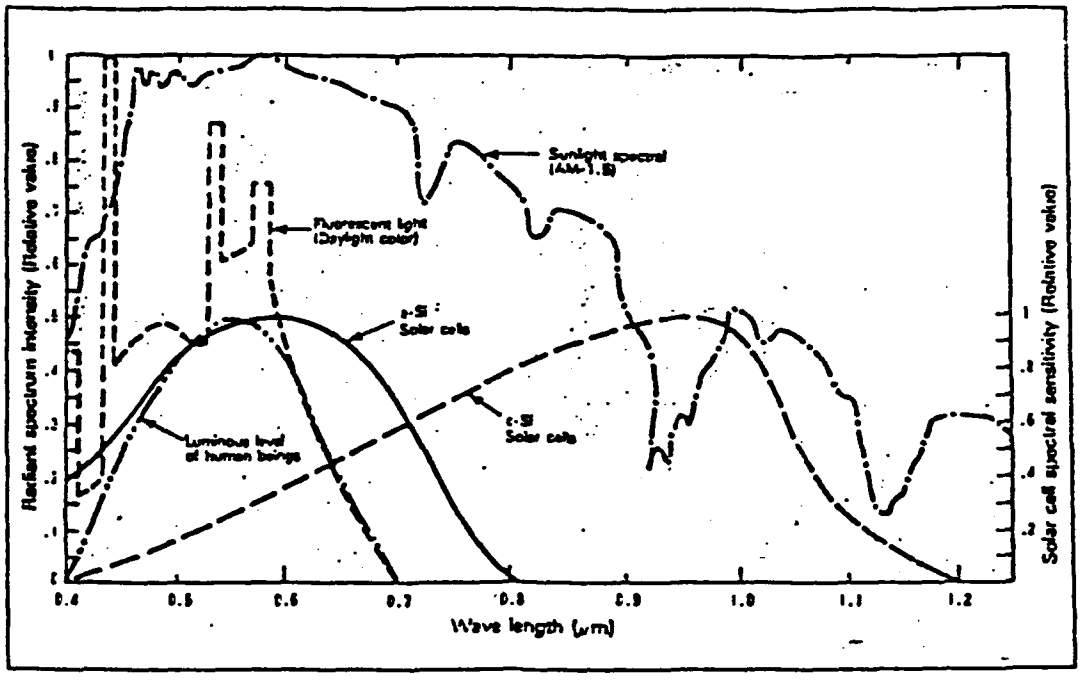

Figure 4.0-8. Radiant Spectrum of Light and Spectral Sensitivity of Solar Cells (Ref. 4.0-3)

Further inaccuracy results from the difficulty in achieving the AM1.5 spectrum in the L'Garde parking lot. The array was tested in Los Angeles smog, near a reflective building, at 33.34° north latitude, near the winter solstice, etc. The tested power output of the array must be normalized to AM1.5. This was done using a crystalline silicon solar cell calibrated to AM1.5.

Other inaccuracies result from differences in the actual temperature and the AM1.5 specified temperature of 25°C, particularly when it's windy. For this, temperature correction factors are used (Ref. 3.0-8) for both the array and reference cell.

The array must be kept perpendicular to the sun. This is done by laying an open box next to the array, and adjusting the array so that there are no shadows in the bottom of the box.

The array was tested to verify the functionality of the bypass diodes by shadowing part of the array. Also, the cosine loss due to off nominal pointing was tested.

The test set-up is shown in Figure 4.0-2.

4.4.3 Array Test Results

The array was originally tested in Ames, Iowa on 11/18/90. Power was 105 watts, AM1.5. It was then brought to Tustin and tested on 11/20/90 (Figure 4.0-10). Power was 101 watts, but a shorting burn failure was noticed on the active area under one of the bussbars (Ref. 3.1-17).

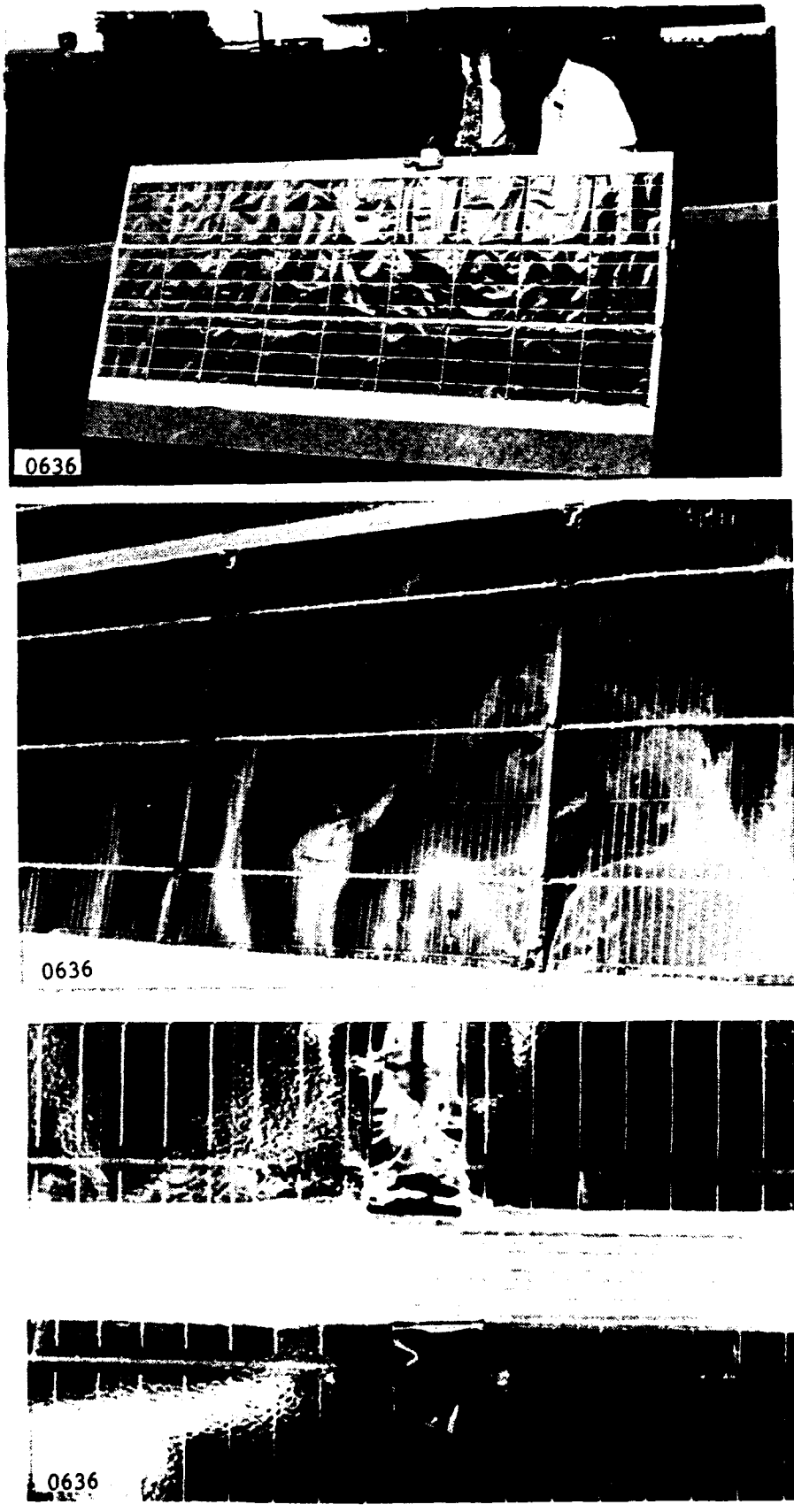

Figure 4.0-9. Solar Array Being Tested at L'Garde, Inc.

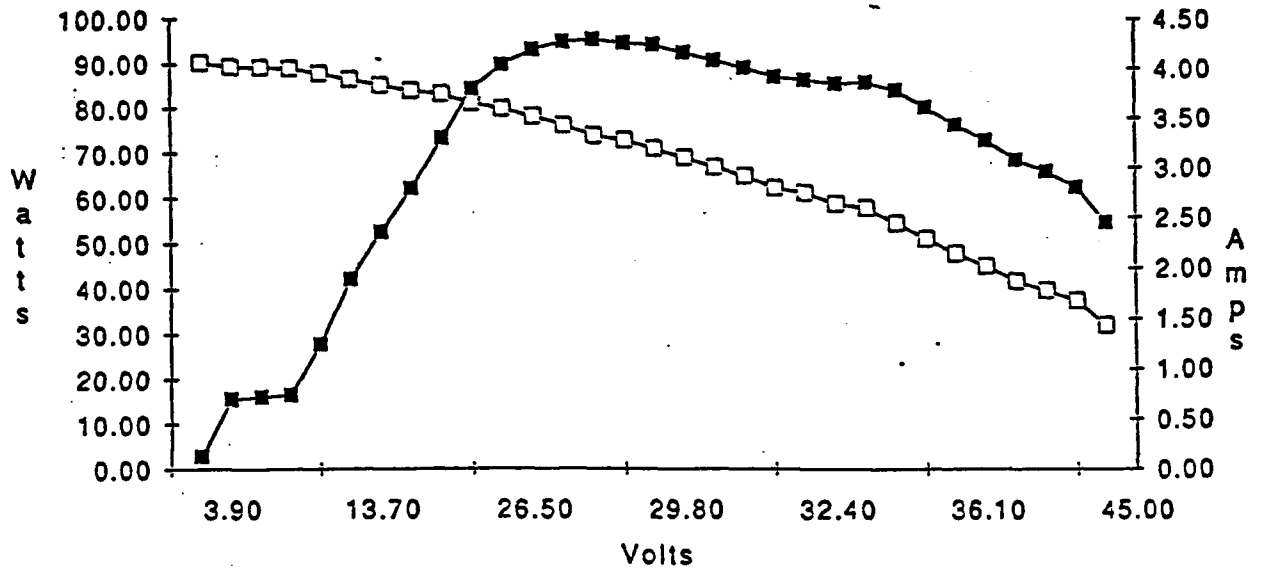

Figure 4.0-10. Solar Array Test in Tustin 11/20/90

The array was brought back to Iowa for replacement of the module, and an inverted bypass diode was installed properly. Also, some shorts were discovered, which were repaired by reverse bias voltage. The array was again brought to Tustin and tested on 4/18 and 4/19/91. The power was 93 watts (Figure 4.0-11).

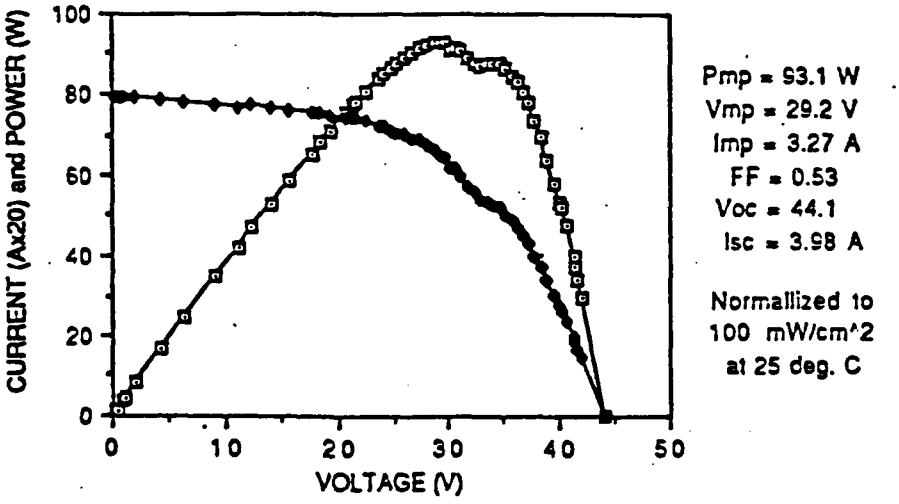

Figure 4.0-11. Solar Array Test in Tustin 4/18/91

The cause of the low power then became the subject of investigation. The culprit appears to be excessive rolling to small diameters during fabrication. This puts the bussbar/active area interface in shear, and probably fractures the cell, causing shorts. A summary of the tests and number of packaging cycles is presented in Table 4.0-2.

TABLE 4.0-2. SUMMARY OF SOLAR ARRAY TESTS BEFORE PACKAGING

	TEST	SUN	TEMP	POWER	Vmp	Imp	FF	Voc	Isc	RESTOWING
#	Location / Date	mW/cm^2	°C	Watt	Volt	Amp		Volt	Amp	# of Prior Cycles
1a	Ames, IA 11/18/90	83	37	105.4	32.2	3.31	0.62	43.2	3.93	4
2a	Tustin, 11/20/90	97	47	101.2	30.9	3.36	0.56	44.2	4.12	6
2d	Tustin, CA 11/20/90	87	43	98.4	29.7	3.38	0.57	44.6	4.05	6
3	Tustin, CA 4/18/91	103	46	93.1	29.2	3.27	0.53	44.1	3.98	15
4	Tustin, CA 4/19/91	102	47	93.2	29.1	3.20	0.54	43.8	3.95	16

The array was then left flat while the torus was developed. The original purpose of the testing was to verify conversion efficiency and investigate array damage due to packaging and deployment. The sensitivity to handling became apparent well before the packaging tests. However, packaging did not cause any damage; power output was 93 watts before and after packaging (Figure 4.0-12).

The bypass diodes were found to work properly, and the cosine loss with incidence angle was verified.

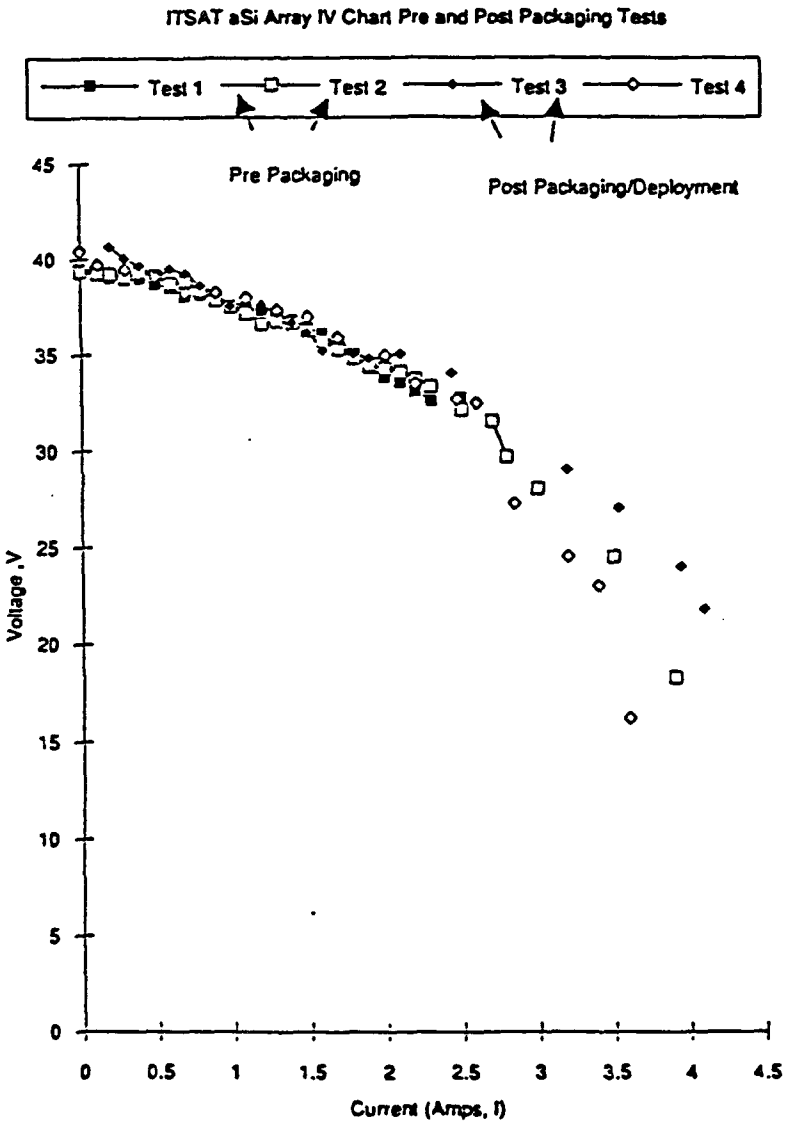

Figure 4.0-12. Solar Array Tests Pre and Post Packaging

5.0 POINT DESIGN UPDATE

Part of the final task of the study was to update six of the point designs incorporating the results of this study. Four designs were required by the statement of work and two were selected by L'Garde.

The four required configurations are:

a. Tubular configuration in a 740 kilometer polar orbit, delivering 200 watts after 3 years.
b. Tubular configuration in a 740 kilometer polar orbit, delivering 200 watts after 3 years, attached to a STEP-type satellite bus.
c. Tubular configuration in a 740 kilometer polar orbit, delivering 200 watts after 3 years, attached to a TECHSTARS-type satellite bus.
d. Tubular configuration in a 6 hour Molniya orbit, delivering 200 watts after 3 years, attached to a TECHSTARS-type satellite bus.

The two selected by L'Garde are:

e. Tubular configuration in a 740 kilometer polar orbit, 1500 watts.
f. Tubular configuration in a 740 kilometer polar orbit, 5000 watts.

A review of the point designs considering the prototype design and test results indicates they are still accurate for aSi arrays. However, the results of the array technology study indicate the aSi technology is not sufficiently mature to support the ITSAT Phase 2 and 3 schedule. In fact, only the APSA type system incorporating crystalline silicon cells, of the flexible array technologies is sufficiently advanced to do so.

Therefore, the above point designs were updated to replace the aSi array with the APSA blanket crystalline silicon configuration. Because this configuration is more efficient then the aSi array the same size APSA type as the aSi array will deliver significantly more power. In order to simplify the update it was decided to keep the array area the same, i.e., a single 1 x 2m array for configurations a through d. In addition, the updated weights include only the array, the support structure and the deployment system. This was done to make comparisons with other technologies possible since the stowage systems and control system are normally driven by the specific applications.

The results are as follows:

5.1 TUBULAR CONFIGURATION IN A 740 KILOMETER POLAR ORBIT, APSA TYPE SYSTEM

Torus Diameter	4 Inches
Laminate Thickness	4 mil plastic / 3 mil Al / 4 mil plastic
Inflation System Wgt.	.6 lb
BOL Power (Panel)	255 Watts
Array Dimensions	.91m x 2.36m = 2.15m^2

Aspect Ratio	2.6
Max G-Load	.03
Cell Thickness	2 mil
Shield Thickness	2 mil
Array Weight	0.93 Kg
Structure/Deploy Wgt.	3.4 lb (1.54 Kg)
Total Weight	2.46 Kg
Watts/Kilogram	103
% Structural Weight	62%

5.2 TUBULAR CONFIGURATION IN A 740 KILOMETER POLAR ORBIT, APSA TYPE SYSTEM, ATTACHED TO A STEP-TYPE SATELLITE BUS

This configuration is the same as configuration a and is shown in Figure 6.0-1.

5.3 TUBULAR CONFIGURATION IN A 740 KILOMETER POLAR ORBIT, APSA TYPE SYSTEM, ATTACHED TO A TECHSTARS-TYPE SATELLITE BUS

This configuration is the same as configuration a and b, but attached to a Techstars bus. The mounting is essentially the same as that shown in Drawing 21012, Appendix 2.

5.4 TUBULAR CONFIGURATION IN A 6 HOUR MOLNIYA ORBIT, APSA TYPE SYSTEM, ATTACHED TO A TECHSTARS-TYPE SATELLITE BUS

Torus Diameter	4 Inches
Laminate Thickness	4 mil plastic / 3 mil Al / 4 mil plastic
Inflation System Wgt.	.6 lb
BOL Power (Panel)	255 Watts
Array Dimensions	.91m x 2.36m = 2.15m^2
Aspect Ratio	2.6
Max G-Load	.03
Cell Thickness	2 mil
Shield Thickness	24 mil
Array Weight	2.2 Kg
Structure/Deploy Wgt.	3.4 lb (1.54 Kg)
Total Weight	3.74 Kg
Watts/Kilogram	68
% Structural Weight	41%

The physical configuration is shown in Drawing 21012, Appendix 2.

5.5 TUBULAR CONFIGURATION IN A 740 KILOMETER POLAR ORBIT, 1500 WATTS, APSA TYPE SYSTEM

Torus Diameter	5 Inches
Laminate Thickness	4 mil plastic / 4 mil Al / 4 mil plastic
Inflation System Wgt.	2.4 lb
BOL Power (Panel)	1500 Watts
Array Dimensions	1.6m x 7.9m = 12.64m^2
Aspect Ratio	5
Max G-Load	.03
Cell Thickness	2 mil
Shield Thickness	2 mil
Array Weight	5.43 Kg
Structure/Deploy Wgt.	3.26 Kg
Total Weight	8.69 Kg
Watts/Kilogram	172
% Structural Weight	38%

5.6 TUBULAR CONFIGURATION IN A 740 KILOMETER POLAR ORBIT, 5800 WATTS, APSA TYPE SYSTEM

Torus Diameter	6 Inches
Material Thickness	12 mil
Inflation System Wgt.	6.5 lb
BOL Power (Panel)	5800 Watts
Array Dimensions	4.0m x 12.25m = 49m^2
Aspect Ratio	3
Max G-Load	.03
Cell Thickness	2 mil
Shield Thickness	2 mil
Array Weight	21.08 Kg
Structure/Deploy Wgt.	10.77 Kg
Total Weight	31.85 Kg
Watts/Kilogram	182
% Structural Weight	34%

6.0 PREFLIGHT READINESS TEST CONFIGURATION

The final task of Phase 1 of the program was to "use all available information to recommend a pre-flight readiness test (PFRT) inflatable solar array concept. This concept shall minimize system mass and packaged volume, have approximately two square meters of deployed solar cell area, be designed to operate for three years in a 740 kilometer polar orbit, be completely self-contained, and be suitable for a thermal vacuum chamber test or a space flight experiment. This concept shall demonstrate inflatable solar array operations yet have packaging and deployment requirements that are as simple as possible. The contractor shall consider project cost, schedule, and technical risk for this recommendation."

Results of the concept definition study (Section 2.0) indicate the use of an inflatable deployed rigidizable tubular structure for the PFRT. Feasibility of this type of structure was proven in the packaging and deployment test. Results of the Phase 1 studies also indicate that an aSi or CIS array deployed and supported by an inflatable structure will potentially provide the maximum packaging flexibility, and cleft Gallium arsenide array the highest watts per kilogram.

The lack of availability of these types of arrays for this program dictates the use of the APSA blanket system with the crystalline silicon cells for the PFRT. This configuration is shown in Figure 6.0-1A and B.

The two arrays are packaged in a rectangular housing shown mounted on the base of a STEP type satellite. Each array is mounted on arms that are hinged to allow the panel to be rotated 180° and latched so the panel is outboard of the satellite. The arm also contains a swivel joint to allow the panels to be pointed in a nominal sun direction and then held in position. This approach eliminates the need for an active pointing and control system, thus minimizing the cost of the experiment.

After the support arms are deployed the arrays are then extended with the following sequence of events:

a. Actuate cable cutters to release housing.
b. Actuate GN_2 bottle pyrotechnic valve.
c. Release of gas pressure closes the vent valve.
d. GN_2 flows thru the controlling solenoid valve into the two inflatable tubes. Pressure is controlled by the valve and the pressure control system to provide a constant deployment pressure.
e. The accordion folded tubes extend causing the accordion folded array to extend.
f. The tube inflation pressure is then increased to 13 psi to rigidize the structure.

The housing and housing cover provide the end members of the support structure and the inflatable tubes provide the side structure.

Both the array and side tubes are accordion folded on 6.28 centers (⅓ the tube circumference). The folds in the tubes are oriented at 90° to the folds in

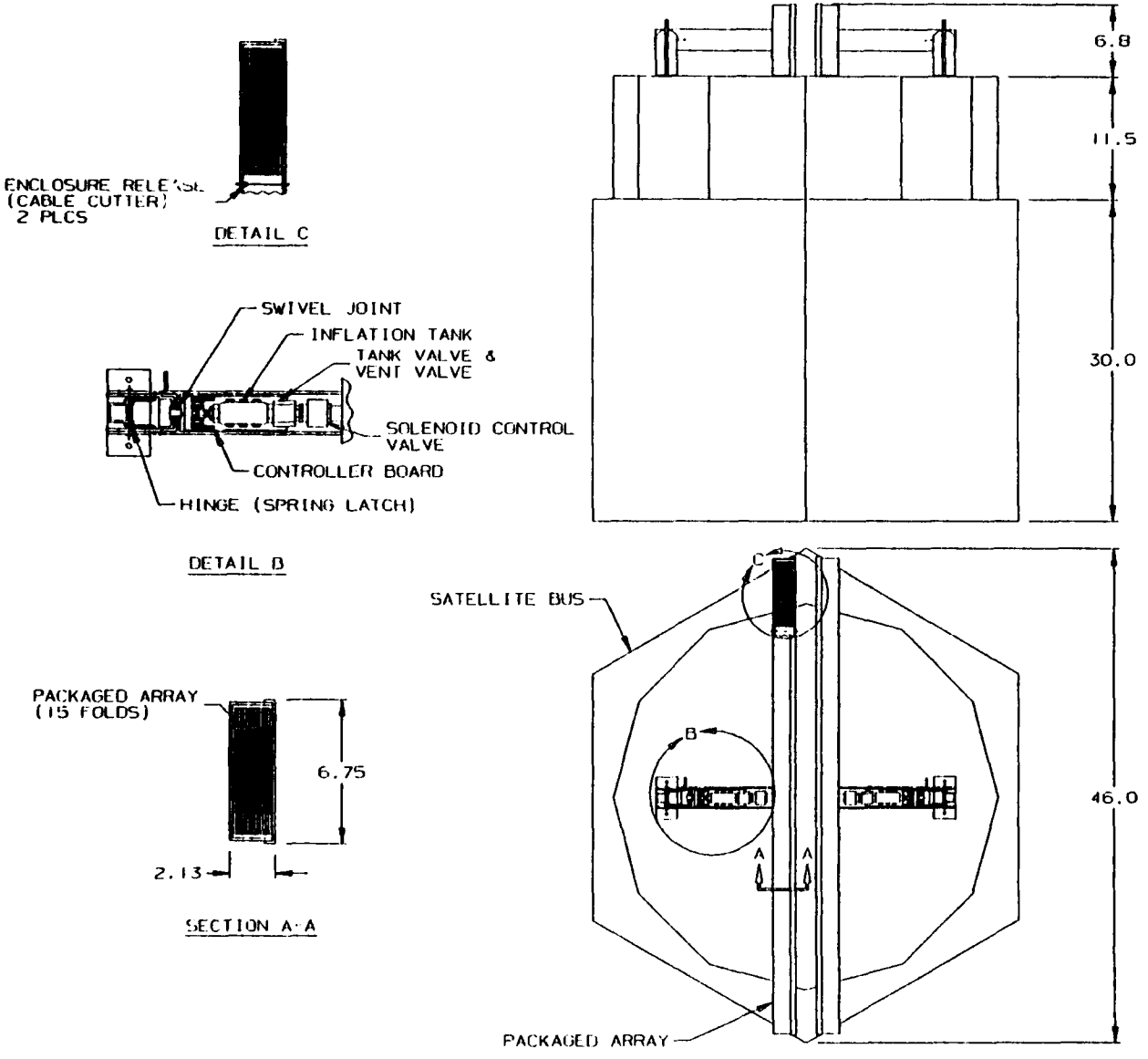

Figure 6.0-1A PFRT Configuration

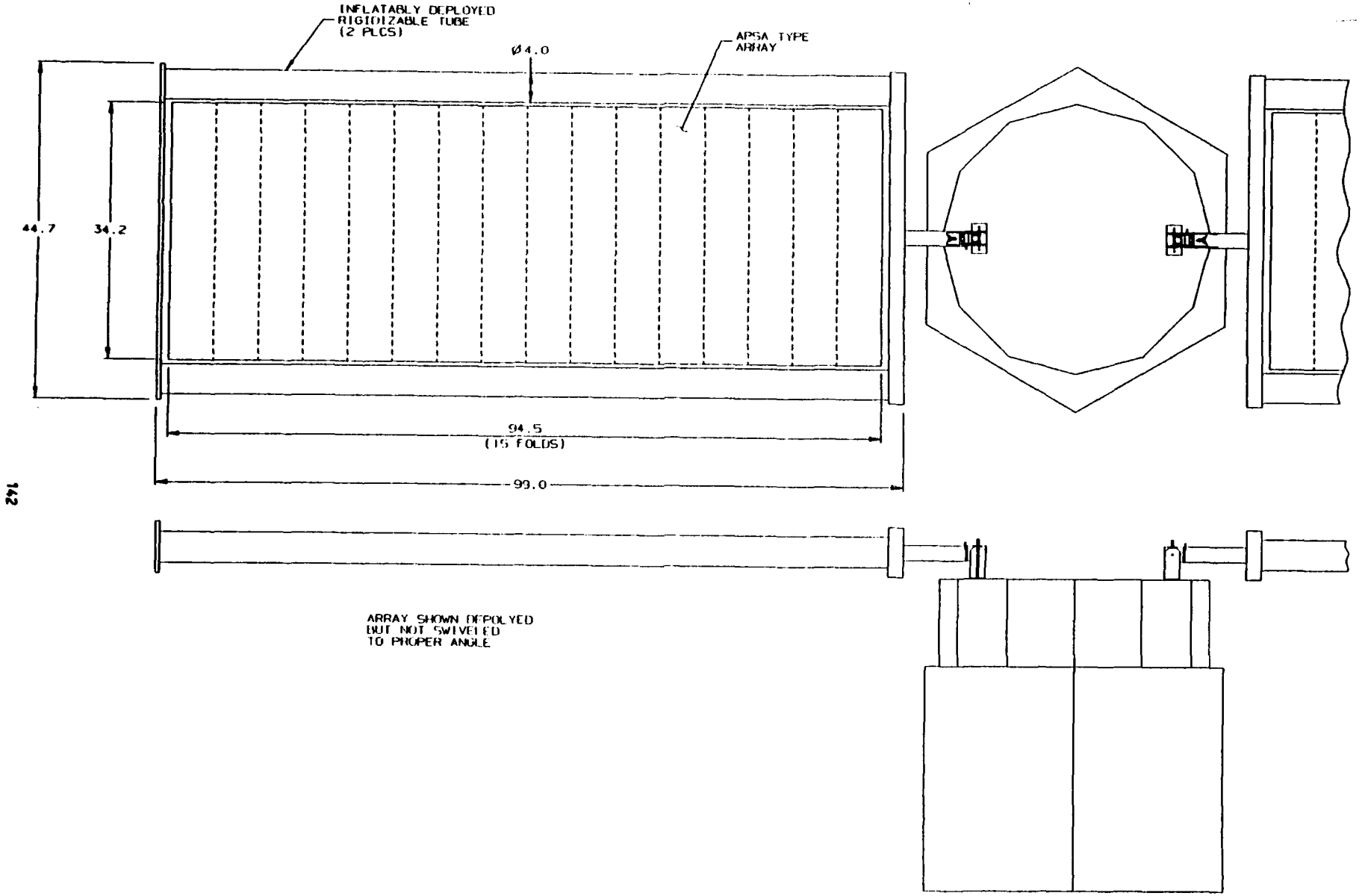

Figure 6.0-1B. PFRT Configuration (Cont)

the array with a flexible tie between the array and tubes at every other fold line. The 90° orientation of the folds provides considerable stability during the deployment process eliminating a concern identified during the packaging deployment testing.

The array itself (to be supplied by Spectro Lab Inc.) will consist of 2 mil crystalline silicon cells mounted on a two mil thick Kapton substrate. Two mil thick glass cover slides will be mounted on the front side for a total thickness of 7.5 mils. For the experiment only, it is recommended (for cost purposes) that only 10% of the array will be populated with real cells and 90% simulated mass representative units. Each cell will be approximately 1.18 x 3.1 in. The panel output voltage will be nominally 28 VDC with protection diodes.

The packaged system will require approximately 600 in^3 for the array, support structure and deployment system. The weight breakdown is shown in Table 6.0-1.

TABLE 6.0-1. SYSTEM WEIGHT SUMMARY
(LBS)

Housing			.74
Base	.44		
Cover	.30		
Inflatable Tubes			1.475
.738 each			
Array			2.04
Controller Sequencer			.03
Inflation System			1.0
Tank, Pyro Valve	.6		
Vent Valve	.15		
Solenoid Valve	.25		
Cable Cutters			0.1
.05 each			
Support Structure			.218
Arm & End Fitting	.138		
Bearing	.02		
Bracket	.04		
Spring & Pin	.02		
		Sub Total	5.603 lbs
Misc & Contingency			.397 lbs
			6.000 lbs

7.0 CONCLUSIONS

The studies and testing performed during Phase 1 of the ITSAT Program establish the feasibility of using an inflatable structure to deploy a flexible solar array. The concept provides a higher power to mass ratio then all current technologies, especially for small arrays. In addition, it provides low packaged volume and latitude in packaged shapes. These last two features are extremely important for the spacecraft designer who is trying to package multiple spacecraft in a relatively small booster such as the Pegasus. In addition, there are a number of other conclusions:

1. The amorphous silicon and especially CIS arrays in conjunction with an inflatable structure have the greatest potential for providing the lowest volume and the most packaging flexibility of all technologies.

2. The cleft Gallium arsenide arrays have the most potential for providing the highest power to mass ratio.

3. It appears that the amorphous silicon, CIS, or cleft Gallium arsenide technologies will not be sufficiently advanced to support the ITSAT schedule.

4. The APSA type system with 2 mil crystalline silicon cells mounted on an aluminum laminate rigidizable structure can provide a higher power to mass ratio then any currently developed technology.

5. Of the three configurations studied - spherical, pillow and tubular, the tubular proved to be best.

6. For applications involving mission lives of more than a few weeks a rigidizable structure (as opposed to inflated) will be required.

7. The aluminum laminate structure is appropriate for arrays up to a few kilowatts. Larger arrays will require either a UV cured resin or water soluble gel system.

8. Further work is required to firmly establish the inherent deployment reliability of the inflatable structure concept.

8.0 RECOMMENDATIONS

L'Garde recommends that the ITSAT Program proceed into the Phase 2 Preflight Readiness Test Phase. The PFRT configuration consisting of an APSA type system with 2 mil crystalline silicon cells supported and deployed by a rigidizable aluminum laminate structure (Section 6) should be the baseline design concept. This concept should form the basis for detail design, development testing, environmental testing including thermal cycling in vacuum and finally a deployment/functional test in a vacuum chamber.

Since this type array has been space qualified the primary concern will be space qualification of the rigidizable structure. Special attention must be directed towards the selection of the plastic film and adhesives used in the structural laminate.

Another area that should be addressed further is reliability. The "one shot" nature of PFRT configuration precludes repeated preflight testing. L'Garde recommends, therefore, that the structure be treated as any other one shot device and establish its reliability by lot acceptance testing. This testing could be performed during the Phase 3 Space Flight Experiment as part of the formal qualification testing.

References

2.0-1 Visentine, J.T., DurCanin, J.T. and Chalmers, D.R.: The Definition of Environment and its Effects on Thermal Control Materials, AIAA-87-1599.

2.0-2 Denman, J.E., and Maldoon, L.C., Hughes Aircraft Co., SAMPE 31st International Symposium, 5/8/86, Las Vegas.

2.0-3 Yeaple F., Design News, Page 190, 3/27/89.

2.0-4 Williams, Geoff and Friese, Gil, Gas Loss Due to Meteoroid and Debris Damage, L'Garde Report LTR-87-GW-007, June 1990.

2.0-5 Williams, Geoff, Meteoroid Penetration Analysis, L'Garde Report LTR-87-GW-031, Nov 1987.

2.0-6 White, Frank M., Fluid Mechanics, McGraw-Hill Book Co., 1979, ISBN 0-07-069667-5.

2.0-7 Friese, Gil, Leak Testing of Space Inflatables, L'Garde Report LTR-87-GF-027, 20 October 1987.

2.0-8 Gay, C.F., Potter, R.R., Tanner, D.P. and Anspauch, B.E., Proc. 17th IEEE Photovoltaic Specialists Conf.

2.0-9 L'Garde, Inc., "Highly Accurate Inflatable Reflectors, Phase II Final Report", LTR-86-GV-129, 1/16/87

2.0-10 Bernasconi, M.C., "Study on Large Ultralight Structures in Space. Phase II Final Report", Contraves Corp., July 1982.

2.0-11 L'Garde, Inc., "Inflatable/Rigidizable Material, Final Report", LTR-89-DC-009, May 1989

2.0-12 Kouba, Lt. E., "STEP & Techstars", fax to L'Garde, 7/24/90.

3.0-1 L'Garde,Inc. subcontract (PO# SC2247) to Apogee Corp., Attachment 2, "UL-125 Mechanical Specifications".

3.0-2 C. Riordan and R. Hulstrom, SERI, "What is an Air Mass 1.5 Spectrum?", 21st IEEE Photovoltaic Specialists Conference, May, 1990.

3.0-3 J. Woodyard, "Annealing Characteristics of Amorphous Silicon Alloy Solar Cells Irradiated with 1.00 MeV Protons", XI Space Photovoltaic Research and Technology Conference, May 1991.

3.0-4 JPL, Solar Cell Array Design Handbook, Oct., 1986.

3.0-5 Hanak et al., "Deployable Aerospace Photovoltaic Array Based on Amorphous Silicon Alloys"

References - Continued

3.0-6 Hanak, J. Apogee Corp., letter to L'Garde, Inc., Mar 1991

3.0-7 Stafford, B., et al., "Status of the DOE/SERI Amorphous Silicon Research Project: Recent Advances and Future Directions", 21st IEEE PVSC, May 1990.

3.0-8 C. Osterwald et al., "Comparison of the Temperature Coefficients of the Basic I-V Parameters for Various Types of Solar Cells".

3.0-9 NASA JPL Publications 82-69, Solar Cell Radiation Handbook 3rd Edition.

3.0-10 Gidanian, K., L'Garde Technical Report LTR-90-KG-020, "Optically Transparent/Colorless Polyimide Films for Solar Array Applications", Sept., 1990.

3.0-11 Hanak, J. "Notes on the Fabrication, Testing, and Performance Characteristics of the FLX-125 Photovoltaic Array", letter to L'Garde, Inc., May 15, 1991.

3.0-12 Derbes, L'Garde Memo LM-BD-494, "Report on Trip to Check Status of Solar Array Fabrication at Apogee", Nov., 1990.

3.0-13 Hanak, et al., "Integral Bypass Diodes in an Amorphous Silicon Alloy Photovoltaic Module", SPRAT, 1990.

3.0-14 Hanak, "Stowable Large Area Solar Power Module", US Patent No. 4,713,492, Dec., 1987.

3.0-15 "Buckling of thin-walled circular cylinders", National Aeronautics and Space Administration, September 1968.

3.0-16 Shigley and Mitchell, "Mechanical Engineering Design", McGraw Hill, N.Y., 1983.

4.0-1 L'Garde, Inc., "ITSAT Test Plan", CDRL A010, May, 1991.

4.0-2 B. Derbes, L'Garde Memo LM-90-BD-544, "ISA Solar Array Test at L'Garde", Dec., 1990.

4.0-3 Sanyo Corp., "Sanyo Electric Announces New Amorton™ Flexible Solar Cell Film Material", News Release, June, 1990.

APPENDIX A1

TUBE BENDING AND BUCKLING

A1. BENDING AND BUCKLING

In order to analyze buckling of the tubes of interest, which have large length to radius ratios, the bending buckling data of Figure A1-3 was extrapolated using a log least squares method. The results are in Figure A1-1 and A1-2. The results were coded into a fortran program called "torusbend", which was used to analyze the torus structures of interest. The listing is enclosed.

The resulting analysis involves much extrapolation, and as such is useful only for conceptual studies. Generally, it is desirable to avoid very large length to radius ratios as much as possible in the selection of a tube.

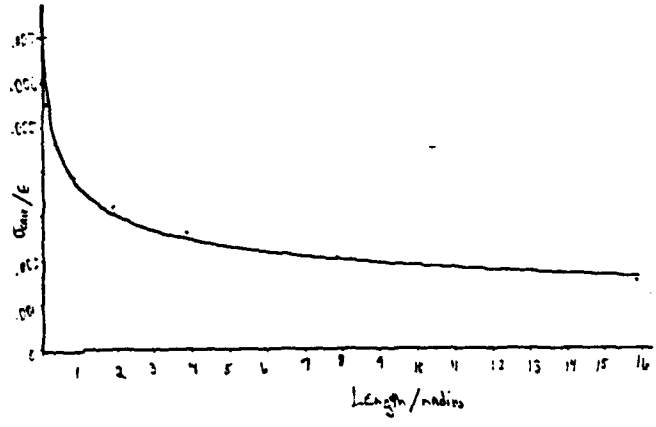

Figure A1-1. Critical Stress/E vs. Length/Radius for Radius/Thick=100

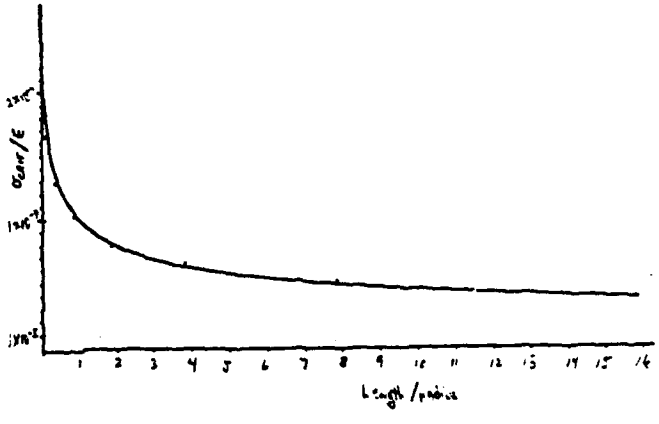

Figure A1-2. Critical Stress/E vs. Length/Radius for Radius/Thick=1000

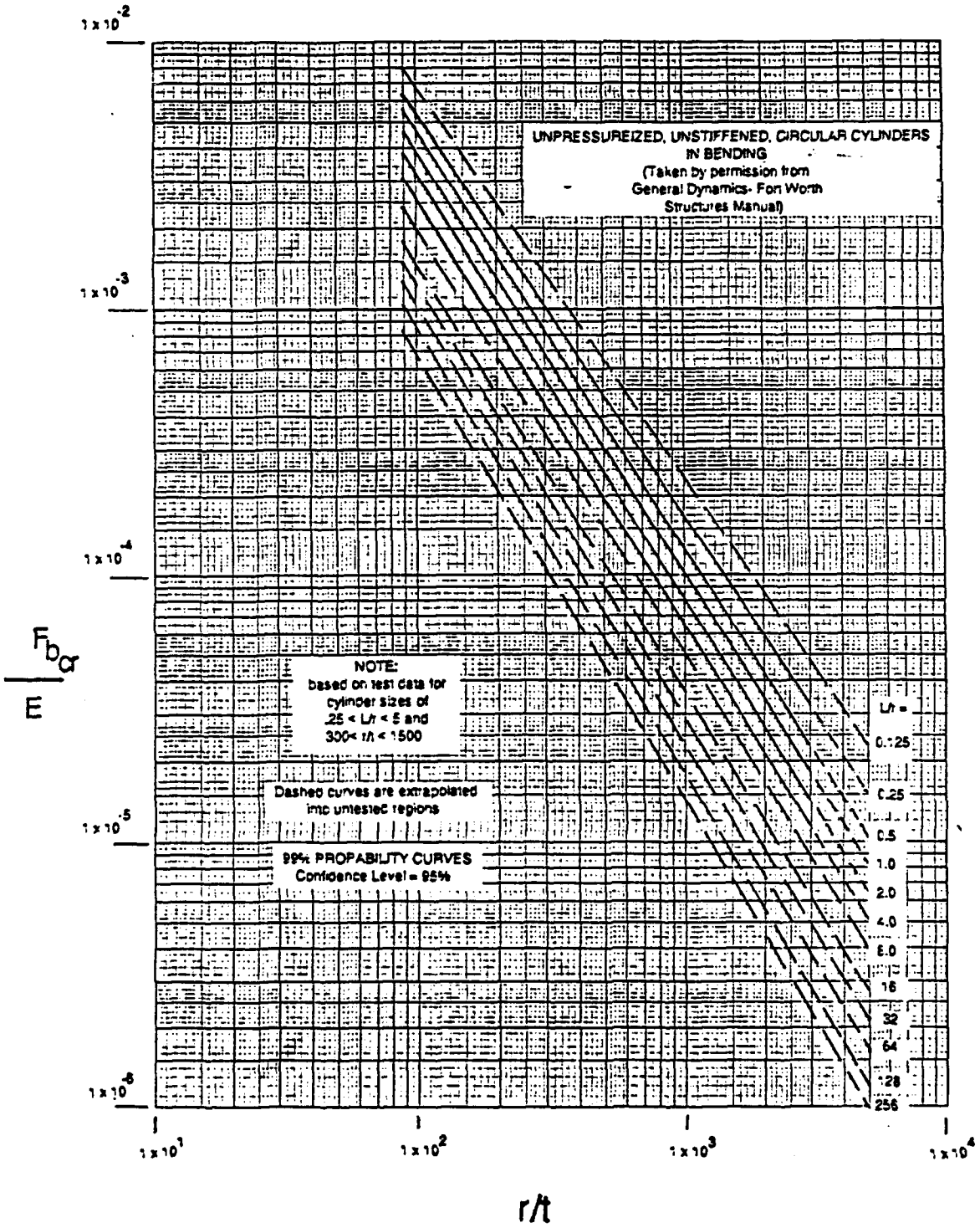

Figure A1-3. Critical Stress/E vs. Length/Radius and Radius/Thick

```
      program torusbend

C This program optimizes beam diameter and thickness for bending.
C Weight is traded as a function of radius & thickness for a specified
C     solar array.
C This assumes there are 'numtubes' bundled tubes, equally loaded.
C When more than one tube is used, results are for each tube.
C Assumes torus design, so loads are divided in half (born by two tubes).
C Assumes 1/4 mil mylar coat on each side.
C User includes dynamics/safety factor in acceleration input.
C All results and input are for one solar paddle.
C All results are printed to a file called 'bendout'.
C Negative values of 'delta' represent failure.

      implicit none
      real r,t,w,l,dia,area,M,Iz,loadstress,lor,rot,E,critstress,
     1     numtubes,salength, sawidth, saweight, tubedensity,
     2     inithick,delthick,initdia,deldia,accel
      integer i,j
      real PI
      PI = 3.141592654


      write(9,*)'number of tubes in bundle ?'
      read(9,*)numtubes
      write(9,*)'aluminum  density = .098;  E = 3.7e6'
      write(9,*)'Kevlar/UV density = .051;  E = 1.0e6'
      write(9,*)'tube material density, lb/in3 (excluding mylar coat) ?'
      read(9,*)tubedensity
      write(9,*)'E of tube material, psi ?'
      read(9,*)E
      write(9,*)'accel, ft/sec2 (include dynamics/safety factor) ?'
      read(9,*)accel
      write(9,*)'length from spacecraft of solar array itself,inches ?'
      read(9,*)salength
      write(9,*)'width of one side solar array itself, inches ?'
      read(9,*)sawidth
      write(9,*)'weight of one side solar array itself, pounds ?'
      read(9,*)saweight
      write(9,*)'initial thickness, inches ?'
      read(9,*)inithick
      write(9,*)'delta thickness, inches ?'
      read(9,*)delthick
      write(9,*)'initial diameter, inches ?'
      read(9,*)initdia
      write(9,*)'delta diameter, inches ?'
      read(9,*)deldia
      open(1,file='bendout',status='new')
      write(1,*)'numtubes =',numtubes
      write(1,*)'tubedensity =',tubedensity
      write(1,*)'E =',E
      write(1,*)'accel =',accel
      write(1,*)'salength =',salength
      write(1,*)'sawidth =',sawidth
      write(1,*)'saweight =',saweight
      write(1,*) ' dia   t    w,sa+tube loadstress critstress    delta'

      dia = initdia - deldia
      do 10 i=1,17
        dia = dia + deldia
        r = dia/2.
```

```
          t= inithick - delthick
          do 20 j=1,20
            t = t + delthick

            l = salength + 2.*dia
            area = 2.*(salength+sawidth+(2.*dia))*PI*dia
            w = saweight + numtubes*(area*.0005*.0512
     1          + area*(t-.0005)*tubedensity)
            M = (accel*w/32.2)*(l/2.)*.5/numtubes
            Iz = PI*(r**4. - (r-t)**4.)/4.
            loadstress = M*r/Iz

            lor = l/r
            rot = r/t
            call curves(lor,rot,E,critstress,r,t,l)

            write(1,100) dia,t,w,loadstress,critstress,
     1                   (critstress-loadstress)

         20   continue
         10 continue

            write(9,*)'See bendout for results'

        100 format(f5.2,f6.4,f8.2,2x,f8.1,4x,f8.1,4x,f8.1)

            stop
            end


            subroutine curves(lor,rot,E,critstress,r,t,l)
            implicit none
            real lor,rot,E,critstress,lor32(15),lor64(15),lor128(15),lor32a,
           1     lor64a,lor128a,FbcroE,r,t,l,lor256(15),lor256a

        C Data taken from General Dynamics Structures Manual.
        C Also see Appendix 5 of L'Garde, Inc.,
        C       "Inflatable Solar Array Conceptual Designs", August, 1990

            lor32(1) = 1.32e-3
            lor64(1) = 1.07e-3
            lor128(1) = 8.67e-4
            lor256(1) = 7.03e-4

            lor32(2) = 4.26e-4
            lor64(2) = 3.42e-4
            lor128(2) = 2.75e-4
            lor256(2) = 2.21e-4

            lor32(3) = 2.18e-4
            lor64(3) = 1.74e-4
            lor128(3) = 1.38e-4
            lor256(3) = 1.1e-4

            lor32(4) = .000138
            lor64(4) = .000108
            lor128(4) = .000085
            lor256(4) = .0000675

            lor32(5) = .000096
            lor64(5) = .000075
            lor128(5) = .000058
            lor256(5) = .000046
```

```
      lor32(6) = .00007
      lor64(6) = .000056
      lor128(6) = .000043
      lor256(6) = .000034

      lor32(7) = .000056
      lor64(7) = .000043
      lor128(7) = .000033
      lor256(7) = .000026

      lor32(8) = .000044
      lor64(8) = .0000345
      lor128(8) = .000026
      lor256(8) = .000021

      lor32(9) = .000037
      lor64(9) = .000028
      lor128(9) = .0000215
      lor256(9) = .000017

      lor32(10) = 3.01e-5
      lor64(10) = 2.34e-5
      lor128(10) = 1.82e-5
      lor256(10) = 1.42e-5

      lor32(11) = .0000265
      lor64(11) = .00002
      lor128(11) = .000015
      lor256(11) = .000012

      lor32(12) = .000023
      lor64(12) = .0000175
      lor128(12) = .000013
      lor256(12) = .0000105

      lor32(13) = .00002
      lor64(13) = .000015
      lor128(13) = .0000115
      lor256(13) = .0000092

      lor32(14) = .000018
      lor64(14) = .0000135
      lor128(14) = .00001
      lor256(14) = .000008

      lor32(15) = .000016
      lor64(15) = .000012
      lor128(15) = .000009
      lor256(15) = .0000071

C  32 ≤ l/r ≤ 256
C 100 ≤ r/t ≤ 1500

      if ((rot .ge. 100.) .and. (rot .le. 200.)) then
         if ((lor .ge. 32.) .and. (lor .le. 64.)) then
           call interp(lor32(1),lor32(2),100.,rot,200.,lor32a)
           call interp(lor64(1),lor64(2),100.,rot,200.,lor64a)
           call interp(lor32a,lor64a,32,lor,64,FbcroE)
         else if ((lor .gt. 64.) .and. (lor .le. 128.)) then
           call interp(lor64(1),lor64(2),100.,rot,200.,lor64a)
           call interp(lor128(1),lor128(2),100.,rot,200.,lcr128a)
           call interp(lor64a,lor128a,64,lor,128,FbcroE)
```

```
      else if ((lor .gt. 128.) .and. (lor .le. 256.)) then
        call interp(lor128(1),lor128(2),100.,rot,200.,lor128a)
        call interp(lor256(1),lor256(2),100.,rot,200.,lor256a)
        call interp(lor128a,lor256a,128,lor,256,FbcroE)
      else
        write(9,*) 'lor range exceeded (CR)',lor,l,r,t
        pause
      end if
    else if ((rot .gt. 200.) .and. (rot .le. 300.)) then
      if ((lor .ge. 32.) .and. (lor .le. 64.)) then
        call interp(lor32(2),lor32(3),200.,rot,300.,lor32a)
        call interp(lor64(2),lor64(3),200.,rot,300.,lor64a)
        call interp(lor32a,lor64a,32,lor,64,FbcroE)
      else if ((lor .gt. 64.) .and. (lor .le. 128.)) then
        call interp(lor64(2),lor64(3),200.,rot,300.,lor64a)
        call interp(lor128(2),lor128(3),200.,rot,300.,lor128a)
        call interp(lor64a,lor128a,64,lor,128,FbcroE)
      else if ((lor .gt. 128.) .and. (lor .le. 256.)) then
        call interp(lor128(2),lor128(3),200.,rot,300.,lor128a)
        call interp(lor256(2),lor256(3),200.,rot,300.,lor256a)
        call interp(lor128a,lor256a,128,lor,256,FbcroE)
      else
        write(9,*) 'lor range exceeded (CR)',lor,l,r,t
        pause
      end if
    else if ((rot .gt. 300.) .and. (rot .le. 400.)) then
      if ((lor .ge. 32.) .and. (lor .le. 64.)) then
        call interp(lor32(3),lor32(4),300.,rot,400.,lor32a)
        call interp(lor64(3),lor64(4),300.,rot,400.,lor64a)
        call interp(lor32a,lor64a,32,lor,64,FbcroE)
      else if ((lor .gt. 64.) .and. (lor .le. 128.)) then
        call interp(lor64(3),lor64(4),300.,rot,400.,lor64a)
        call interp(lor128(3),lor128(4),300.,rot,400.,lor128a)
        call interp(lor64a,lor128a,64,lor,128,FbcroE)
      else if ((lor .gt. 128.) .and. (lor .le. 256.)) then
        call interp(lor128(3),lor128(4),300.,rot,400.,lor128a)
        call interp(lor256(3),lor256(4),300.,rot,400.,lor256a)
        call interp(lor128a,lor256a,128,lor,256,FbcroE)
      else
        write(9,*) 'lor range exceeded (CR)',lor,l,r,t
        pause
      end if
    else if ((rot .gt. 400.) .and. (rot .le. 500.)) then
      if ((lor .ge. 32.) .and. (lor .le. 64.)) then
        call interp(lor32(4),lor32(5),400.,rot,500.,lor32a)
        call interp(lor64(4),lor64(5),400.,rot,500.,lor64a)
        call interp(lor32a,lor64a,32,lor,64,FbcroE)
      else if ((lor .gt. 64.) .and. (lor .le. 128.)) then
        call interp(lor64(4),lor64(5),400.,rot,500.,lor64a)
        call interp(lor128(4),lor128(5),400.,rot,500.,lor128a)
        call interp(lor64a,lor128a,64,lor,128,FbcroE)
      else if ((lor .gt. 128.) .and. (lor .le. 256.)) then
        call interp(lor128(4),lor128(5),400.,rot,500.,lor128a)
        call interp(lor256(4),lor256(5),400.,rot,500.,lor256a)
        call interp(lor128a,lor256a,128,lor,256,FbcroE)
      else
        write(9,*) 'lor range exceeded (CR)',lor,l,r,t
        pause
      end if
    else if ((rot .gt. 500.) .and. (rot .le. 600.)) then
      if ((lor .ge. 32.) .and. (lor .le. 64.)) then
        call interp(lor32(5),lor32(6),500.,rot,600.,lor32a)
```

```
          call interp(lor64(5),lor64(6),500.,rot,600.,lor64a)
          call interp(lor32a,lor64a,32,lor,64,FbcroE)
        else if ((lor .gt. 64.) .and. (lor .le. 128.)) then
          call interp(lor64(5),lor64(6),500.,rot,600.,lor64a)
          call interp(lor128(5),lor128(6),500.,rot,600.,lor128a)
          call interp(lor64a,lor128a,64,lor,128,FbcroE)
        else if ((lor .gt. 128.) .and. (lor .le. 256.)) then
          call interp(lor128(5),lor128(6),500.,rot,600.,lor128a)
          call interp(lor256(5),lor256(6),500.,rot,600.,lor256a)
          call interp(lor128a,lor256a,128,lor,256,FbcroE)
        else
          write(9,*) 'lor range exceeded (CR)',lor,l,r,t
          pause
        end if
      else if ((rot .gt. 600.) .and. (rot .le. 700.)) then
        if ((lor .ge. 32.) .and. (lor .le. 64.)) then
          call interp(lor32(6),lor32(7),600.,rot,700.,lor32a)
          call interp(lor64(6),lor64(7),600.,rot,700.,lor64a)
          call interp(lor32a,lor64a,32,lor,64,FbcroE)
        else if ((lor .gt. 64.) .and. (lor .le. 128.)) then
          call interp(lor64(6),lor64(7),600.,rot,700.,lor64a)
          call interp(lor128(6),lor128(7),600.,rot,700.,lor128a)
          call interp(lor64a,lor128a,64,lor,128,FbcroE)
        else if ((lor .gt. 128.) .and. (lor .le. 256.)) then
          call interp(lor128(6),lor128(7),600.,rot,700.,lor128a)
          call interp(lor256(6),lor256(7),600.,rot,700.,lor256a)
          call interp(lor128a,lor256a,128,lor,256,FbcroE)
        else
          write(9,*) 'lor range exceeded (CR)',lor,l,r,t
          pause
        end if
      else if ((rot .gt. 700.) .and. (rot .le. 800.)) then
        if ((lor .ge. 32.) .and. (lor .le. 64.)) then
          call interp(lor32(7),lor32(8),700.,rot,800.,lor32a)
          call interp(lor64(7),lor64(8),700.,rot,800.,lor64a)
          call interp(lor32a,lor64a,32,lor,64,FbcroE)
        else if ((lor .gt. 64.) .and. (lor .le. 128.)) then
          call interp(lor64(7),lor64(8),700.,rot,800.,lor64a)
          call interp(lor128(7),lor128(8),700.,rot,800.,lor128a)
          call interp(lor64a,lor128a,64,lor,128,FbcroE)
        else if ((lor .gt. 128.) .and. (lor .le. 256.)) then
          call interp(lor128(7),lor128(8),700.,rot,800.,lor128a)
          call interp(lor256(7),lor256(8),700.,rot,800.,lor256a)
          call interp(lor128a,lor256a,128,lor,256,FbcroE)
        else
          write(9,*) 'lor range exceeded (CR)',lor,l,r,t
          pause
        end if
      else if ((rot .gt. 800.) .and. (rot .le. 900.)) then
        if ((lor .ge. 32.) .and. (lor .le. 64.)) then
          call interp(lor32(8),lor32(9),800.,rot,900.,lor32a)
          call interp(lor64(8),lor64(9),800.,rot,900.,lor64a)
          call interp(lor32a,lor64a,32,lor,64,FbcroE)
        else if ((lor .gt. 64.) .and. (lor .le. 128.)) then
          call interp(lor64(8),lor64(9),800.,rot,900.,lor64a)
          call interp(lor128(8),lor128(9),800.,rot,900.,lor128a)
          call interp(lor64a,lor128a,64,lor,128,FbcroE)
        else if ((lor .gt. 128.) .and. (lor .le. 256.)) then
          call interp(lor128(8),lor128(9),800.,rot,900.,lor128a)
          call interp(lor256(8),lor256(9),800.,rot,900.,lor256a)
          call interp(lor128a,lor256a,128,lor,256,FbcroE)
        else
```

```
        write(9,*) 'lor range exceeded (CR)',lor,l,r,t
        pause
      end if
    else if ((rot .gt. 900.) .and. (rot .le. 1000.)) then
      if ((lor .ge. 32.) .and. (lor .le. 64.)) then
        call interp(lor32(9),lor32(10),900.,rot,1000.,lor32a)
        call interp(lor64(9),lor64(10),900.,rot,1000.,lor64a)
        call interp(lor32a,lor64a,32,lor,64,FbcroE)
      else if ((lor .gt. 64.) .and. (lor .le. 128.)) then
        call interp(lor64(9),lor64(10),900.,rot,1000.,lor64a)
        call interp(lor128(9),lor128(10),900.,rot,1000.,lor128a)
        call interp(lor64a,lor128a,64,lor,128,FbcroE)
      else if ((lor .gt. 128.) .and. (lor .le. 256.)) then
        call interp(lor128(9),lor128(10),900.,rot,1000.,lor128a)
        call interp(lor256(9),lor256(10),900.,rot,1000.,lor256a)
        call interp(lor128a,lor256a,128,lor,256,FbcroE)
      else
        write(9,*) 'lor range exceeded (CR)',lor,l,r,t
        pause
      end if
    else if ((rot .gt. 1000.) .and. (rot .le. 1100.)) then
      if ((lor .ge. 32.) .and. (lor .le. 64.)) then
        call interp(lor32(10),lor32(11),1000.,rot,1100.,lor32a)
        call interp(lor64(10),lor64(11),1000.,rot,1100.,lor64a)
        call interp(lor32a,lor64a,32,lor,64,FbcroE)
      else if ((lor .gt. 64.) .and. (lor .le. 128.)) then
        call interp(lor64(10),lor64(11),1000.,rot,1100.,lor64a)
        call interp(lor128(10),lor128(11),1000.,rot,1100.,lor128a)
        call interp(lor64a,lor128a,64,lor,128,FbcroE)
      else if ((lor .gt. 128.) .and. (lor .le. 256.)) then
        call interp(lor128(10),lor128(11),1000.,rot,1100.,lor128a)
        call interp(lor256(10),lor256(11),1000.,rot,1100.,lor256a)
        call interp(lor128a,lor256a,128,lor,256,FbcroE)
      else
        write(9,*) 'lor range exceeded (CR)',lor,l,r,t
        pause
      end if
    else if ((rot .gt. 1100.) .and. (rot .le. 1200.)) then
      if ((lor .ge. 32.) .and. (lor .le. 64.)) then
        call interp(lor32(11),lor32(12),1100.,rot,1200.,lor32a)
        call interp(lor64(11),lor64(12),1100.,rot,1200.,lor64a)
        call interp(lor32a,lor64a,32,lor,64,FbcroE)
      else if ((lor .gt. 64.) .and. (lor .le. 128.)) then
        call interp(lor64(11),lor64(12),1100.,rot,1200.,lor64a)
        call interp(lor128(11),lor128(12),1100.,rot,1200.,lor128a)
        call interp(lor64a,lor128a,64,lor,128,FbcroE)
      else if ((lor .gt. 128.) .and. (lor .le. 256.)) then
        call interp(lor128(11),lor128(12),1100.,rot,1200.,lor128a)
        call interp(lor256(11),lor256(12),1100.,rot,1200.,lor256a)
        call interp(lor128a,lor256a,128,lor,256,FbcroE)
      else
        write(9,*) 'lor range exceeded (CR)',lor,l,r,t
        pause
      end if
    else if ((rot .gt. 1200.) .and. (rot .le. 1300.)) then
      if ((lor .ge. 32.) .and. (lor .le. 64.)) then
        call interp(lor32(12),lor32(13),1200.,rot,1300.,lor32a)
        call interp(lor64(12),lor64(13),1200.,rot,1300.,lor64a)
        call interp(lor32a,lor64a,32,lor,64,FbcroE)
      else if ((lor .gt. 64.) .and. (lor .le. 128.)) then
        call interp(lor64(12),lor64(13),1200.,rot,1300.,lor64a)
        call interp(lor128(12),lor128(13),1200.,rot,1300.,lor128a)
```

```
            call interp(lor64a,lor128a,64,lor,128,FbcroE)
            else if ((lor .gt. 128.) .and. (lor .le. 256.)) then
            call interp(lor128(12),lor128(13),1200.,rot,1300.,lor128a)
            call interp(lor256(12),lor256(13),1200.,rot,1300.,lor256a)
            call interp(lor128a,lor256a,128,lor,256,FbcroE)
          else
            write(9,*) 'lor range exceeded (CR)',lor,l,r,t
            pause
          end if
        else if ((rot .gt. 1300.) .and. (rot .le. 1400.)) then
          if ((lor .ge. 32.) .and. (lor .le. 64.)) then
            call interp(lor32(13),lor32(14),1300.,rot,1400.,lor32a)
            call interp(lor64(13),lor64(14),1300.,rot,1400.,lor64a)
            call interp(lor32a,lor64a,32,lor,64,FbcroE)
          else if ((lor .gt. 64.) .and. (lor .le. 128.)) then
            call interp(lor64(13),lor64(14),1300.,rot,1400.,lor64a)
            call interp(lor128(13),lor128(14),1300.,rot,1400.,lor128a)
            call interp(lor64a,lor128a,64,lor,128,FbcroE)
          else if ((lor .gt. 128.) .and. (lor .le. 256.)) then
            call interp(lor128(13),lor128(14),1300.,rot,1400.,lor128a)
            call interp(lor256(13),lor256(14),1300.,rot,1400.,lor256a)
            call interp(lor128a,lor256a,128,lor,256,FbcroE)
          else
            write(9,*) 'lor range exceeded (CR)',lor,l,r,t
            pause
          end if
        else if ((rot .gt. 1400.) .and. (rot .le. 1500.)) then
          if ((lor .ge. 32.) .and. (lor .le. 64.)) then
            call interp(lor32(14),lor32(15),1400.,rot,1500.,lor32a)
            call interp(lor64(14),lor64(15),1400.,rot,1500.,lor64a)
            call interp(lor32a,lor64a,32,lor,64,FbcroE)
          else if ((lor .gt. 64.) .and. (lor .le. 128.)) then
            call interp(lor64(14),lor64(15),1400.,rot,1500.,lor64a)
            call interp(lor128(14),lor128(15),1400.,rot,1500.,lor128a)
            call interp(lor64a,lor128a,64,lor,128,FbcroE)
          else if ((lor .gt. 128.) .and. (lor .le. 256.)) then
            call interp(lor128(14),lor128(15),1400.,rot,1500.,lor128a)
            call interp(lor256(14),lor256(15),1400.,rot,1500.,lor256a)
            call interp(lor128a,lor256a,128,lor,256,FbcroE)
          else
            write(9,*) 'lor range exceeded (CR)',lor,l,r,t
            pause
          end if
        else
          write(9,*) 'rot range exceeded',rot,r,t,l
        end if

        critstress = FbcroE*E

        return
        end



        subroutine interp(y1,y3,x1,x2,x3,y2)
        implicit none
        real y1,y3,x1,x2,x3,y2

        y2 = (x2-x1)*(y3-y1)/(x3-x1) + y1

        return
        end
```

APPENDIX A2

DRAWINGS OF POINT DESIGNS

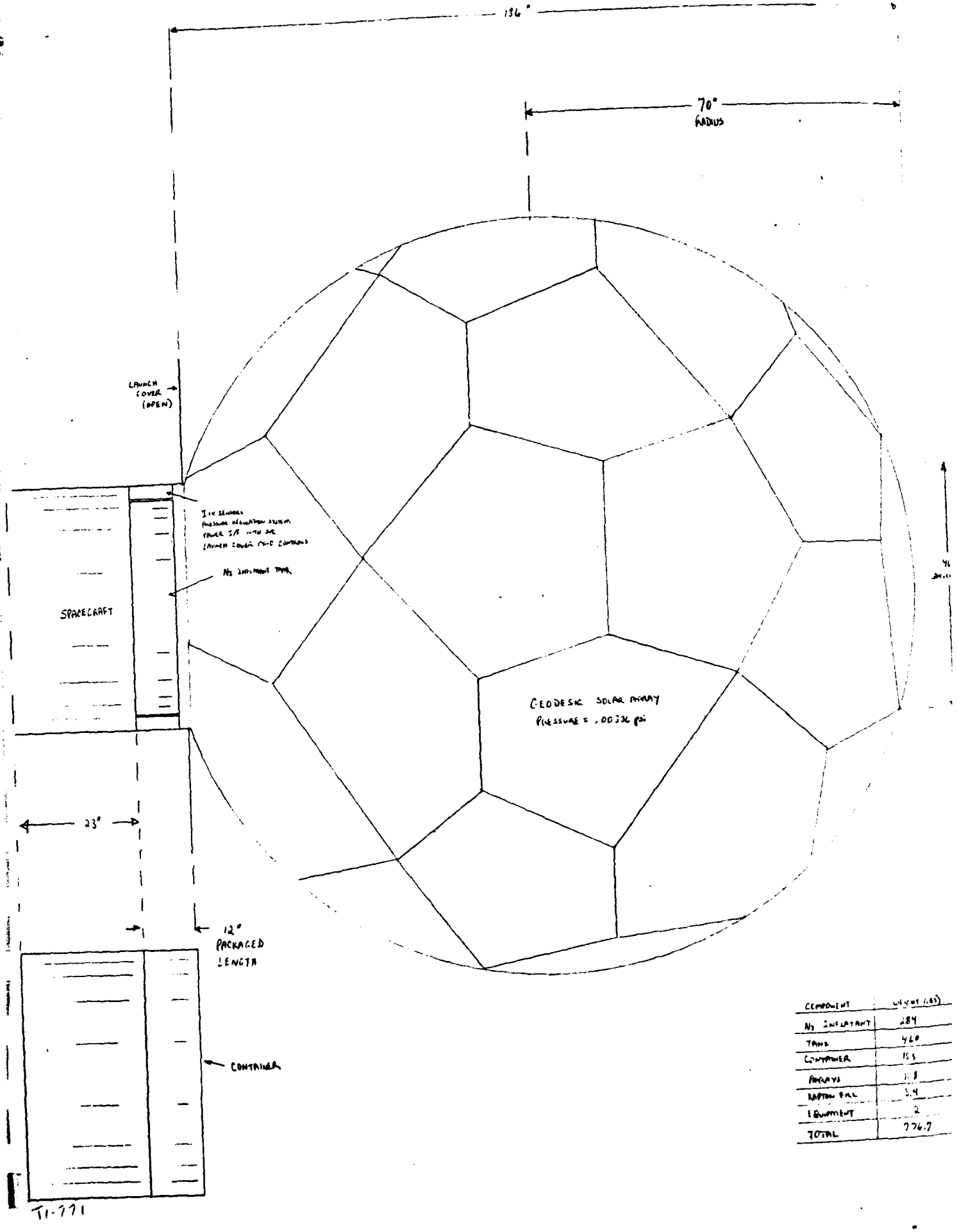

COMPONENT	WEIGHT (LBS)
N_2 INFLATANT	284
TANK	460
CONTAINER	155
PANELS	1.8
KAPTON FILL	3.4
EQUIPMENT	2
TOTAL	776.7

TI-771

200 W INFLATABLE

NON-RIGIDIZED SPHERICA

AMORPHOUS SILIC

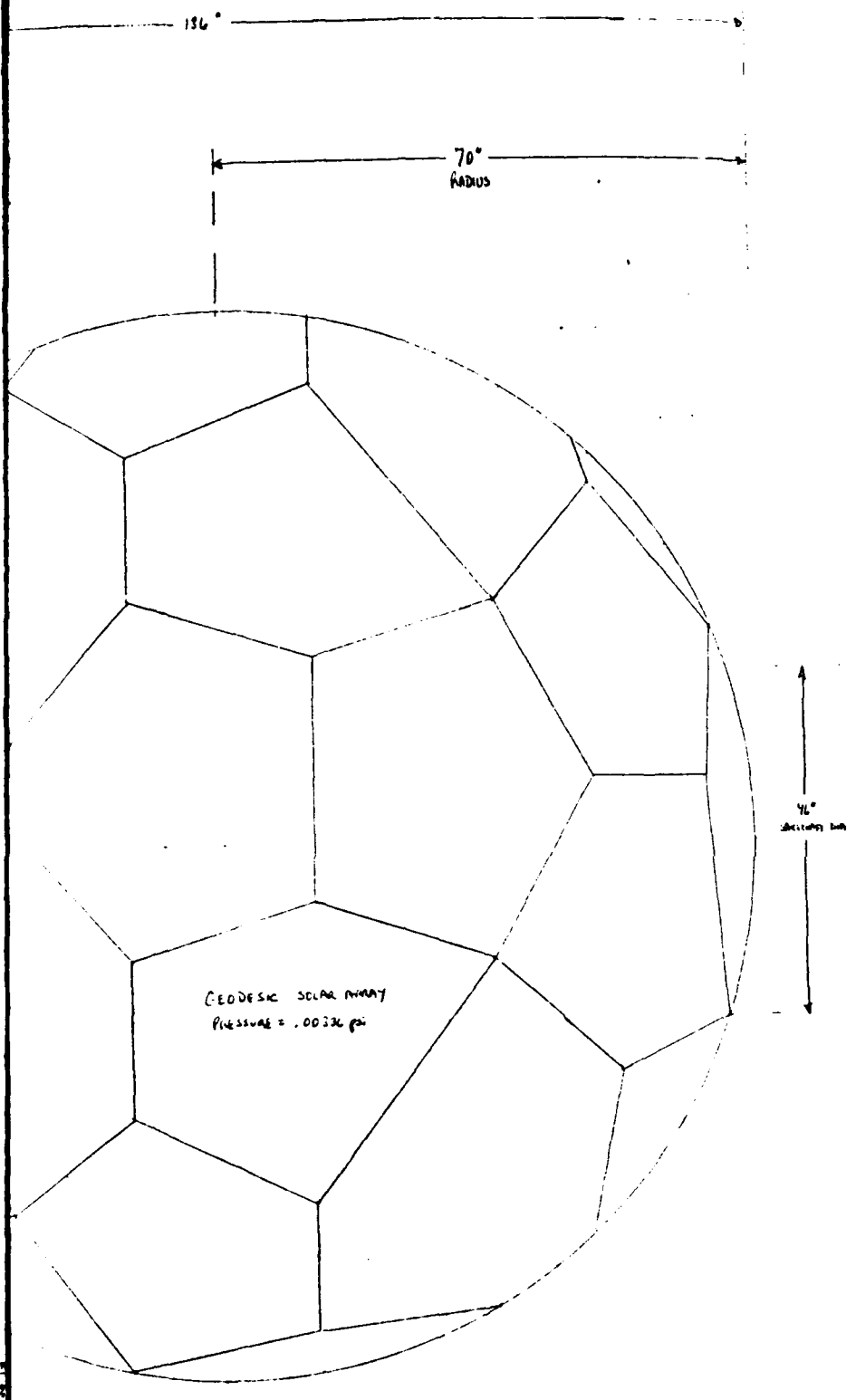

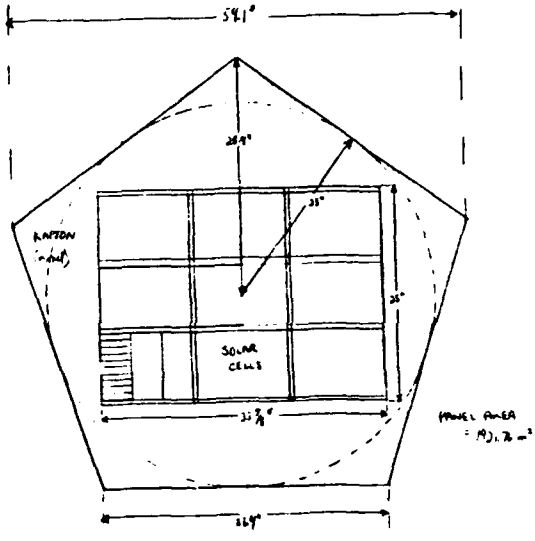

CAP PANEL (REGULAR PENTAGON)

ALL OTHER PANELS ARE IRREGULAR PENTAGONS, SIMILAR AREA

TOTAL NUMBER OF PANELS : 31 (5 A + 1)

NUMBER OF PANELS EXPOSED, ORBIT AVERAGE : 11.5

PANEL VOLTAGE : 32.9 V DC

PANEL POWER (FULLY ILLUMINATED, BOL) : 32.2 W

SOLAR CELLS ARE HEAVILY POPULATED WITH BLOCKING DIODES

COMPONENT	WEIGHT (LBS)	% TOTAL
N_2 INFLATANT	284	36.6 %
TANK	460	59.2 %
CONTAINER	15.5	2.0 %
ARRAYS	11.8	1.5 %
KAPTON FILL	3.4	.4 %
EQUIPMENT	2	.3 %
TOTAL	776.7	

200 W INFLATABLE SOLAR ARRAY; GEO;

NON-RIGIDIZED SPHERICAL CONFIGURATION

AMORPHOUS SILICON ARRAY

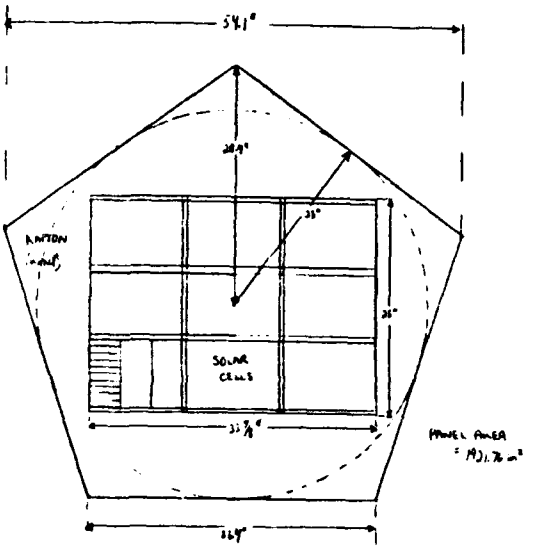

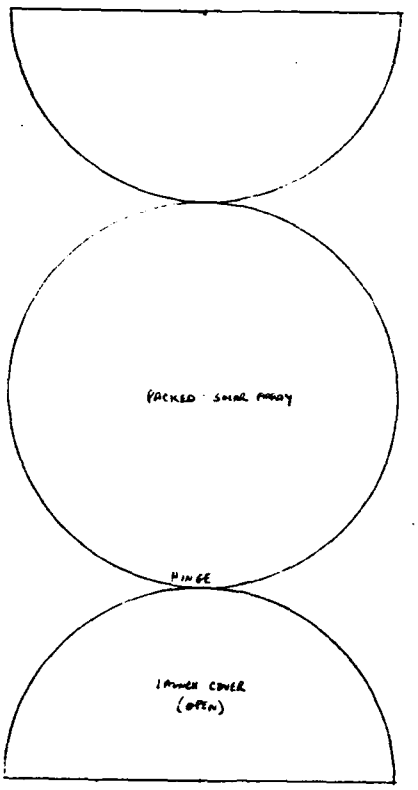

CAP PANEL (REGULAR PENTAGON)

ALL OTHER PANELS ARE IRREGULAR PENTAGONS, SIMILAR AREA

TOTAL NUMBER OF PANELS : 31 (5 & 1)

NUMBER OF PANELS EXPOSED, ORBIT AVERAGE : 11.5

PANEL VOLTAGE : 33.9 V DC

PANEL POWER (FULLY ILLUMINATED, BOL) : 32.2 W

SOLAR CELLS ARE HEAVILY POPULATED WITH BLOCKING DIODES

	% TOTAL
	36.6 %
	59.2 %
	2.0 %
	1.5 %
	.4 %
	.3 %
.7	

			200 W INFLATABLE SOLAR ARRAY;
			GEO; NON-RIGIDIZED SPHERICAL CONFIG
	DRAWN Dennis	6/12/	
			SIZE 21001 REV
			SCALE 1/4 SHEET 1 of 1

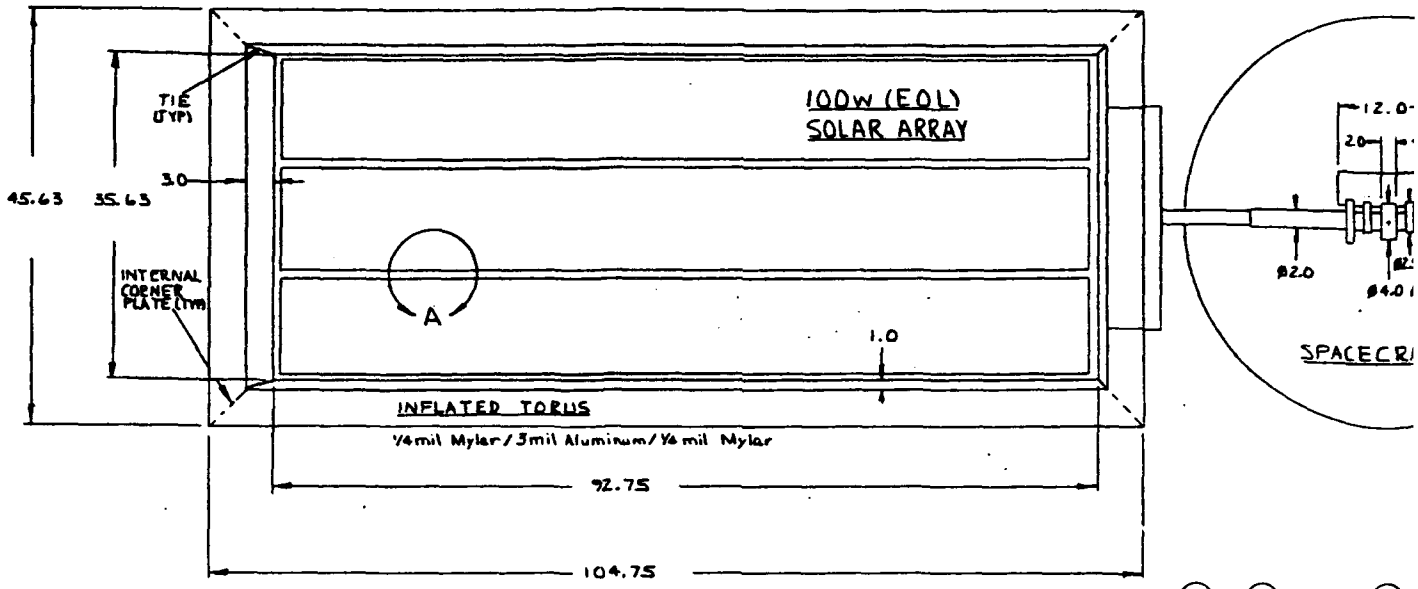
100W (EOL)
SOLAR ARRAY
TIE (TYP)
3.0
45.63
35.63
INTERNAL CORNER PLATE (TYP)
A
1.0
INFLATED TORUS
¼mil Mylar/3mil Aluminum/¼mil Mylar
92.75
104.75
12.0
2.0
Ø2.0
Ø4.0
SPACECR

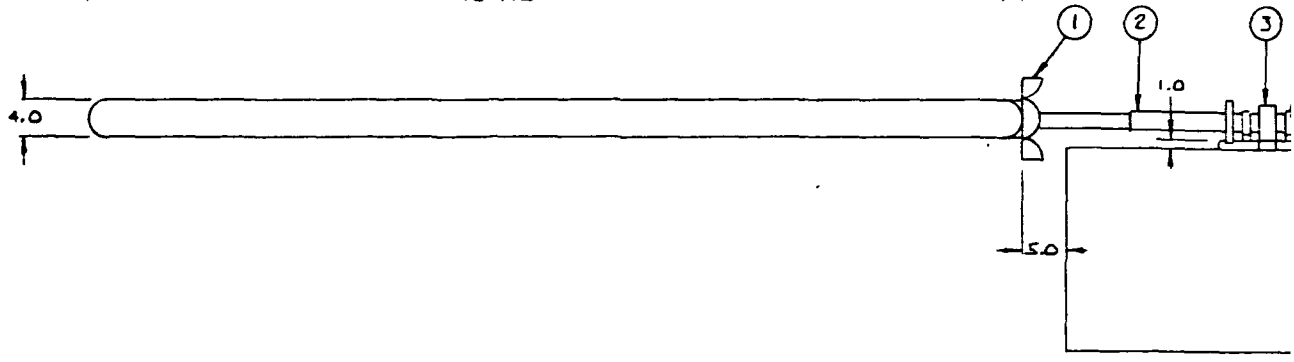
1
2
3
1.0
4.0
5.0

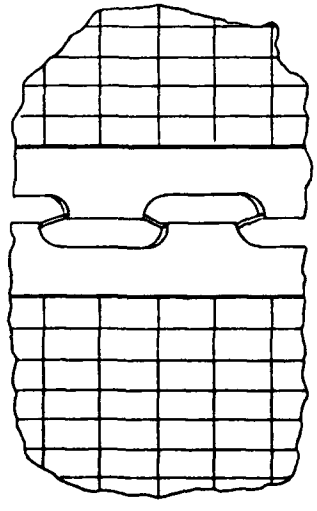

VIEW A

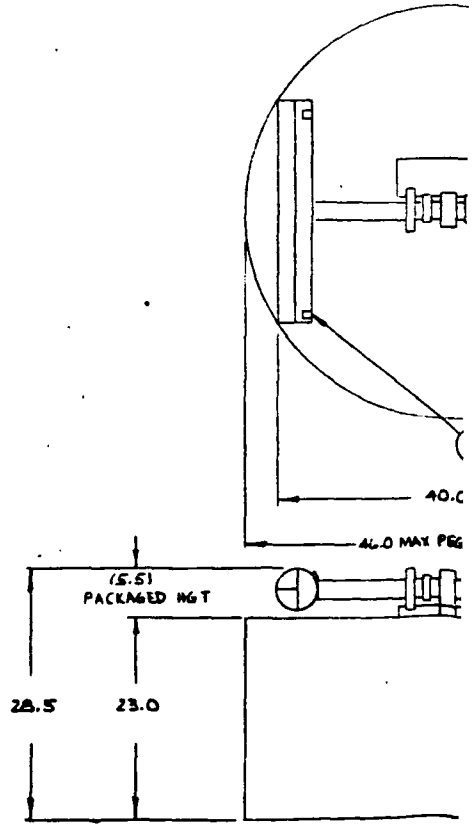
40.0
46.0 MAX PEG
(5.5)
PACKAGED HGT
28.5
23.0

TI-772

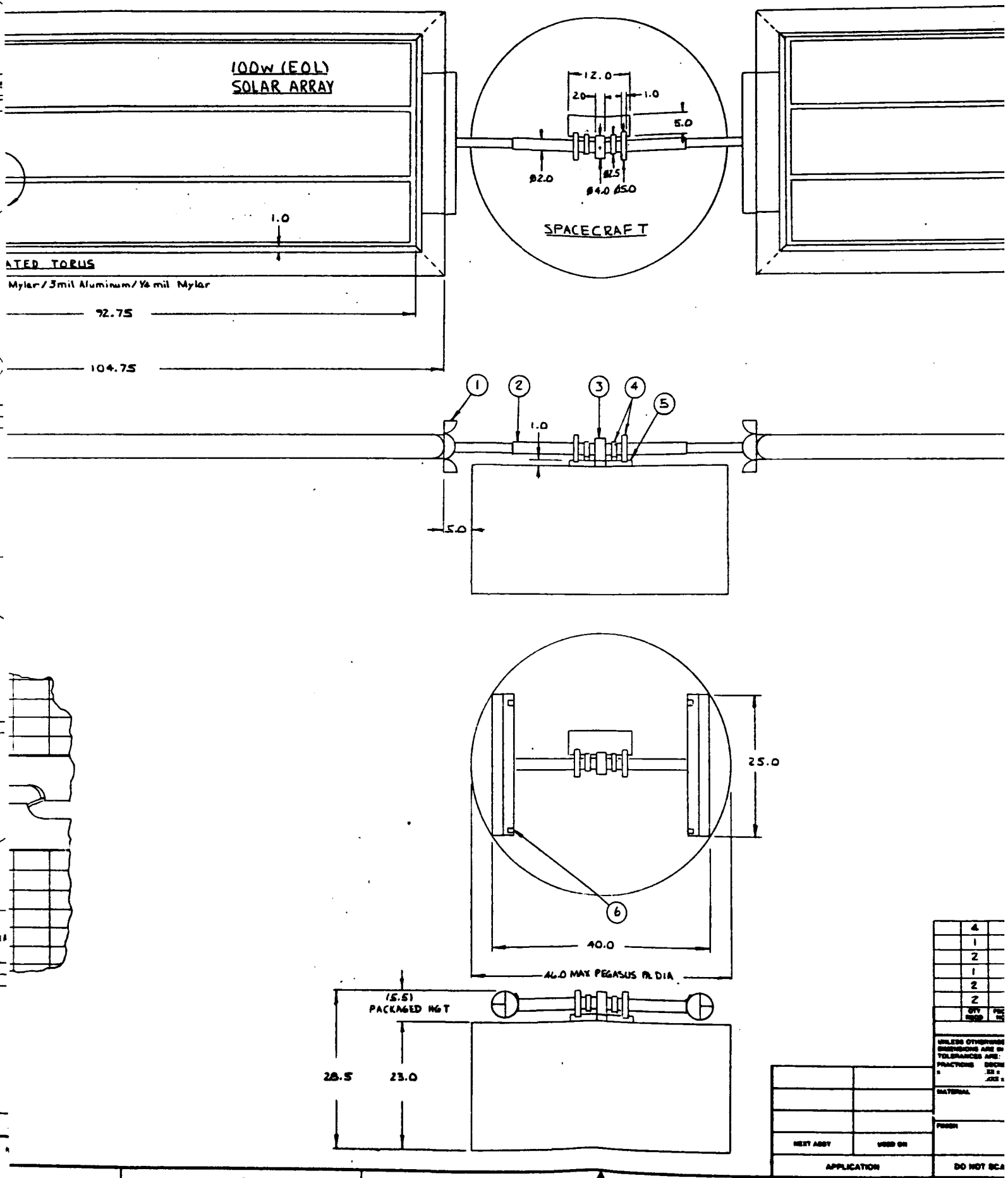
100w (EOL)
SOLAR ARRAY
12.0
2.0
1.0
5.0
Ø2.0
Ø2.5
Ø4.0 Ø5.0
SPACECRAFT
1.0
ATED TORUS
Mylar/3mil Aluminum/½ mil Mylar
92.75
104.75
1
2
3
4
5
1.0
5.0
6
25.0
40.0
46.0 MAX PEGASUS FL DIA
(5.5)
PACKAGED HGT
28.5
23.0
7
6
5
4
3

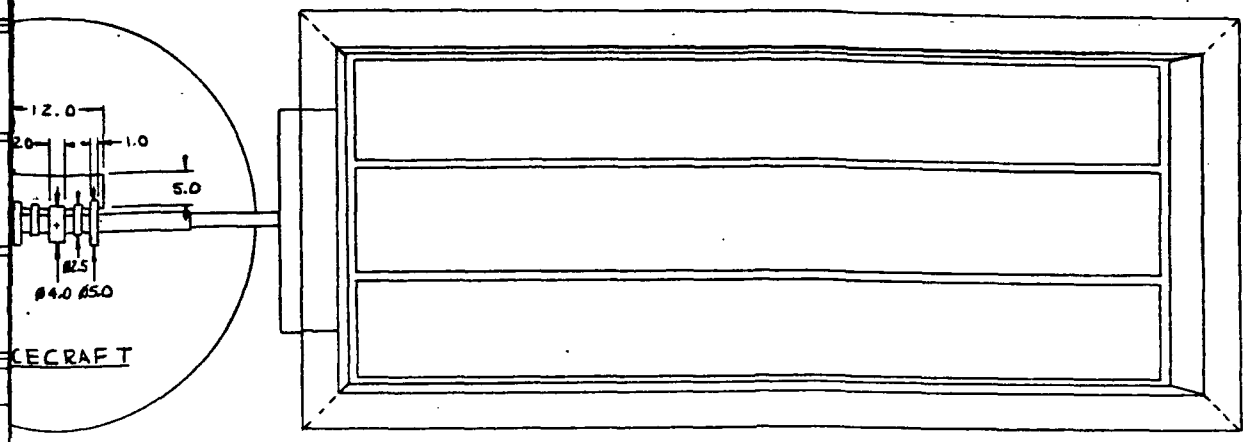

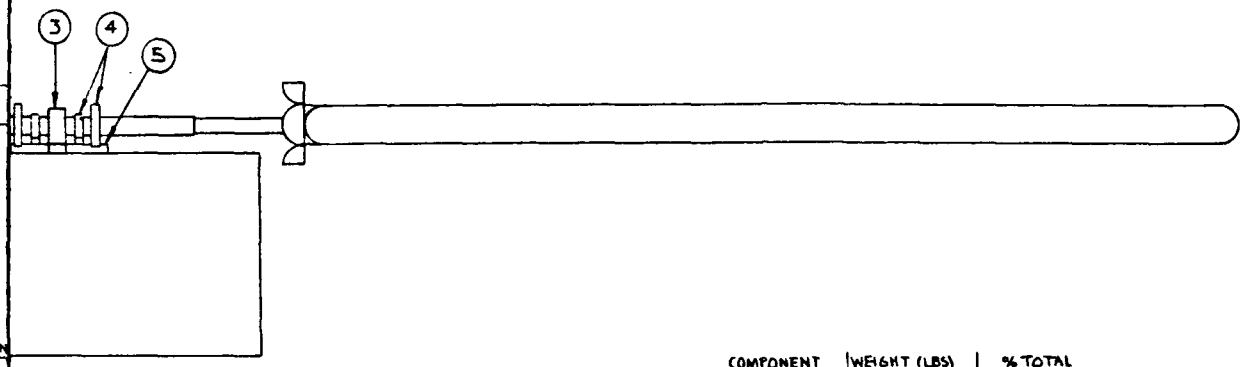

COMPONENT	WEIGHT (LBS)	% TOTAL
SOLAR CELLS	1.47 x 2 = 2.94	26.3
TORUS	1.16 x 2 = 2.32	20.8
VALVES, TANK	.53 x 2 = 1.06	9.5
ARM, CASE	1.8 x 2 = 3.60	32.2
MOTOR MOUNT	.25	2.2
COMPUTER, CABLES	1.00	9.0
TOTAL	11.17	

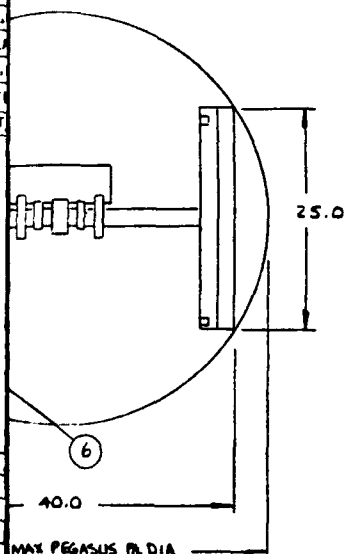

QTY REQD	ITEM NO.	PART OR IDENTIFYING NO.	NOMENCLATURE OR DESCRIPTION	MATERIAL DESCRIPTION	ITEM NO.
4			PYRO CABLE CUTTERS TO OPEN CLAMSHELLS		6
1			MOTOR CONTROLLER COMPUTER		5
2			FLEX RIBBON POWER&SIGNAL TRANSFER RING		4
1			DRIVE MOTOR & RESOLVER		3
2			TELESCOPING ARM		2
2			CLAMSHELL LAUNCH CASE		1

PARTS LIST

NEXT ASSY	USED ON
APPLICATION	

UNLESS OTHERWISE SPECIFIED DIMENSIONS ARE IN INCHES
TOLERANCES ARE:
FRACTIONS ± DECIMALS .XX ± .XXX ± ANGLES ±

MATERIAL

FINISH

DO NOT SCALE DRAWING

CONTRACT NO.

APPROVALS	DATE
DRAWN TUMMOND	7/16/90
CHECKED	
ISSUED	

L'GARDE, INC. 16181 WOODLAWN AVENUE TUSTIN, CALIFORNIA 92680

200w INFLATABLE SOLAR ARRAY, L.E.O., RIGIDIZED ALUMINUM TORUS, AMORPHOUS SILICON ARRAY

SIZE D | FSCM NO. 1F668 | DWG. NO. 21002 | REV.

SCALE 1:10 | SHEET 1 OF 1

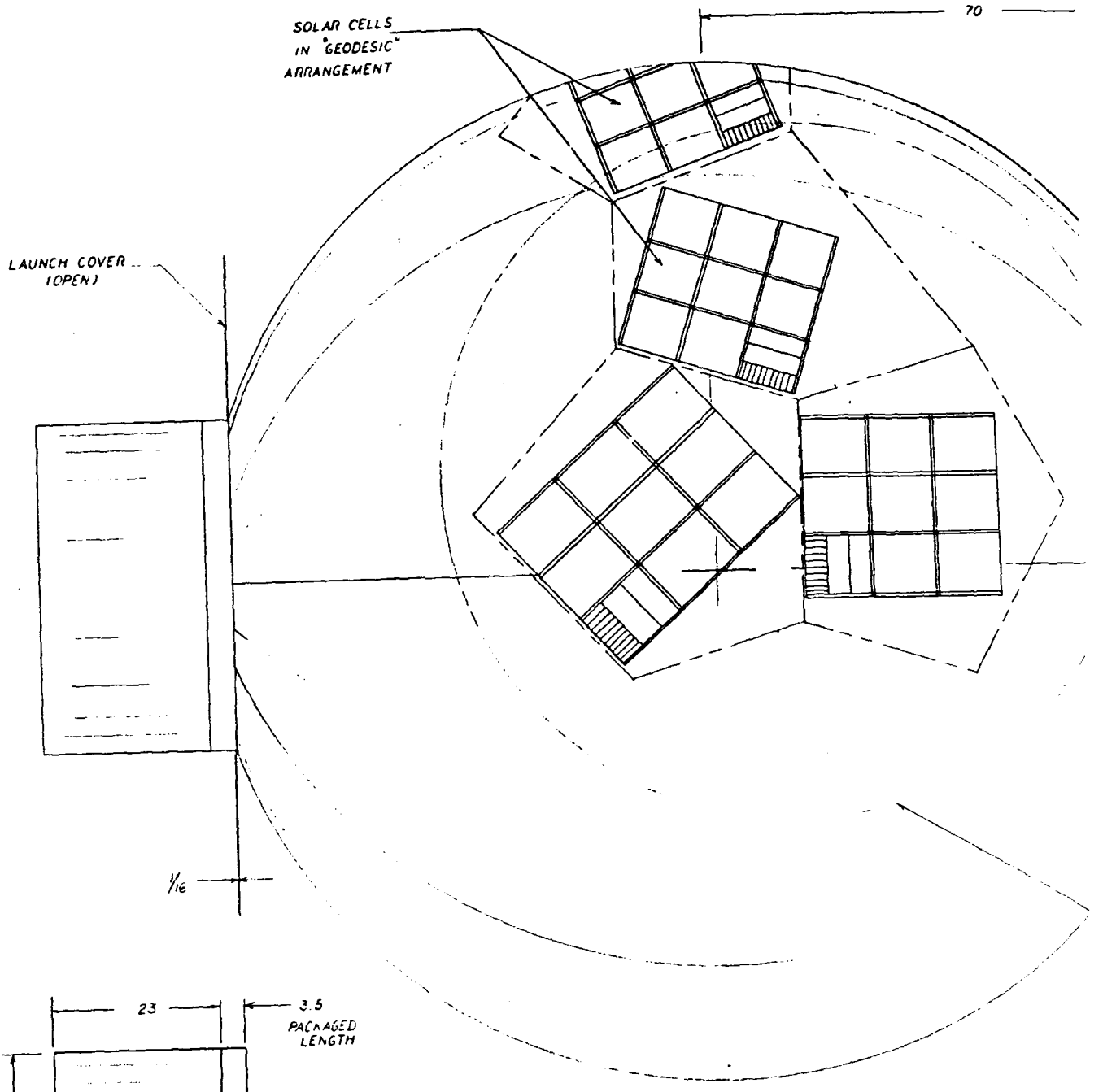

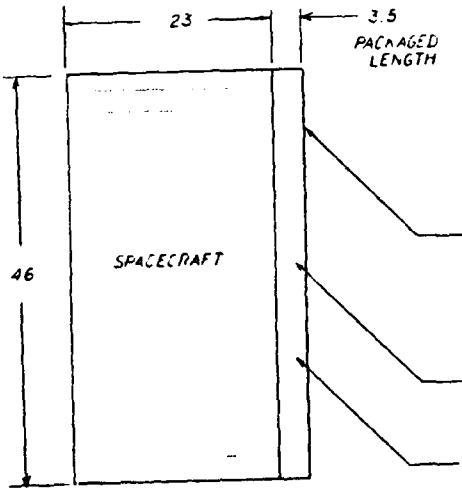

COMPONENT	WEI
N_2 INFLATANT	
N_2 TANK	
BALLOON CONTAINER	
ARRAYS	
ALUMINUM BALLOON	
EQUIPMENT	
TOTAL	

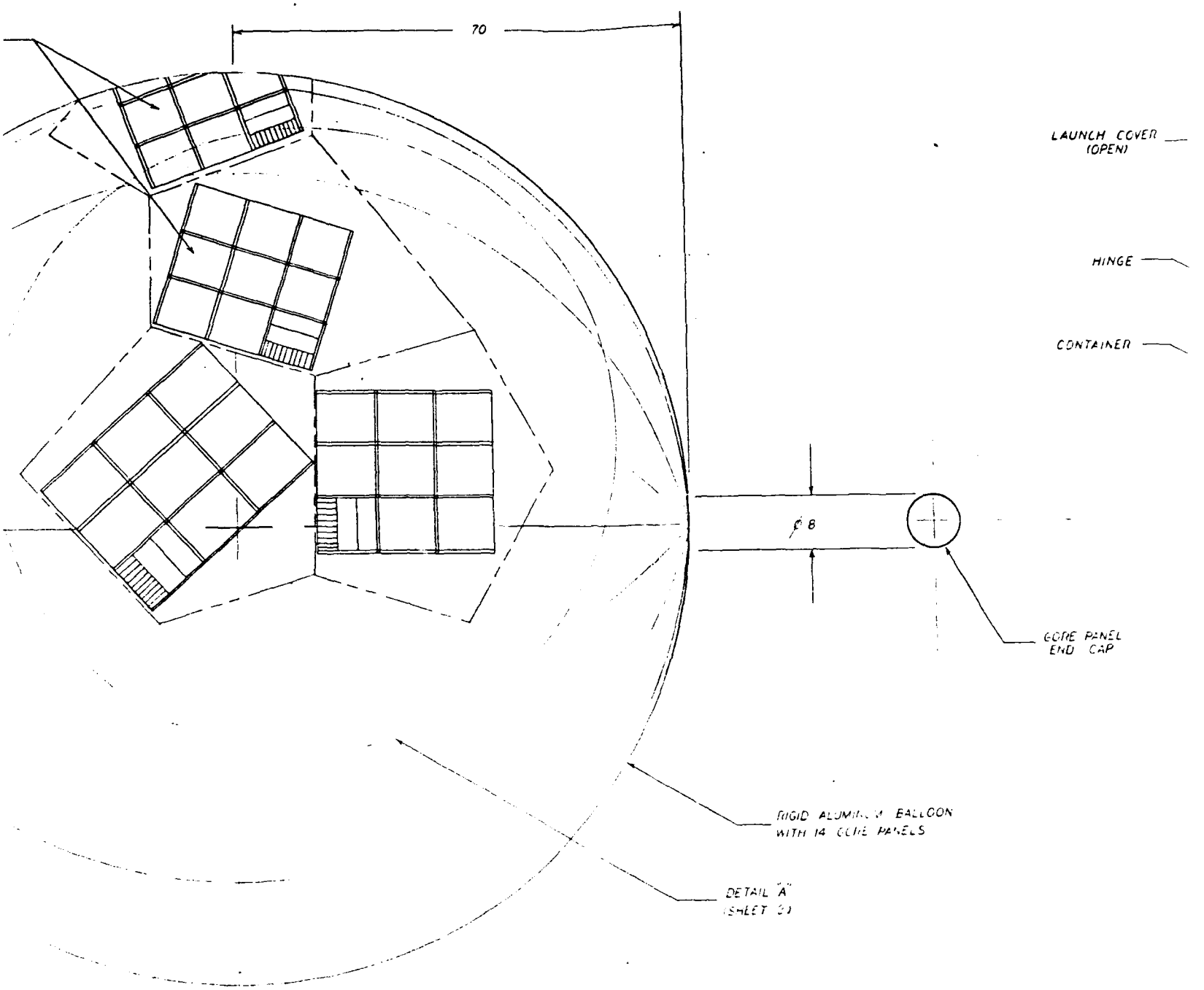

COMPONENT	WEIGHT (LBS)	%
N_2 INFLATANT	3.3	5.3
N_2 TANK	13.2	21.4
BALLOON CONTAINER	13.3	21.6
ARRAYS	11.6	18.1
ALUMINUM BALLOON	16.1	25.3
EQUIPMENT	2.0	3.2
TOTAL	61.7	

QTY REQD	FSCM NO	PART OR IDENTIFYING NO
UNLESS OTHERWISE SPECIFIED DIMENSIONS ARE IN INCHES TOLERANCES ARE: FRACTIONS DECIMALS ANGLES		CONTRACT NO
MATERIAL		APPRO
FINISH		DRAWN CHECKED ISSUED
NEXT ASSY	USED ON	
APPLICATION	DO NOT SCALE DRAWING	

REVISIONS				
ZONE	REV.	DESCRIPTION	DATE	APPROVED

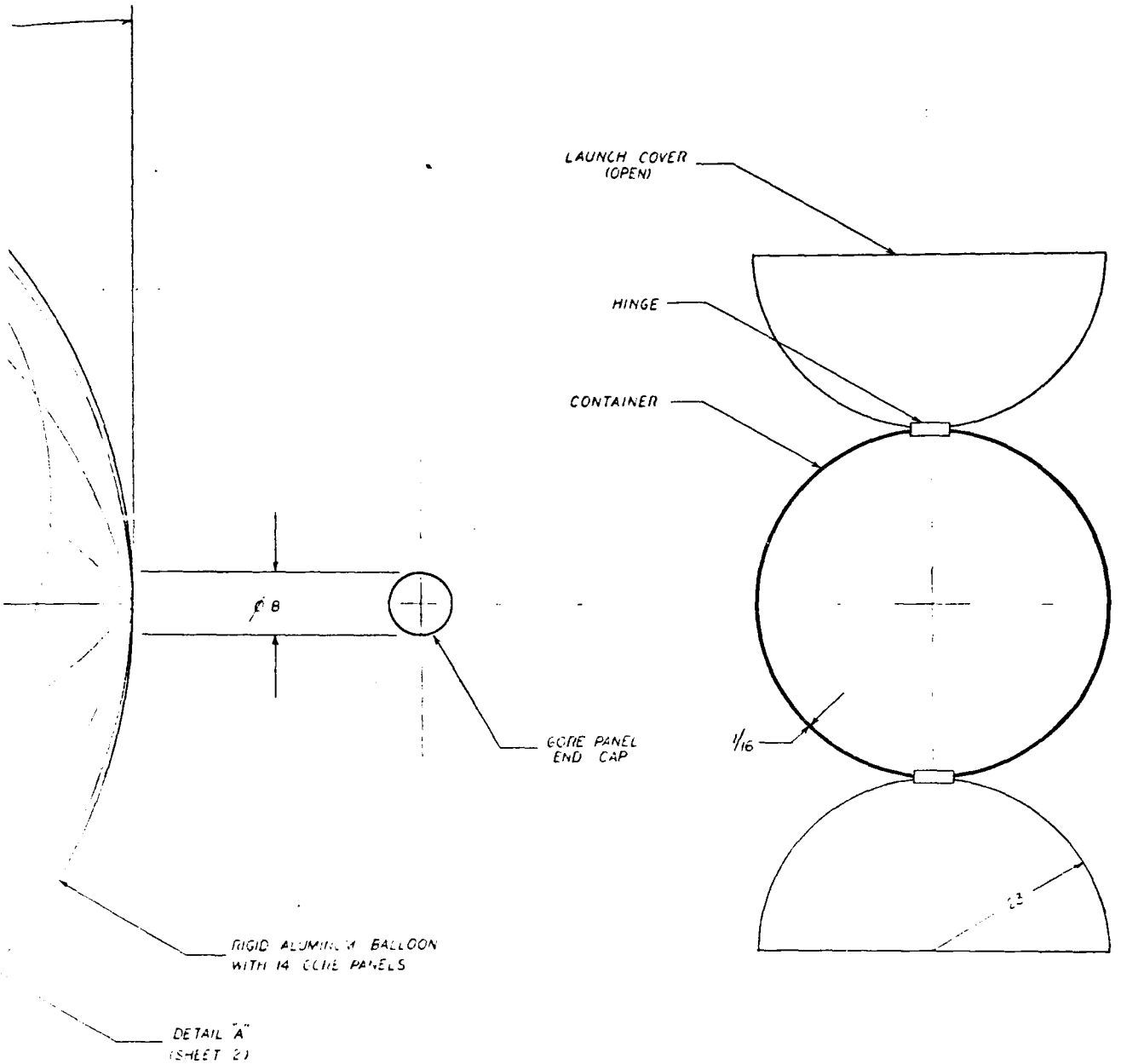

(LES)	%
3.1	5.3
3.2	21.4
.3	21.6
	19.1
	29.3
C	3.2
7	

QTY REQD	FSCM NO.	PART OR IDENTIFYING NO.	NOMENCLATURE OR DESCRIPTION	MATERIAL SPECIFICATION

PARTS LIST

UNLESS OTHERWISE SPECIFIED DIMENSIONS ARE IN INCHES
TOLERANCES ARE:
FRACTIONS ± DECIMALS .XX ± .XXX ± ANGLES ±

MATERIAL

FINISH

NEXT ASSY | USED ON

APPLICATION

DO NOT SCALE DRAWING

CONTRACT NO. 5542

APPROVALS	DATE
DRAWN D. BIANET	6-26-90
CHECKED	
ISSUED	

L'GARDE, INC. 15181 WOODLAWN AVENUE TUSTIN, CALIFORNIA 92680

200 W INFLATABLE SOLAR ARRAY
RIGID ALUMINUM SPHERE CONFIGURATION
AMORPHOUS SILICON ARRAY

SIZE	FSCM NO.	DWG. NO.	REV
D	1FBCE	21003	

SCALE 1/10 SHEET 1 OF 2

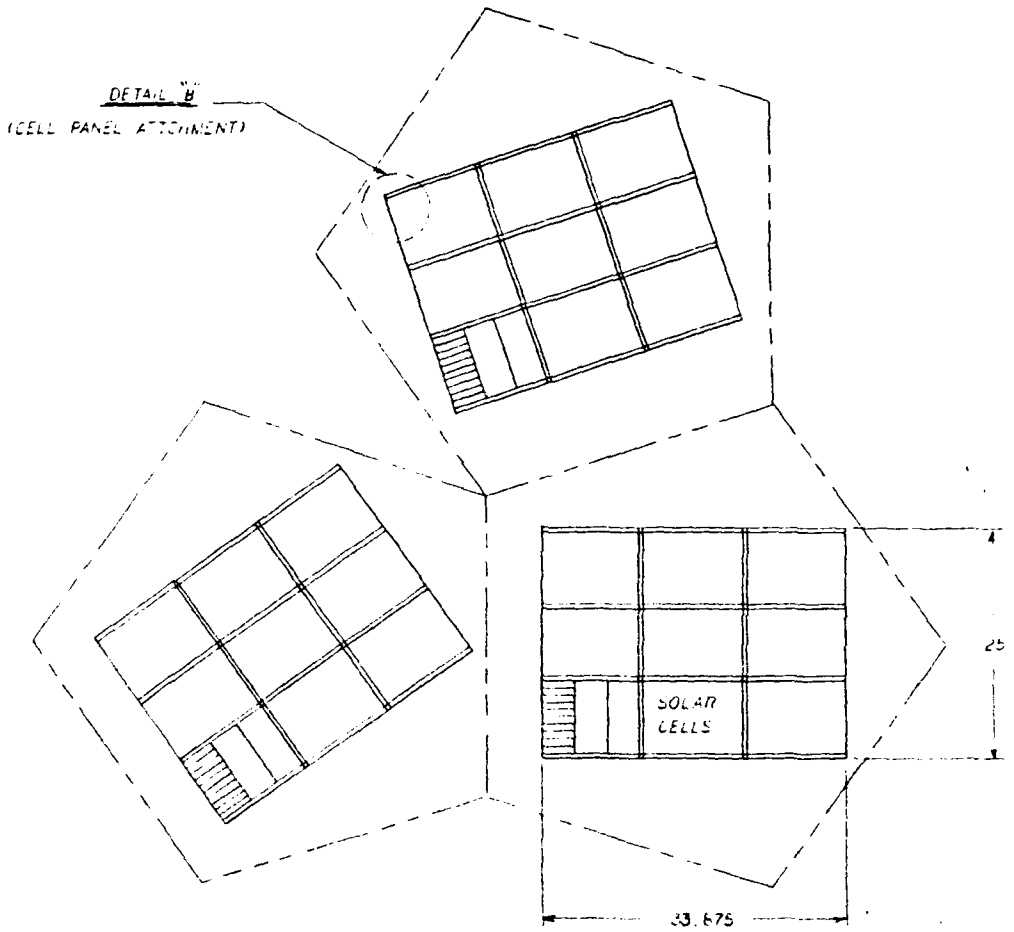

DETAIL "A"

TOTAL NUMBER OF CELL PANELS: 31
NUMBER OF PANELS EXPOSED SUNLIGHT AVERAGE:
PANEL VOLTAGE: 32.4 VDC
PANEL POWER (FULL ILLUMINATED SUN): 32.2 W

41-174

ELASTIC CORD SEWED TO BALLOON & CELL PANEL

OPTION 1

REINFORCED HOLE

ELASTIC CORD

PLASTIC FASTENER

OPTION 2

LOCKING TEETH

LOCKING DISK

OPTION 3

ELASTIC STRAP

ADHESIVE BOND

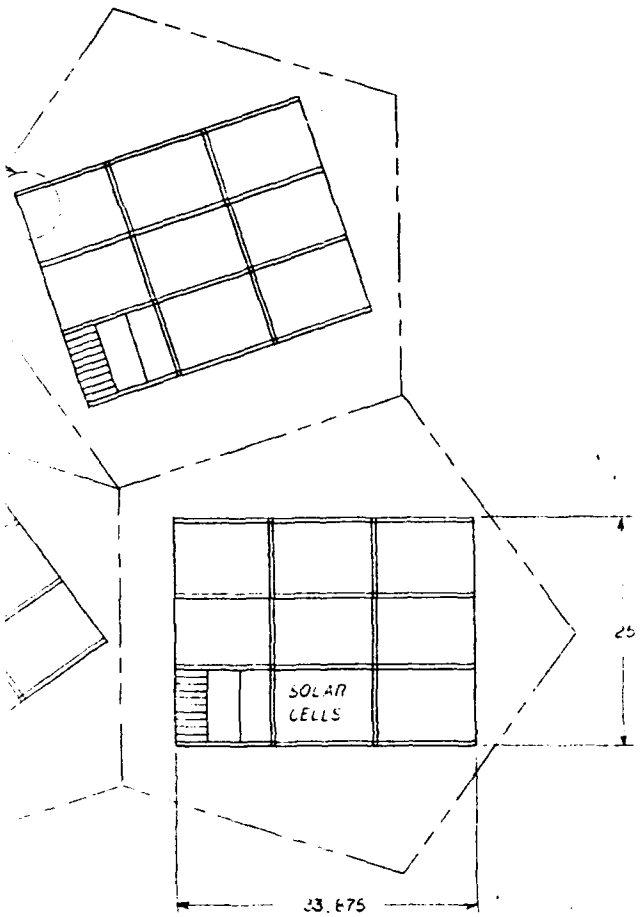

DETAIL "A"

TOTAL NUMBER OF CELL PANELS: 31
NUMBER OF PANELS EXPOSED, ORBIT AVERAGE: 15.5
PANEL VOLTAGE: 32.4 VDC
PANEL POWER (FULLY ILLUMINATED, BOL): 32.2 W

	UNIT	PROD NO	

UNLESS OTHERWISE SPECIFIED DIMENSIONS ARE IN INCHES
TOLERANCES ARE:
FRACTIONS DECIMALS ANGLES
± .XX ±
.XXX ±

MATERIAL

FINISH

NEXT ASSY	USED ON
APPLICATION	DO NOT SCALE DRAWIN

DWG. NO.	SH	REV.
21003	2 OF 2	

ZONE	REV.	REVISIONS DESCRIPTION	DATE	APPROVED

OPTION 1

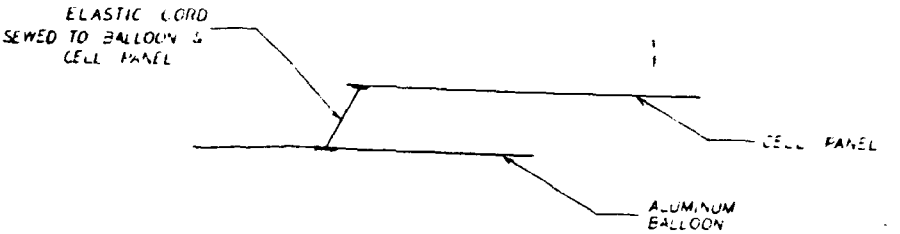

OPTION 2

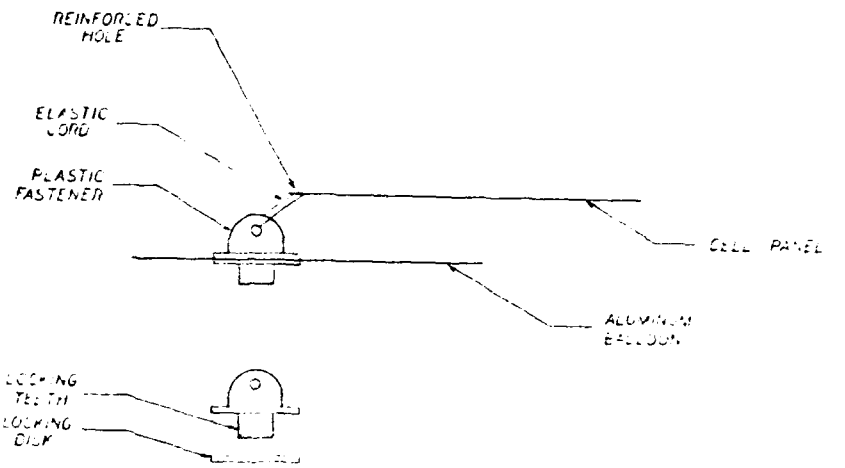

OPTION 3

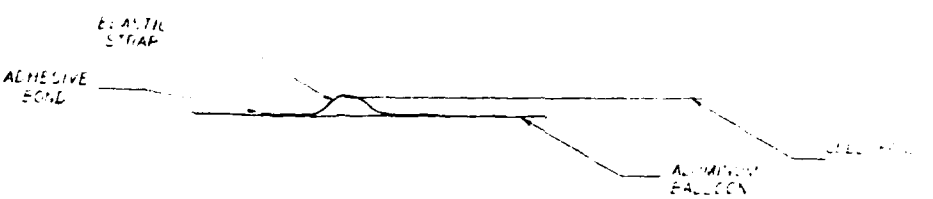

AVERAGE 15.5

32.2 W

DETAIL E
NOT TO SCALE

QTY PER	ITEM NO	PART OR IDENTIFYING NO	NOMENCLATURE OR DESCRIPTION	MATERIAL SPECIFICATION

PARTS LIST

UNLESS OTHERWISE SPECIFIED DIMENSIONS ARE IN INCHES
TOLERANCES ARE:
FRACTIONS DECIMALS ANGLES
.XX ±
.XXX ±

MATERIAL

FINISH

NEXT ASSY | USED ON

APPLICATION

DO NOT SCALE DRAWING

CONTRACT NO: SI-42

APPROVALS	DATE
DRAWN D. BRANDT	7-2 90
CHECKED	
ISSUED	

L'GARDE, INC. 15181 WOODLAWN AVENUE TUSTIN, CALIFORNIA 92680

ZCC W INFLATABLE SOLAR ARRAY

SOLAR CELL PANEL ARRANGEMENT, AMORPHOUS SILICON ARRAY

SIZE	FSCM NO	DWG NO	REV
D	1FCC8	21003	

SCALE NONE SHEET 2 OF 2

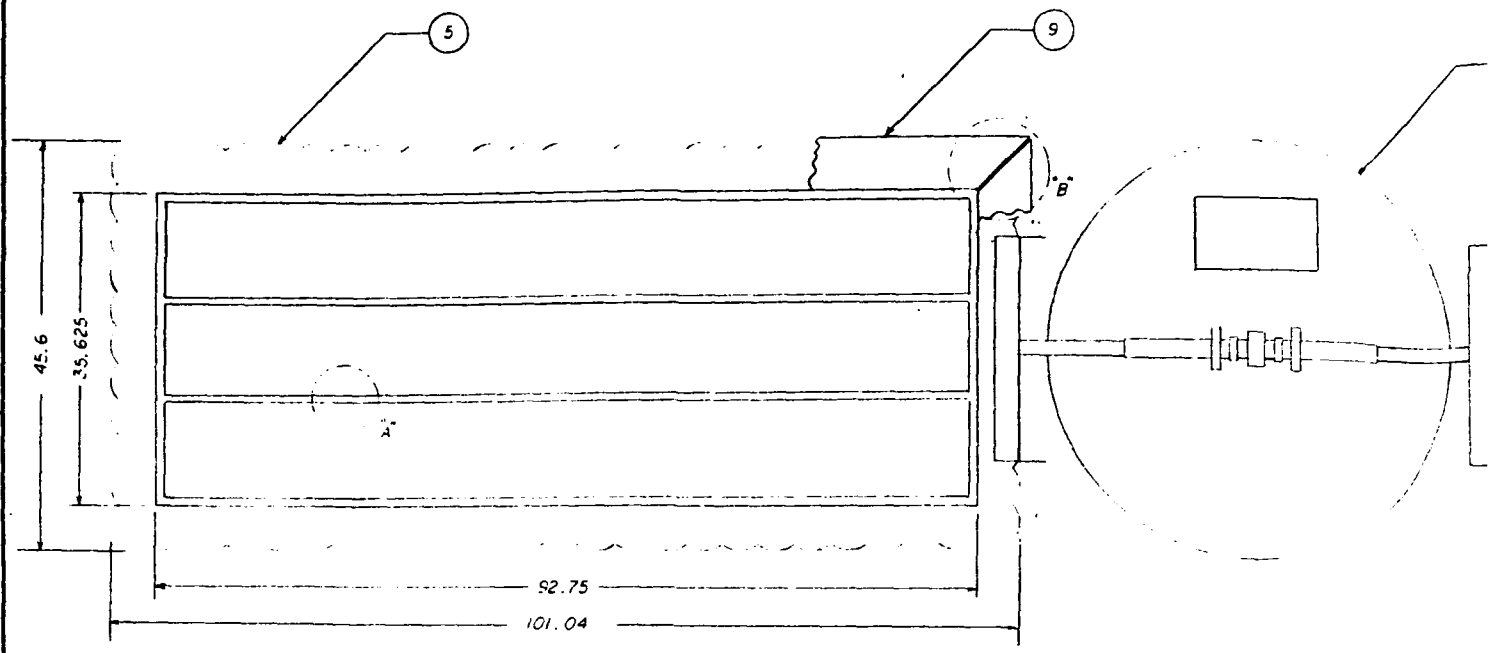

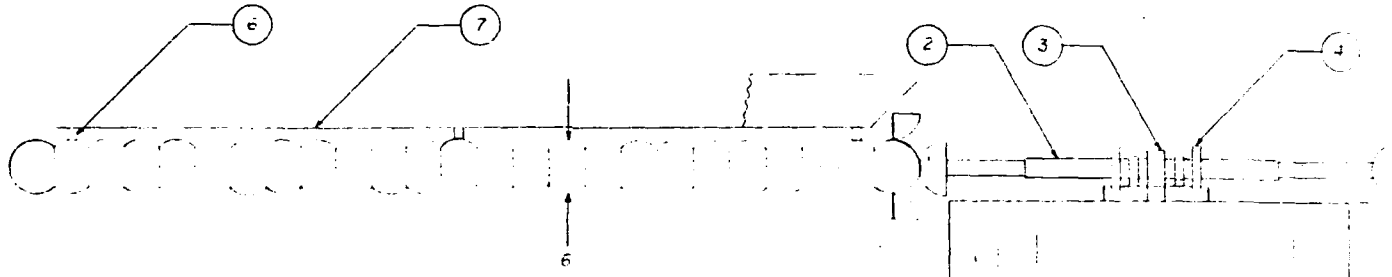

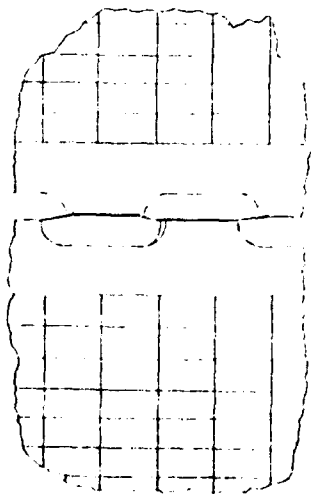

DETAIL A
NOT TO SCALE

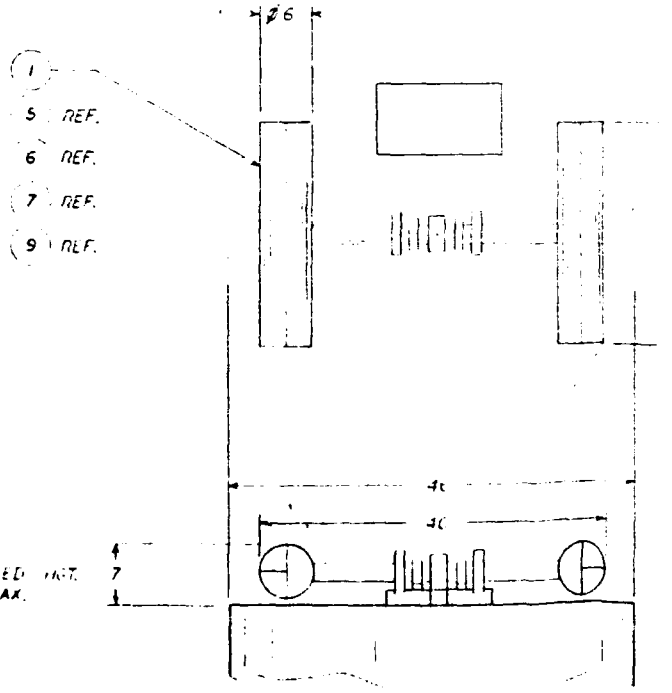

T1-115

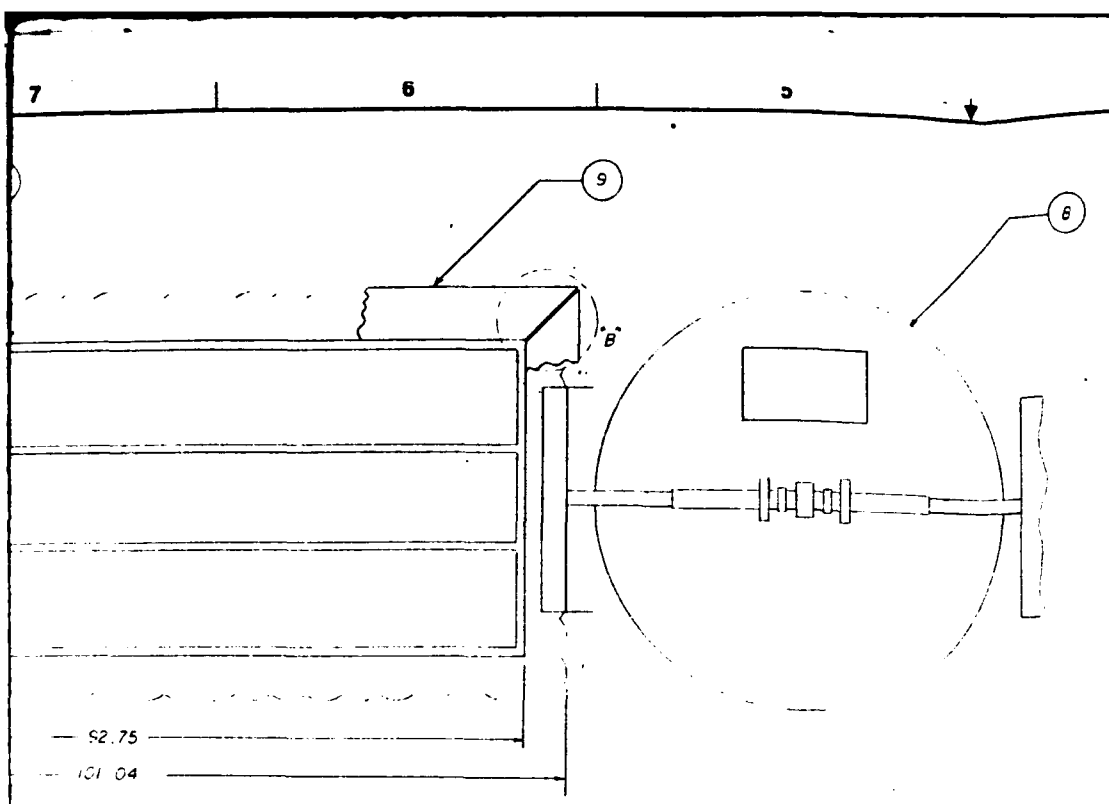

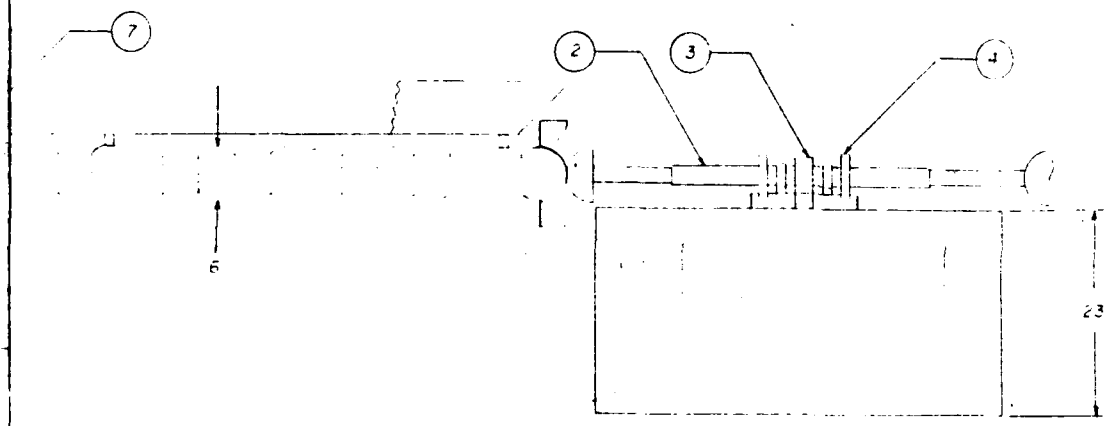

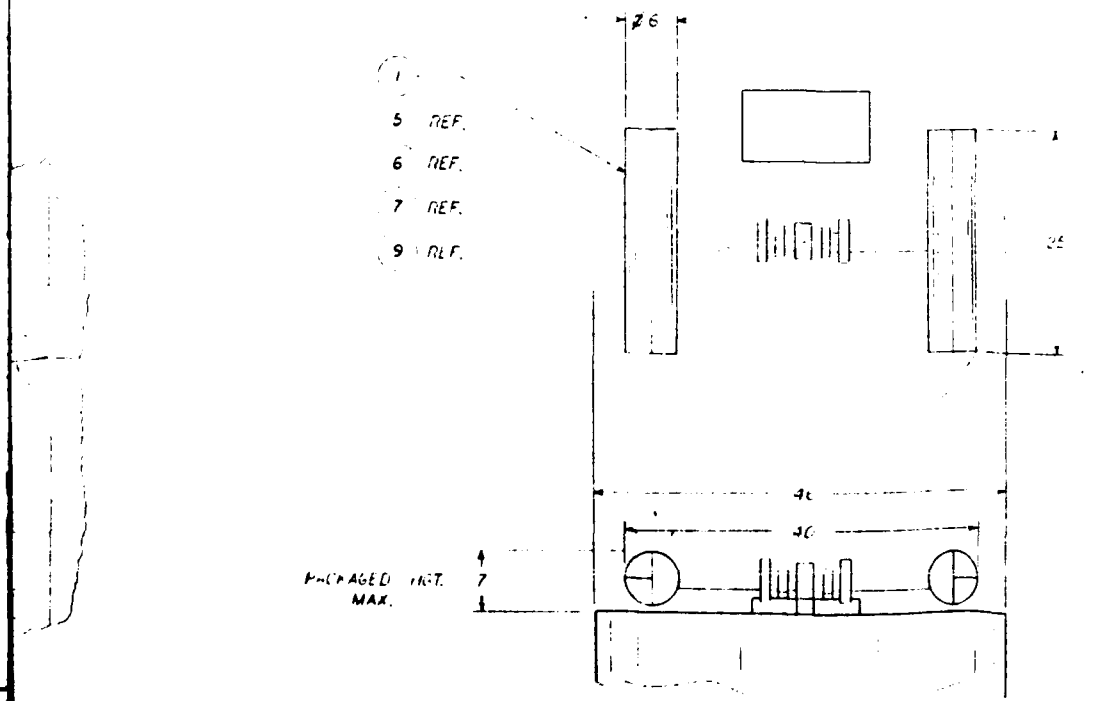

NEXT ASSY	USED ON
APPLICATION	

	QTY REQD	PSCN NO

UNLESS OTHERWISE SPEC
DIMENSIONS ARE IN INCH
TOLERANCES ARE:
FRACTIONS DECIMALS
± .XX ±
.XXX ±

MATERIAL

FINISH

DO NOT SCALE

REVISIONS				
ZONE	REV.	DESCRIPTION	DATE	APPROVED

CORNES SEWN. SUCH THAT
OUTER EDGES "STAND UP"

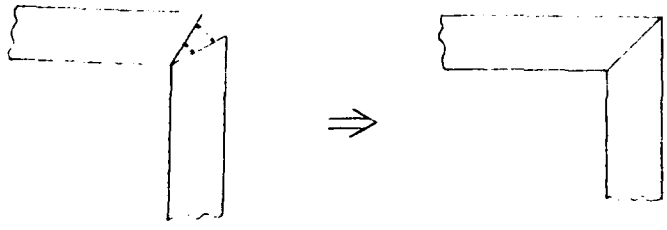

DETAIL "B"
NOT TO SCALE

COMPONENT	WEIGHT (LBS)	% TOTAL
SOLAR CELLS	1.47 x 2 = 2.94	7.74
INFLATABLE	4.41 x 2 = 8.82	23.21
ARM, CABLE, ETC	4.89 x 2 = 9.78	25.74
MOTOR, MOUNT	C.50	1.32
VALVES, TANK	7.4 x 2 = 14.8	38.95
INFLATANT	1.16	3.05
TOTAL	38.00	

QTY REQD	PSCM NO	PART OR IDENTIFYING NO	NOMENCLATURE OR DESCRIPTION	MATERIAL SPECIFICATION	ITEM
1			SUN SHADE		9
1			SPACECRAFT		8
2			SOLAR ARRAY PANEL		7
5			STAND OFFS (INFLATABLE)		6
2			RIGID PILLOW (INFLATABLE)	ALUM	5
2			FLEX RIBBON, POWER & SIGNAL XFER RINGS		4
1			DRIVE MOTOR & RECEIVER GEARED		3
2			TELESCOPING ARM W/INFLATION TANK	ALUM / SS	2
2			CLAMSHELL LAUNCH CASE (CLOSED)	ALUM	1

PARTS LIST

UNLESS OTHERWISE SPECIFIED DIMENSIONS ARE IN INCHES
TOLERANCES ARE:
FRACTIONS ± DECIMALS .XX ± .XXX ± ANGLES ±

MATERIAL

FINISH

NEXT ASSY | USED ON

APPLICATION

DO NOT SCALE DRAWING

CONTRACT NO. 5542

APPROVALS	DATE
DRAWN D. BRAULT	7-10
CHECKED	
ISSUED	

L'GARDE, INC. 15181 WOODLAWN AVENUE TUSTIN, CALIFORNIA 92680

200W INFLATABLE SOLAR ARRAY
RIGIDIZED PILLOW CONFIGURATION,
AMORPHOUS SILICON ARRAY

SIZE	FSCM NO.	DWG NO.	REV
D	11468	21004	

SCALE 1:10 SHEET 1 OF 1

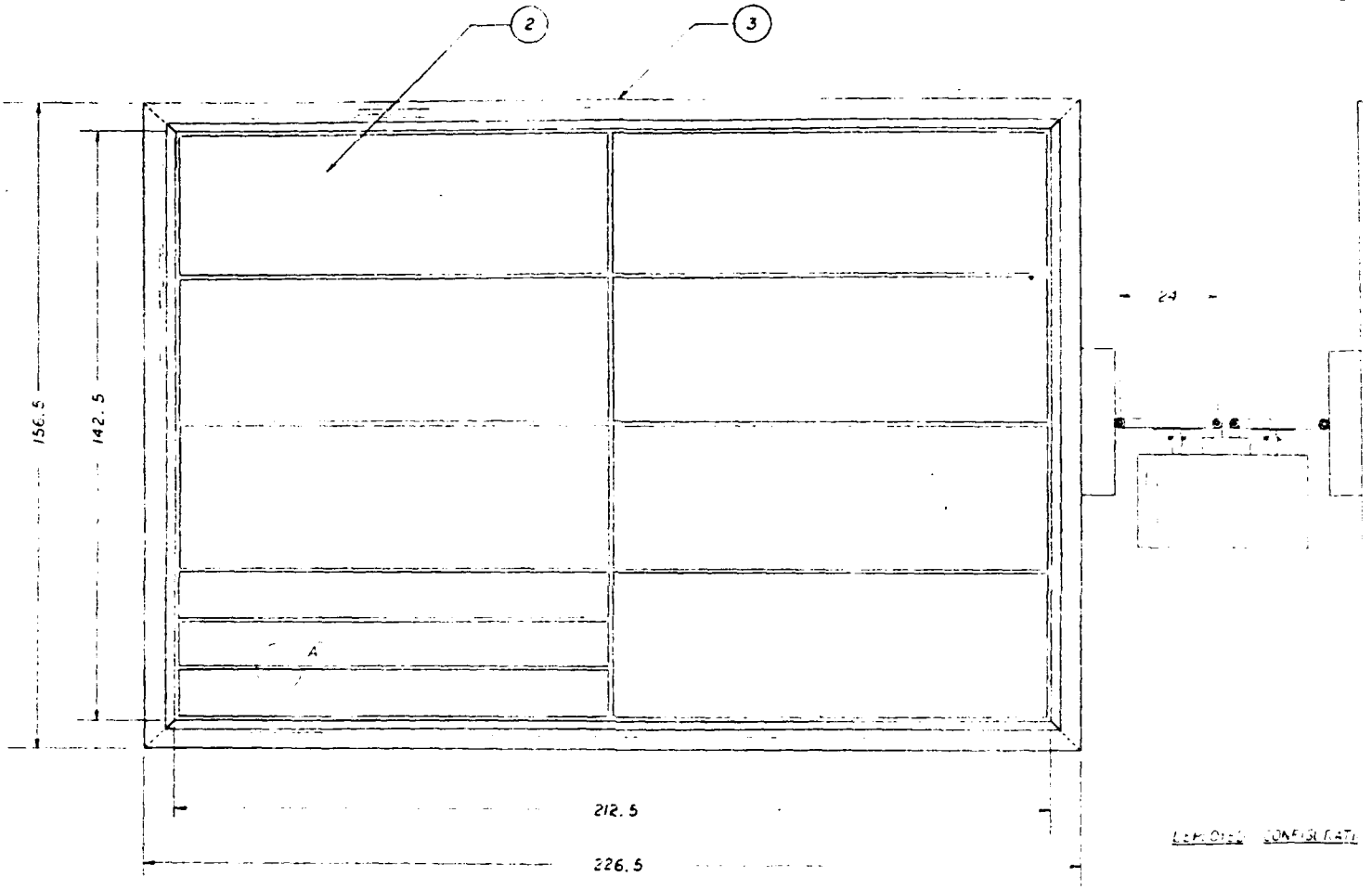

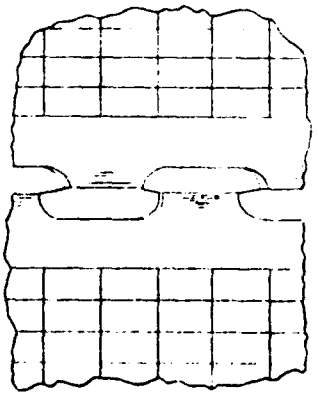

DETAIL "A"
NOT TO SCALE

71-774

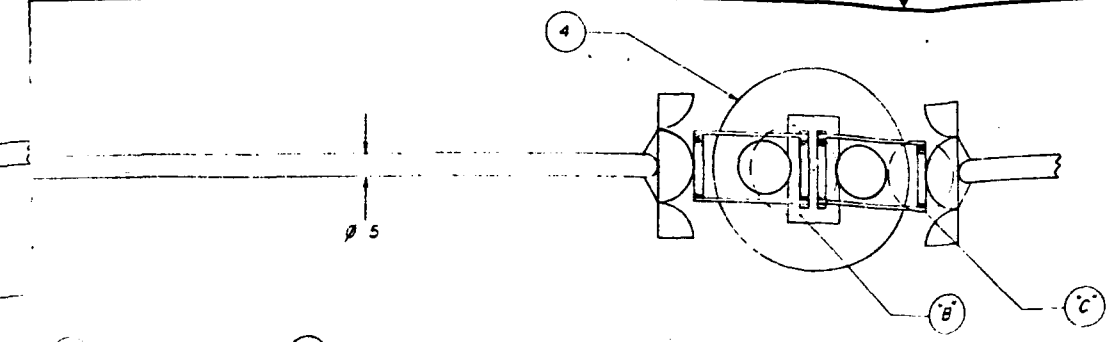

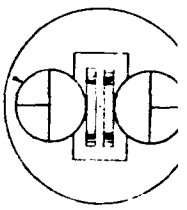

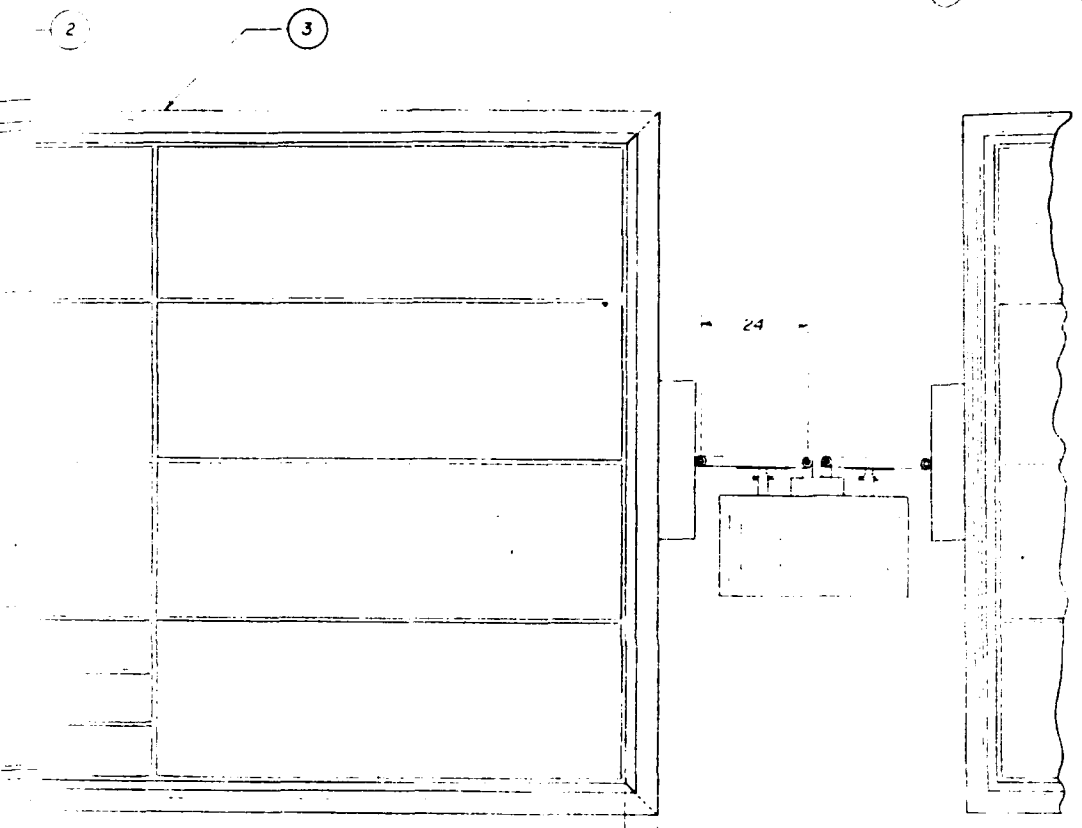

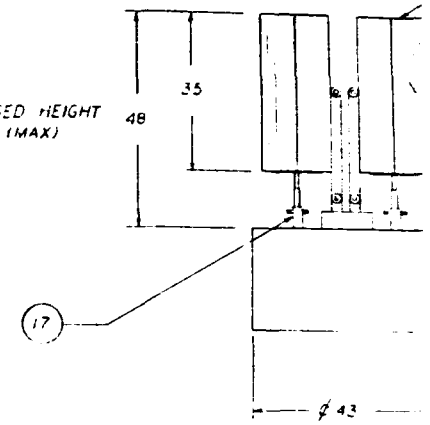

PACKAGED

DEPLOYED CONFIGURATION

COMPONENT	WEIGHT (LBS)	%
SOLAR ARRAY	129.2	54.6
TORUS	22.0	9.2
ARMS, CASE, ETC	57.2	24.0
ARM MOUNT	≈ 9.2	3.9
MOTOR DRIVE ASS	≈ 16.1	6.8
INFLATION SYS.	≈ 5.0	2.1
TOTAL	≈ 238.5	

QTY REQD	FROM NO	PART IDENTIFY
2		
4		
8		
6		
6		
6		
2		
2		
2		
2		
6		
2		
4		
6		
1		
2		
2		
2		

UNLESS OTHERWISE SPECIFIED
DIMENSIONS ARE IN INCHES
TOLERANCES ARE
FRACTIONS DECIMALS ANGLES
.XX ±
.XXX ±

MATERIAL

FINISH

DO NOT SCALE DRAWING

NEXT ASSY | USED ON

APPLICATION

REVISIONS				
ZONE	REV.	DESCRIPTION	DATE	APPROVED

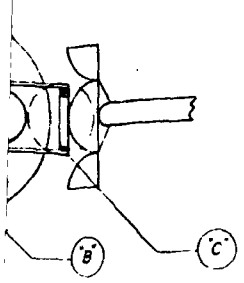

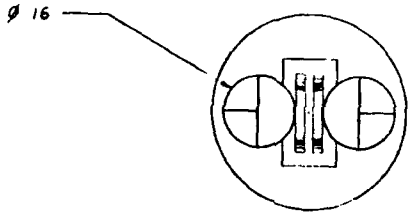

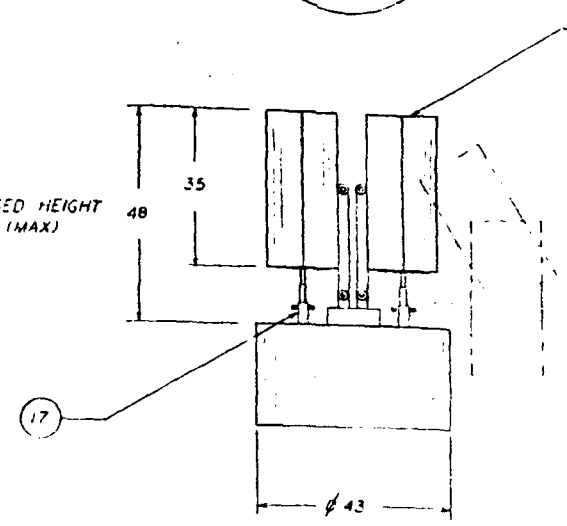

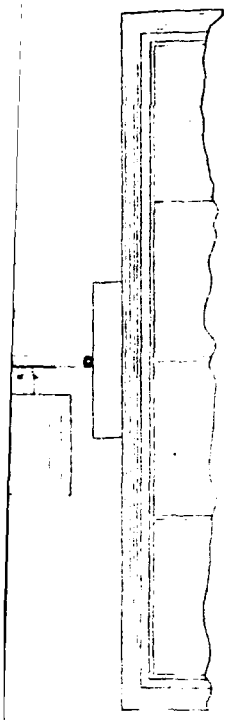

PACKAGED CONFIGURATION

CONFIGURATION

COMPONENT	WEIGHT (LES)	%
SOLAR ARRAY	129.2	54.2
TORUS	22.0	9.2
ARMS, CABLE, ETC	57.2	24.0
ARM MOUNT	≈ 9.2	3.9
MOTOR DRIVE ASS	≈ 16.1	6.8
INFLATION SYS.	≈ 5.0	2.1
TOTAL	≈ 238.5	

QTY REQD	PSCM NO	PART OR IDENTIFYING NO	NOMENCLATURE OR DESCRIPTION	MATERIAL SPECIFICATION	ITEM
2			LAUNCH LOAD SUPPORT STRUT		17
4			.5" PRESS FIT SHAFT		16
8			BOLT		15
6			SPACER DISC		14
6			COMPRESSION SPRING		13
6			DETENT PIN		12
2			MOTOR DRIVE		11
2			WORM		10
2			GEAR		9
6			PIN		8
2			.5" SUPPORT SHAFT		7
4			2" SHAFT		6
8			TORSIONAL SPRING		5
1			SPACECRAFT		4
2			TORUS		3
2			SOLAR ARRAY PANEL		2
2			(EARTH?) LAUNCH CASE (DISCARD)		1

PARTS LIST

HEAT ASSY	USED ON
APPLICATION	

UNLESS OTHERWISE SPECIFIED DIMENSIONS ARE IN INCHES TOLERANCES ARE: FRACTIONS DECIMALS ANGLES .XX ± .XXX ±

MATERIAL

FINISH

DO NOT SCALE DRAWING

CONTRACT NO. 1542

APPROVALS	DATE
DRAWN D. BRANDT	7-10-80
CHECKED	
ISSUED	

L'GARDE, INC. 15181 WOODLAWN AVENUE TUSTIN, CALIFORNIA 92680

1000 W INFLATABLE SOLAR ARRAY
RIGID KEVLAR TORUS CONFIGURATION, AMORPHOUS SILICON ARRAY

SIZE	PSCM NO.	DWG. NO.	REV.
D	1-166	21005	

SCALE 1:20 SHEET 1 OF 2

4 3 2 1

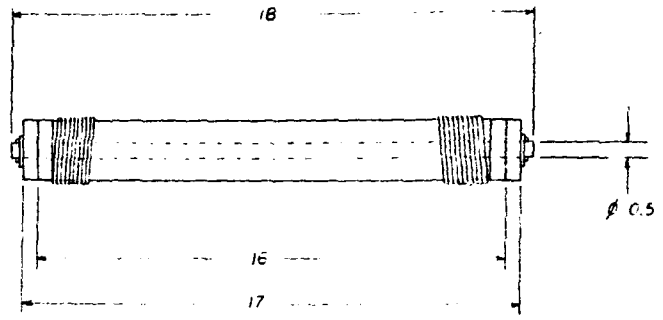

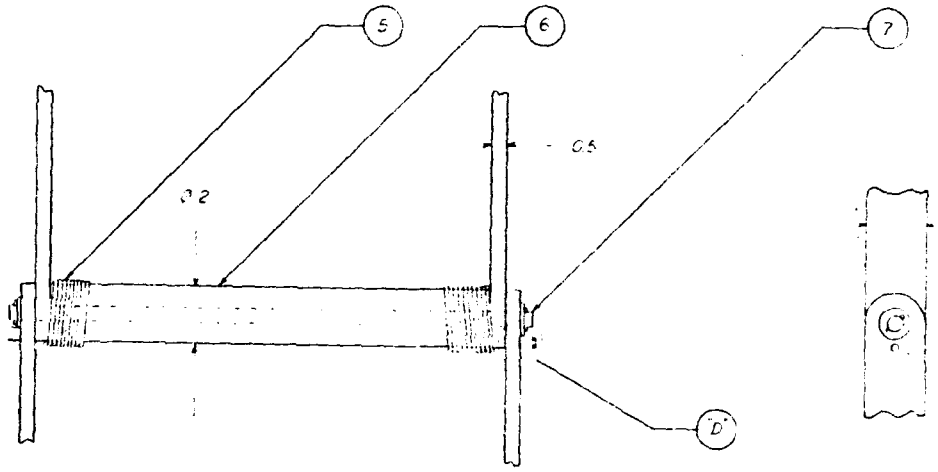

DETAIL "B"

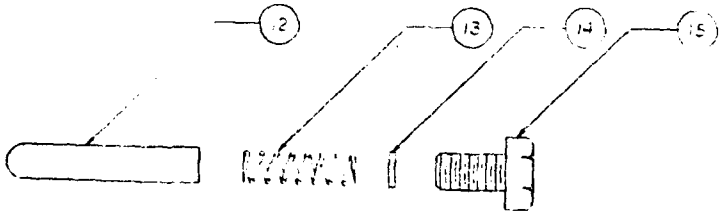

EXPLODED VIEW "D"
NOT TO SCALE

11-777

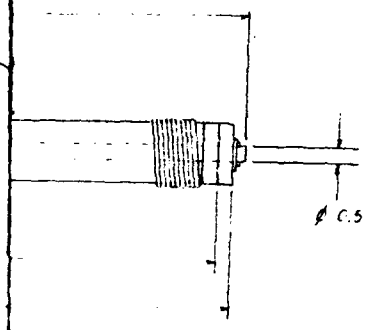

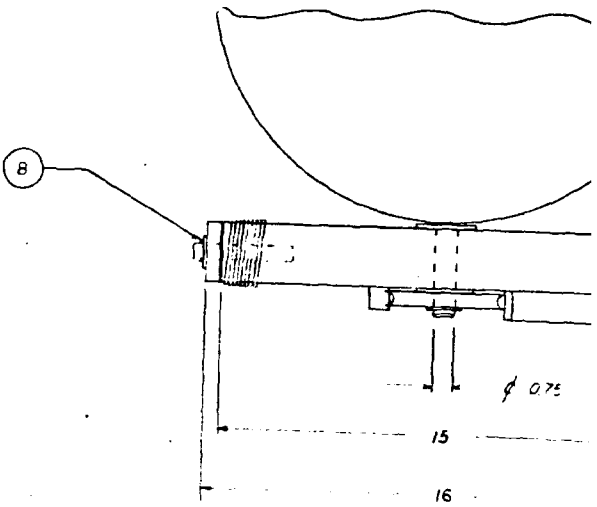

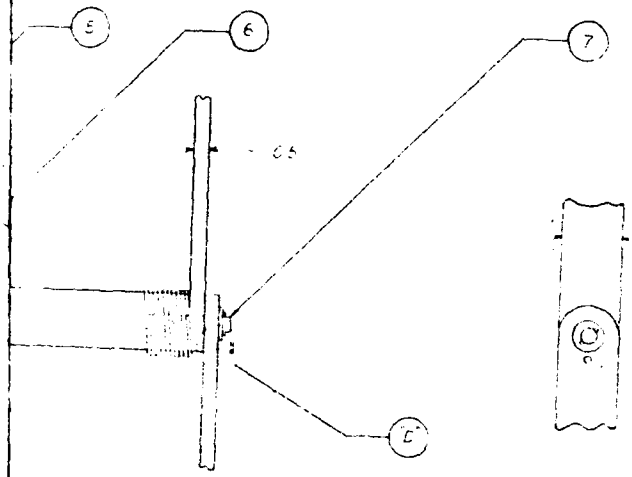

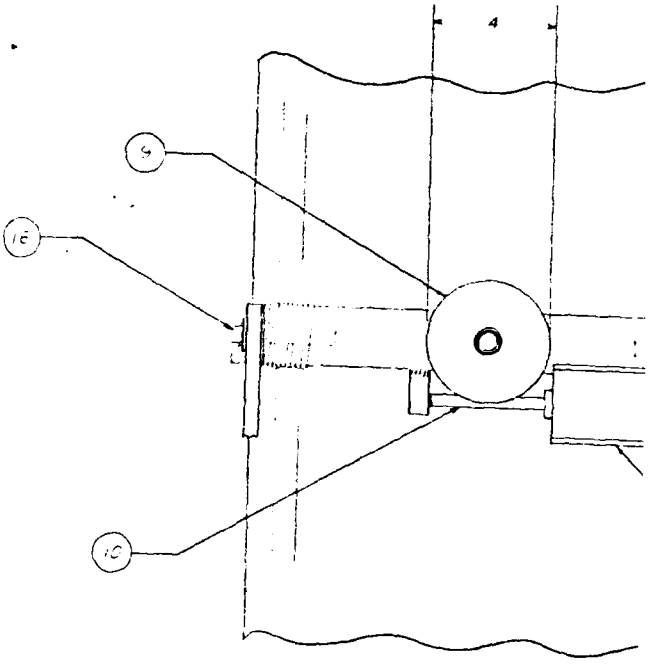

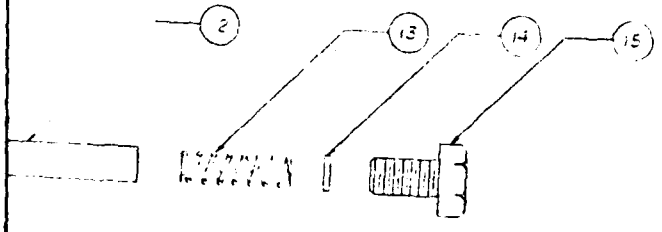

EXPLODED VIEW 'B'
NOT TO SCALE

NEXT ASSY	USED ON		
APPLICATION		DO NOT SCA	

UNLESS OTHERWISE
DIMENSIONS ARE IN
TOLERANCES ARE,
FRACTIONS
MATERIAL
FINISH

DWG. NO. 21005 SH. 2 OF 2 REV

REVISIONS				
ZONE	REV.	DESCRIPTION	DATE	APPROVED

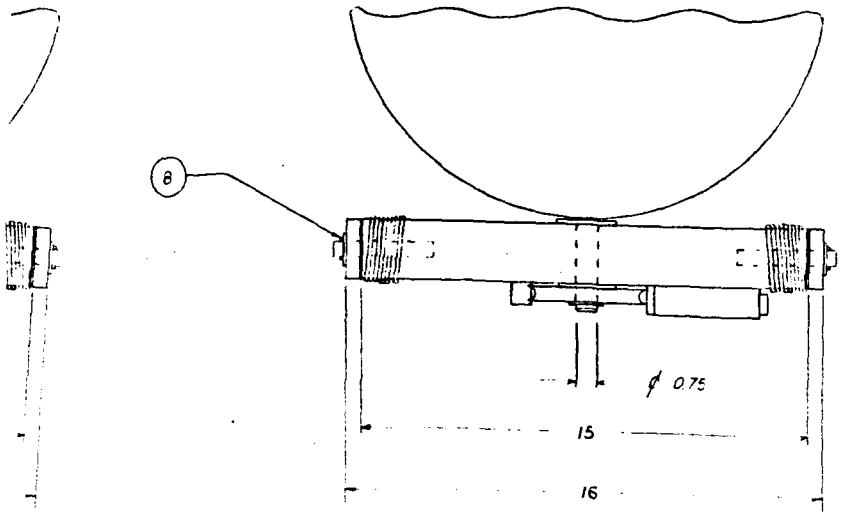

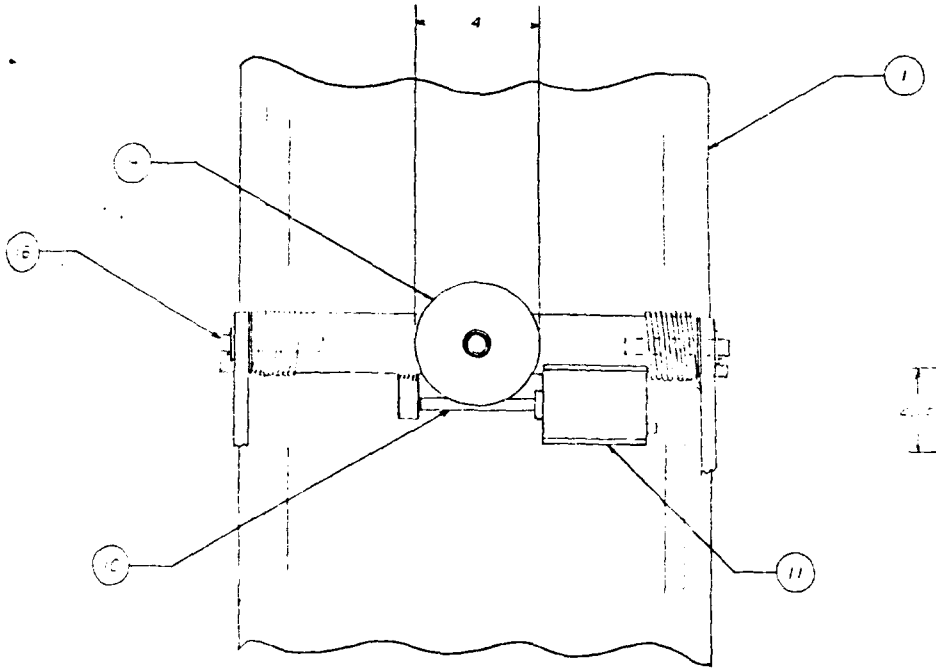

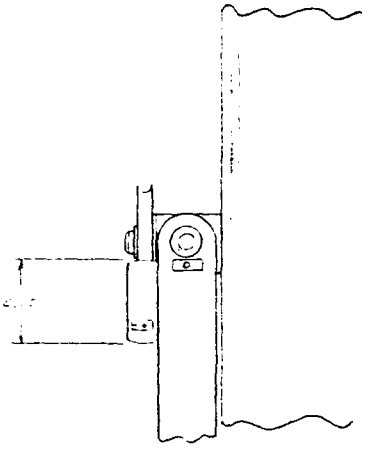

DETAIL "C"

QTY REQD	FSCM NO	PART OR IDENTIFYING NO.	NOMENCLATURE OR DESCRIPTION	MATERIAL SPECIFICATION
			PARTS LIST	

UNLESS OTHERWISE SPECIFIED DIMENSIONS ARE IN INCHES
TOLERANCES ARE:
FRACTIONS ± DECIMALS .XX ± .XXX ± ANGLES °

MATERIAL

FINISH

NEXT ASSY | USED ON

APPLICATION

DO NOT SCALE DRAWING

CONTRACT NO. 5542

APPROVALS	DATE
DRAWN F. BRANDT	7-1-92
CHECKED	
ISSUED	

L'GARDE, INC. 15181 WOODLAWN AVENUE TUSTIN, CALIFORNIA 92680

1000 W INFLATABLE SOLAR ARRAY, AMORPHOUS SILICON

SIZE D | FSCM NO. 11066 | DWG NO. 21005 | REV

SCALE 1:3 | SHEET 2 OF 2

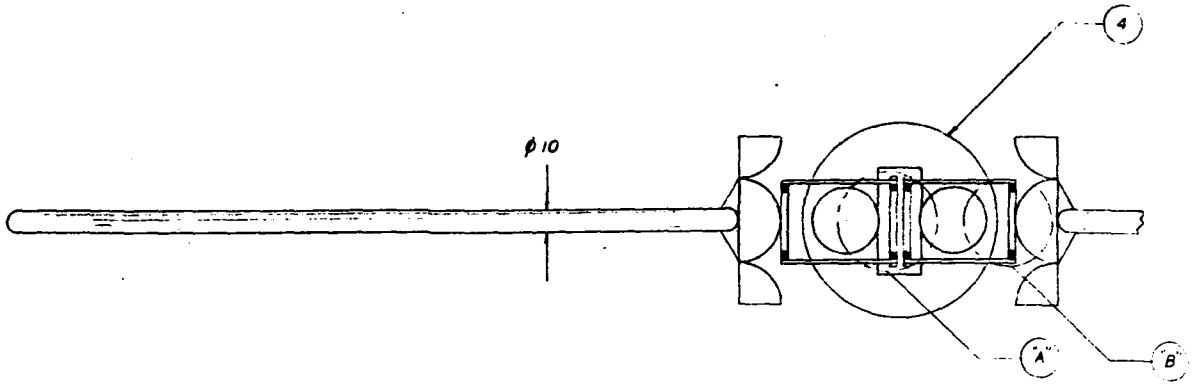

DEPLOYED CONFIGURATION

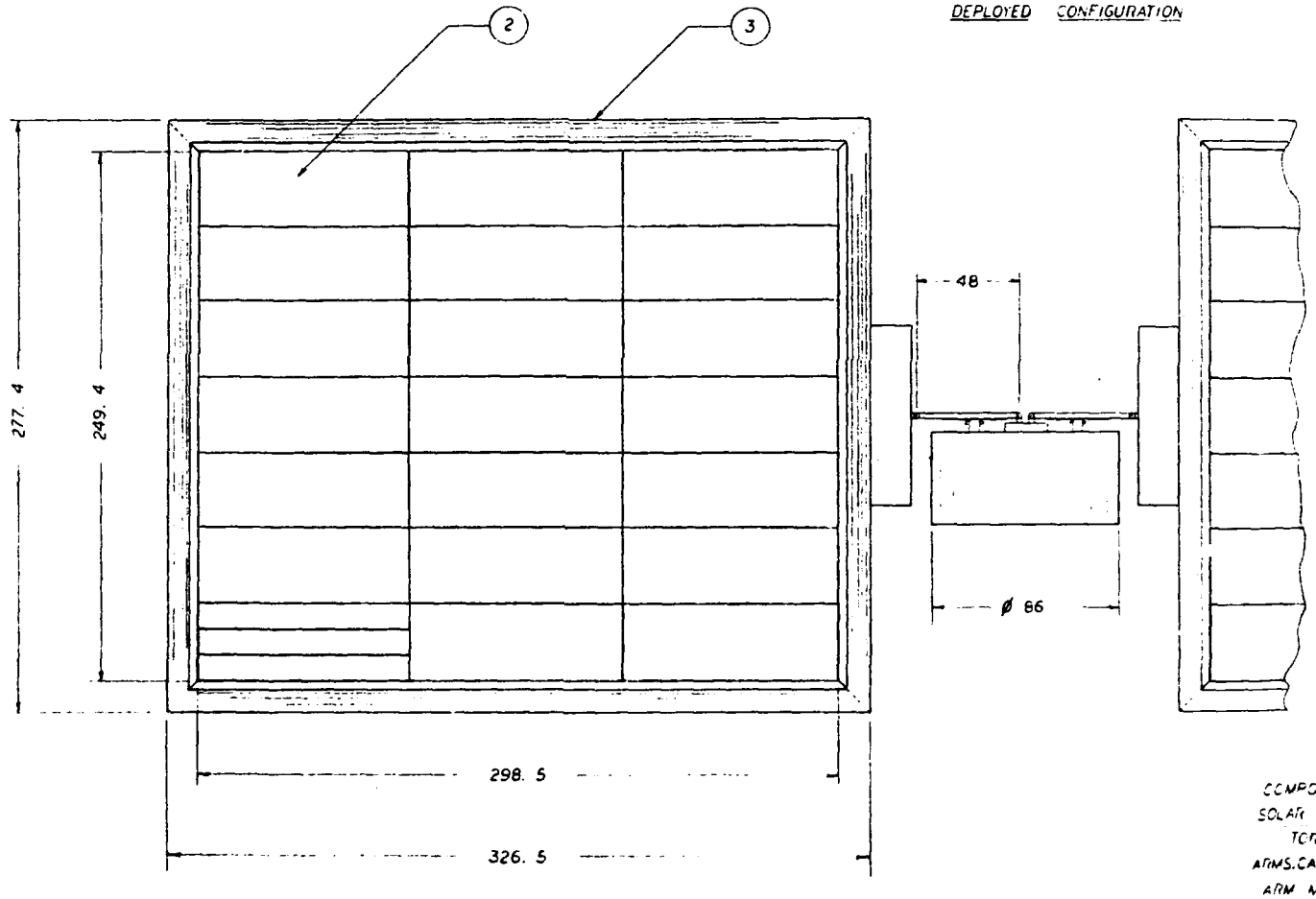

COMPONE
SOLAR AR
TORUS
ARMS.CASE
ARM MOU
MOTOR DRIV.
INFLATION
TOTAL

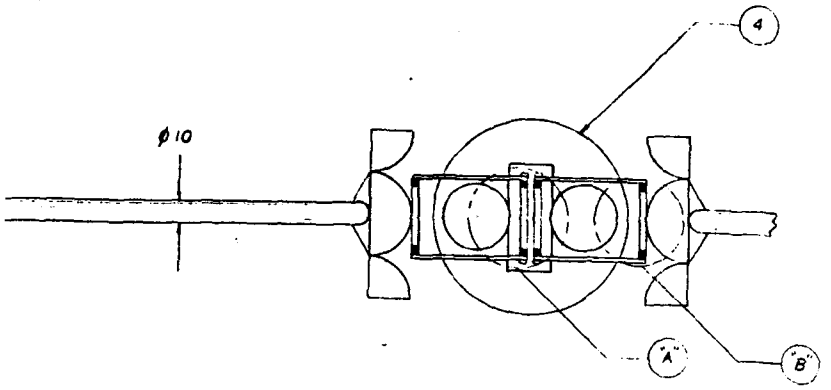

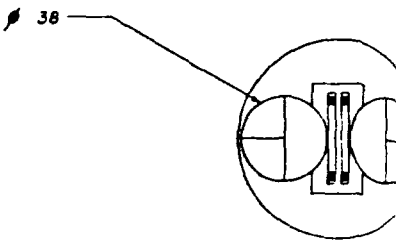

DEPLOYED CONFIGURATION

PACKAGED CONFI

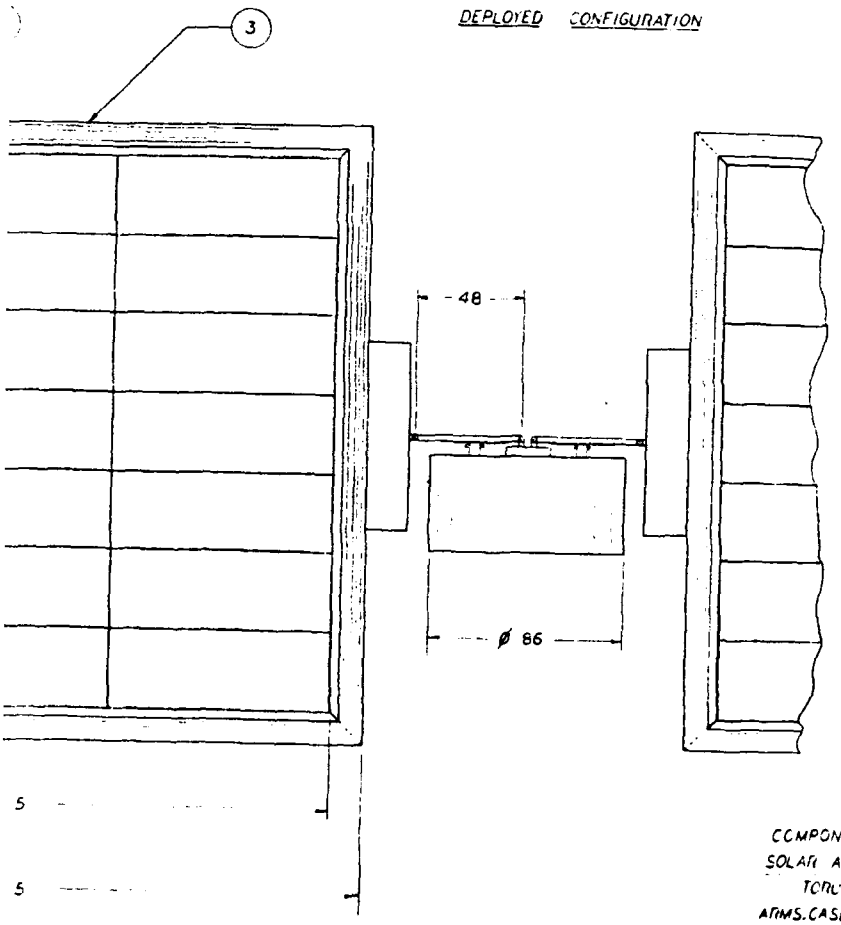

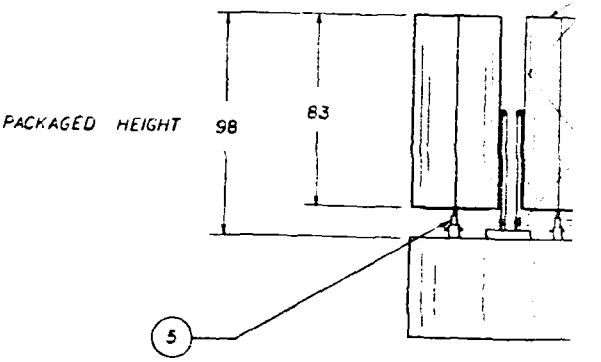

COMPONENT	WEIGHT (LBS)	%
SOLAR ARRAY	1603	75.3
TORUS	177.2	8.3
ARMS, CASE, ETC	269.3	12.6
ARM MOUNT	≈ 30.0	1.4
MOTOR DRIVE ASS.	≈ 34.5	1.6
INFLATION SYS.	≈ 15.0	0.70
TOTAL	≈ 2129.0	

8		
8		
6		
6		
2		
2		
2		
4		
4		
6		
2		
1		
2		
2		
2		
QTY REQD	PIECE NO.	PART OR IDENTIFYING NO.

UNLESS OTHERWISE SPECIFIED
DIMENSIONS ARE IN INCHES
TOLERANCES ARE:
FRACTIONS DECIMALS ANGLES
± .XX ±
.XXX ±

MATERIAL

FINISH

NEXT ASSY | USED ON

APPLICATION

DO NOT SCALE DRAWING

CONTRACT NO.

APPVD

DRAWN D. BI

CHECKED

ISSUED

DWG. NO. 21006	SH 1	REV.

REVISIONS

ZONE	REV.	DESCRIPTION	DATE	APPROVED

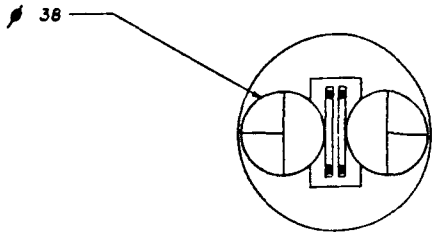

PACKAGED CONFIGURATION

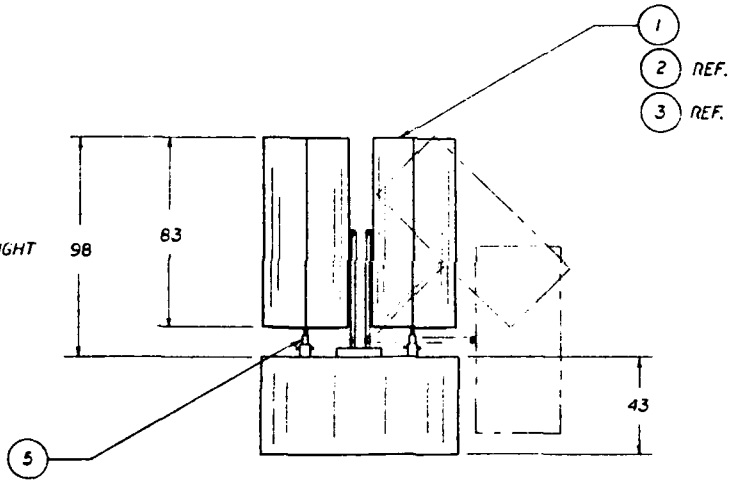

COMPONENT	WEIGHT (LBS)	%
ARR ARRAY	1603	75.3
TORUS	177.2	8.3
S.CASE ETC	269.3	12.6
M MOUNT	≈ 30.0	1.4
N DRIVE ASS.	≈ 34.5	1.6
LATION SYS.	≈ 15.0	0.70
TOTAL	≈ 2129.0	

QTY PER	PICK NO.	PART OR IDENTIFYING NO.	NOMENCLATURE OR DESCRIPTION	MATERIAL SPECIFICATION	ITEM NO.
8			BOLT		15
8			SPACER DISC		14
8			COMPRESSION SPRING		13
8			DETENT PIN		12
2			MOTOR DRIVE		11
2			WORM		10
2			GEAR		9
4			0.75" SUPPORT SHAFT		8
4			2.5" SHAFT		7
8			TORSIONAL SPRING		6
2			LAUNCH LOAD SUPPORT STRUT		5
1			SPACECRAFT		4
2			TORUS		3
2			SOLAR ARRAY PANEL		2
2			CLAMSHELL LAUNCH CASE (CLOSED)		1

PARTS LIST

NEXT ASSY	USED ON
APPLICATION	

UNLESS OTHERWISE SPECIFIED DIMENSIONS ARE IN INCHES
TOLERANCES ARE:
FRACTIONS ± DECIMALS .XX ± .XXX ± ANGLES ±

MATERIAL

FINISH

DO NOT SCALE DRAWING

CONTRACT NO. 5542

APPROVALS	DATE
DRAWN D. BRANDT	7-16-90
CHECKED	
ISSUED	

L'GARDE, INC. 15181 WOODLAWN AVENUE TUSTIN, CALIFORNIA 92680

2500 W INFLATABLE SOLAR ARRAY
RIGID KEVLAR TORUS CONFIGURATION,
AMORPHOUS SILICON ARRAY

SIZE	PICK NO.	DWG. NO.	REV.
D	IF668	21006	

SCALE 1:40 SHEET 1 OF 2

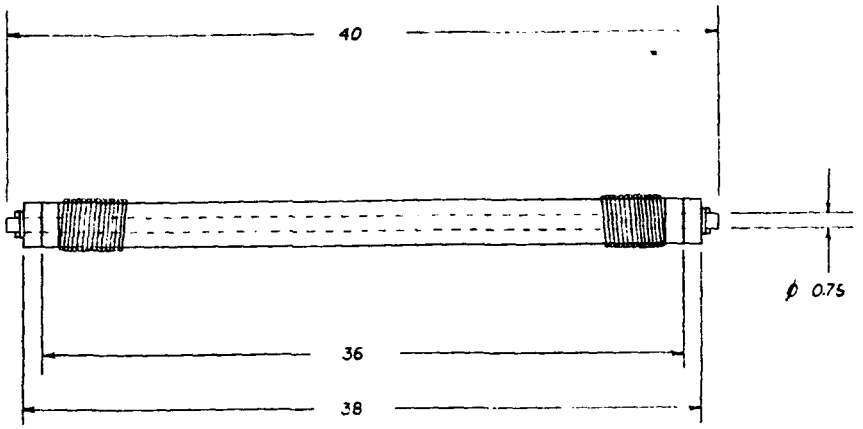

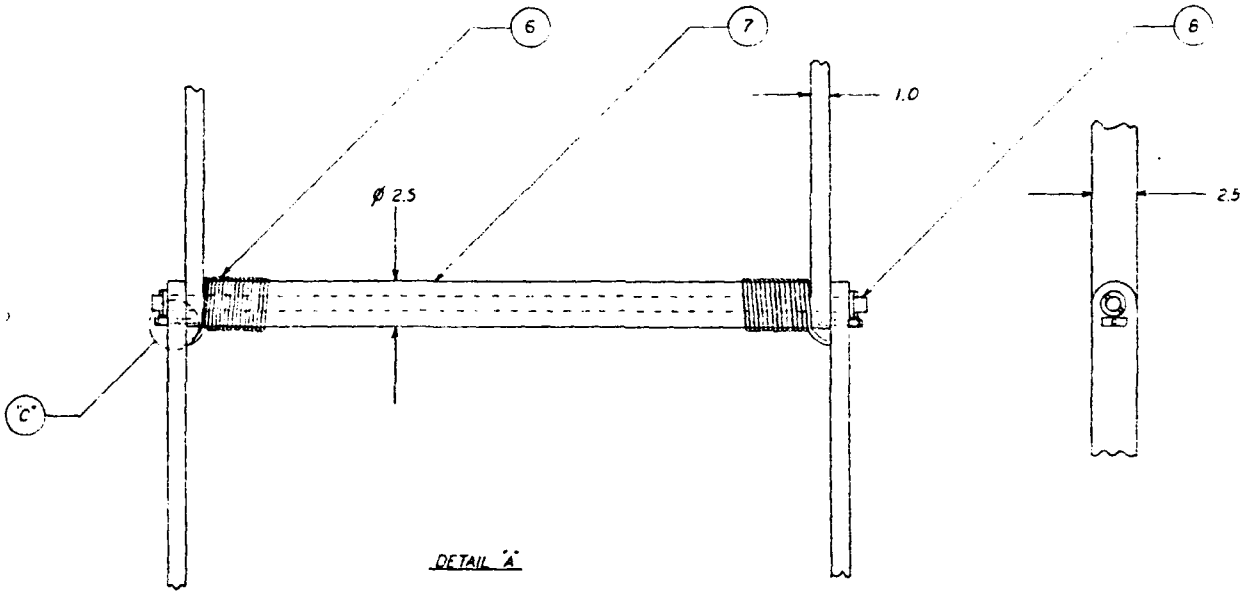

DETAIL "A"

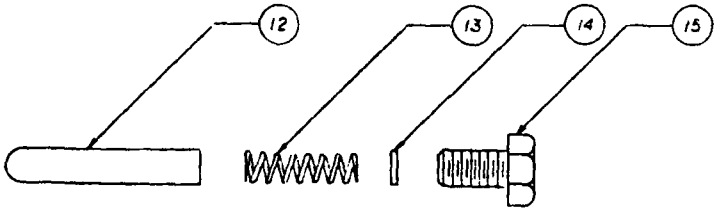

EXPLODED VIEW "C"

NOT TO SCALE

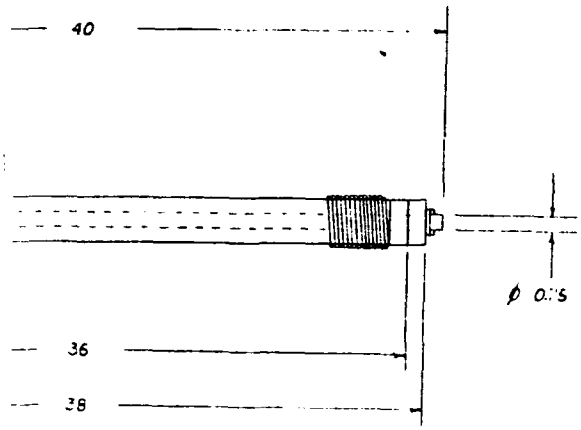

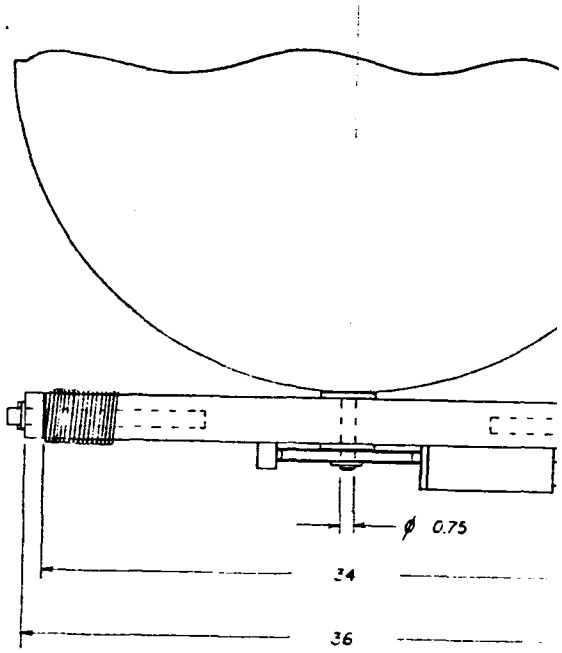

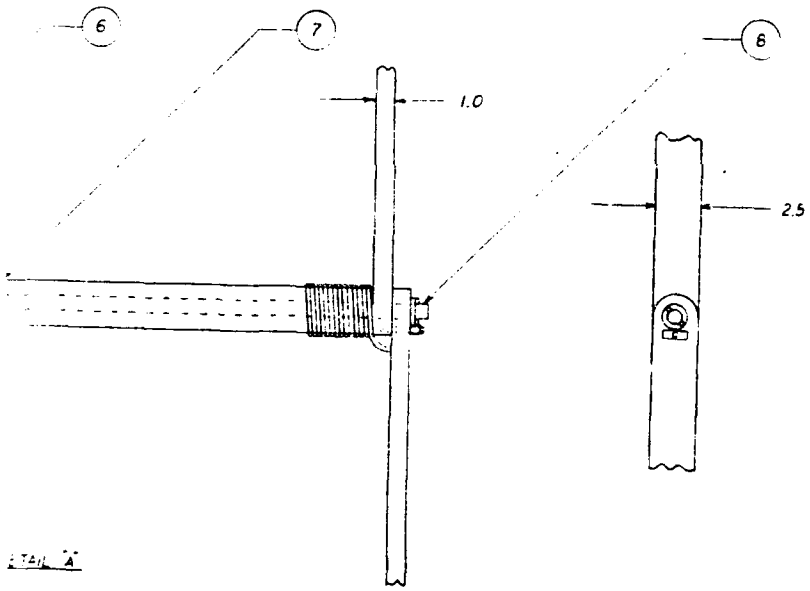

DETAIL "A"

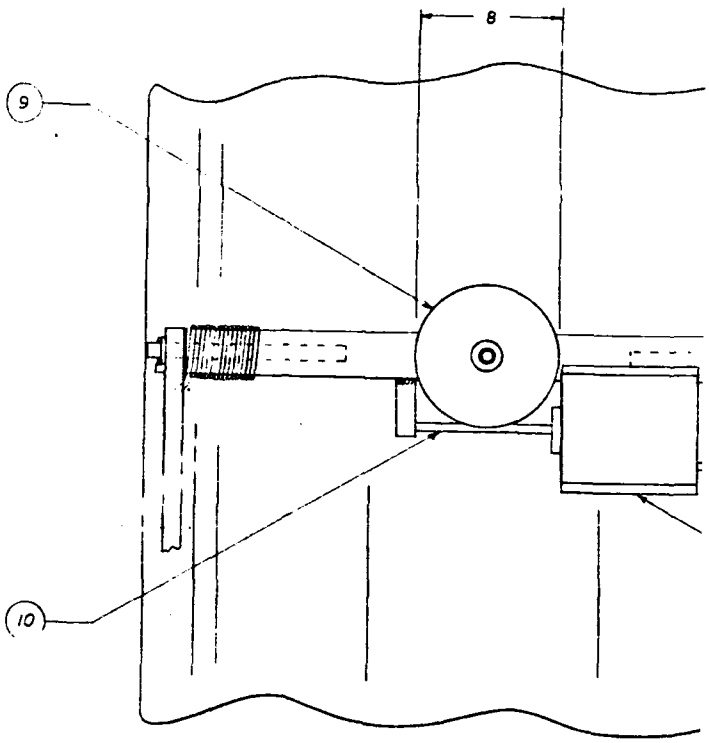

DETAIL "B"

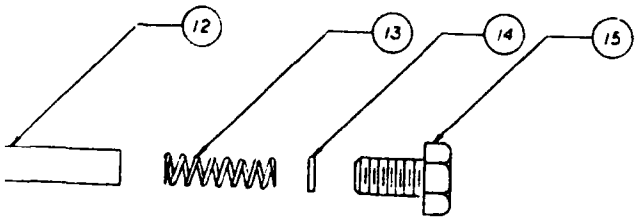

EXPLODED VIEW "C"

NOT TO SCALE

NEXT ASSY	USED ON
APPLICATION	

UNLESS OTHERWISE SPECIFIED DIMENSIONS ARE IN INCHES
TOLERANCES ARE:
FRACTIONS DECIMALS ANG
X .XX ±
.XXX ±

MATERIAL

FINISH

DO NOT SCALE DRAW

DWG. NO. 21006 SH. 2 REV. 1

ZONE	REV.	REVISIONS DESCRIPTION	DATE	APPROVED

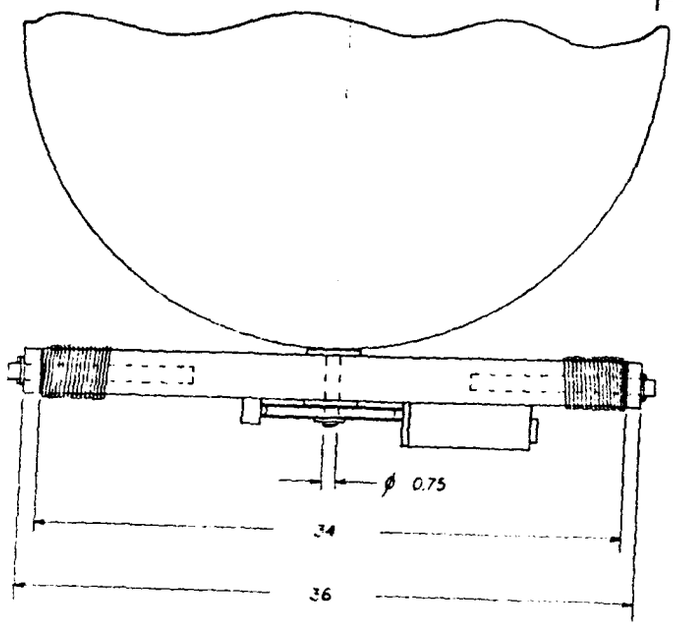

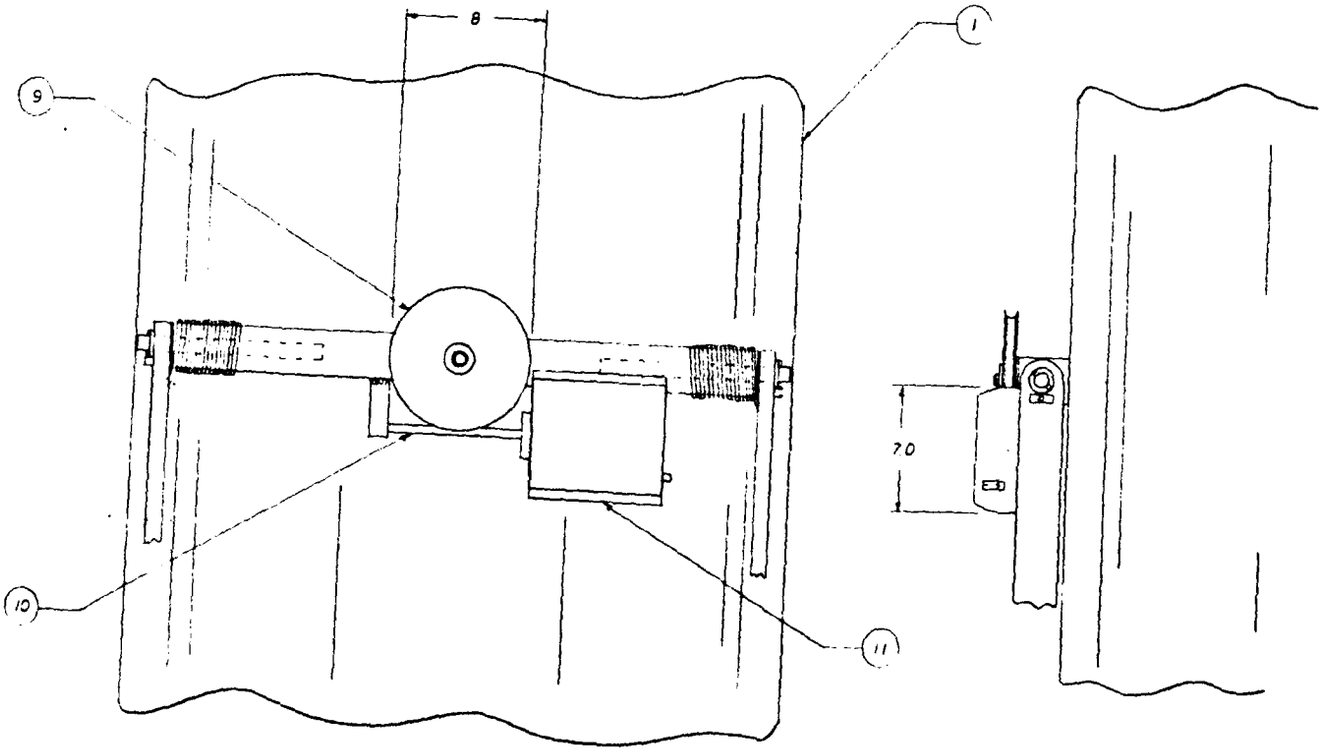

DETAIL "B"

PARTS LIST

QTY REQD	ITEM NO.	PART OR IDENTIFYING NO.	NOMENCLATURE OR DESCRIPTION	MATERIAL SPECIFICATION

UNLESS OTHERWISE SPECIFIED DIMENSIONS ARE IN INCHES
TOLERANCES ARE:
FRACTIONS ± DECIMALS .XX ± .XXX ± ANGLES °

MATERIAL

FINISH

NEXT ASSY | USED ON

APPLICATION

DO NOT SCALE DRAWING

CONTRACT NO. 5542

APPROVALS	DATE
DRAWN D BRANDT	7-20-90
ENGINEER	
ISSUED	

L'GARDE, INC. 15181 WOODLAWN AVENUE TUSTIN, CALIFORNIA 92680

2500 W INFLATABLE SOLAR ARRAY, AMORPHOUS SILICON

SIZE D | FSCM NO. 1FE68 | DWG. NO. 21006 | REV.

SCALE 1:5 | SHEET 2 OF 2

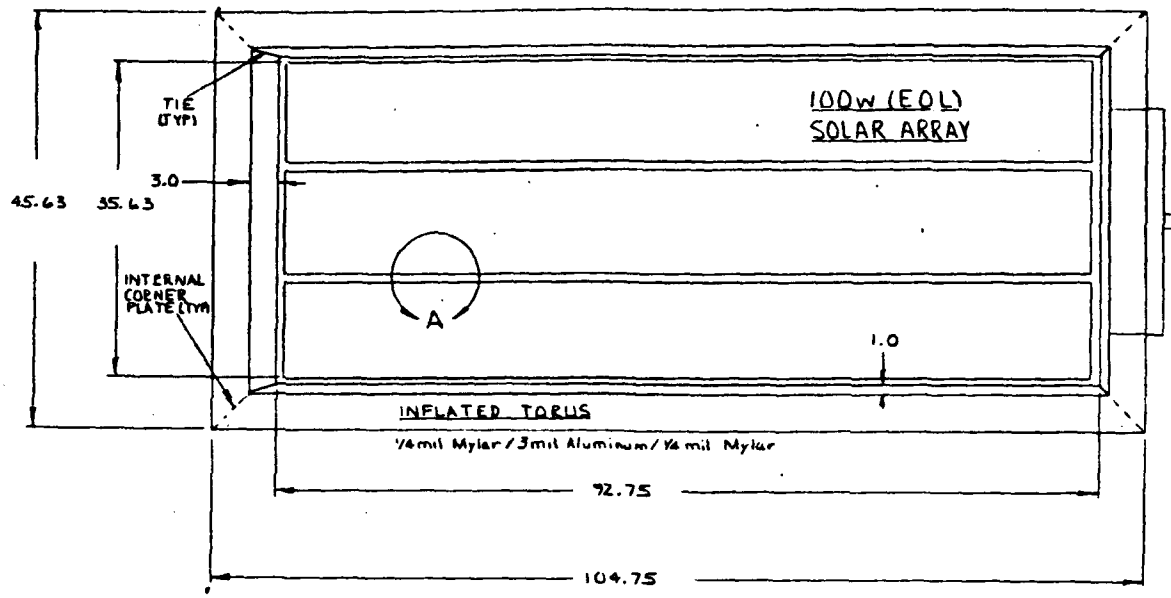
100w (EOL)
SOLAR ARRAY
TIE
(TYP)
3.0
45.63
35.63
INTERNAL
CORNER
PLATE (TYP)
A
1.0
INFLATED TORUS
¼mil Mylar / 3mil Aluminum / ¼ mil Mylar
92.75
104.75

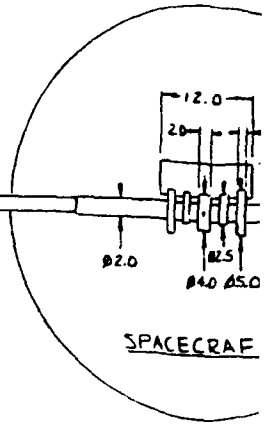
12.0
2.0
Ø2.0
Ø2.5
Ø4.0
Ø5.0
SPACECRAF

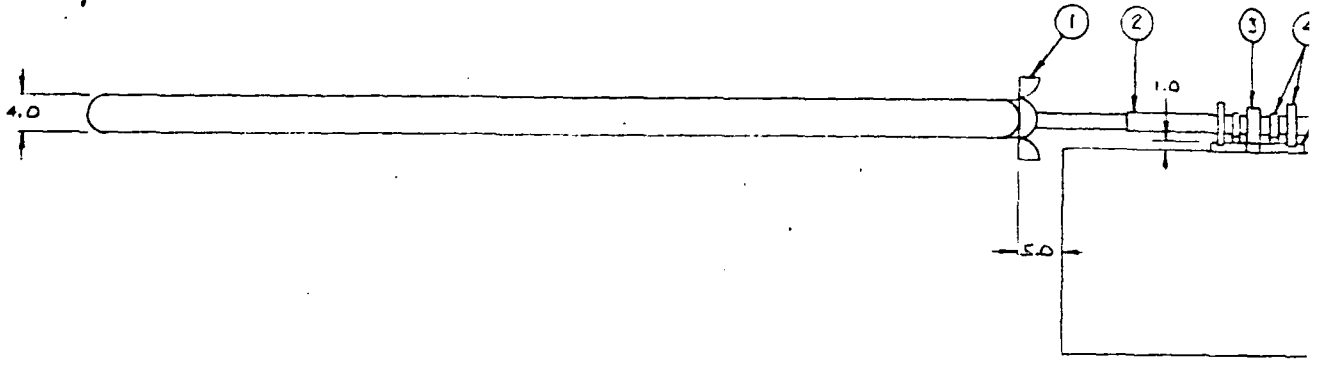
1
2
3
4
4.0
1.0
5.0

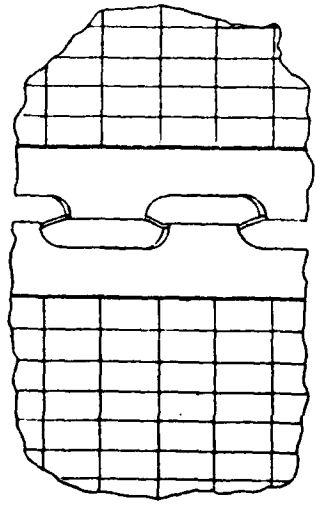

VIEW A

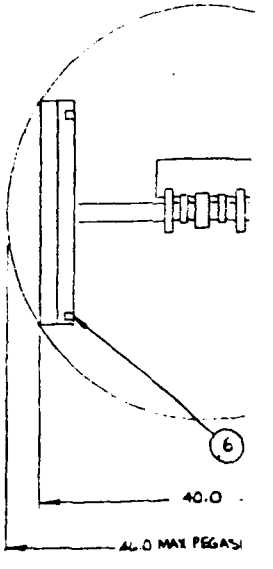
6
40.0

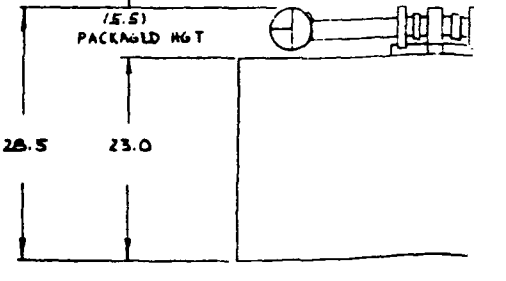
(5.5)
PACKAGED HGT
28.5
23.0

11-780

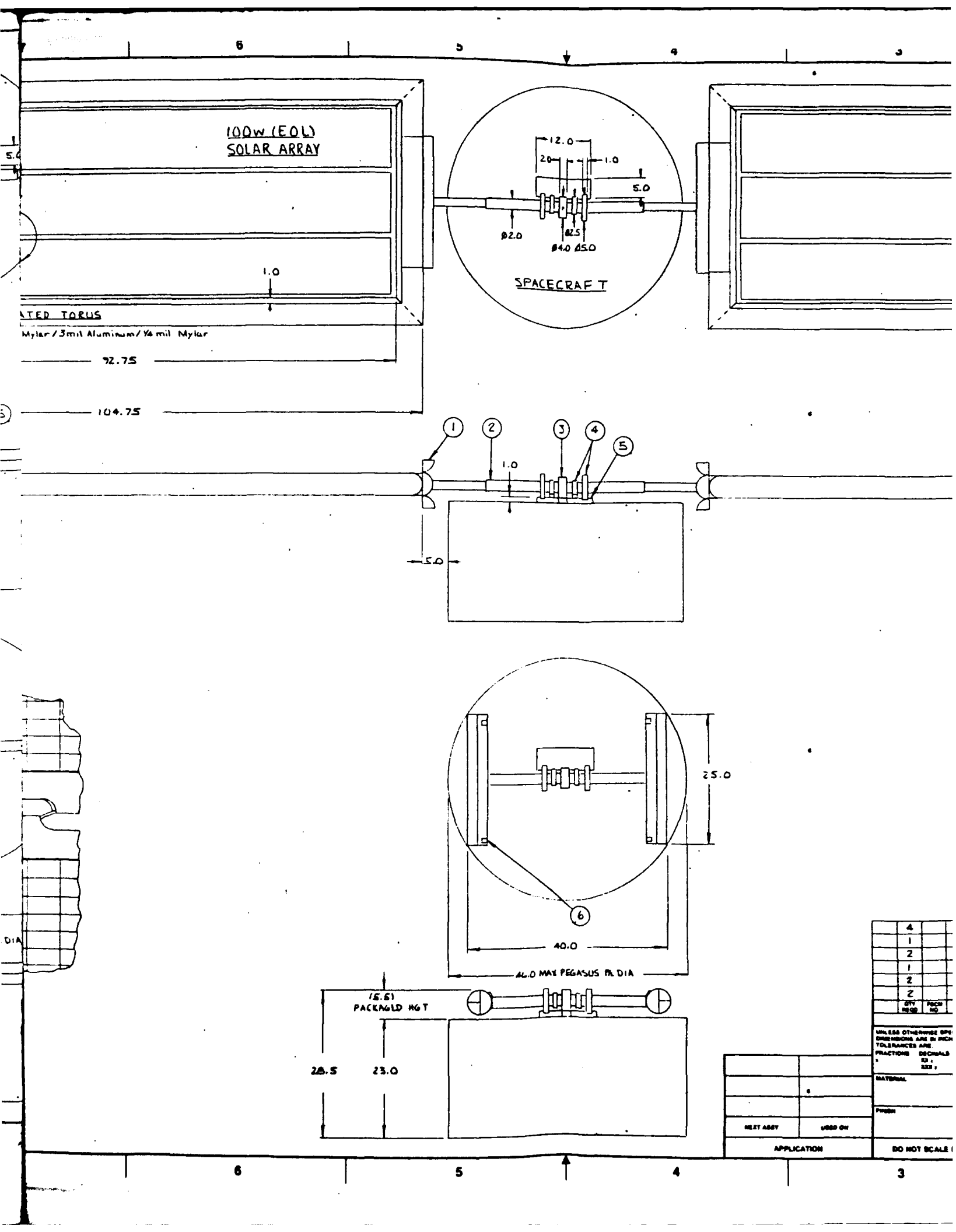
100w (EOL)
SOLAR ARRAY
12.0
2.0
1.0
5.0
Ø2.0
Ø2.5
Ø4.0 Ø5.0
SPACECRAFT
1.0
TED TORUS
Mylar/3mil Aluminum/¼ mil Mylar
92.75
104.75
1
2
3
4
5
1.0
5.0
25.0
6
40.0
44.0 MAX PEGASUS FR DIA
(15.5)
PACKAGED HGT
28.5
23.0
4
1
2
1
2
2
QTY REQD
PIECE NO
UNLESS OTHERWISE SPE
DIMENSIONS ARE IN INCH
TOLERANCES ARE
FRACTIONS
DECIMALS
X.X ±
X.XX ±
MATERIAL
FINISH
NEXT ASSY
USED ON
APPLICATION
DO NOT SCALE
6
5
4
3

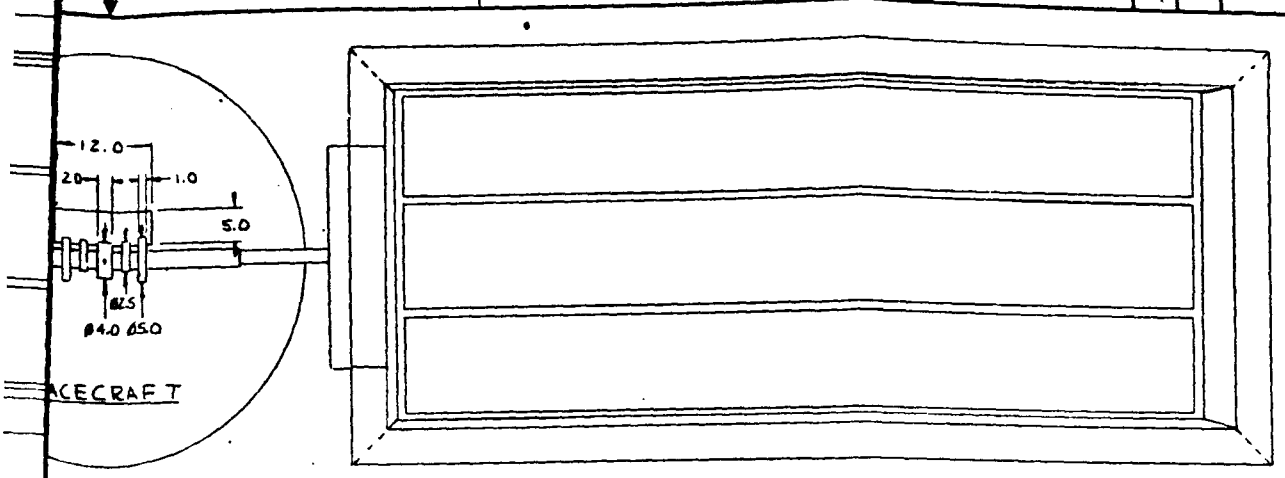

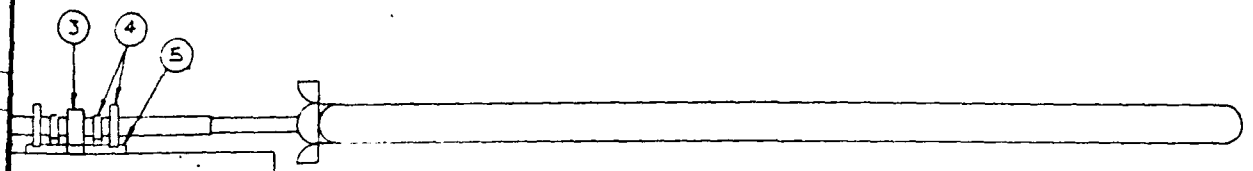

COMPONENT	WEIGHT (LBS)	% TOTAL
SOLAR CELLS	1.47×2= 2.94	26.3
TORUS	1.16×2=2.32	20.8
VALVES, TANK	.53×2= 1.06	9.5
ARM, CASE	1.8×2 = 3.60	32.2
MOTOR, MOUNT	.25	2.2
COMPUTER, CABLES	1.00	9.0
TOTAL	11.17	

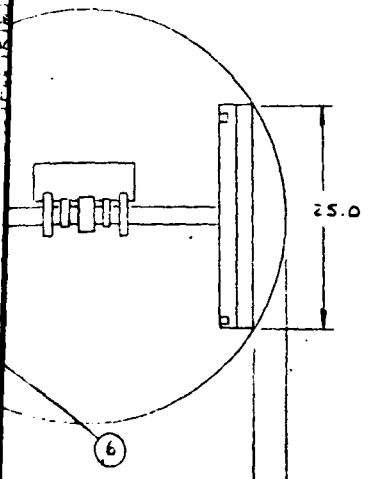

QTY REQD	FIND NO	PART OR IDENTIFYING NO	NOMENCLATURE OR DESCRIPTION	MATERIAL SPECIFICATION	ITEM NO.
4			PYRO CABLE CUTTERS TO OPEN CLAMSHELLS		6
1			MOTOR CONTROLLER COMPUTER		5
2			FLEX RIBBON POWER & SIGNAL TRANSFER RING		4
1			DRIVE MOTOR & RESOLVER		3
2			TELESCOPING ARM		2
2			CLAMSHELL LAUNCH CASE		1

PARTS LIST

UNLESS OTHERWISE SPECIFIED DIMENSIONS ARE IN INCHES
TOLERANCES ARE:
FRACTIONS ± DECIMALS ± ANGLES °
.XX ±
.XXX ±

MATERIAL

FINISH

NEXT ASSY | USED ON

APPLICATION

DO NOT SCALE DRAWING

CONTRACT NO

APPROVALS	DATE
DRAWN TUMMOND	7/16/90
CHECKED	
ISSUED	

L'GARDE, INC. 19181 WOODLAWN AVENUE, TUSTIN, CALIFORNIA 92680

200W INFLATABLE SOLAR ARRAY, G.E.O., RIGIDIZED ALUMINUM TORUS, AMORPHOUS SILICON ARRAY

SIZE D | FSCM NO 1F668 | DWG NO 21007 | REV

SCALE 1:10 | SHEET 1 OF 6

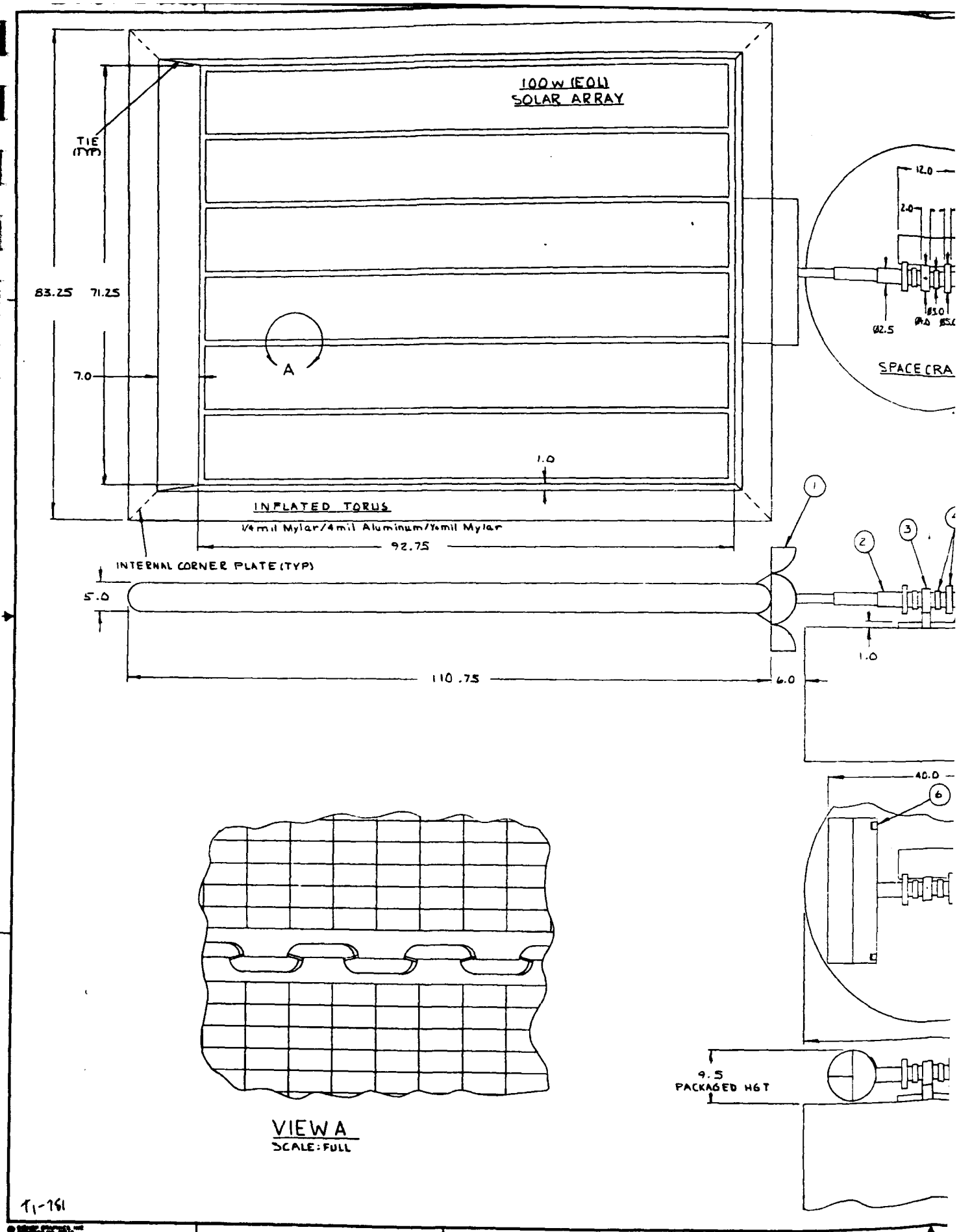

VIEW A
SCALE: FULL

T1-761

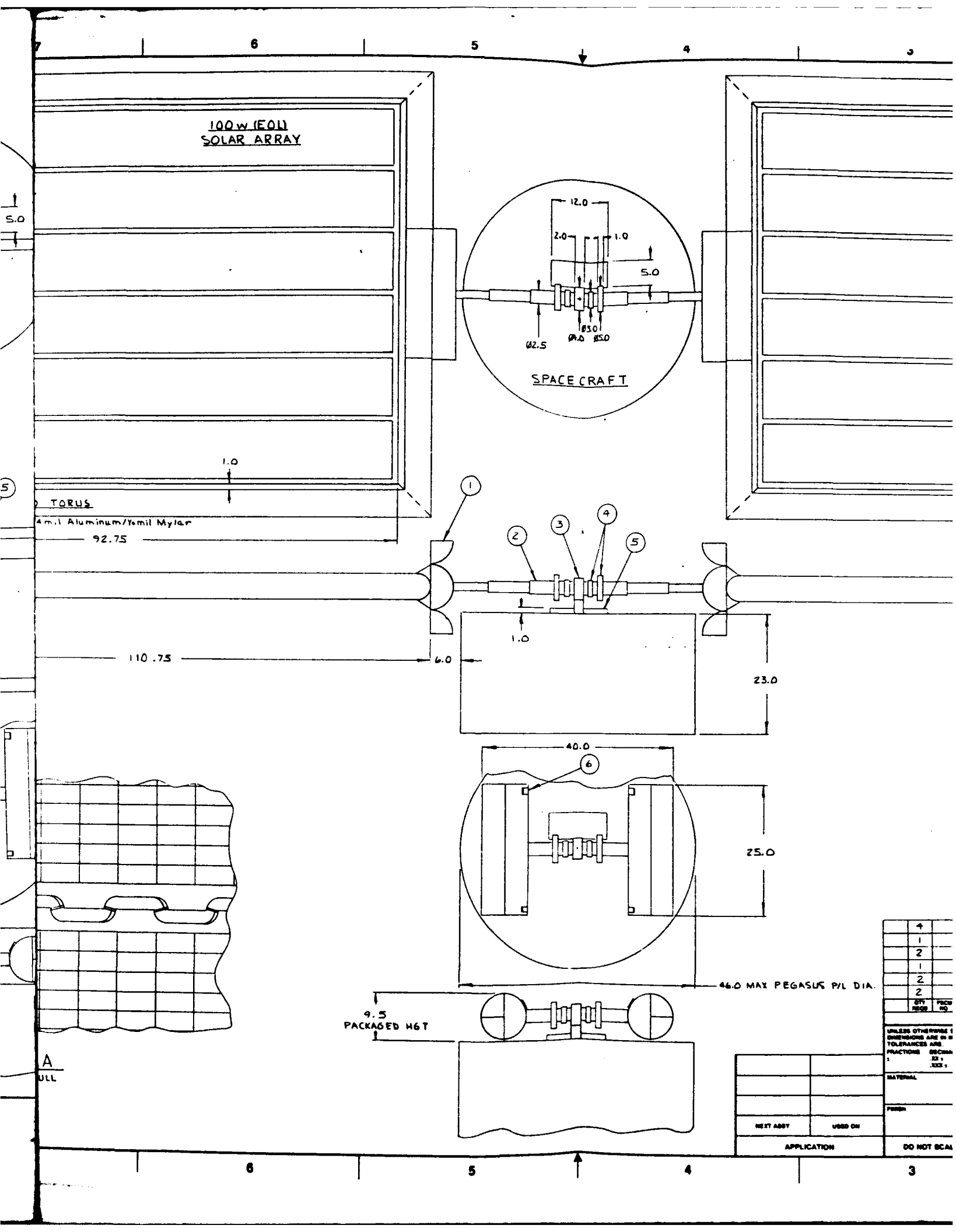
100w (EOL)
SOLAR ARRAY
12.0
2.0
1.0
5.0
Ø3.0
Ø2.5
Ø4.0
Ø5.0
SPACE CRAFT
1.0
TORUS
4mil Aluminum/½mil Mylar
92.75
110.75
6.0
1.0
23.0
40.0
25.0
46.0 MAX PEGASUS P/L DIA.
9.5
PACKAGED HGT
1
2
3
4
5
6
4
1
2
1
2
2
QTY REQD
NEXT ASSY
USED ON
APPLICATION
DO NOT SCAL

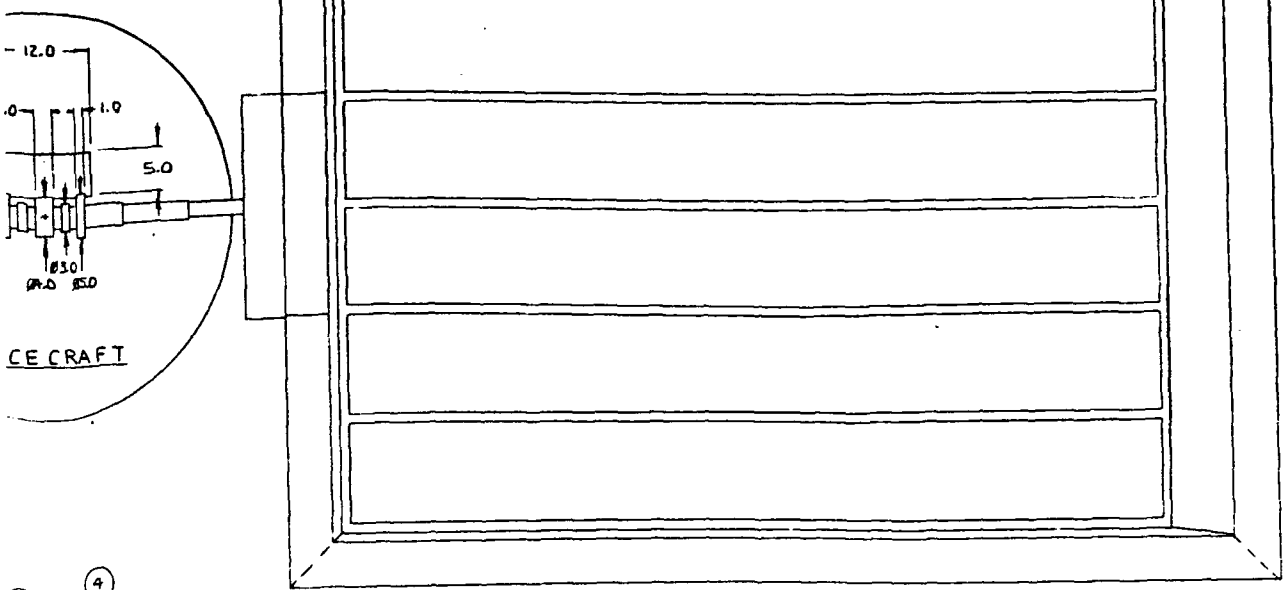

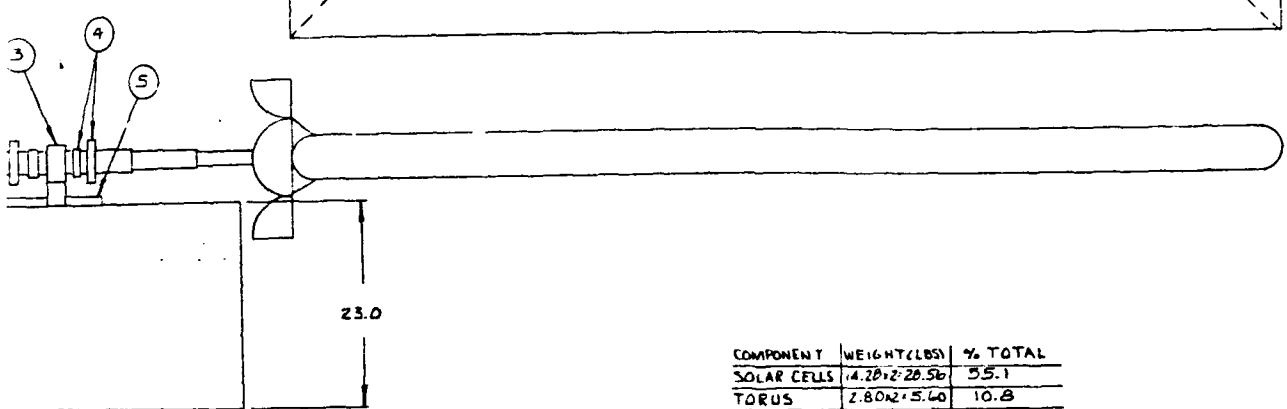

23.0

COMPONENT	WEIGHT (LBS)	% TOTAL
SOLAR CELLS	14.28×2=28.56	55.1
TORUS	2.80×2=5.60	10.8
VALVES, TANK	.87×2 = 1.74	3.4
ARM, CASE	7.20×2=14.40	27.8
MOTOR MOUNT	.50	1.0
COMPUTER, CABLE	1.00	1.9
TOTAL	51.80	

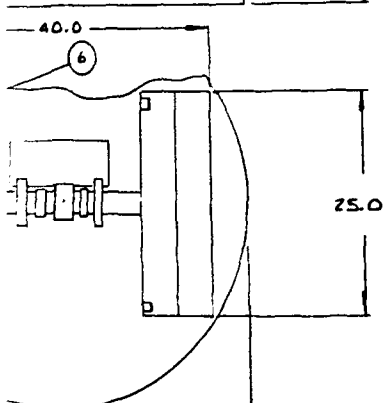

25.0

46.0 MAX PEGASUS P/L DIA.

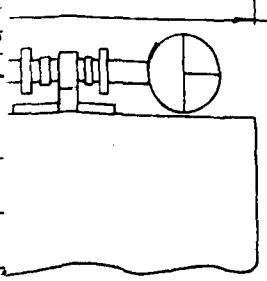

QTY REQD	FSCM NO	PART OR IDENTIFYING NO	NOMENCLATURE OR DESCRIPTION	MATERIAL SPECIFICATION	ITEM NO
1			PYRO CABLE CUTTERS TO OPEN CLAMSHELLS		6
1			MOTOR CONTROLLER COMPUTER		5
2			FLEX RIBBON POWER & SIGNAL TRANSFER RING		4
1			DRIVE MOTOR & RESOLVER		3
2			TELESCOPING ARM		2
2			CLAMSHELL LAUNCH CASE		1

PARTS LIST

UNLESS OTHERWISE SPECIFIED DIMENSIONS ARE IN INCHES
TOLERANCES ARE:
FRACTIONS DECIMALS ANGLES
± .XX ± °
.XXX ±

MATERIAL

FINISH

NEXT ASSY | USED ON

APPLICATION

DO NOT SCALE DRAWING

CONTRACT NO

APPROVALS	DATE
DRAWN TLIMMOND	7/17/90
CHECKED	
ISSUED	

L'GARDE, INC. 15181 WOODLAWN AVENUE TUSTIN, CALIFORNIA 92680

200w INFLATABLE SOLAR ARRAY,
MOLNIYA, RIGIDIZED ALUMINUM TORUS,
AMORPHOUS SILICON ARRAY

SIZE D | FSCM NO. 1F668 | DWG NO. 21008 | REV

SCALE 1:10 | SHEET 1 OF 1

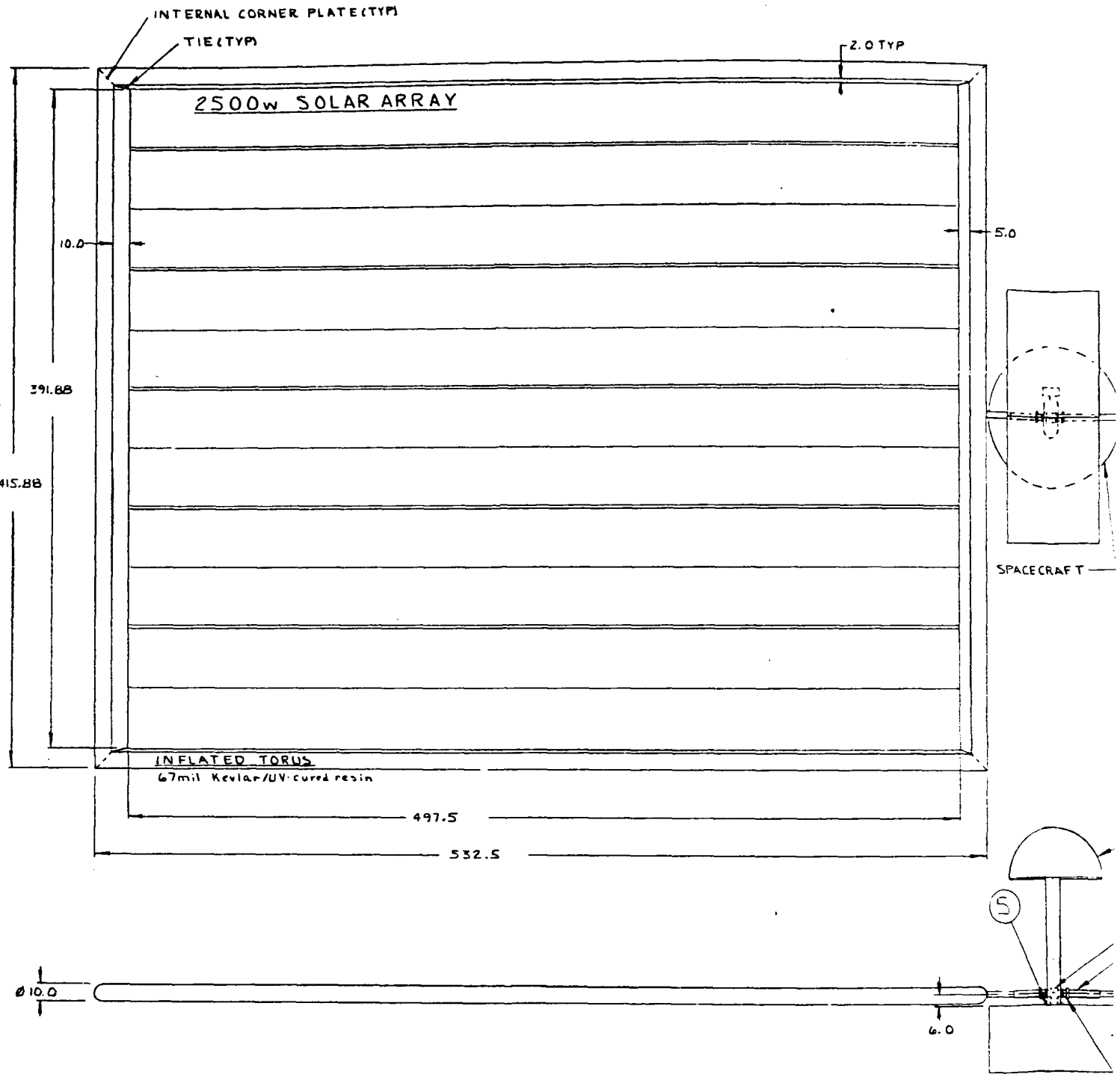

COMPONENT	WEIGHT (LBS)	% TOTAL
SOLAR CELLS	7015 x 2 = 140	73.43
TORUS	215 x 2 = 430	22.51
VALVES, TANK	17	0.89
ARM, CASE	58	3.04
MOTOR, MOUNT	0.6	0.03
COMPUTER/CABLES	2.0	0.10
TOTAL	1910.6	

T1-142

RRAY

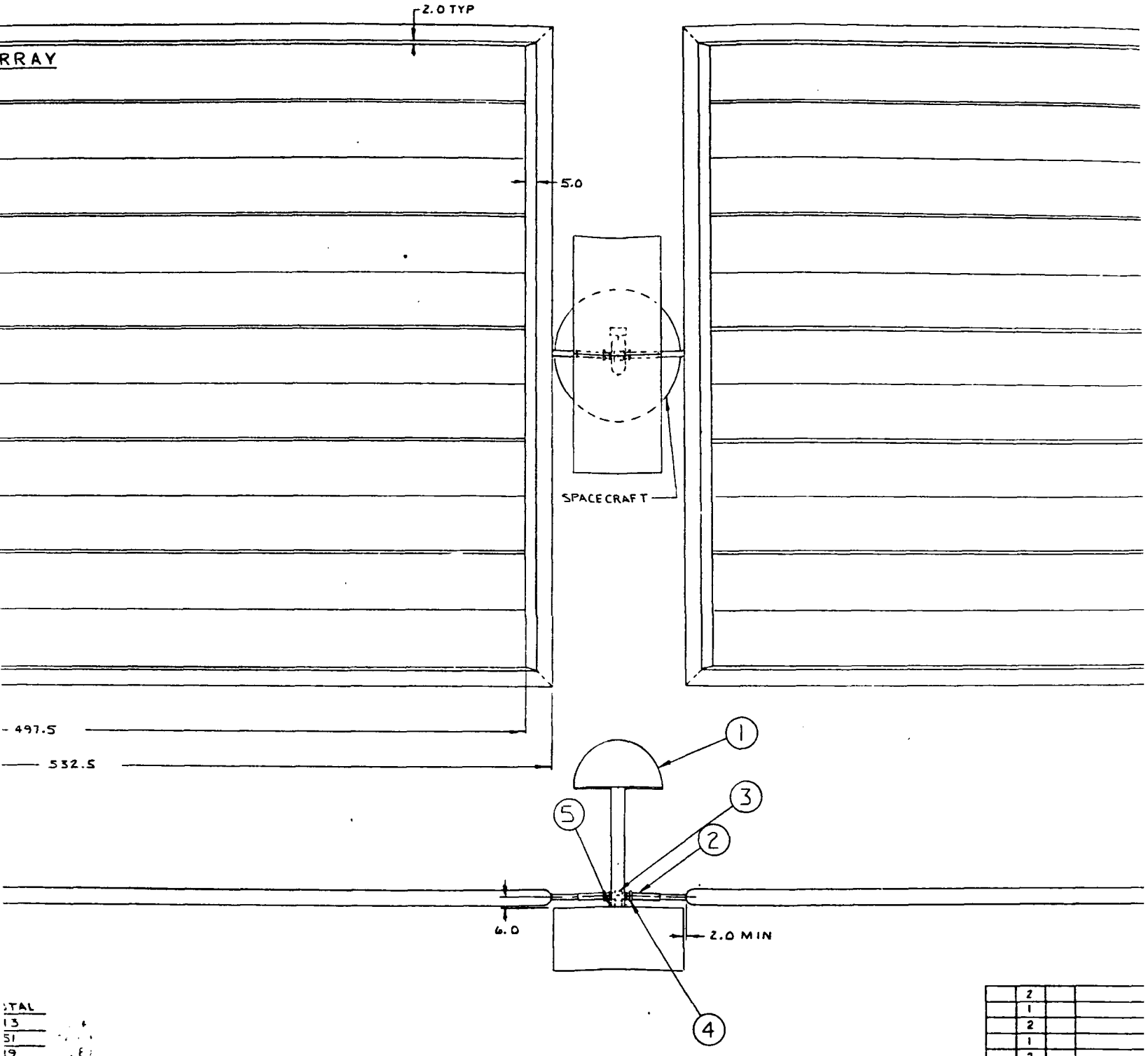

TAL
13
51
19
4
3
0

	QTY REQD	FSCM NO	PART OR IDENTIFYING
	2		
	1		
	2		
	1		
	2		
	2		

UNLESS OTHERWISE SPECIFIED
DIMENSIONS ARE IN INCHES
TOLERANCES ARE:
FRACTIONS ± DECIMALS .XX ± .XXX ± ANGLES ±

MATERIAL

FINISH

NEXT ASSY	USED ON
APPLICATION	DO NOT SCALE DRAWING

DWG. NO.	SH	REV.
21009	1	

REVISIONS

ZONE	REV.	DESCRIPTION	DATE	APPROVED

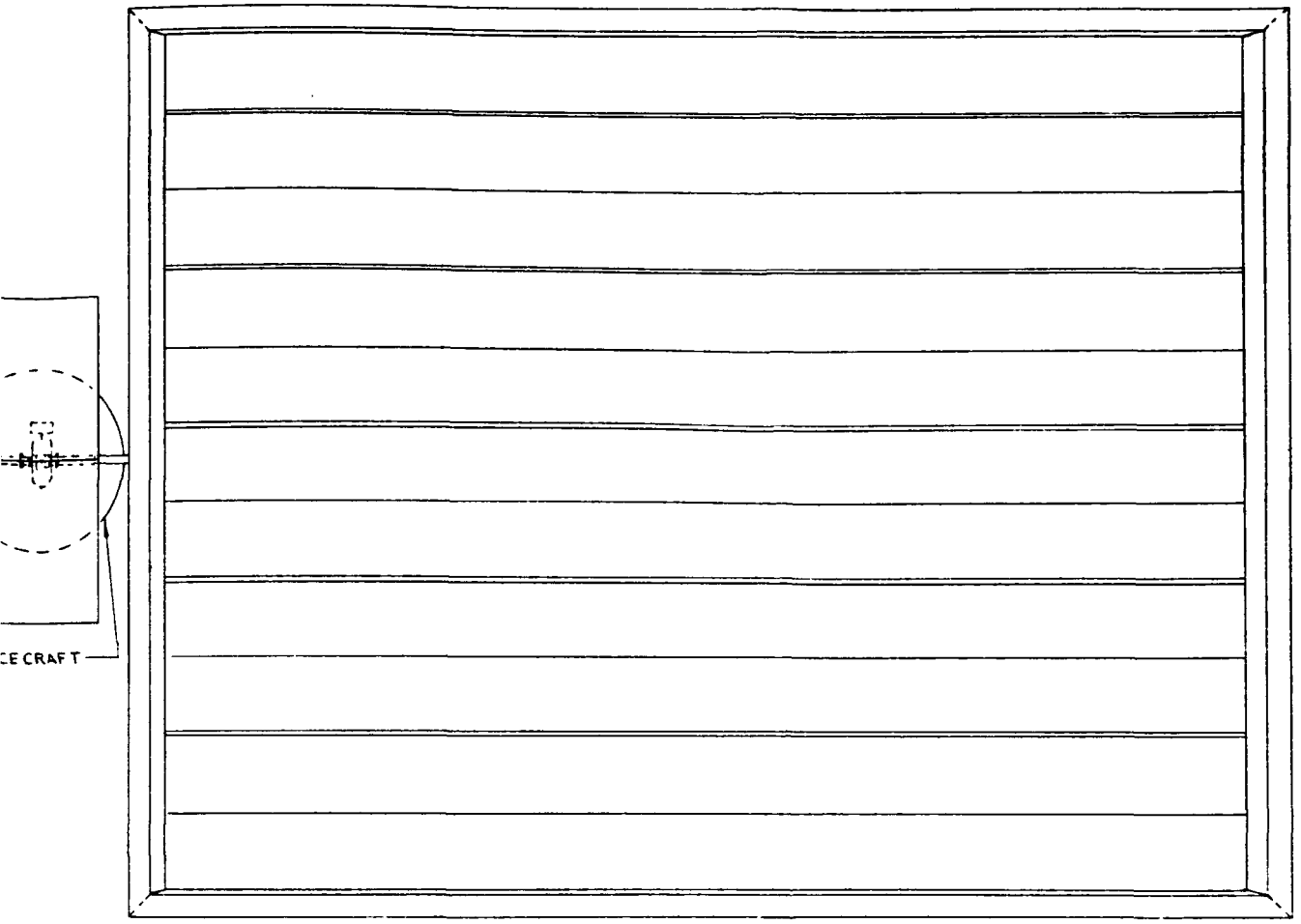

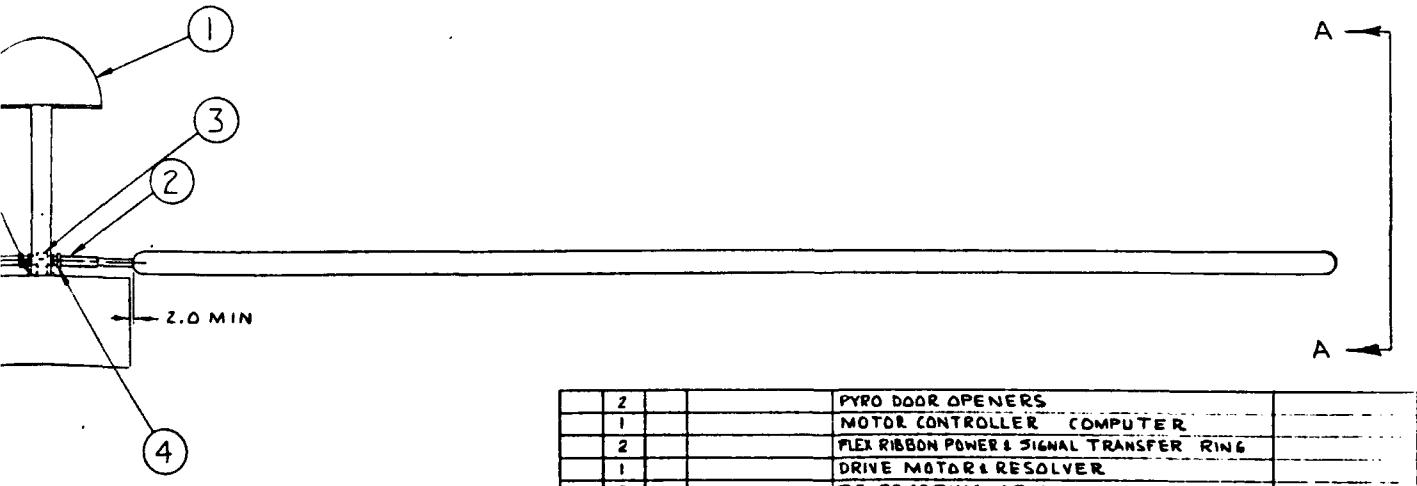

QTY REQD	FSCM NO.	PART OR IDENTIFYING NO.	NOMENCLATURE OR DESCRIPTION	MATERIAL SPECIFICATION	ITEM NO.
2			PYRO DOOR OPENERS		6
1			MOTOR CONTROLLER COMPUTER		5
2			FLEX RIBBON POWER & SIGNAL TRANSFER RING		4
1			DRIVE MOTOR & RESOLVER		3
2			TELESCOPING ARM		2
2			CLAMSHELL LAUNCH CASE		1

PARTS LIST

UNLESS OTHERWISE SPECIFIED DIMENSIONS ARE IN INCHES
TOLERANCES ARE:
FRACTIONS ± DECIMALS .XX ± .XXX ± ANGLES °

MATERIAL

FINISH

NEXT ASSY | USED ON

APPLICATION

DO NOT SCALE DRAWING

CONTRACT NO.

APPROVALS	DATE
DRAWN TUMMOND	8/2/90
CHECKED	
ISSUED	

L'GARDE, INC. 15181 WOODLAWN AVENUE, TUSTIN, CALIFORNIA 92680

5000w INFLATABLE SOLAR ARRAY, AMORPHOUS SILICON

SIZE	FSCM NO.	DWG. NO.	REV
D	1F668	21009	

SCALE 1:40 SHEET 1 OF 2

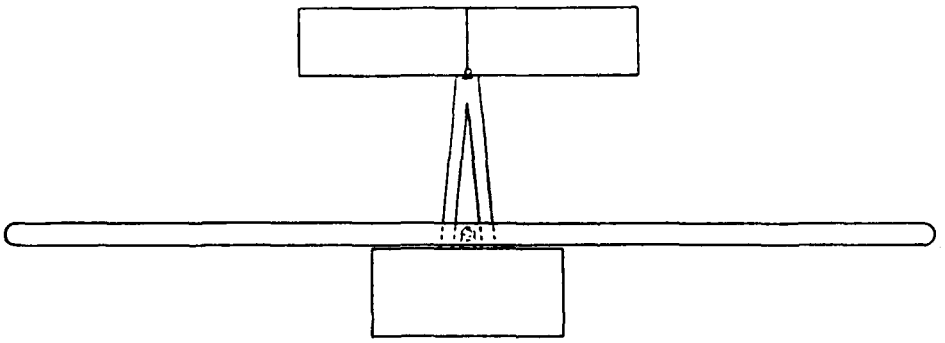

VIEW A-A

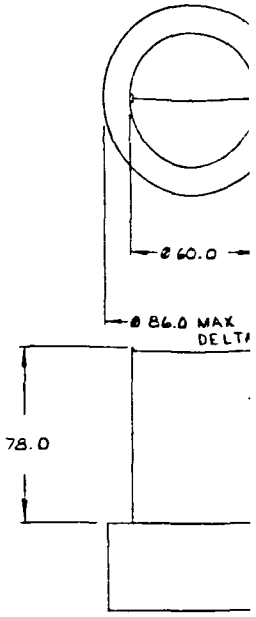

TI-983

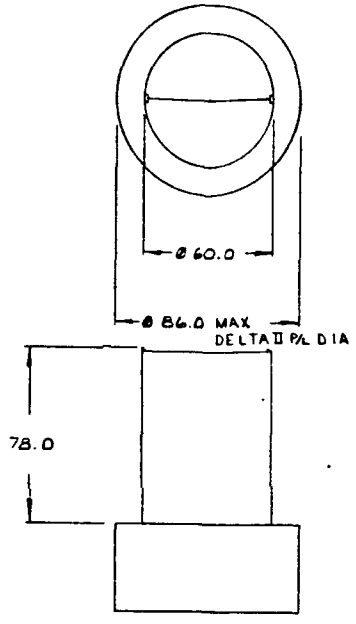

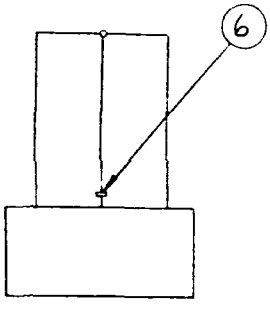

PACKAGED ARRAY

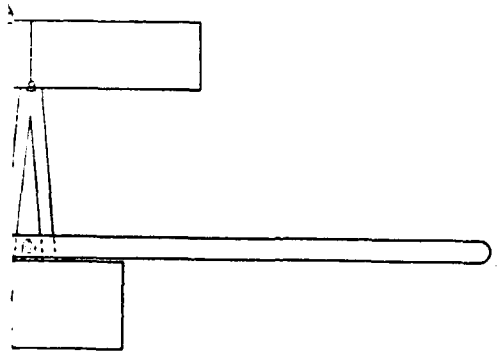

A-A

NEXT ASSY	USED ON
APPLICATION	

	QTY	REV	

UNLESS OTHERWISE SPECIFIED
DIMENSIONS ARE IN INCHES
TOLERANCES ARE:
FRACTIONS DECIMALS ANGLES
± .XX ±
.XXX ±

MATERIAL

FINISH

DO NOT SCALE DRAWIN

21009

REVISIONS				
ZONE	REV.	DESCRIPTION	DATE	APPROVED

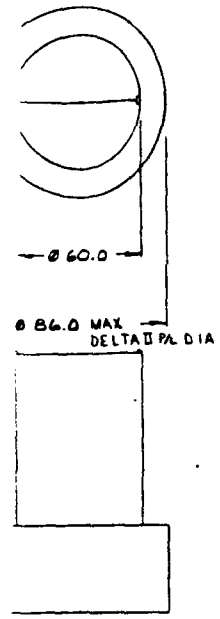

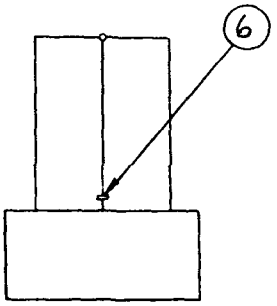

PACKAGED ARRAY

PARTS LIST

QTY REQD	FIGURE NO.	PART OR IDENTIFYING NO.	NOMENCLATURE OR DESCRIPTION	MATERIAL SPECIFICATION

UNLESS OTHERWISE SPECIFIED DIMENSIONS ARE IN INCHES
TOLERANCES ARE:
FRACTIONS ± | DECIMALS .XX ± .XXX ± | ANGLES °

MATERIAL

FINISH

NEXT ASSY | USED ON

APPLICATION

DO NOT SCALE DRAWING

CONTRACT NO.

APPROVALS	DATE
DRAWN TUMMOND	8/2/90
CHECKED	
ISSUED	

L'GARDE, INC. 16181 WOODLAWN AVENUE, TUSTIN, CALIFORNIA 92680

5000w INFLATABLE SOLAR ARRAY, AMORPHOUS SILICON

SIZE	FSCM NO.	DWG. NO.	REV
D	1F668	21009	

SCALE 1:40 SHEET 2 OF 2

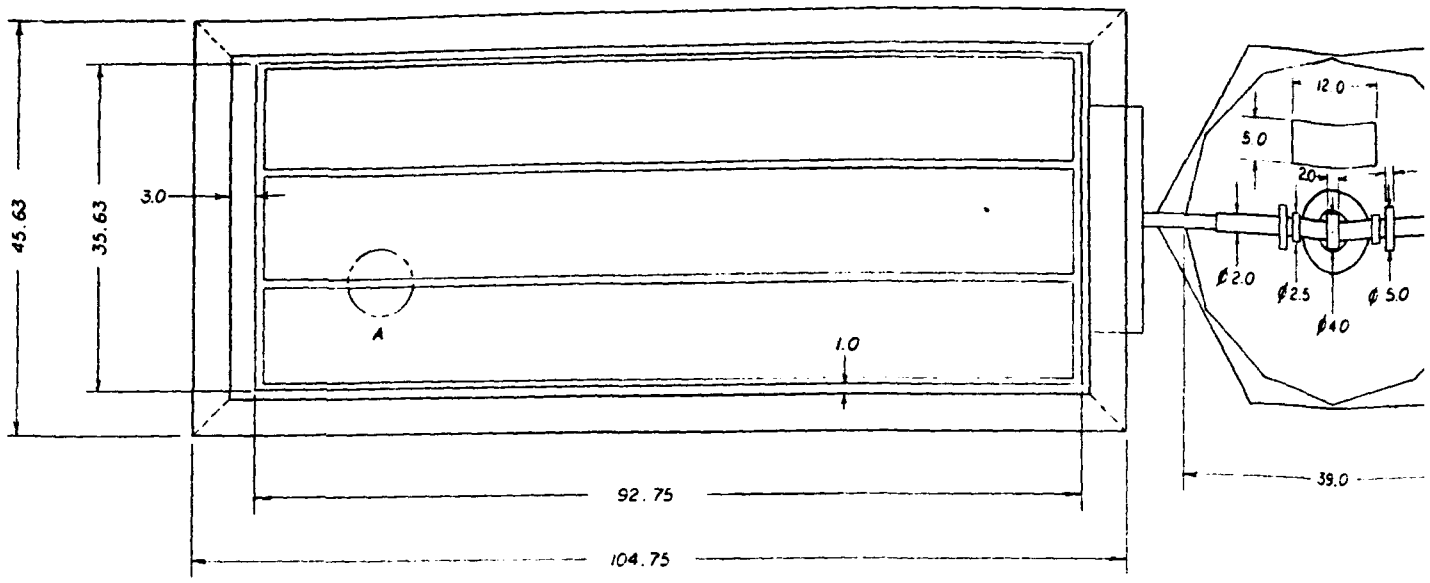

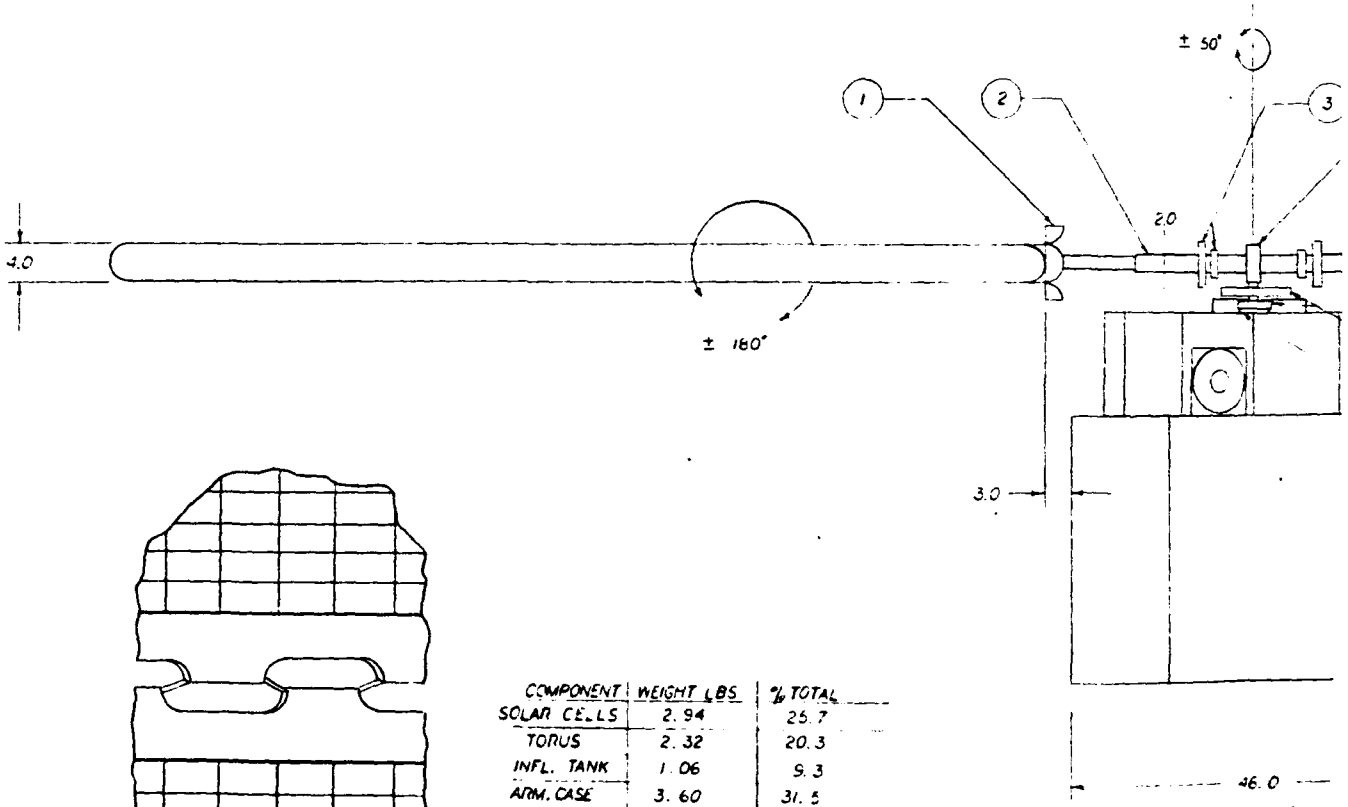

DETAIL A
NOT TO SCALE

COMPONENT	WEIGHT LBS	% TOTAL
SOLAR CELLS	2.94	25.7
TORUS	2.32	20.3
INFL. TANK	1.06	9.3
ARM. CASE	3.60	31.5
COMPUTER	1.00	8.8
MOTOR DRIVES	0.50	4.4
TOTAL	11.42	

T1-49

8 7 6 5

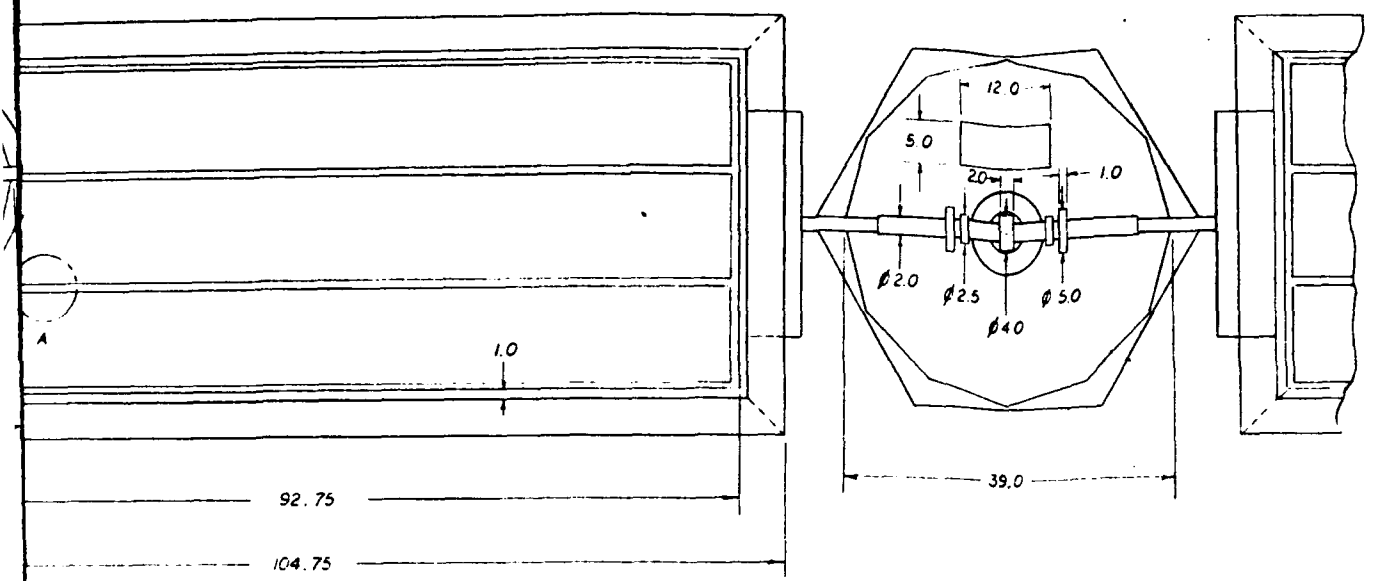

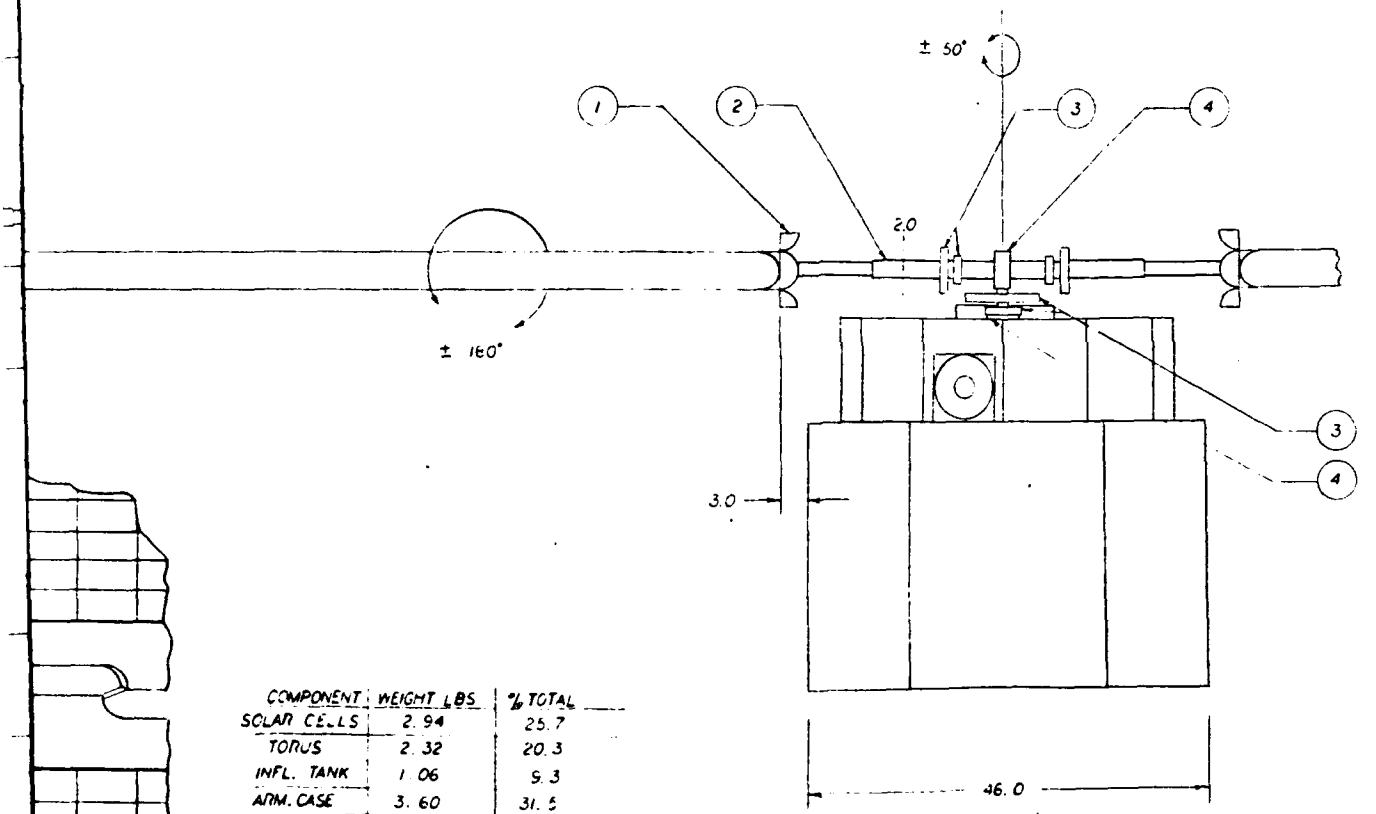

(MAX. PEGASUS P/L DIA.)

COMPONENT	WEIGHT LBS	% TOTAL
SOLAR CELLS	2.94	25.7
TORUS	2.32	20.3
INFL. TANK	1.06	9.3
ARM. CASE	3.60	31.5
COMPUTER	1.00	8.8
MOTOR DRIVES	0.50	4.4
TOTAL	11.42	

IL A
SCALE

21010

ZONE	REV	REVISIONS DESCRIPTION	DATE	APPROVED

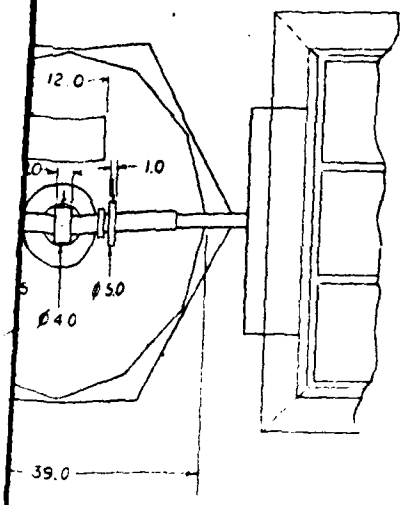

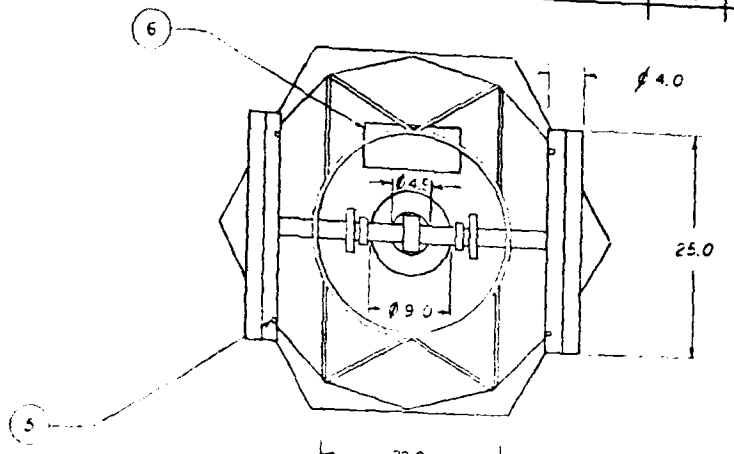

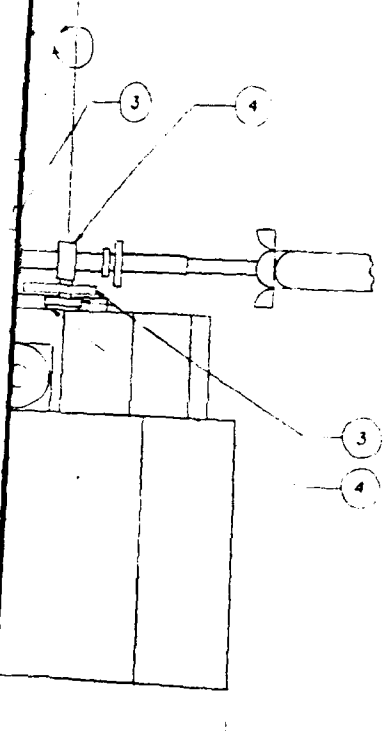

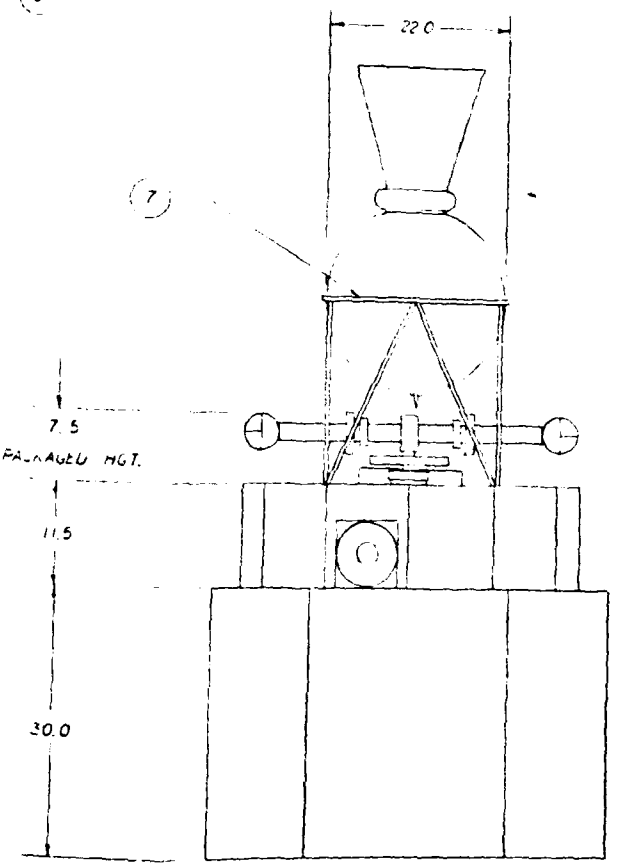

46.0
(ASUS P/L DIA.)

QTY REQD	ITEM NO.	PART OR IDENTIFYING NO.	NOMENCLATURE OR DESCRIPTION	MATERIAL SPECIFICATION	ITEM #
1			22" MARMEN RING		7
1			MOTOR CONTROL COMPUTER		6
4			PYRO CABLE CUTTER		5
2			MOTOR DRIVE & RESOLVER		4
6			FLEX RIBBON POWER TRANSFER RINGS		3
2			TELESCOPING ARM		2
2			CLAMSHELL LAUNCH CASE		1

PARTS LIST

UNLESS OTHERWISE SPECIFIED DIMENSIONS ARE IN INCHES
TOLERANCES ARE:
FRACTIONS ± DECIMALS ± ANGLES ±
.XX ±
.XXX ±

MATERIAL

FINISH

NEXT ASSY | USED ON

APPLICATION

DO NOT SCALE DRAWING

CONTRACT NO. 5542

APPROVALS	DATE
DRAWN D. BRANDT	E-15-90
CHECKED	
ISSUED	

L'GARDE, INC. 15181 WOODLAWN AVENUE TUSTIN, CALIFORNIA 92680

200 W INFLATABLE SOLAR ARRAY
G.E.D., RIGID ALUMINUM TORUS
(ON "STEP" SATELLITE), AMORPHOUS SILICON ARRAY

SIZE	FSCM NO.	DWG. NO.	REV
D	1F668	21010	

SCALE 1:10 SHEET 1 OF 1

4 3 2 1

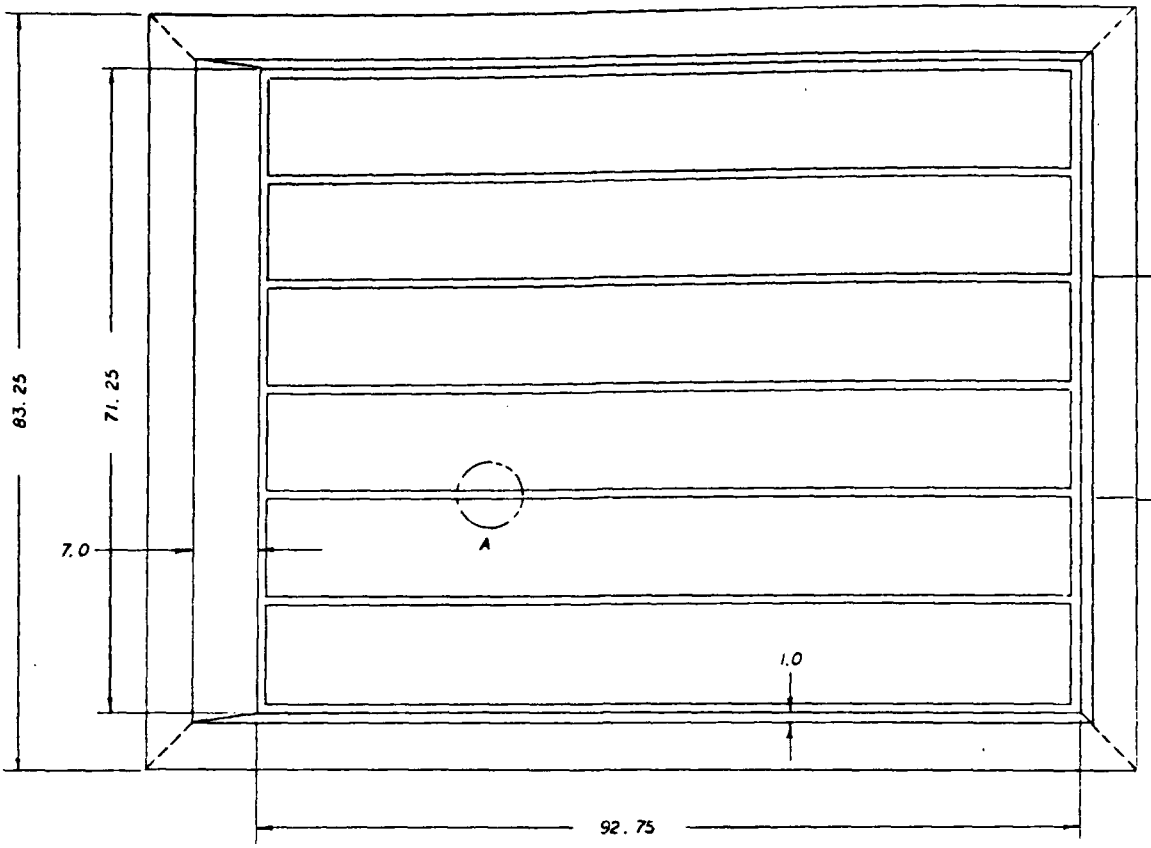

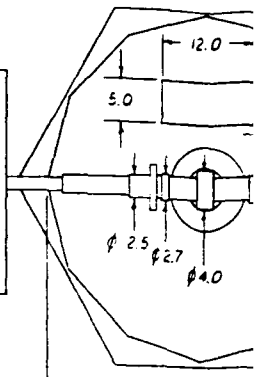

39.0

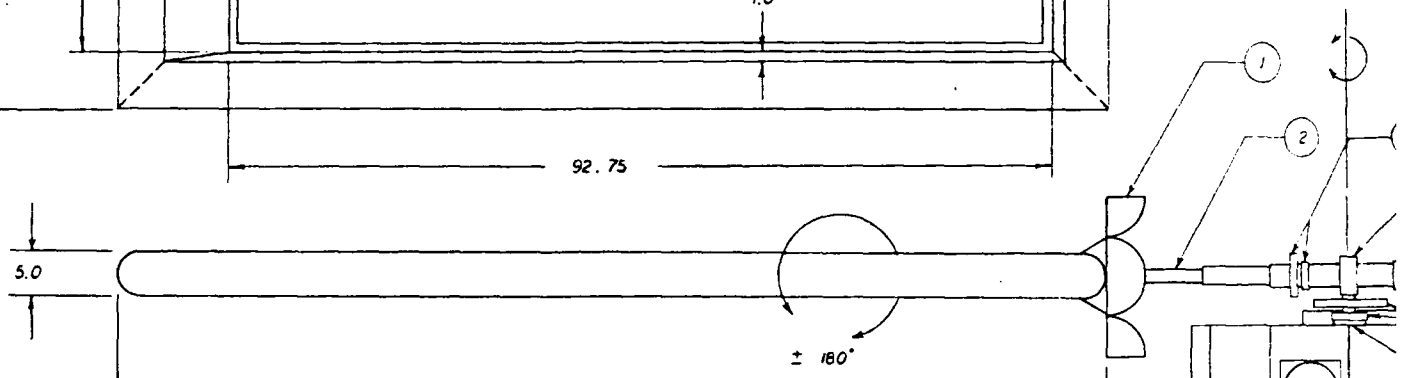

110.75

6.0

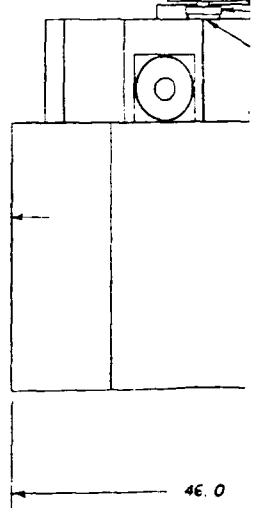

46.0

(MAX. PEGASUS P/L

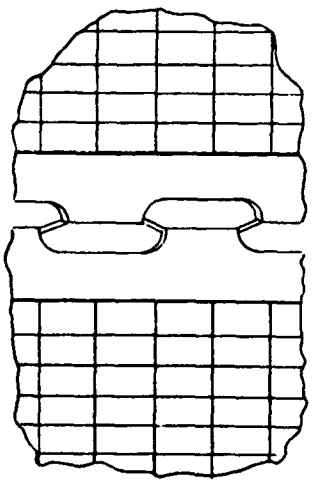

DETAIL A
NOT TO SCALE

COMPONENT	WEIGHT (LBS)	% TOTAL
SOLAR CELLS	28.56	54.6
TORUS	5.60	10.7
INFL. TANK	1.74	3.3
ARM, CASE	14.40	27.5
COMPUTER	1.00	1.9
MOTOR DRIVES	1.00	1.9
TOTAL	52.30	

T1-786

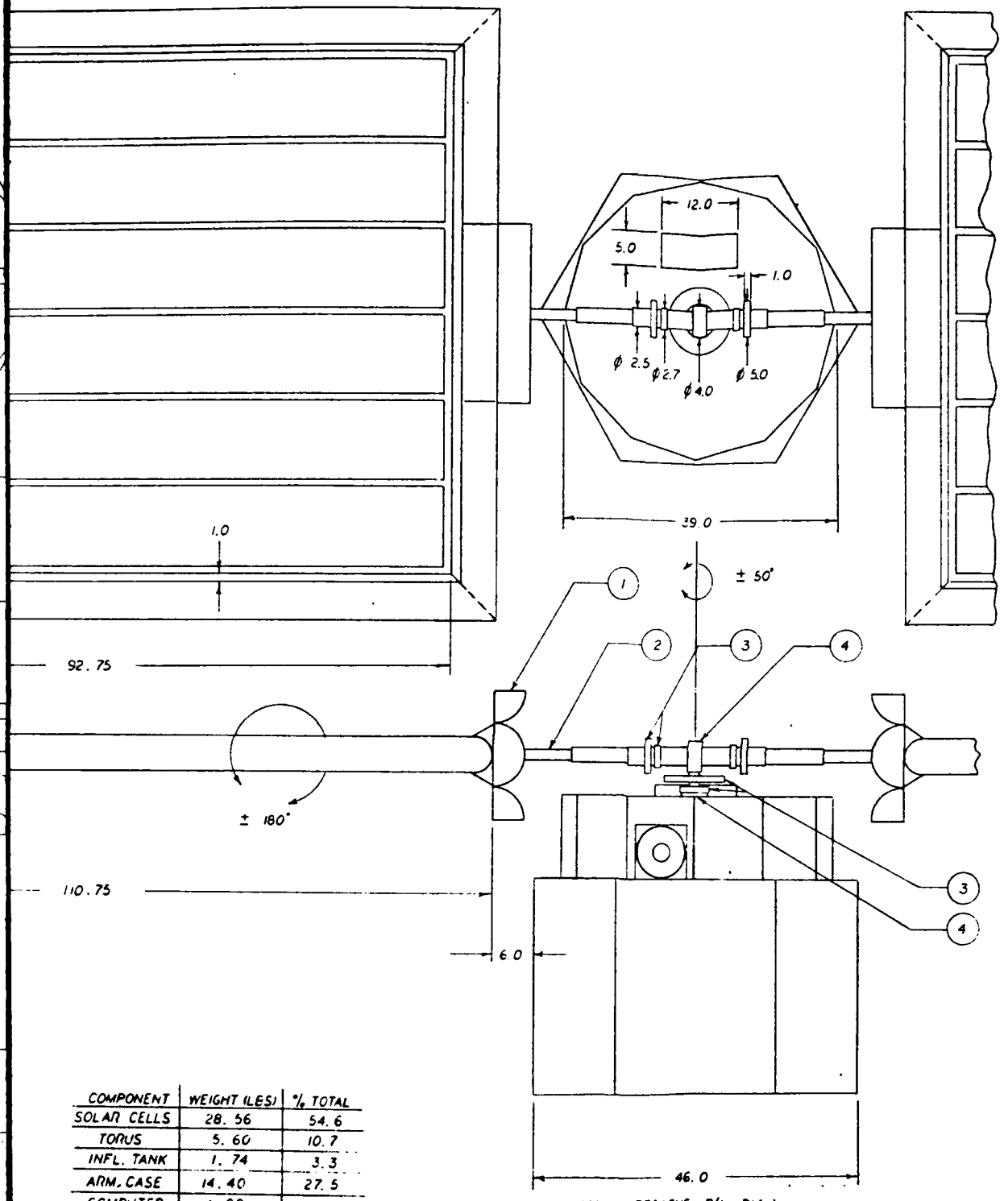

COMPONENT	WEIGHT (LBS)	% TOTAL
SOLAR CELLS	28.56	54.6
TORUS	5.60	10.7
INFL. TANK	1.74	3.3
ARM. CASE	14.40	27.5
COMPUTER	1.00	1.9
MOTOR DRIVES	1.00	1.9
TOTAL	52.30	

5

10.0
PACKAGED HG

11.5

30.0

1		
1		
4		
2		
6		
2		
2		

QTY | PROD NO | PART IDENTIFY

UNLESS OTHERWISE SPECIFIED DIMENSIONS ARE IN INCHES
TOLERANCES ARE:
FRACTIONS ± | DECIMALS .XX ± .XXX ± | ANGLES ±

MATERIAL

FINISH

NEXT ASSY | USED ON

APPLICATION

DO NOT SCALE DRAWING

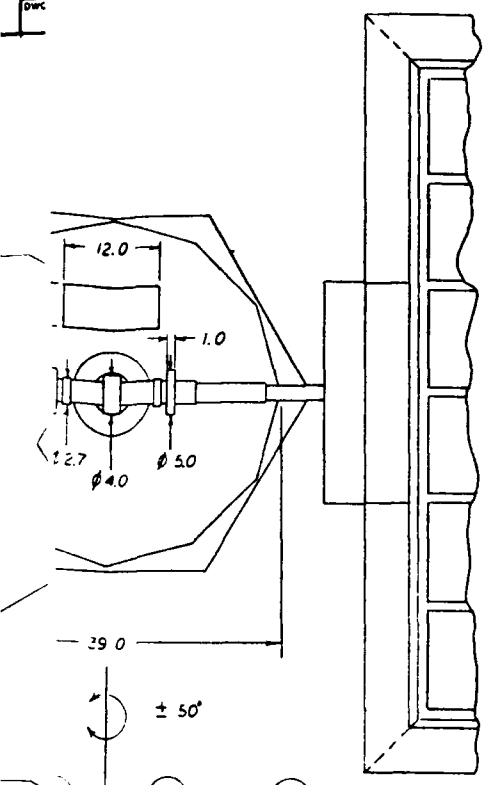

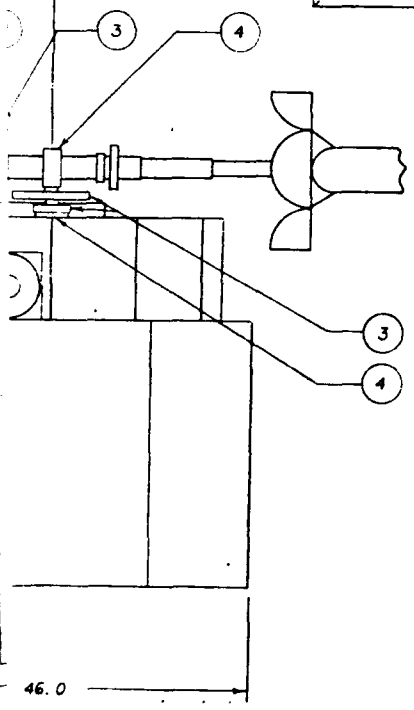

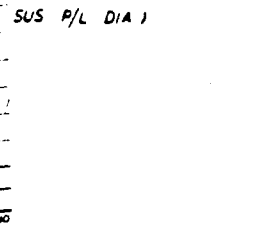

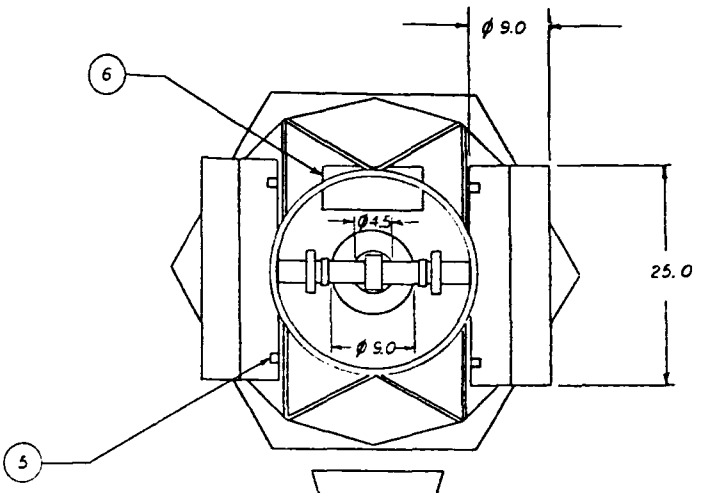

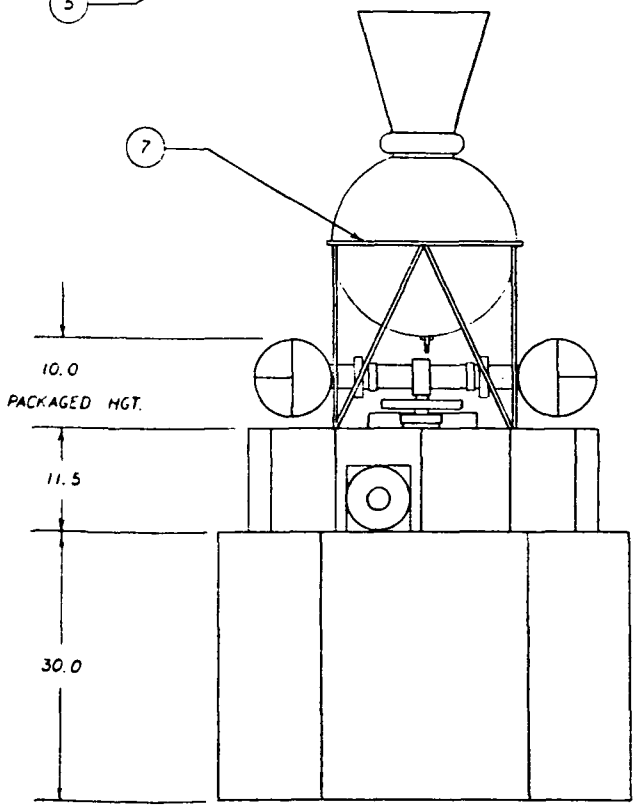

1			22" MARMEN RING		7
1			MOTOR CONTROL COMPUTER		6
4			PYRO CABLE CUTTER		5
2			MOTOR DRIVE & RESOLVER		4
6			FLEX RIBBON POWER TRANSFER RINGS		3
2			TELESCOPING ARM		2
2			CLAMSHELL LAUNCH CASE		1
QTY REQD	FIGURE NO.	PART OR IDENTIFYING NO.	NOMENCLATURE OR DESCRIPTION	MATERIAL SPECIFICATION	ITEM NO.

PARTS LIST

UNLESS OTHERWISE SPECIFIED DIMENSIONS ARE IN INCHES
TOLERANCES ARE:
FRACTIONS ± DECIMALS .XX ± .XXX ± ANGLES °

MATERIAL

FINISH

NEXT ASSY | USED ON

APPLICATION

DO NOT SCALE DRAWING

CONTRACT NO. 5542

APPROVALS	DATE
DRAWN D. BRANDT	8-16-90
CHECKED	
ISSUED	

L'GARDE, INC. 15181 WOODLAWN AVENUE TUSTIN, CALIFORNIA 92680

200 W INFLATABLE SOLAR ARRAY
MOLNIYA, RIGID ALUMINUM TORUS
(ON "STEP" SATELLITE), AMORPHOUS SILICON ARRAY

SIZE D | FSCM NO. 1F668 | DWG. NO. 21011 | REV.

SCALE 1:10 | SHEET 1 OF 1

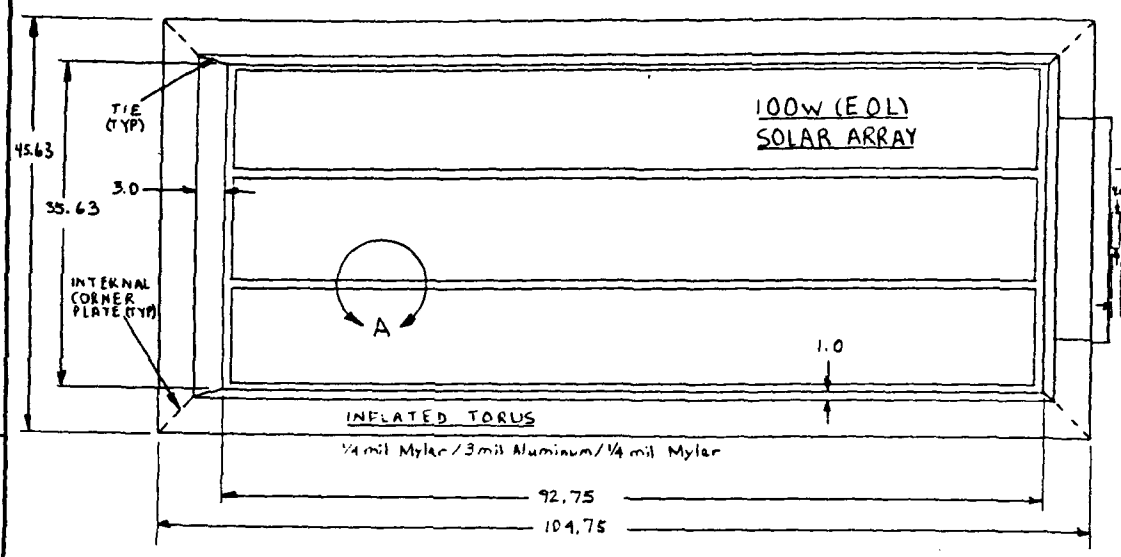

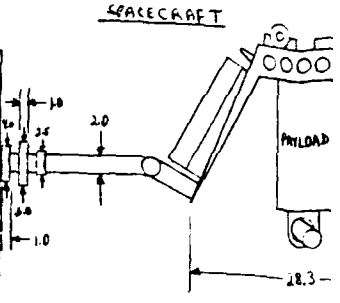

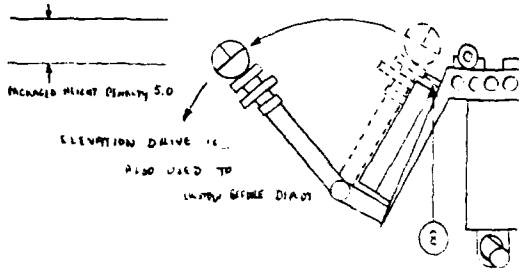

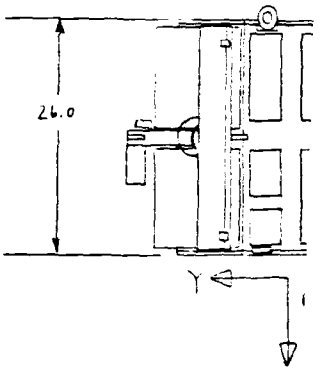

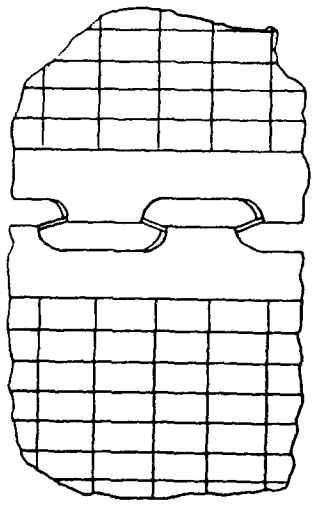

VIEW A

COMPONENT	WEIGHT (LBS)	% TOTAL
SOLAR CELLS	1.47 X 2 = 2.94	23.7
TORUS	1.16 X 2 = 2.32	18.7
VALVES, TANK	.53 X 2 = 1.06	8.5
ARM, CASE	1.8 X 2 = 3.60	29.0
MOTORS, MOUNT	.75 X 2 = 1.5	12.1
COMPUTER, CABLES	1.00	8.0
TOTAL	12.42	

11-796

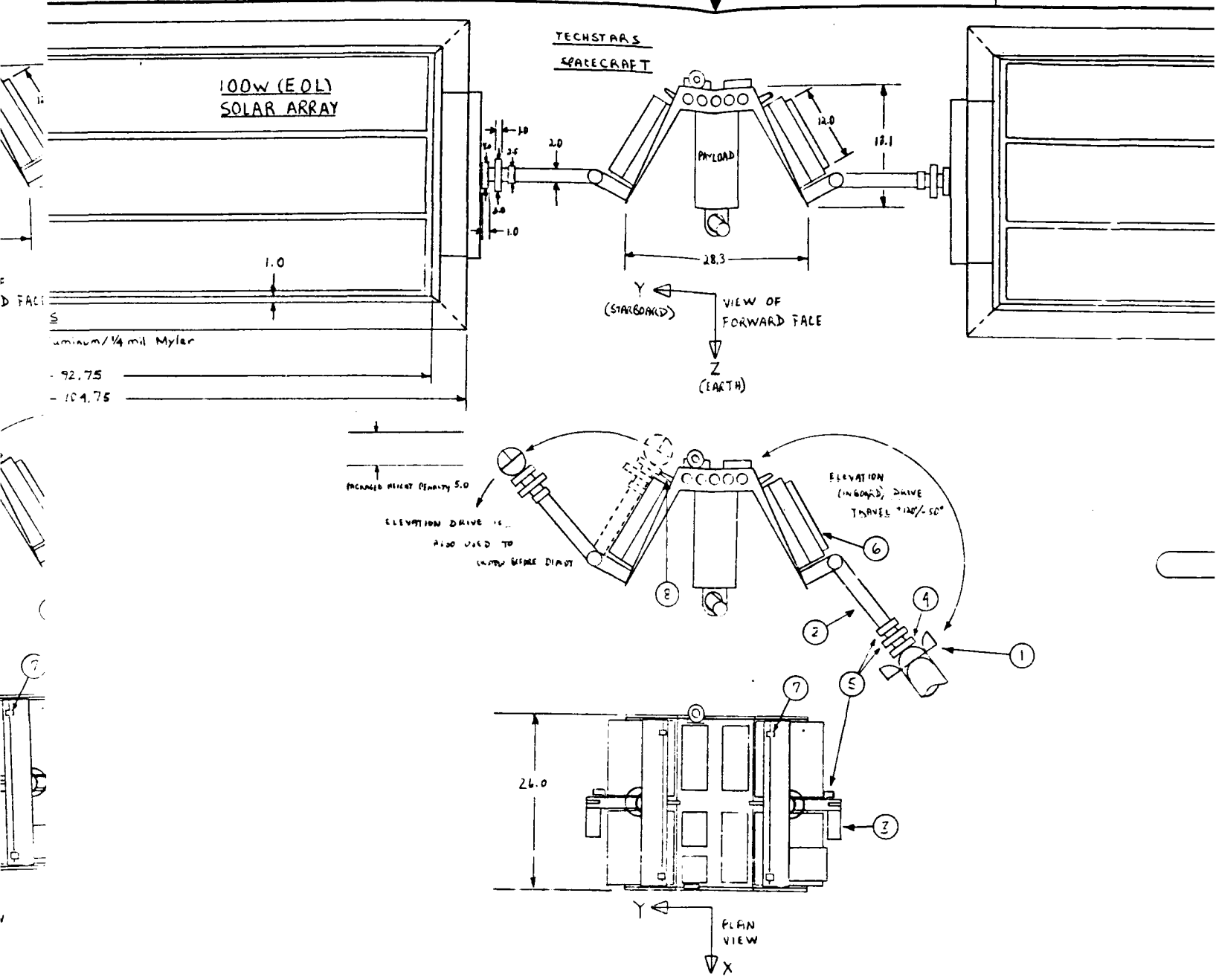

COMPONENT	WEIGHT (LBS)	% TOTAL
SOLAR CELLS	1.47 X 2 = 2.94	23.7
TORUS	1.16 X 2 = 2.32	18.7
VALVES, TANK	.53 X 2 = 1.06	8.5
ARM, CASE	1.8 X 2 = 3.60	29.0
MOTORS, MOUNT	.75 X 2 = 1.5	12.1
COMPUTER, CABLES	1.00	8.0
TOTAL	12.42	

	QTY REQD	PIECE NO
2		
4		
1		
6		
2		
2		
2		
2		

UNLESS OTHERWISE SPECIFI
DIMENSIONS ARE IN INCHES
TOLERANCES ARE:
FRACTIONS DECIMALS A
± .XX ±
.XXX ±

MATERIAL

FINISH

NEXT ASSY	USED ON
APPLICATION	DO NOT SCALE DRA

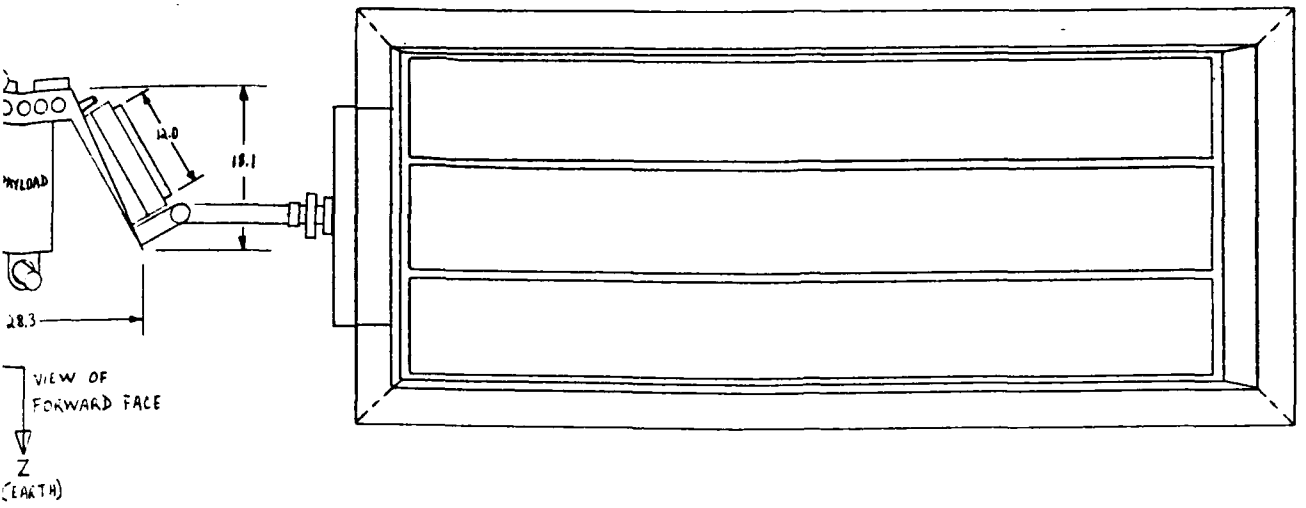

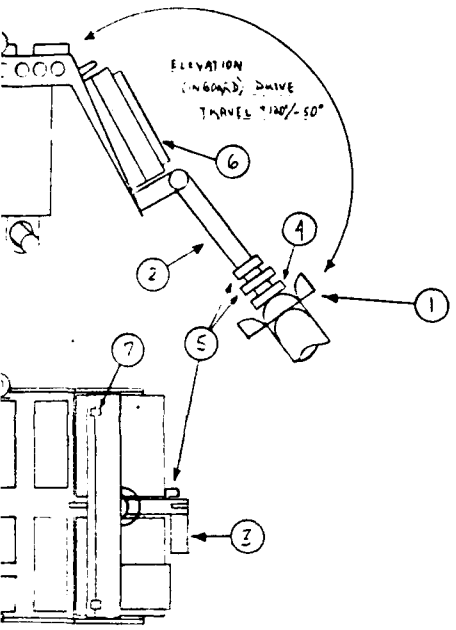

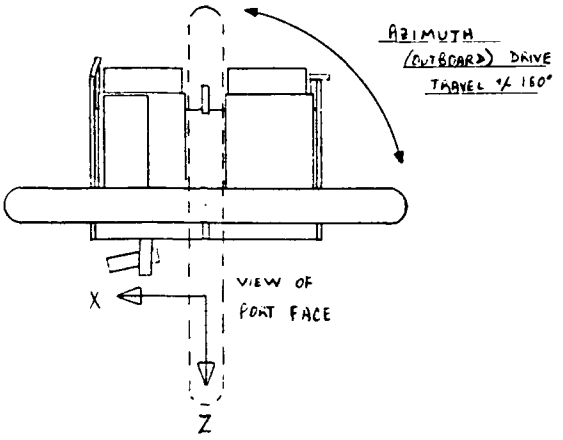

QTY REQD	FSCM NO	PART OR IDENTIFYING NO	NOMENCLATURE OR DESCRIPTION	MATERIAL SPECIFICATION	
2			PYRO PIN-PULLER TO RELEASE FROM SPACECRAFT		8
4			PYRO CABLE CUTTERS TO OPEN CLAMSHELLS		7
1			MOTOR CONTROLLERS + COMPUTER		6
8			FLEX RIBBON POWER + SIGNAL TRANSFER RINGS		5
2			AZIMUTH DRIVE MOTOR + RESOLVER		4
2			ELEVATION DRIVE MOTOR + RESOLVER		3
2			DRIVE ARM		2
2			CLAMSHELL LAUNCH CASE		1

PARTS LIST

UNLESS OTHERWISE SPECIFIED DIMENSIONS ARE IN INCHES
TOLERANCES ARE:
FRACTIONS ± DECIMALS .XX ± .XXX ± ANGLES ±

MATERIAL

FINISH

DO NOT SCALE DRAWING

CONTRACT NO.

APPROVALS	DATE
DRAWN DEREES	8/14/90
CHECKED	
ISSUED	

L'GARDE, INC. 15181 WOODLAWN AVENUE, TUSTIN, CALIFORNIA 92680

200 W SOLAR ARRAY - TITUS, ALUMINUM RIGID, GEO, TECHSTARS SATELLITE, AMORPHOUS SILICON ARRAY

SIZE D | FSCM NO. 1F669 | DWG. NO. 21012 | REV

SCALE 1:10 | SHEET 1 OF 1

NEXT ASSY | USED ON

APPLICATION

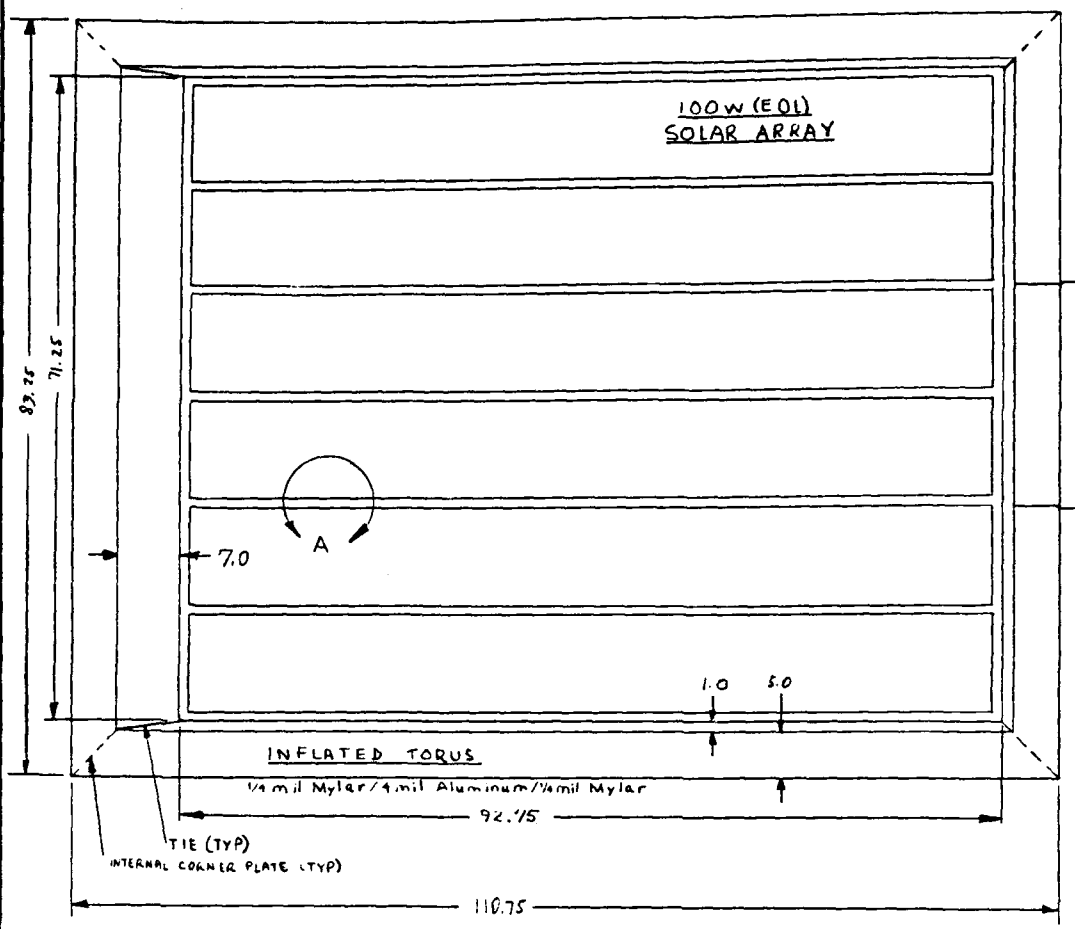

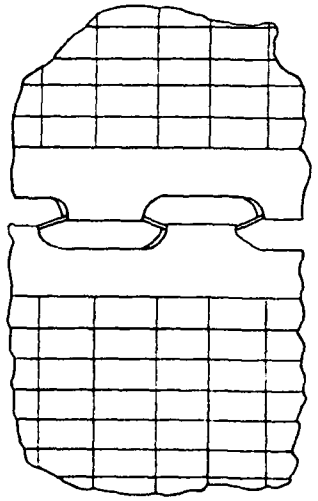

VIEW A

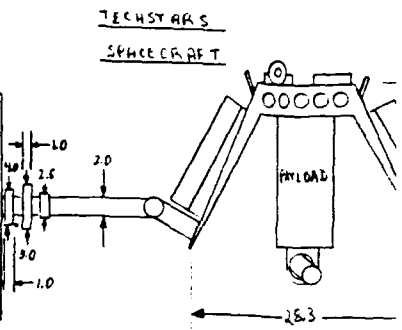

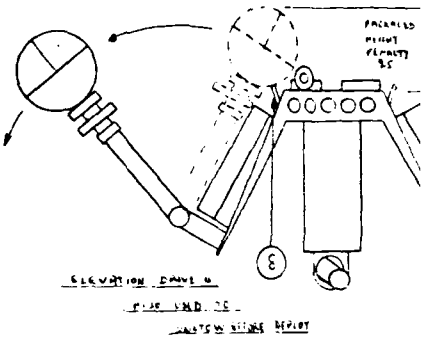

ELEVATION

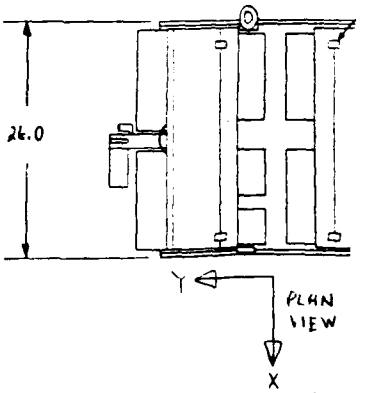

COMPONENT	WEIGHT (LBS)	% TOTAL
SOLAR CELLS	19.28 X 2 = 38.56	53.1
TORUS	2.80 X 2 = 5.6	10.4
VALVES, TANK	.87 X 2 = 1.74	3.2
ARM, CASE	7.2 X 2 = 14.4	26.8
MOTORS, MOUNT	1.25 X 2 = 2.5	4.6
COMPUTER, CABLES	1.00	1.9
TOTAL	53.80	

TI-197

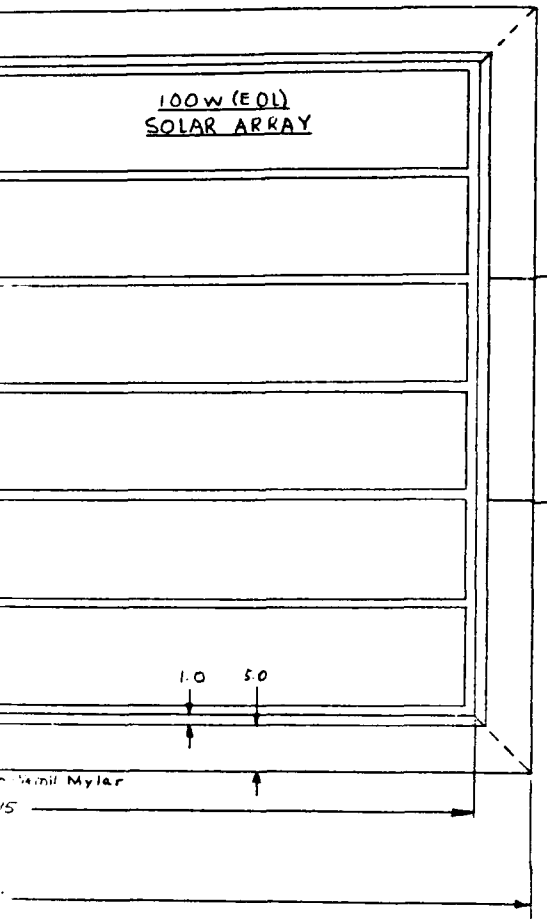

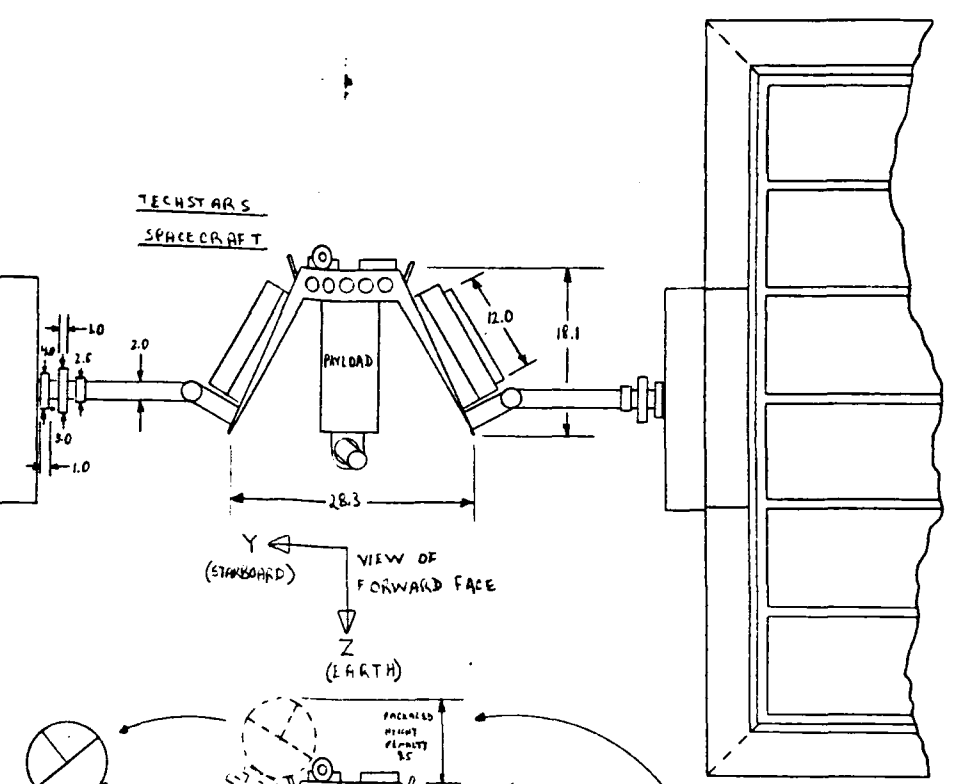

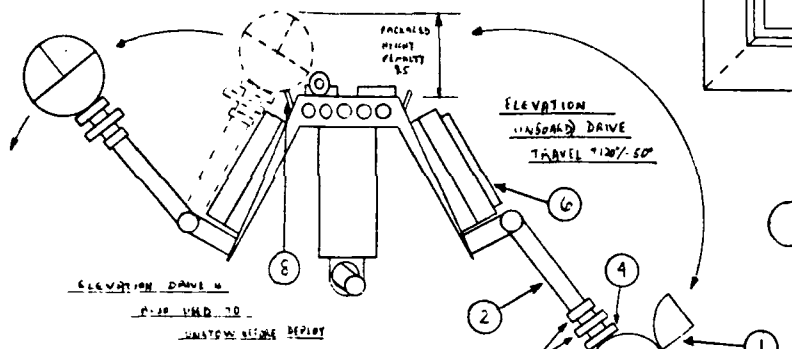

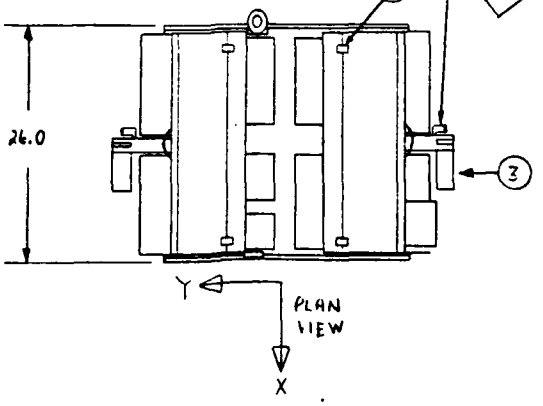

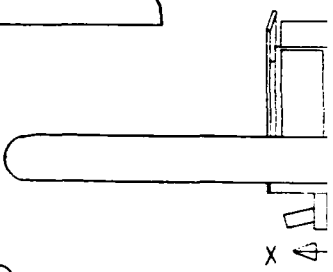

COMPONENT	WEIGHT (LBS)	% TOTAL
SOLAR CELLS	14.28 X 2 = 28.56	53.1
TORUS	2.80 X 2 = 5.6	10.4
VALVES, TANK	.87 X 2 = 1.74	3.2
ARM, CASE	7.2 X 2 = 14.4	26.8
MTORS, MOUNT	1.25 X 2 = 2.5	4.6
COMPUTER, CABLES	1.00	1.9
TOTAL	53.80	

	2		
	4		
	1		
	8		
	2		
	2		
	2		
	2		
	QTY REQD	PICK NO	PART OR IDENTIFYING

UNLESS OTHERWISE SPECIFIED
DIMENSIONS ARE IN INCHES
TOLERANCES ARE:
FRACTIONS DECIMALS ANGLES
± .XX ± ±
.XXX ±

MATERIAL

FINISH

NEXT ASSY	USED ON
APPLICATION	

DO NOT SCALE DRAWING

6 5 4 3

REVISIONS				
ZONE	REV	DESCRIPTION	DATE	APPROVED

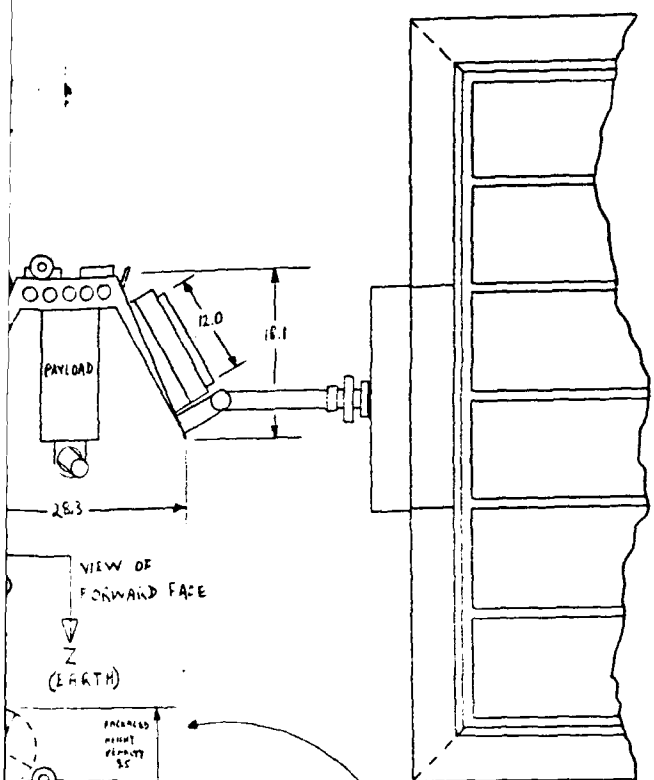

VIEW OF FORWARD FACE

Z (EARTH)

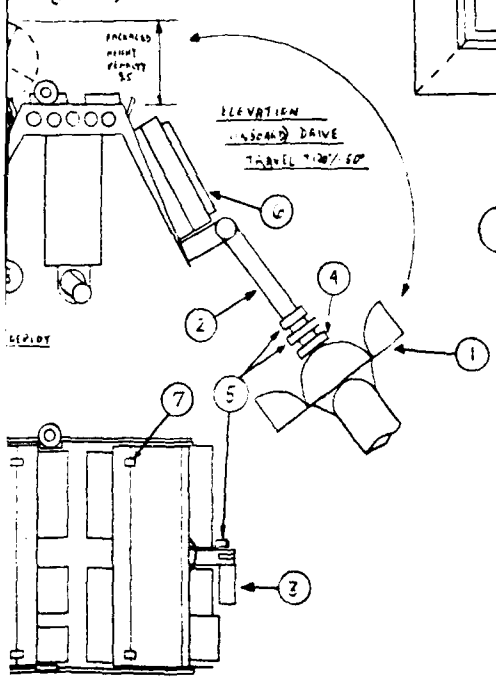

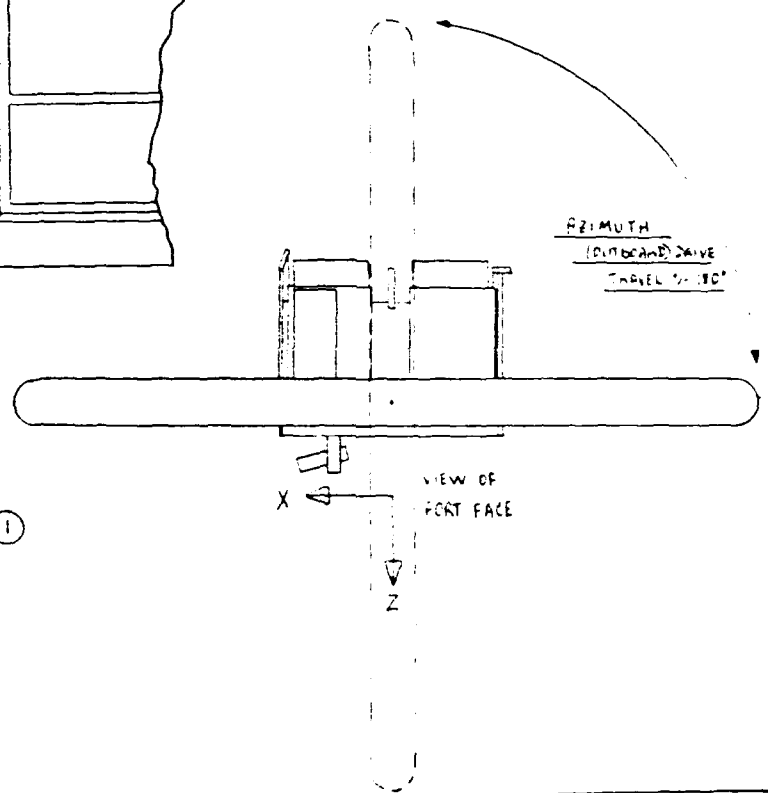

VIEW OF PORT FACE

PLAN VIEW

X

QTY REQD	FSCM NO	PART OR IDENTIFYING NO	NOMENCLATURE OR DESCRIPTION	MATERIAL DESIGNATION	
2			PYRO PIN PULLER TO RELEASE FROM SPACECRAFT		8
4			PYRO CABLE CUTTERS TO OPEN CLAMSHELLS		7
1			MOTOR CONTROLLERS + COMPUTER		6
8			FLEX FIBER POWER + SIGNAL TRANSFER RINGS		5
2			AZIMUTH DRIVE MOTOR + RESOLVER		4
2			ELEVATION DRIVE MOTOR + RESOLVER		3
2			DRIVE ARM		2
2			CLAMSHELL LAUNCH CASE		1

PARTS LIST

UNLESS OTHERWISE SPECIFIED DIMENSIONS ARE IN INCHES. TOLERANCES ARE: FRACTIONS ± , DECIMALS .XX ± , .XXX ± , ANGLES ±

MATERIAL

FINISH

NEXT ASSY | USED ON

APPLICATION

DO NOT SCALE DRAWING

CONTRACT NO

APPROVALS	DATE
DRAWN DENDES	5/16/90
CHECKED	
ISSUED	

L'GARDE, INC. 15181 WOODLAWN AVENUE TUSTIN, CALIFORNIA 92680

600W SOLAR ARRAY - TDRSS, ALUMINUM RIGID, GEO, TECHSTAR II SATELLITE, AMORPHOUS SILICON ARRAY

SIZE D | FSCM NO. 1F668 | SHPL. NO. 21013 | REV

SCALE 1:6 | SHEET 1 OF 1

D

C

B

A

4 3 2 1

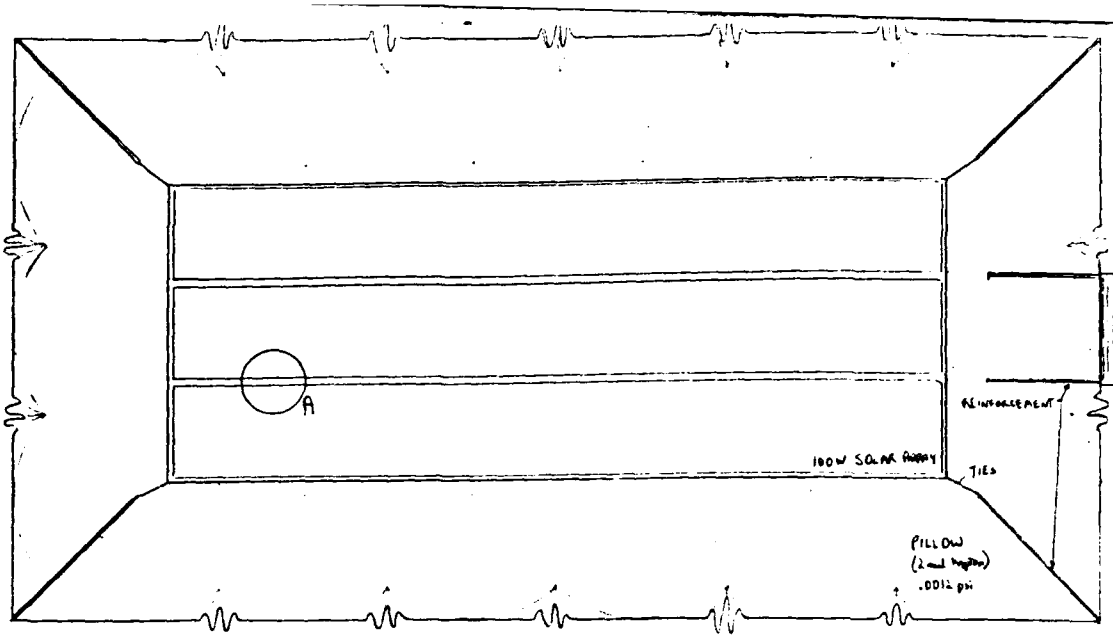

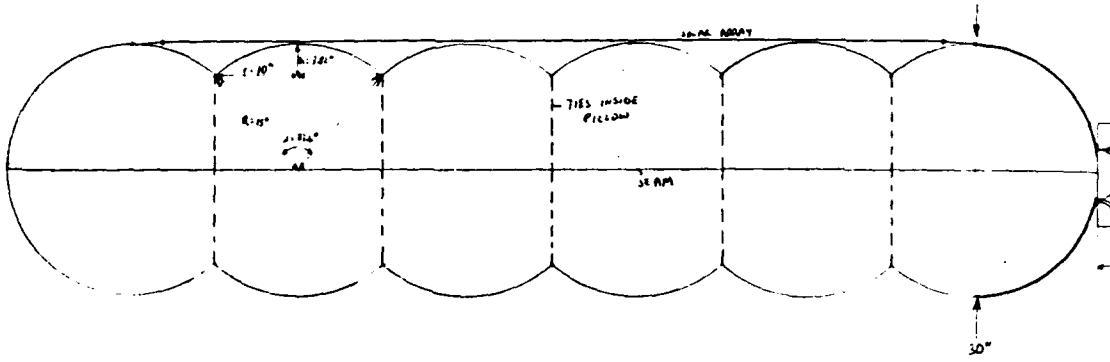

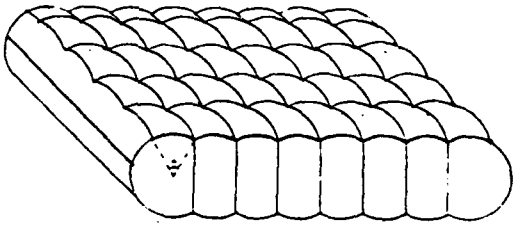

PILLOW CONCEPT

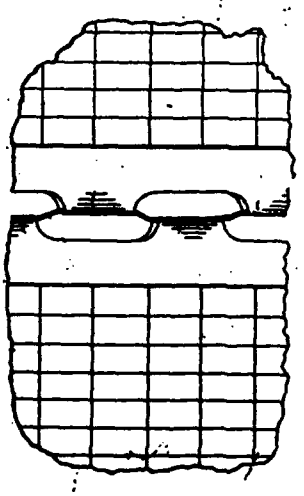

DETAIL "A"

TI-788

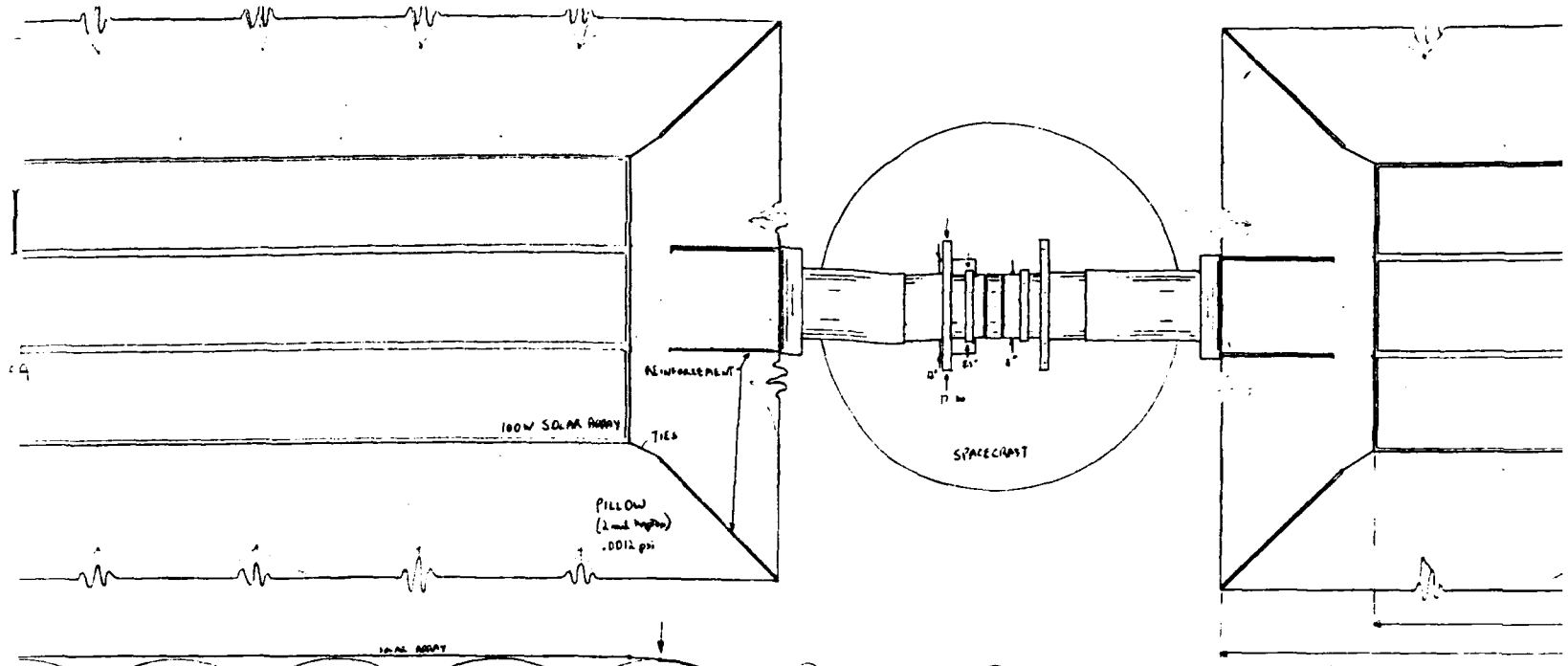

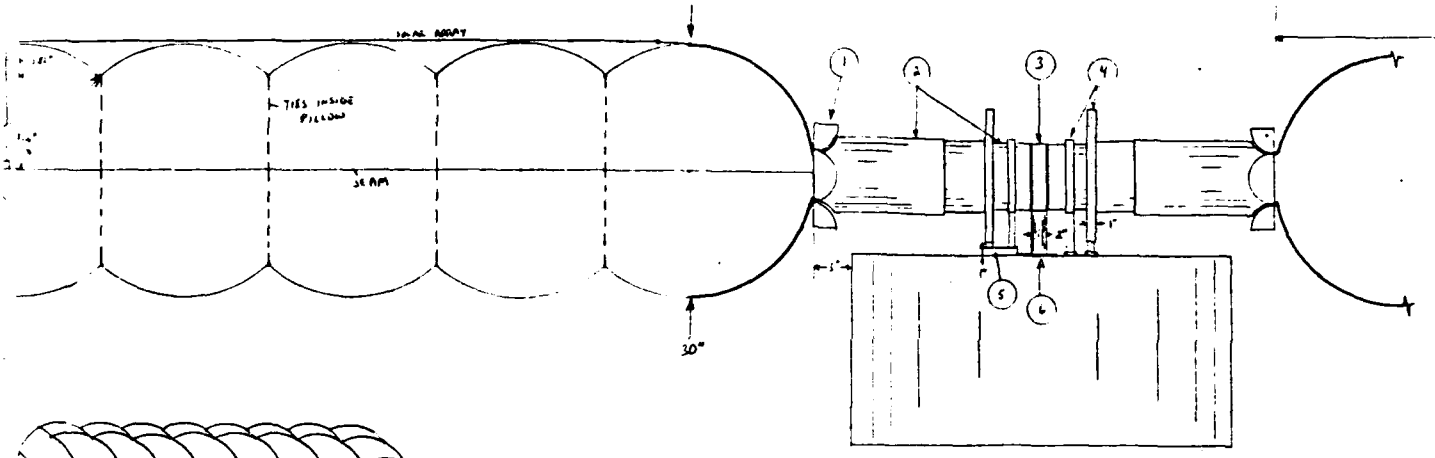

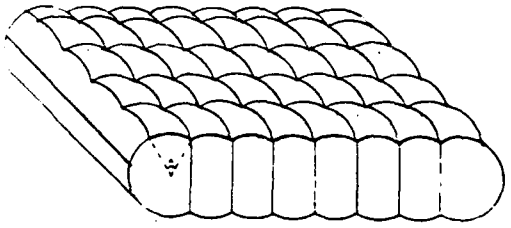

PILLOW CONCEPT

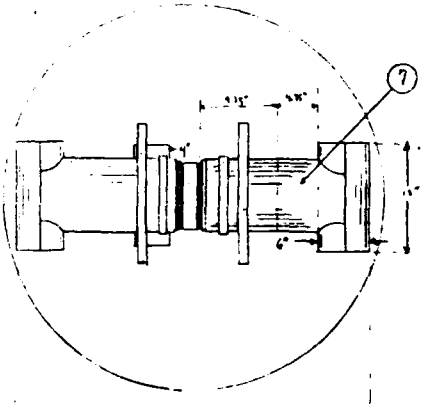

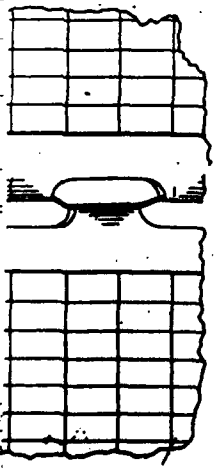

DETAIL "A"

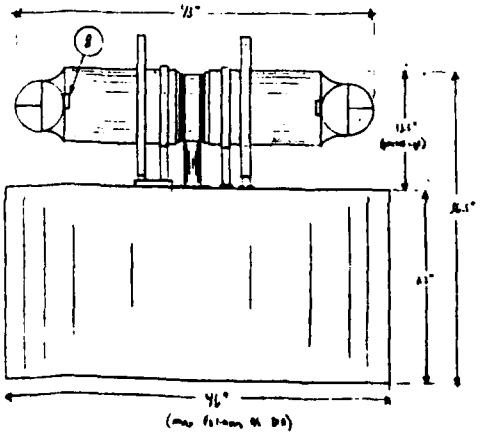

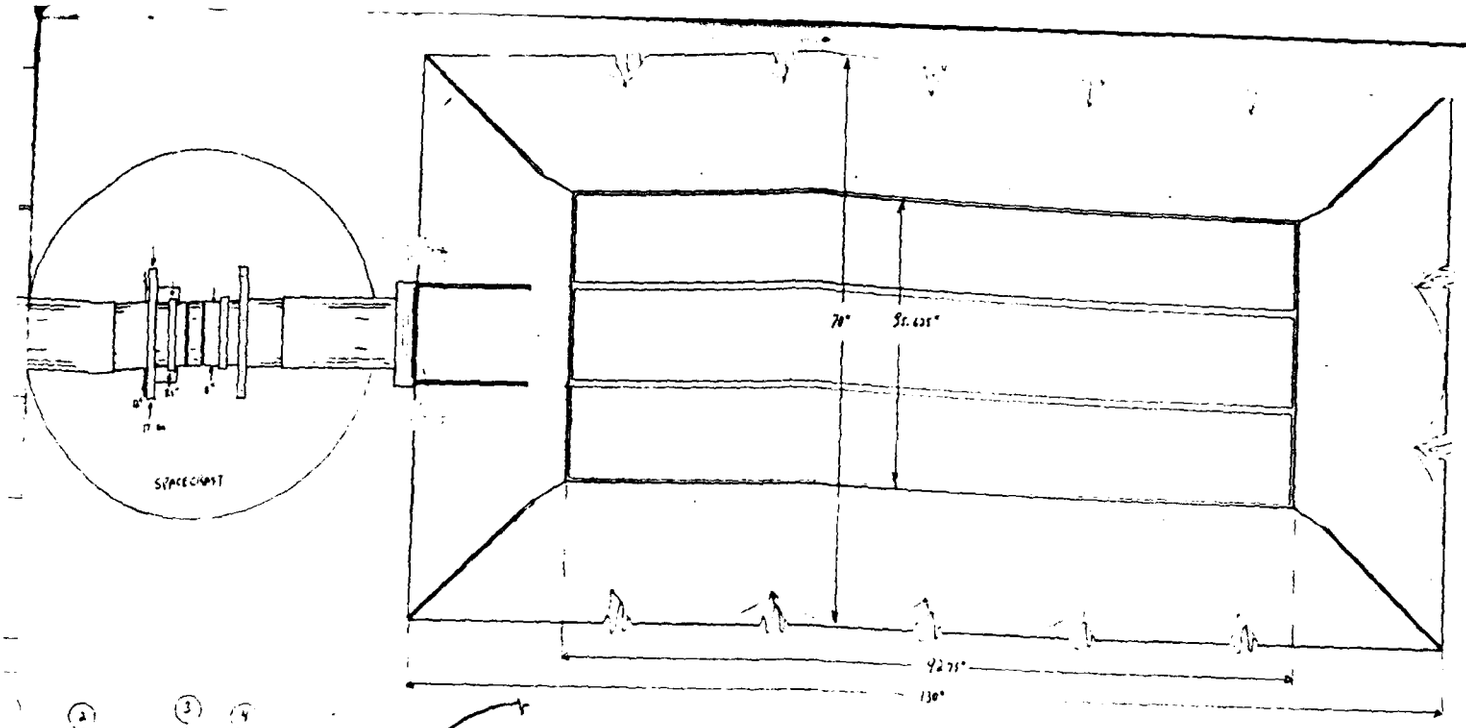

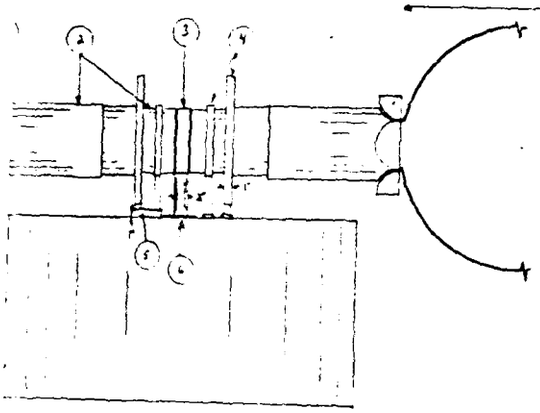

200 W SOLAR ARRAY
PILLOW CONFIGURATION
GED

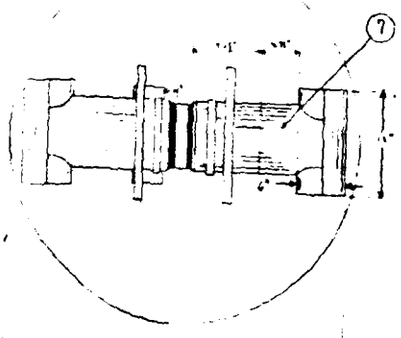

COMPONENT	WEIGHT (LBS)	% TOTAL
[illegible]	2 @ 26.7 = 53.3	34.1 %
[illegible]	4 @ 33 = 66	55.2 %
[illegible]	16 @ 1/8 = 2.93	2.5 %
[illegible]	4 @ 2.35 = 5.87	4.9 %
[illegible] (8)	1	.8 %
[illegible] (7)	2 @ 1 = 2	1.7 %
[illegible]	1	.8 %
	119.6	

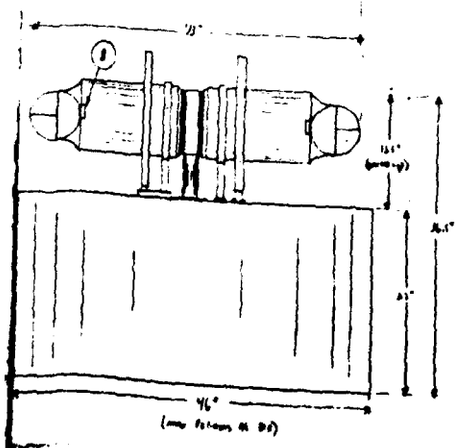

1	CLAMSHELL LATCH COMPONENT, OPEN
2	TELESCOPING ARM - INNERMOST CYLINDER [illegible] THICK, .058" STEEL
3	DRIVE MOTOR + GEARBOX; [illegible]; [illegible]
4	[illegible]
5	ATTITUDE CONTROLLER, COMPUTER, 3-V HEATERS, LOWER HEATER CONTROL, VEHICLE HARDWARE BOARD
6	VEHICLE MOUNT
7	LATCH RELEASE VALVE, RELIEF VALVE, RELEASE HEATER, [illegible]
8	CABLE CUTTERS TO OPEN CLAMSHELL

	200 W INFLATABLE SOLAR ARRAY - GED
	NON-WOVEN GED PILLOW CONFIGURATION ANDERSON'S PILLOW ARRAY
	DWG NO. 21000
	SCALE 1/10 SHEET 1 of 1